frontiers | Research Topics

Bariatric and metabolic surgery for obesity and related diseases: Effects and mechanisms

Edited by
Shaozhuang Liu, Sanyuan Hu, Peng Zhang,
Daniel Guerron and Wah Yang

Published in
Frontiers in Endocrinology

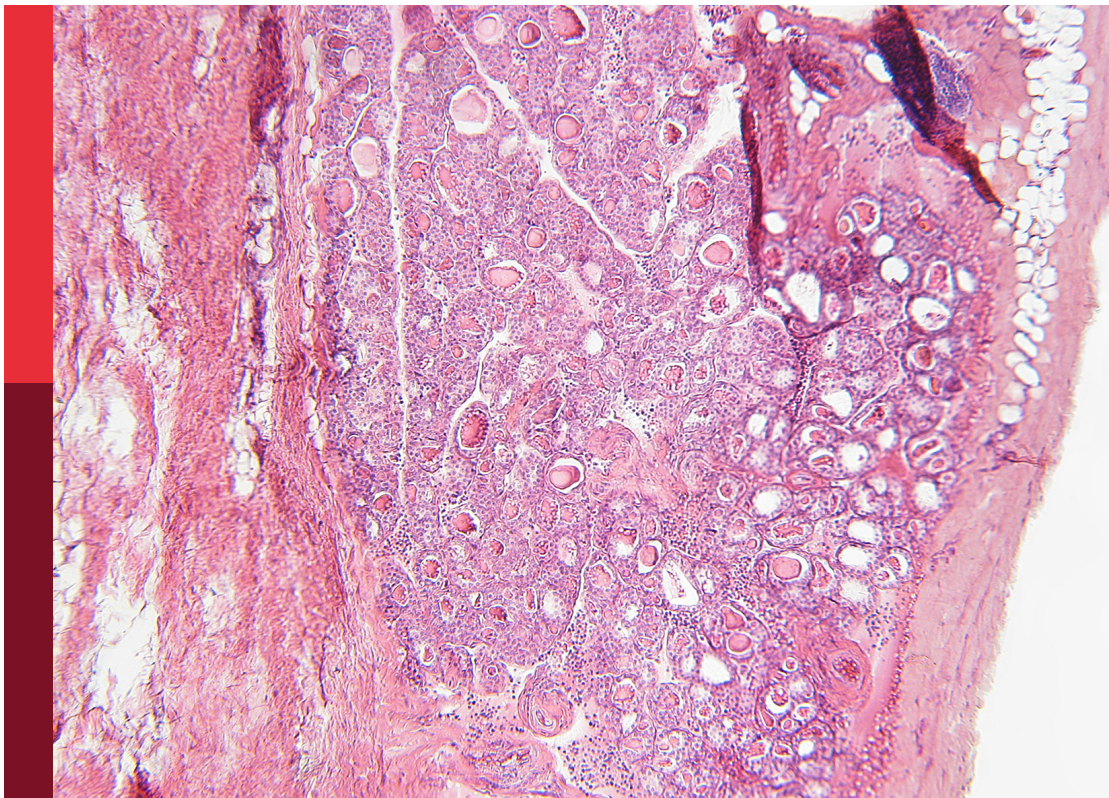

ISSN 1664-8714
ISBN 978-2-8325-2666-8
DOI 10.3389/978-2-8325-2666-8

About Frontiers

Frontiers is more than just an open access publisher of scholarly articles: it is a pioneering approach to the world of academia, radically improving the way scholarly research is managed. The grand vision of Frontiers is a world where all people have an equal opportunity to seek, share and generate knowledge. Frontiers provides immediate and permanent online open access to all its publications, but this alone is not enough to realize our grand goals.

Frontiers journal series

The Frontiers journal series is a multi-tier and interdisciplinary set of open-access, online journals, promising a paradigm shift from the current review, selection and dissemination processes in academic publishing. All Frontiers journals are driven by researchers for researchers; therefore, they constitute a service to the scholarly community. At the same time, the *Frontiers journal series* operates on a revolutionary invention, the tiered publishing system, initially addressing specific communities of scholars, and gradually climbing up to broader public understanding, thus serving the interests of the lay society, too.

Dedication to quality

Each Frontiers article is a landmark of the highest quality, thanks to genuinely collaborative interactions between authors and review editors, who include some of the world's best academicians. Research must be certified by peers before entering a stream of knowledge that may eventually reach the public - and shape society; therefore, Frontiers only applies the most rigorous and unbiased reviews. Frontiers revolutionizes research publishing by freely delivering the most outstanding research, evaluated with no bias from both the academic and social point of view. By applying the most advanced information technologies, Frontiers is catapulting scholarly publishing into a new generation.

What are Frontiers Research Topics?

Frontiers Research Topics are very popular trademarks of the *Frontiers journals series*: they are collections of at least ten articles, all centered on a particular subject. With their unique mix of varied contributions from Original Research to Review Articles, Frontiers Research Topics unify the most influential researchers, the latest key findings and historical advances in a hot research area.

Find out more on how to host your own Frontiers Research Topic or contribute to one as an author by contacting the Frontiers editorial office: frontiersin.org/about/contact

Bariatric and metabolic surgery for obesity and related diseases: Effects and mechanisms

Topic editors

Shaozhuang Liu — Shandong University, China
Sanyuan Hu — Shandong Provincial Qianfoshan Hospital, China
Peng Zhang — Capital Medical University, China
Daniel Guerron — Duke University, United States
Wah Yang — The First Affiliated Hospital of Jinan University, China

Citation

Liu, S., Hu, S., Zhang, P., Guerron, D., Yang, W., eds. (2023). *Bariatric and metabolic surgery for obesity and related diseases: Effects and mechanisms*. Lausanne: Frontiers Media SA. doi: 10.3389/978-2-8325-2666-8

Table of contents

05 Altered Glucose Metabolism and Glucose Transporters in Systemic Organs After Bariatric Surgery
Ju Hun Oh, Chan Woo Kang, Eun Kyung Wang, Jung Ho Nam, Soohyun Lee, Kyeong Hye Park, Eun Jig Lee, Arthur Cho and Cheol Ryong Ku

14 Metabolomics analysis of stool in rats with type 2 diabetes mellitus after single-anastomosis duodenal–ileal bypass with sleeve gastrectomy
Lun Wang, Zeyu Wang, Yang Yu, Zhaoheng Ren, Yongheng Jia, Jinfa Wang, Shixing Li and Tao Jiang

24 Metabolomics analysis of stool in rats with type 2 diabetes mellitus after single-anastomosis duodenal–ileal bypass with sleeve gastrectomy
Lun Wang, Zeyu Wang, Yang Yu, Zhaoheng Ren, Yongheng Jia, Jinfa Wang, Shixing Li and Tao Jiang

27 Association between liver-type fatty acid-binding protein and hyperuricemia before and after laparoscopic sleeve gastrectomy
Hui You, Huihui Ma, Xingchun Wang, Xin Wen, Cuiling Zhu, Wangjia Mao, Le Bu, Manna Zhang, Jiajing Yin, Lei Du, Xiaoyun Cheng, Haibing Chen, Jun Zhang and Shen Qu

36 Upregulation of hypothalamic POMC neurons after biliary diversion in GK rats
Shengnan Zhou, Weijie Chen, Xuesong Bai, Jiemin Chen, Qiang Xu, Liangbo Dong, Wei Chen, Qiang Qu and Xiaodong He

48 Sleeve gastrectomy attenuated diabetes-related cognitive decline in diabetic rats
Huanxin Ding, Chuxuan Liu, Shuo Zhang, Bingjun Li, Qian Xu, Bowen Shi, Songhan Li, Shuohui Dong, Xiaomin Ma, Yun Zhang, Mingwei Zhong and Guangyong Zhang

61 Can we abandon foregut exclusion for an ideal and safe metabolic surgery?
Jason Widjaja, Yuxiao Chu, Jianjun Yang, Jian Wang and Yan Gu

68 Gastroesophageal reflux related changes after sleeve gastrectomy and sleeve gastrectomy with fundoplication: A retrospective single center study
Aikebaier Aili, Maimaitiaili Maimaitiming, Pierdiwasi Maimaitiyusufu, Yusujiang Tusuntuoheti, Xin Li, Jianyu Cui and Kelimu Abudureyimu

76 Cognition and brain oxygen metabolism improves after bariatric surgery-induced weight loss: A pilot study
Nareen Anwar, Wesley J. Tucker, Nancy Puzziferri, T. Jake Samuel, Vlad G. Zaha, Ildiko Lingvay, Jaime Almandoz, Jing Wang, Edward A. Gonzales, Robert Matthew Brothers, Michael D. Nelson and Binu P. Thomas

85 Preoperative circulating peroxiredoxin 1 levels as a predictor of non-alcoholic fatty liver disease remission after laparoscopic bariatric surgery
Xiaoyun Cheng, Zhibing Fu, Wei Xie, Liyong Zhu and Jie Meng

98 Sleeve gastrectomy improves lipid dysmetabolism by downregulating the USP20-HSPA2 axis in diet-induced obese mice
Wenjie Zhang, Bowen Shi, Shirui Li, Zenglin Liu, Songhan Li, Shuohui Dong, Yugang Cheng, Jiankang Zhu, Guangyong Zhang and Mingwei Zhong

109 Increased plasma genistein after bariatric surgery could promote remission of NAFLD in patients with obesity
Geng Wang, Yu Wang, Jie Bai, Gang Li, Yang Liu, Shichang Deng, Rui Zhou, Kaixiong Tao and Zefeng Xia

123 Effects of bariatric surgery on testosterone level and sexual function in men with obesity: A retrospective study
Guoji Chen, Luping Sun, Shuwen Jiang, Xiaomei Chen, Jie Zhu, Xin Zhao, Shuqing Yu, Zhiyong Dong, Yuan Chen, Wen Zhang, Wah Yang and Cunchuan Wang

134 Bariatric Surgery: Targeting pancreatic β cells to treat type II diabetes
Tiantong Liu, Xi Zou, Rexiati Ruze and Qiang Xu

frontiers | Frontiers in Endocrinology

ORIGINAL RESEARCH
published: 14 July 2022
doi: 10.3389/fendo.2022.937394

Altered Glucose Metabolism and Glucose Transporters in Systemic Organs After Bariatric Surgery

Ju Hun Oh[1,2], Chan Woo Kang[2], Eun Kyung Wang[2], Jung Ho Nam[1,2], Soohyun Lee[2], Kyeong Hye Park[4], Eun Jig Lee[2], Arthur Cho[3] and Cheol Ryong Ku[2]**

[1] Brain Korea 21 PLUS Project for Medical Science, Yonsei University, College of Medicine, Seoul, South Korea, [2] Department of Internal Medicine, Endocrinology, Institute of Endocrine Research, Yonsei University College of Medicine, Seoul, South Korea, [3] Department of Nuclear Medicine, Yonsei University College of Medicine, Seoul, South Korea, [4] Division of Endocrinology and Metabolism, Department of Internal Medicine, National Health Insurance Service Ilsan Hospital, Goyang, South Korea

OPEN ACCESS

Edited by:
Shaozhuang Liu,
Shandong University, China

Reviewed by:
Sang Ouk Chin,
Kyung Hee University, South Korea
Chang-Myung Oh,
Seoul National University Hospital, South Korea
Zhenyu Hong,
The First Affiliated Hospital of Xinxiang Medical University, China
Jae Won Hong,
Inje University Ilsan Paik Hospital, South Korea
Wonjin Kim,
Cha Medical Center Gangnam, South Korea

***Correspondence:**
Cheol Ryong Ku
cr079@yuhs.ac
Arthur Cho
artycho@yuhs.ac

Specialty section:
This article was submitted to Obesity, a section of the journal Frontiers in Endocrinology

Received: 06 May 2022
Accepted: 20 June 2022
Published: 14 July 2022

Citation:
Oh JH, Kang CW, Wang EK, Nam JH, Lee S, Park KH, Lee EJ, Cho A and Ku CR (2022) Altered Glucose Metabolism and Glucose Transporters in Systemic Organs After Bariatric Surgery. Front. Endocrinol. 13:937394. doi: 10.3389/fendo.2022.937394

The Roux-en-Y gastric bypass (RYGB) is highly effective in the remission of obesity and associated diabetes. The mechanisms underlying obesity and type 2 diabetes mellitus remission after RYGB remain unclear. This study aimed to evaluate the changes in continuous dynamic FDG uptake patterns after RYGB and examine the correlation between glucose metabolism and its transporters in variable endocrine organs using ^{18}F-fluoro-2-deoxyglucose positron emission tomography images. Increased glucose metabolism in specific organs, such as the small intestine and various fat tissues, is closely associated with improved glycemic control after RYGB. In Otsuka Long-Evans Tokushima Fatty rats fed with high-fat diets, RYGB operation increases intestine glucose transporter expression and various fat tissues' glucose transporters, which are not affected by insulin. The fasting glucose decrement was significantly associated with RYGB, sustained weight loss, post-RYGB oral glucose tolerance test (OGTT) area under the curve (AUC), glucose transporter, or glycolytic enzymes in the small bowel and various fat tissues. High intestinal glucose metabolism and white adipose tissue-dependent glucose metabolism correlated with metabolic benefit after RYGB. These findings suggest that the newly developed glucose biodistribution accompanied by increased glucose transporters is a mechanism associated with the systemic effect of RYGB.

Keywords: bariatric surgery, diabetes mellitus, glucose metabolism, glucose transporter, obesity

INTRODUCTION

Bariatric surgery provides a long-term solution for patients with severe obesity. Bariatric surgeries are effective for both substantial weight loss and improved glucose metabolism, resulting in the remission of type 2 diabetes mellitus (DM) (1–7), especially in patients with a history of diabetes for less than 5 years (4, 5, 8), and the effects are superior to conventional non-surgical diabetes therapy (4, 5). Among bariatric surgeries, Roux-en Y gastric bypass (RYGB) has the most powerful therapeutic effect on the resolution of DM and obesity. In most patients undergoing RYGB, improved glycemic control occurs initially within days before sustained weight loss, implicating the

possibility of a weight-independent mechanism of bariatric surgery (9). In addition, several studies indicated that bariatric surgeries enhance the systemic hormone levels or signaling peptides, including GLP-1, GLP-2, CCK, 5-HT, PYY, and IGFBP-2 (10–16), causing alterations in bile acids and related pathways (17–19). However, to date, most studies mainly focused on the intestine after bariatric surgery (20–24), which cannot fully explain clinical improvement (16, 17, 25). Meanwhile, few studies focus on systemic metabolism change.

^{18}F-fluoro-2-deoxyglucose (FDG) positron emission tomography (PET)/computed tomography (CT) is used in the diagnosis of cancer malignancies by capturing the high FDG uptake of cancer cells. Also, the FDG uptake pattern shows the biodistribution of physiological glucose disposal. We previously reported that after bariatric surgery, intestinal glycolysis and glucose excretion through the intestine were substantially increased, which contributed to the rapid and lasting beneficial effect on glycemic control that is predominantly weight loss independent (21, 24). Moreover, in this study, we observed the change of systemic glucose metabolism not only in robust intestinal FDG uptake but also in various organs. Although systemic increment of glucose metabolism was observed, whether this newly developed glucose metabolism is correlated with metabolic improvement after RYGB remains unclear.

This study aimed to evaluate the changes in continuous dynamic FDG uptake patterns after RYGB and examine the correlation between glucose metabolism and its transporters in variable endocrine organs.

METHODS

Animals

All animal experiments were carried out under an Institutional Animal Care and Use Committee-approved protocol and institutional guidelines for the proper and humane use of animals. Four-week-old male Otsuka Long-Evans Tokushima Fatty (OLETF) rats were provided by the Tokushima Research Institute (Otsuka Pharmaceutical). OLETF rats were fed a high-fat diet (D12492, Research Diets, USA) for 16 weeks and were assigned to two types of surgery (RYGB: n=10 and sham surgery: n=4). The rats were housed at 22 ± 1°C under a 12-12 h light-dark cycle, with *ad libitum* access to water and food. Positron emission tomography (PET) was performed after an overnight fast before the surgery and 2, 4, and 8 weeks post-surgery and was processed as described below.

Roux-En Y Gastric Bypass

RYGB was performed under anesthesia as described in a previous study (21). The length of the entire small intestine was measured from the Treitz ligament. The jejunum was cut 18 cm downstream from the Treitz ligament. In a jejuno-gastric anastomosis, an end-to-side gastrojejunostomy was performed, and the other end of the cut jejunum was anastomosed to the small intestine 20 cm distal to the gastrojejunostomy resulting in a long common limb.

Sham Operation

The Sham group was used as a control. The sham surgery was performed as described in a previous study (21). Briefly, sham surgery consisted of laparotomy, a 1-cm enterotomy on the jejunum, and re-anastomosis without transection of jejunum and stomach.

Micro-Positron Emission Tomography and Radiotracer Counting

μPET imaging was performed according to a previously published paper protocol (21, 24). After an overnight fast, approximately 1 mCi of 18F-fluoro-2-deoxyglucose (FDG) was injected *via* tail vein injection. One hour after FDG injection, a 10 min μPET scan was conducted using Inveon PET (Siemens Medical Solutions, Knoxville, KY, USA). The maximum standardized uptake value (SUVmax), averaged uptake value (SUVmean), SUVmax normalized to rodents' weight (maxSUV), and SUVmean normalized to rodents' weight (meanSUV) were measured with the volume of interest (VOI) drawn on multiple tissues on PET images using the pMOD software (version 4.3, Switzerland). The SUVmax of the VOI was measured using the following formula: (decay-corrected activity [kBq] per tissue volume [mL])/(injected 18F-FDG activity [kBq] per body mass [g]). Immediately after μPET scan, the rats were euthanized in a CO_2 chamber, and tissues were excised, weighted, and subjected to gamma counting (Wallac Wizard 3" 1480 Gamma Counter; PerkinElmer, Akron, OH, USA). FDG tissue biodistribution data were decay-corrected according to the time of FDG injection and normalized to both the tissue weight (g) and radioactivity level. In counting FDG activity in the various tissues, the counts per minute were normalized to the dose of radioactivity injected.

Quantitative real-Time Polymerase Chain Reaction

Total RNA from tissues was isolated using the RNeasy Mini Kit (Qiagen, Germantown, MD, USA) according to the manufacturer's protocol. cDNA was synthesized using the ReverTra Ace (Toyobo, Osaka, Japan). qRT-PCR was performed using the ABI StepOne Plus Real-Time PCR machine (Applied Biosystems, Foster City, CA, USA). The primers used in this study are listed in **Table S1**. The relative transcriptional expression of target genes was evaluated by Eq. $2^{-\Delta Ct}$ (ΔCt = Ct of target gene minus Ct of reference gene of each organ tissue).

Statistical Analysis

All data were expressed as means ± SEM. Statistical analyses were performed using the Prism software version 4.0.0 (GraphPad, La Jolla, CA, USA). Each experiment was performed at least three times. All data were analyzed for statistical significance using the student's t test. In addition, Spearman correlation analyses were performed for comparing post-op OGTT AUC, post-op fasting glucose, post-op weight, post-op FDG radioactivity, post-op glucose transporter and glucose metabolism enzyme mRNA level. Also, in the RYGB column, sham group was set as 0 and RYGB group was set as 1, and correlation analysis was performed to analyze the correlation between operation type and glucose biodistribution.

Statistical significance was set at $p < 0.05$, and differences are indicated using asterisks (*$p < 0.05$, **$p < 0.01$, ***$p < 0.001$).

RESULT

FDG PET/CT Scanning Cases of Changes in Systemic Glucose Biodistribution After Gastrectomy in Human and RYGB in Rodents

Previous our study showed that increased intestinal glycolysis significantly correlated with reduction in HbA1c levels (21, 24). To further characterize the systemic glucose metabolism, we focused not only on small bowel but also the whole-body organs. We performed baseline and post-surgical FDG μPET in RYGB-operated rats. Pre-operated OLETF rats showed that low FDG uptake in the intestine and fat layer (**Figures 1A-C**). After RYGB surgery, it was confirmed that robust FDG uptake was observed in the intestine and subcutaneous layer (**Figures 1D-F**). We gained similar observations in patients who underwent FDG-PET/CT 1 year after Roux-en-Y gastroesophagectomy for gastric cancer. FDG-PET/CT showed elevated FDG uptake not only in small bowel but also in the subcutaneous fat layer (**Figures 1 G-J**), which is similar to observations from RYGB-operated rats (**Figures 1D-F**). Thus, these results indicated that newly developed glucose metabolism occurred in surgical groups after bariatric surgery.

Altered Glucose Distribution After RYGB

When comparing PET images of patients who underwent bariatric surgery with PET images after RYGB with OLETF rats examined in this experiment, it was confirmed that, similar to humans, changes in systemic glucose metabolism and small intestine occurred in OLETF rats after RYGB (**Figure 1**).

To confirm our previous finding of the occurrence of a newly FDG uptake pattern and unexpected glucose retention and secretion in the intestine (21, 24), OLETF rats were fed a 60% high-fat diet for 16 weeks and were subjected to RYGB. All sham-operated rats gained or maintained weight, whereas those that were subjected to RYGB lost weight robustly and sustainably for 8 weeks (**Figure 2A**). We conducted OGTT and measured fasting glucose at 8 weeks post-surgery. As expected, compared to sham operation, RYGB resulted in improved glucose control (**Figures 2B, C**). Absolute body weight (702.1 ± 10.67 vs. 590.23 ± 6.25 g, $p<0.01$), fasting glucose levels (10.439 ± 0.212 vs. 7.849 ± 0.169 mmol/L, $p<0.01$), and body weight changes (%reduction compared with preoperative weight, +4.06% vs. –

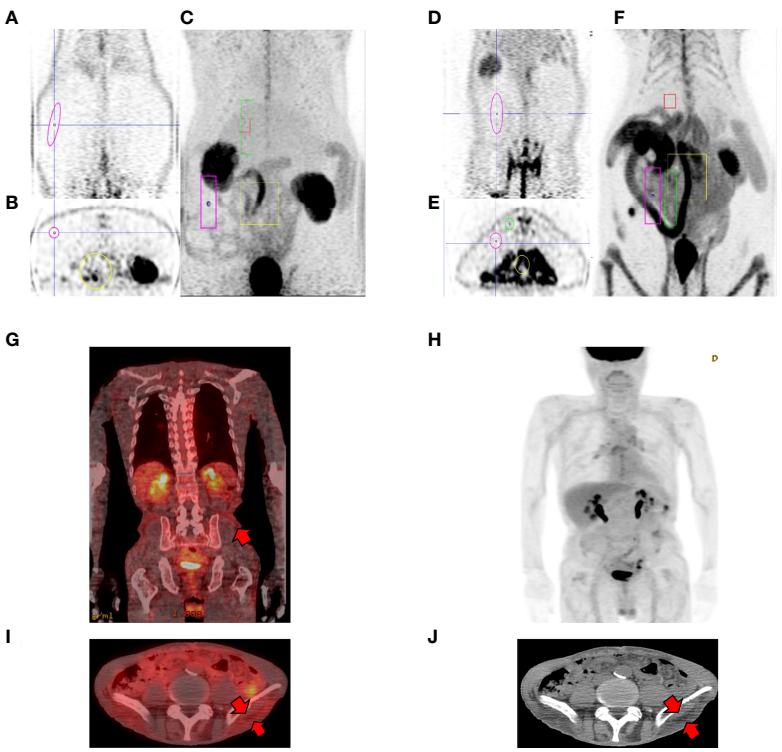

FIGURE 1 | Representative PET cases of altered systemic glucose distribution. **(A-C)** pre-operative OLETFrat showing low FDG uptake in the subcutaneous fat layer. Note low FDG uptake in the bowel in MIP images. **(D-F)** post-operative OLETFrat showing increased FDG uptake in the subcutaneous layer 2 months after surgery. (**A**, **D** coronal PET, **B**, **E** axial PET, **C, F** maximum intensity projection (MIP) **(G-J)** Representative case of changes in biodistribution after gastrectomy. A 49-year-old male patient underwent Roux-en-Y gastroesophagectomy due to stomach cancer. FDG PET/CT was performed one year after surgery for surveillance. Fusion coronal **(G)** and axial fusion **(I)** images shows elevated FDG uptake in the corresponding subcutaneous fat layer (arrows, **J**).

25.2%, respectively), fasting glucose changes (%reduction compared with preoperative glucose, +15.9% vs. -42.6%, respectively) were significantly lower in RYGB-operated rats (**Figures 2A-C**).

To evaluate whether RYGB enhanced systemic glucose uptake, we performed baseline and post-RYGB dynamic FDG μPET. List-mode-time-of-flight data acquisition started immediately after the intravenous FDG administration and lasted for 1 h. Dynamic PET images were reconstructed, and six spherical regions of interest (ROI), each with 20 mm diameter, were placed on the six segments of each organ, avoiding any blood vessels. The averaged FDG activity in all six ROIs was extracted from the dynamic images to form a global Time Activity Curves (TAC) (**Figures 2D-G**). ^{18}FDG distribution was characterized by rapid liver uptake, followed by clearance through the other organ, including the kidney and bladder (**Figures 1B**, **2D**). Rapid liver uptake of FDG was increased in RYGB rats but preceded a washout of FDG radioactivity over 60 min, and the difference between the two groups disappeared (**Figure 2D**). This phenomenon also occurred in muscles (**Figure 2F**). In contrast, compared to sham surgery rats, fat-specific radioactivity was still retained at 60 min in RYGB-operated rats (**Figure 2G**). Also, a previous study (21) showed that although FDG did not accumulate in the intestine of sham-surgery rats, the intestine of RYGB-treated rats showed a high accumulation of the FDG (**Figure 2E**).

To evaluate systemic changes in glucose metabolism after RYGB operation, multiple tissues were excised and subjected to

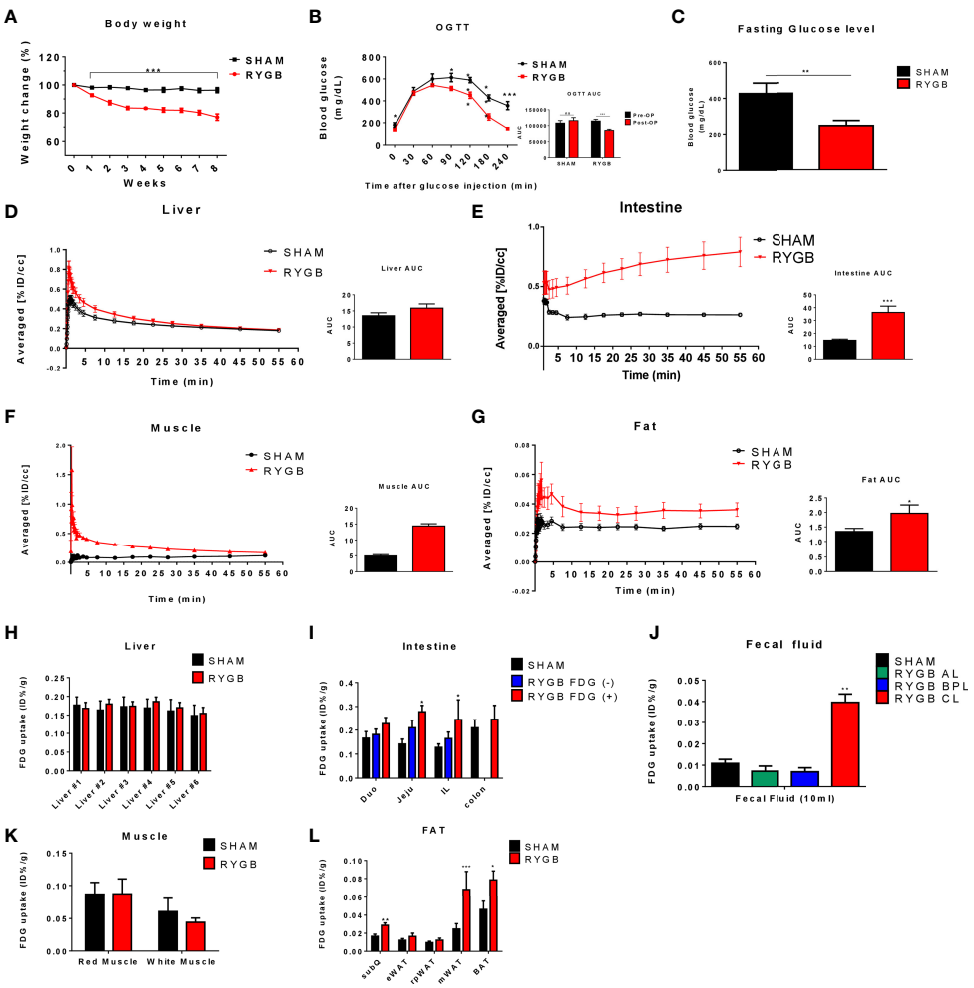

FIGURE 2 | Altered glucose distribution after RYGB. Metabolic parameters in adult male Otsuka Ling-Evans Tokushima fatty (OLETF) rats showing weekly body weight change **(A)** measured every week over 8 weeks, oral glucose tolerance test (OGTT) data **(B)**, and fasting glucose level **(C)** in sham-operated and RYGB-operated rats. Representative 2-Deoxy-2-[18F]-fluoro-D-glucose (FDG)-PET image analysis in OLETF rats. OLETF rats Time Activity Curves (TAC) obtained from 60-min dynamic PET imaging and AUC graph of liver **(D)**, intestine **(E)**, muscle **(F)**, and mesenteric fat **(G)**. Liver #1~#6 denote Right Median Lobe (#1), Right Superior Lobe (#2), Right Median Lobe (#3), Left Median Lobe (#4), Left Lateral Lobe (#5), Caudate Lobe (#6), respectively **(H)**. FDG biodistribution analysis (gamma counting) in RYGB-operated and sham-operated rats in various organs, including the liver **(H)**, intestine **(I)**, intestinal lumen phosphate buffered saline (PBS) washing analysis **(J)**, muscle **(K)**, and various fat tissues **(L)**. Number of mice in all panels **(A–C)** (males; RYGB, 10; sham, 4). All data are presented as mean ± SEM, *p<0.05, **p<0.01, ***p<0.001 vs. sham.

gamma counting of FDG radioactivity immediately after μPET. FDG tissue biodistribution analysis showed that FDG uptake in the intestine and fat was higher in RYGB-operated rats compared with that in sham-operated rats, whereas no difference in the FDG uptake in the liver and muscle was observed (**Figures 2H, K**). Furthermore, excreted FDG into common limbs (CL) of the intestine lumen was increased in RYGB-operated CL compared to that of RYGB-operated alimentary limbs (AL), biliopancreatic limbs (BPL), and sham-operated rats (**Figure 2J**). Taken together, these data indicated that RYGB induced a newly glucose biodistribution through the intestine and fat tissue and that RYGB-induced improved glycemic control might be correlated with this newly glucose biodistribution.

Expression of Glucose Transporters in Various Organs

Because systemic glucose uptake was observed in various tissues after RYGB, we evaluated which glucose uptake and glucose metabolism genes could influence this glucose homeostasis. Glucose transporter (GLUT) and enzyme genes were observed in tissues based on reverse transcription PCR (RT-PCR) analysis (**Figure 3**). In the intestine, we selected regions of each limb of the intestine with higher levels of FDG uptake (FDG +) or basal levels (FDG -) using gamma counting. Corresponding sections of sham-operated rats were used as controls. Consistent with previous study (21), in the AL of the intestine, GLUT1 and Hexokinase (HK) genes showed a sequential increase corresponding to FDG uptake increase patterns (sham jejunum, AL FDG (-), AL FDG (+)) (**Figure 3A**). Other GLUT genes were unchanged or decreased in sham and RYGB. Similarly, in CL, GLUT1 and HK genes were upregulated in FDG (+) AL (**Figure 3B**). However, no genes in the BPL of the intestine were differently regulated in RYGB rats (**Figure 3C**). We removed various fat tissues, including the inguinal white adipose tissue (iWAT), epididymal WAT (eWAT), brown adipose tissue (BAT), retroperitoneal WAT (rpWAT), and mesentery WAT (mWAT), to identify which fats contribute to the improvement of glucose homeostasis of RYGB-operated rats. In all fats, except for eWAT, GLUT1 expression was increased in RYGB-operated rats than that in sham rats (**Figures 3D-H**). In the rpWAT of RYGB-operated rats, GLUT1-5 expressions were significantly increased (**Figure 3D**). In the liver, GLUT1 and GLUT2 showed a significantly increased in RYGB-operation rats (**Figure 3I**). In accordance with above dynamic PET data, no genes were significantly altered in the muscle (**Figures 3J, K**). These results indicated that GLUT and HK are robustly associated with systemic and newly glucose biodistribution by RYGB.

Correlation Analysis Between Glucose Distribution and Glucose Transporters

To document the relationships between glucose uptake and metabolism related genes and system metabolic changes, we conducted correlation analysis. Operation type, post-op OGTT AUC, post-op fating glucose level, post-op weight, FDG radioactivity, and GLUT1-5 genes were used as multiple parameters for Pearson or Spearman correlation analysis. Since FDG uptake was increased in the AL of the intestine, CL of the intestine, and various adipose tissues among various organs, we conducted a correlation analysis with intestine and WAT (**Figure 4**). Correlation analysis showed that: (1) operation type, post-op AUC, post-op fasting glucose, and post-op weight were positively correlated (**Figures 4A-E**); (2) in the AL of intestine, RYGB surgery correlated with FDG radioactivity and GLUT1 expression, whereas post-op AUC, fasting glucose level, and weight were negatively associated with FDG uptake and GLUT1 expression (**Figure 4A**); (3) in the CL of intestine, RYGB surgery correlated with CL FDG radioactivity and CL GLUT1 expression, whereas post-op AUC, fasting glucose level, and weight were negatively associated with CL FDG uptake, CL GLUT1 expression, and SGLT1 expression (**Figure 4B**); (4) in iWAT, RYGB surgery correlated with iWAT FDG radioactivity, iWAT GLUT1 expression, and GLUT5 expression, whereas post-op AUC, fasting glucose level, and weight were negatively associated with iWAT FDG uptake and GLUT1 expression, while post-FDG uptake was positively associated with GLUT2, GLUT3, and SGLT1 expression (**Figure 4C**); (5) in mWAT, post-op AUC negatively associated with mWAT GLUT1, GLUT2, and SLGT2 expression, whereas post-op fasting glucose level and weight were negatively associated with mWAT FDG uptake (**Figure 4D**); (6) in rpWAT, RYGB surgery correlated with rpWAT FDG radioactivity, rpWAT GLUT1 expression, and GLUT5 expression (**Figure 4E**), whereas post-op AUC, fasting glucose level, and weight were negatively associated with iWAT FDG uptake and GLUT1 expression. These data are consistent with systemic glucose metabolism changes in RYGB-operated patients and rats. These results indicated that systemic glucose metabolism changes are robustly associated with upregulation of GLUT1, and related transporter genes underwent RYGB.

DISCUSSION

The biological mechanism of improved hyperglycemia and weight loss by bariatric remains unelucidated. Previous studies focused on the anatomical changes of the intestine or gut oriented hormones, such as glucagon-like peptide 1. Here, we demonstrate that the potential image-based semi-quantitative FDG activity of systemic glycolytic activity correlated with improved glycemic control and robust weight loss brought by RYGB in a rodent model. We analyzed the correlation between increased systemic glucose metabolism and RYGB-induced improvement in metabolic changes. We have shown that (1) the increased glucose metabolism not only in AL and CL of the intestine but also in mWAT, rpWAT, and iWAT; (2) the increased expression of glucose transporter subtypes in organs showed improved glucose metabolism after RYGB; and (3) the correlation between increased organ-specific glucose metabolism and improved hyperglycemia in rats after RYGB.

Insulin-induced glucose disposal occurs in muscle, fat, and various organs in normal physiology (26). After bariatric surgery

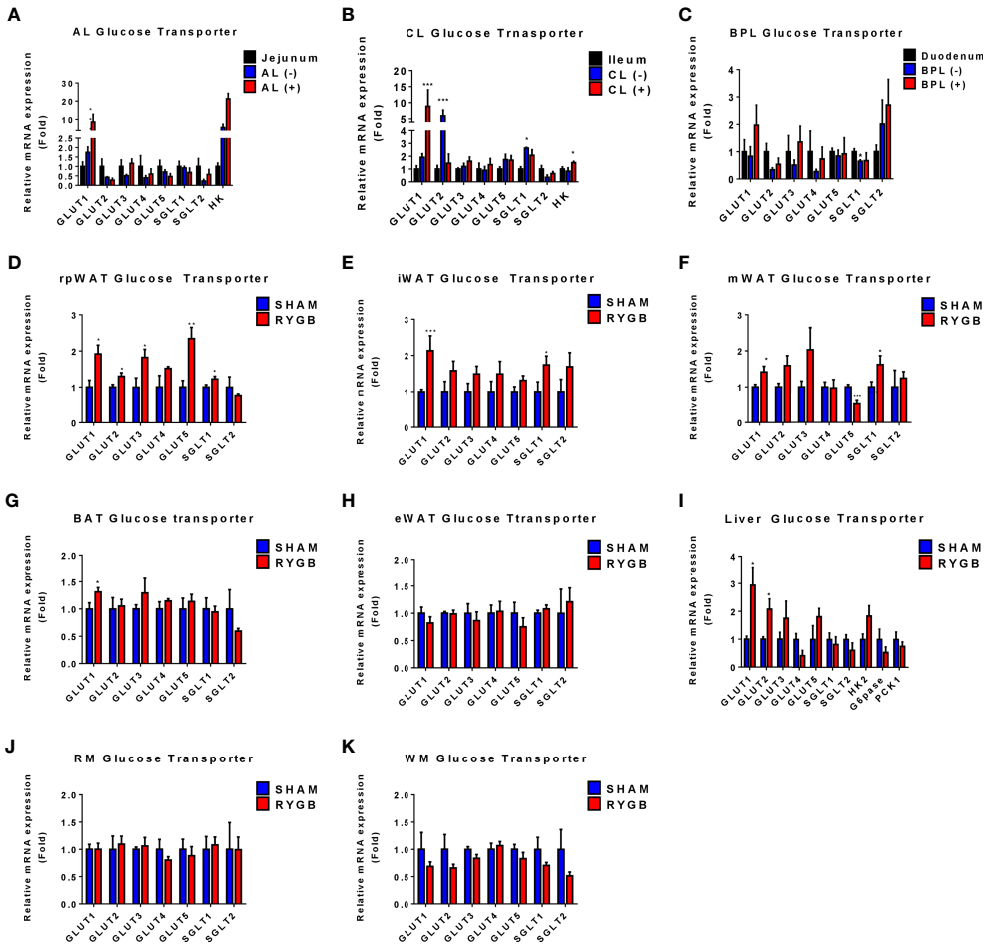

FIGURE 3 | Expression of Glucose transporters in various organs. Subtypes of glucose transporters are altered in RYGB-operated OLETF rats. The expression of glucose transporter subtype in alimentary limbs (AL), common limb (CL), and biliopancreatic limb (BPL) of RYGB-operated rats and the corresponding limbs of sham-operated rats **(A-C)**. The fold change was calculated based on the corresponding sham-operated bowel (jejunum for the CL, duodenum for the biliopancreatic limbs (BPL), and ileum for the CL). (–) or (+) denotes FDG negativity or positivity of individual rats, respectively. The expression of glucose transporter subtype in retroperitoneal white adipose tissue (rpWAT) **(D)**, inguinal WAT (iWAT) **(E)**, mesentery WAT (mWAT) **(F)**, brown adipose tissue (BAT) **(G)**, epididymal WAT (eWAT) **(H)**, liver **(I)**, red muscle (RM) **(J)**, and white muscle (WM) **(K)**. The fold change was calculated based on the corresponding sham-operated rats' organs. All data are presented as mean ± SEM, *p<0.05, **p<0.01, ***p<0.001 vs. sham.

in obese patients with T2D, micro-PET analysis revealed a possible increase in systemic glucose uptake (**Figures 1**, **2**). FDG uptake was not changed in the muscle, a representative glucose disposed organ, but newly increased in the intestine and various fat tissues. According to the TAC graph, FDG was trapped for over 60 min in both the intestine and fat, unlike in muscles and liver (**Figure 2**). Some studies showed that bariatric surgery leads to a significant improvement in hepatic insulin sensitivity, which is accompanied by increased hepatic glucose uptake and reduced endogenous glucose production in human T2D or non-T2D patients (27). However, our results showed that hepatic glucose uptake was comparable. Several studies demonstrated that FDG uptake in the liver was lower or comparable in RYGB-operated groups (20, 21), which may be caused by a glucose analogue in which FDG cannot be metabolized. It is postulated that Glucose-6-phophatase (G6pase) is expressed in liver and this enzyme may affect the retention of FDG in liver. Also, in the muscle, an earlier FDG uptake surge was observed but preceded a slow washout of FDG radioactivity over the remaining 60 min and showed that insulin-induced glucose disposal does not change. Previous studies showed that bariatric surgery induced improvement in glycemic control independently with insulin secretion or sensitivity (20, 21, 28, 29). Unlike in liver or muscle, FDG retention is maintained in various fat tissues, including mWAT, iWAT, and rpWAT, which are the organ where glucose is uptaken by insulin-induced GLUT4 activity (30). However, our data showed that although GLUT4 expression is comparable, the expression of GLUT1 was increased. This result indicated that the high expression of GLUT1, whose activity is independent of insulin, contributes to increased glucose uptake after RYGB surgery. Similar to reprogrammed intestinal glucose

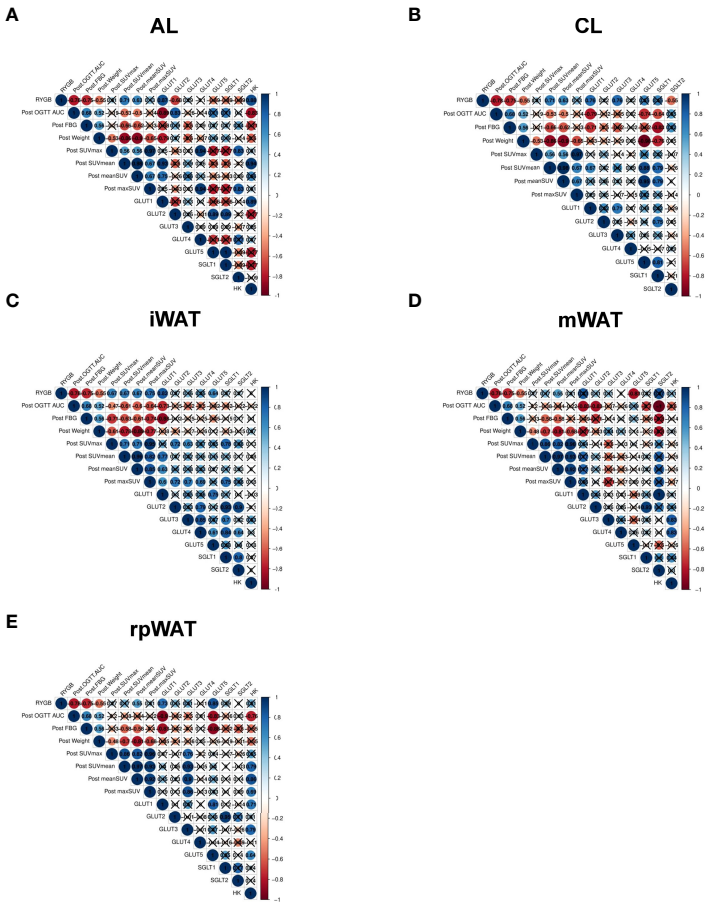

FIGURE 4 | Correlation analysis between glucose distribution and glucose transporters Spearman's correlation among post-operated OGTT AUC, post-operated weight, postoperated fasting glucose, operation type, the maximum standardized FDG uptake value (SUVmax), the averaged standardized FDG value, and each normalized to weight (maxSUV, meanSUV), and the expression levels of glucose transporters in **(A)** AL, **(B)** CL, **(C)** iWAT, **(D)** mWAT, and **(E)** rpWAT, representing significant FDG uptake in TAC images in RYGB-operated OLETF rats. Nonsignificant correlations (p-value > 0.05) are indicated by crosses.

metabolism after RYGB is mediated by GLUT1, GLUT1 contributes to glucose absorption in various fat tissues. Accordingly, systemic reprogrammed glucose absorption patterns were mediated independently of insulin-mediated effects.

Our results indicate that compared with sham-operated rats, GLUT1 is upregulated in organs with increased FDG uptake of RYGB-operated animals. GLUT1 and glycolysis genes are increased in the intestine after bariatric surgery (20, 21, 23, 28, 31). Consistent with previous studies (23, 32), intestinal glucose transporter GLUT2 and SGLT1 expression were downregulated in the AL and CL of RYGB-operated rats. In organs with a high FDG uptake, GLUT1 expression was increased. mWAT, iWAT, and rpWAT showed the increased expression of GLUT1 after RYGB surgery. Conversely, GLUT1 expression was comparable in the organ with no change in FDG uptake after RYGB. It can be inferred that the insulin-independent higher FDG uptake in fat is due to the increase in GLUT1. GLUT1 is rarely expressed in mature intestine and white adipose tissue (33). Intestinal hypertrophy and increasing villus length are caused by intestinal glucose uptake through GLUT1 after RYGB (20, 21, 34, 35). In our previous study, Amphiregulin (AREG)/Epidermal growth factor receptor (EGFR) signaling is upregulated in RYGB rats and human intestine, and AREG increases glucose uptake and secretion through EGFR-mediated GLUT1 expression and trafficking (21). Also, oxygen is insufficient due to numerous build-up processes occurring in the small intestine, which leads to the overexpression of GLUT1 by HIF1-a (36). We speculate that soluble factors such as AREG not only affect the intestine, but also affect the various organs through circulating through the blood. AREG may regulate GLUT1 expression in various fats throughout the body. In fact, it was reported that overexpression of AREG in white adipose tissue of db/db mice reduced mouse weight and fat weight and beta-oxidation signaling and TCA cycle would be increased in white adipose tissue (37). Furthermore, the T Helper cell modulates intestinal stem cell renewal and intestinal morphology (38). Previous studies showed that AREG, which originated from T helper 2 cells, results in the upregulation of the GLUT1 expression (21). Therefore, the intestinal derived signal may affect the glucose disposal of fat

tissues independent of insulin action or intestine-derived T helper 2 cells systemically similar to other immune cells (39).

The current study has several limitations. First, we only used ^{18}F-fluoro-2-deoxyglucose (FDG). However, glucose is trapped in the cell in the form of glucose-6-phosphate (G6P). G6P is a late limiting step in glucose metabolism. FDG in the intestine and fat tissues was retained for over 60 min; therefore, if glucose had been used instead of FDG, it would have been metabolized. Also, previous study showed that ^{14}C-Glucose disposal and excretion was similar to those of FDG. Second, we only showed correlation and not causation through experiments. However, to our knowledge, this study is the first to demonstrate the quantitative measurements of post-RYGB FDG uptake in various organs and show dynamic glucose retention. This study supports the RYGB-induced new systemic glucose distribution. Further studies are needed to identify the signaling pathways inducing GLUT1-mediated systemic glucose disposal, which may be new drug targets to mimic the RYGB-induced improvement in metabolic changes.

In conclusion, the induction of GLUT1 levels by RYGB is robust and is correlated with improved metabolic changes. This novel finding may support the unknown mechanism effect of RYGB.

DATA AVAILABILITY STATEMENT

The raw data supporting the conclusions of this article will be made available by the authors without undue reservation.

ETHICS STATEMENT

The studies involving human participants were reviewed and approved by Approved by Severance Hospital's institutional review board. The ethics committee waived the requirement of written informed consent for participation. The animal study was reviewed and approved by Institutional Animal Care and Use Committee (IACUC) at the Yonsei University Health System. Written informed consent was not obtained from the individual(s) for the publication of any potentially identifiable images or data included in this article.

AUTHOR CONTRIBUTIONS

Conceptualization: CKu and AC. Data curation and formal analysis: CKu, JO, KP, and AC. Funding acquisition: CKu. Investigation and methodology: CKu, JO, CKa, EW, JN, SL, and AC. Supervision and validation: CKu, JO and AC. Visualization: CKu, JO, and AC. Writing original draft: CKu, JO, and AC. Writing review and editing: CKu, JO, EL, KP, and AC. All authors contributed to the article and approved the submitted version.

FUNDING

This research was supported by a grant from the Korea Health Technology R&D Project through the Korea Health Industry Development Institute (KHIDI), funded by the Ministry of Health & Welfare, the Republic of Korea (grant number: HR18C0012).

ACKNOWLEDGMENTS

We would like to thank Byung Gon Kim and Jung-Hyun Ji, members of the laboratory animal research Centre of ABMRC at Yonsei University College of Medicine, for their technical support with animal experiments. We also thank the Editage (www. editage. co. kr) for English language editing.

SUPPLEMENTARY MATERIAL

The Supplementary Material for this article can be found online at: https://www.frontiersin.org/articles/10.3389/fendo.2022.937394/full#supplementary-material

REFERENCES

1. Rubino F. Bariatric Surgery: Effects on Glucose Homeostasis. *Curr Opin Clin Nutr Metab Care* (2006) 9(4):497–507. doi: 10.1097/01.mco.0000232914.14978.c5
2. Buchwald H, Avidor Y, Braunwald E, Jensen MD, Pories W, Fahrbach K, et al. Bariatric Surgery: A Systematic Review and Meta-Analysis. *Jama* (2004) 292 (14):1724–37. doi: 10.1001/jama.292.14.1724
3. Mingrone G, Panunzi S, De Gaetano A, Guidone C, Iaconelli A, Leccesi L, et al. Bariatric Surgery Versus Conventional Medical Therapy for Type 2 Diabetes. *N Engl J Med* (2012) 366(17):1577–85. doi: 10.1056/NEJMoa1200111
4. Schauer PR, Bhatt DL, Kirwan JP, Wolski K, Aminian A, Brethauer SA, et al. Bariatric Surgery Versus Intensive Medical Therapy for Diabetes - 5-Year Outcomes. *N Engl J Med* (2017) 376(7):641–51. doi: 10.1056/NEJMoa1600869
5. Mingrone G, Panunzi S, De Gaetano A, Guidone C, Iaconelli A, Nanni G, et al. Bariatric-Metabolic Surgery Versus Conventional Medical Treatment in Obese Patients With Type 2 Diabetes: 5 Year Follow-Up of an Open-Label, Single-Centre, Randomised Controlled Trial. *Lancet* (2015) 386(9997):964–73. doi: 10.1016/S0140-6736(15)00075-6
6. Chambers AP, Jessen L, Ryan KK, Sisley S, Wilson-Pérez HE, Stefater MA, et al. Weight-Independent Changes in Blood Glucose Homeostasis After Gastric Bypass or Vertical Sleeve Gastrectomy in Rats. *Gastroenterology* (2011) 141(3):950–8. doi: 10.1053/j.gastro.2011.05.050
7. Lingvay I, Guth E, Islam A, Livingston E. Rapid Improvement in Diabetes After Gastric Bypass Surgery: Is it the Diet or Surgery? *Diabetes Care* (2013) 36(9):2741–7. doi: 10.2337/dc12-2316
8. Abarca-Gómez L., Abdeen Z.A., Hamid Z.A.., Abu-Rmeileh N.M., Acosta-Cazares B., Acuin C., et al. Worldwide Trends in Body-Mass Index, Underweight, Overweight, and Obesity From 1975 to 2016: A Pooled Analysis of 2416 Population-Based Measurement Studies in 128·9 Million Children, Adolescents, and Adults. *Lancet* (2017) 390(10113):2627–42. doi: 10.1016/S0140-6736(17)32129-3
9. Jørgensen NB, Jacobsen SH, Dirksen C, Bojsen-Møller KN, Naver L, Hvolris L, et al. Acute and Long-Term Effects of Roux-En-Y Gastric Bypass on Glucose Metabolism in Subjects With Type 2 Diabetes and Normal Glucose

Tolerance. *Am J Physiol Endocrinol Metab* (2012) 303(1):E122–31. doi: 10.1152/ajpendo.00073.2012
10. Stefater MA, Wilson-Pérez HE, Chambers AP, Sandoval DA, Seeley RJ. All Bariatric Surgeries Are Not Created Equal: Insights From Mechanistic Comparisons. *Endocr Rev* (2012) 33(4):595–622. doi: 10.1210/er.2011-1044
11. Laferrère B. Do We Really Know Why Diabetes Remits After Gastric Bypass Surgery? *Endocrine* (2011) 40(2):162–7. doi: 10.1007/s12020-011-9514-x
12. Falkén Y, Hellström PM, Holst JJ, Näslund E. Changes in Glucose Homeostasis After Roux-En-Y Gastric Bypass Surgery for Obesity at Day Three, Two Months, and One Year After Surgery: Role of Gut Peptides. *J Clin Endocrinol Metab* (2011) 96(7):2227–35. doi: 10.1210/jc.2010-2876
13. Mumphrey MB, Patterson LM, Zheng H, Berthoud HR. Roux-En-Y Gastric Bypass Surgery Increases Number But Not Density of CCK-, GLP-1-, 5-HT-, and Neurotensin-Expressing Enteroendocrine Cells in Rats. *Neurogastroenterol Motil* (2013) 25(1):e70–9. doi: 10.1111/nmo.12034
14. Holst JJ. Enteroendocrine Secretion of Gut Hormones in Diabetes, Obesity and After Bariatric Surgery. *Curr Opin Pharmacol* (2013) 13(6):983–8. doi: 10.1016/j.coph.2013.09.014
15. Ramracheya RD, McCulloch LJ, Clark A, Wiggins D, Johannessen H, Olsen MK, et al. PYY-Dependent Restoration of Impaired Insulin and Glucagon Secretion in Type 2 Diabetes Following Roux-En-Y Gastric Bypass Surgery. *Cell Rep* (2016) 15(5):944–50. doi: 10.1016/j.celrep.2016.03.091
16. Faramia J, Hao Z, Mumphrey MB, Townsend RL, Miard S, Carreau A-M, et al. IGFBP-2 Partly Mediates the Early Metabolic Improvements Caused by Bariatric Surgery. *Cell Rep Med* (2021) 2(4):100248. doi: 10.1016/j.xcrm.2021.100248
17. Ryan KK, Tremaroli V, Clemmensen C, Kovatcheva-Datchary P, Myronovych A, Karns R, et al. FXR Is a Molecular Target for the Effects of Vertical Sleeve Gastrectomy. *Nature* (2014) 509(7499):183–8. doi: 10.1038/nature13135
18. Flynn CR, Albaugh VL, Cai S, Cheung-Flynn J, Williams PE, Brucker RM, et al. Bile Diversion to the Distal Small Intestine has Comparable Metabolic Benefits to Bariatric Surgery. *Nat Commun* (2015) 6(1):7715. doi: 10.1038/ncomms8715
19. DePaoli AM, Zhou M, Kaplan DD, Hunt SC, Adams TD, Learned RM, et al. FGF19 Analog as a Surgical Factor Mimetic That Contributes to Metabolic Effects Beyond Glucose Homeostasis. *Diabetes* (2019) 68(6):1315–28. doi: 10.2337/db18-1305
20. Saeidi N, Meoli L, Nestoridi E, Gupta NK, Kvas S, Kucharczyk J, et al. Reprogramming of Intestinal Glucose Metabolism and Glycemic Control in Rats After Gastric Bypass. *Science* (2013) 341(6144):406–10. doi: 10.1126/science.1235103
21. Kwon IG, Kang CW, Park JP, Oh JH, Wang EK, Kim TY, et al. Serum Glucose Excretion After Roux-En-Y Gastric Bypass: A Potential Target for Diabetes Treatment. *Gut* (2021) 70(10):1847–56. doi: 10.1136/gutjnl-2020-321402
22. Ribeiro-Parenti L, Jarry A-C, Cavin J-B, Willemetz A, Le Beyec J, Sannier A, et al. Bariatric Surgery Induces a New Gastric Mucosa Phenotype With Increased Functional Glucagon-Like Peptide-1 Expressing Cells. *Nat Commun* (2021) 12(1):110. doi: 10.1038/s41467-020-20301-1
23. Cavin JB, Couvelard A, Lebtahi R, Ducroc R, Arapis K, Voitellier E, et al. Differences in Alimentary Glucose Absorption and Intestinal Disposal of Blood Glucose After Roux-En-Y Gastric Bypass vs Sleeve Gastrectomy. *Gastroenterology* (2016) 150(2):454–64.e9. doi: 10.1053/j.gastro.2015.10.009
24. Ku CR, Lee N, Hong JW, Kwon IG, Hyung WJ, Noh SH, et al. Intestinal Glycolysis Visualized by FDG PET/CT Correlates With Glucose Decrement After Gastrectomy. *Diabetes* (2017) 66(2):385–91. doi: 10.2337/db16-1000
25. Aron-Wisnewsky J, Prifti E, Belda E, Ichou F, Kayser BD, Dao MC, et al. Major Microbiota Dysbiosis in Severe Obesity: Fate After Bariatric Surgery. *Gut* (2019) 68(1):70–82. doi: 10.1136/gutjnl-2018-316103
26. Dimitriadis G, Mitrou P, Lambadiari V, Maratou E, Raptis SA. Insulin Effects in Muscle and Adipose Tissue. *Diabetes Res Clin Pract* (2011) 93:S52–S9. doi: 10.1016/S0168-8227(11)70014-6
27. Immonen H, Hannukainen JC, Iozzo P, Soinio M, Salminen P, Saunavaara V, et al. Effect of Bariatric Surgery on Liver Glucose Metabolism in Morbidly Obese Diabetic and Non-Diabetic Patients. *J Hepatol* (2014) 60(2):377–83. doi: 10.1016/j.jhep.2013.09.012
28. Kim M, Son YG, Kang YN, Ha TK, Ha E. Changes in Glucose Transporters, Gluconeogenesis, and Circadian Clock After Duodenal-Jejunal Bypass Surgery. *Obes Surg* (2015) 25(4):635–41. doi: 10.1007/s11695-014-1434-4
29. Isbell JM, Tamboli RA, Hansen EN, Saliba J, Dunn JP, Phillips SE, et al. The Importance of Caloric Restriction in the Early Improvements in Insulin Sensitivity After Roux-En-Y Gastric Bypass Surgery. *Diabetes Care* (2010) 33(7):1438–42. doi: 10.2337/dc09-2107
30. Leto D, Saltiel AR. Regulation of Glucose Transport by Insulin: Traffic Control of GLUT4. *Nat Rev Mol Cell Biol* (2012) 13(6):383–96. doi: 10.1038/nrm3351
31. Deal RA, Tang Y, Fletcher R, Torquati A, Omotosho P. Understanding Intestinal Glucose Transporter Expression in Obese Compared to Non-Obese Subjects. *Surg Endosc* (2018) 32(4):1755–61. doi: 10.1007/s00464-017-5858-5
32. Stearns AT, Balakrishnan A, Tavakkolizadeh A. Impact of Roux-En-Y Gastric Bypass Surgery on Rat Intestinal Glucose Transport. *Am J Physiol Gastrointest Liver Physiol* (2009) 297(5):G950–7. doi: 10.1152/ajpgi.00253.2009
33. Thorens B. Glucose Transporters in the Regulation of Intestinal, Renal, and Liver Glucose Fluxes. *Am J Physiol* (1996) 270(4 Pt 1):G541–53. doi: 10.1152/ajpgi.1996.270.4.G541
34. Bueter M, Löwenstein C, Olbers T, Wang M, Cluny NL, Bloom SR, et al. Gastric Bypass Increases Energy Expenditure in Rats. *Gastroenterology* (2010) 138(5):1845–53. doi: 10.1053/j.gastro.2009.11.012
35. Hansen CF, Bueter M, Theis N, Lutz T, Paulsen S, Dalbøge LS, et al. Hypertrophy Dependent Doubling of L-Cells in Roux-En-Y Gastric Bypass Operated Rats. *PloS One* (2013) 8(6):e65696. doi: 10.1371/journal.pone.0065696
36. Chen C, Pore N, Behrooz A, Ismail-Beigi F, Maity A. Regulation of Glut1 mRNA by Hypoxia-Inducible Factor-1. Interaction Between H-Ras and Hypoxia. *J Biol Chem* (2001) 276(12):9519–25. doi: 10.1074/jbc.M010144200
37. Yang B, Kumoto T, Arima T, Nakamura M, Sanada Y, Kumrungsee T, et al. Transgenic Mice Specifically Expressing Amphiregulin in White Adipose Tissue Showed Less Adipose Tissue Mass. *Genes Cells* (2018) 23(3):136–45. doi: 10.1111/gtc.12558
38. Biton M, Haber AL, Rogel N, Burgin G, Beyaz S, Schnell A, et al. T Helper Cell Cytokines Modulate Intestinal Stem Cell Renewal and Differentiation. *Cell* (2018) 175(5):1307–20.e22. doi: 10.1016/j.cell.2018.10.008
39. Rojas OL, Pröbstel AK, Porfilio EA, Wang AA, Charabati M, Sun T, et al. Recirculating Intestinal IgA-Producing Cells Regulate Neuroinflammation *via* IL-10. *Cell* (2019) 176(3):610–24.e18. doi: 10.1016/j.cell.2018.11.035

Conflict of Interest: The authors declare that the research was conducted in the absence of any commercial or financial relationships that could be construed as a potential conflict of interest.

frontiers | Frontiers in Endocrinology

TYPE Original Research
PUBLISHED 20 September 2022
DOI 10.3389/fendo.2022.1013959

OPEN ACCESS

EDITED BY
Shaozhuang Liu,
Qilu Hospital, Shandong University, China

REVIEWED BY
Jiangfan Zhu,
Shanghai Tenth People's Hospital, Tongji University, China
Mala Dharmalingam,
Bangalore Endocrinology And Diabetes Research Center, India

*CORRESPONDENCE
Tao Jiang
jiangtao99@jlu.edu.cn

SPECIALTY SECTION
This article was submitted to Obesity, a section of the journal Frontiers in Endocrinology

RECEIVED 08 August 2022
ACCEPTED 29 August 2022
PUBLISHED 20 September 2022

CITATION
Wang L, Wang Z, Yu Y, Ren Z, Jia Y, Wang J, Li S and Jiang T (2022) Metabolomics analysis of stool in rats with type 2 diabetes mellitus after single-anastomosis duodenal–ileal bypass with sleeve gastrectomy. *Front. Endocrinol.* 13:1013959. doi: 10.3389/fendo.2022.1013959

Metabolomics analysis of stool in rats with type 2 diabetes mellitus after single-anastomosis duodenal–ileal bypass with sleeve gastrectomy

Lun Wang, Zeyu Wang, Yang Yu, Zhaoheng Ren, Yongheng Jia, Jinfa Wang, Shixing Li and Tao Jiang*

Department of Bariatric and Metabolic Surgery, China-Japan Union Hospital of Jilin University, Changchun City, China

Background: Single-anastomosis duodenal-ileal bypass with sleeve gastrectomy (SADI-S) is one of the most effective bariatric procedures in the treatment of type 2 diabetes mellitus (T2DM). However, the mechanisms by which SADI-S improves T2DM are not well-known.

Objective: To explore the effects of SADI-S on metabolites in the stool of rats with T2DM.

Methods: Twenty rats were fed on high-fat diet and administered with a low-dose (30mg/kg) of streptozotocin to establish T2DM models. The rats were then randomly assigned to the SADI-S group (n=10) and sham operation group (n=9). Stool samples were collected from all rats at 8 weeks after surgery and stored at -80 °C. Metabolomics analysis was performed to identify differential metabolites through ultra- performance liquid chromatography-mass spectrometry.

Results: At 8-week after surgery, rats of the SADI-S group showed significantly decreased fasting blood glucose, glucose tolerance test 2-hour, glycated haemoglobin, and body weight compared with those of the sham group. A total of 245 differential metabolites were identified between the two groups, among which 8 metabolites were detectable under both the positive ion model and negative ion model. Therefore, a total of 237 differential metabolites were identified in our study which were mainly involved in tryptophan metabolism; cysteine and methionine metabolism; phenylalanine metabolism; phenylalanine; tyrosine and tryptophan biosynthesis; arginine biosynthesis; alanine, aspartate and glutamate metabolism; Arginine and proline metabolism; glyoxylate and dicarboxylate metabolism; alpha-Linolenic acid metabolism; Linoleic acid metabolism; riboflavin metabolism; nicotinate and nicotinamide metabolism; pyrimidine metabolism; porphyrin and chlorophyll metabolism.

Conclusion: SADI-S significantly improved the glucose metabolism in T2DM rats. In addition, SADI-S significantly changed the composition of metabolites in T2DM rats which were involved in tryptophan metabolism pathway, linoleic acid metabolism pathway and so on. This may be the mechanism by which SADI-S improved T2DM.

KEYWORDS

single-anastomosis duodenal–ileal bypass with sleeve gastrectomy, type 2 diabetes mellitus, metabolomics, bariatric surgery, SADI-S, T2DM

Introduction

With the rapid development of social economy and changes in people's lifestyles, the number of people with diabetes has been increasing yearly. According to the latest report by the International Diabetes Federation, the global number of patients with diabetes (aged 20-79 years) was 537 million, and there were 6.7 million deaths due to diabetes in 2021. Moreover, the total health expenditure on diabetes managements was more than 966 billion US dollars in 2021 (1). Approximately, 90% of all patients with diabetes are of type 2 diabetes mellitus (T2DM). Traditional therapeutic strategies, including diet control, exercise, and the utilization of hypoglycemic agents, have not been successful in improving T2DM. Compared with traditional therapeutic strategies, bariatric surgery has been shown to effectively treat T2DM (2–4). For this reason, bariatric surgery is routinely applied in the treatment of T2DM patients.

As one of the currently used bariatric procedures, single-anastomosis duodenal–ileal bypass with sleeve gastrectomy (SADI-S) was first established in 2007 by Torres et al. based on the principle of biliopancreatic diversion with duodenal switch (BPD/DS) (5). SADI-S and BPD/DS are widely acknowledged as the most effective bariatric procedure for T2DM treatment (6–8). Compared with BPD/DS, SADI-S is preferred because it not only maintains similar effects in weight loss and remission of metabolic diseases of BPD/DS, but has a lower operative and malnutritional risk given its ability to reduce one anastomosis and lengthen the common channel of intestine.

Metabolomics is an effective method for quantifying the metabolites of an organism and determine association of metabolites with physiological and pathological changes (9, 10). It has been applied to explore the mechanisms underlying efficacy of bariatric surgery (11). However, the impacts of SADI-S on metabolites in T2DM are currently unknown.Therefore, this study was conducted to explore the effects of SADI-S on metabolites in stool of rats with T2DM, and determine whether changes in metabolites affect the surgery-induced T2DM remission.

Materials and methods

T2DM animal model and groups

Twenty male Wistar rats (8 weeks old) were purchased from the Vital River Laboratory Animal Technology Co., Ltd (Beijing, China). The rats were housed in individual cages under constant ambient temperature and humidity controlled to a 12-h day/night cycle. After 2-week adaptive feeding with an ordinary feed (containing 13.8% fat, 63.4% carbohydrate, and 22.8% protein), the rats were fed with a high-fat diet (containing 45.6% fat, 37.9% carbohydrate, and 16.5% protein) for 8 weeks to induce insulin resistance. 100 mg of streptozotocin (STZ) (Sigma, USA) were dissolved in 10 ml of ice-cold citrate buffer (0.1 mol/L, PH=4.5) to prepare a STZ solution with a concentration of 10 mg/mL. The rats were fasted for 12 h and intraperitoneally injected with STZ (30 mg/kg).

The T2DM rat model was considered successful if rats' random blood glucose was at least 16.7 mmol/L after 72 h from STZ injection. Based on this criterion, the T2DM rat model was successfully established in 19 rats randomly assigned to the SADI-S group (n =10) and sham operation group (n =9). Three weeks after STZ injection, SADI-S and sham operation were performed. All animal protocols were approved by the Animal Experiment Ethics Committee of First hospital of Jilin University, and all rats were cared according to the national guidelines for the care of animal of the People's Republic of China.

Preoperative preparation

The night before surgery, rats were placed in a cage with a raised wire platforms to avoid coprophagy and fasted for approximately 12 h. To prevent hyperglycemia which will increase the risk of surgery, blood glucose was regularly measured before surgery. An appropriate dose of insulin was injected subcutaneously if blood sugar was too high. The rats were anaesthetized through intraperitoneal injection of

pentobarbital sodium solution (10 mg/mL).

The abdominal fur of rat was shaved from the sternum to groin using an electric hair clipper. Part of the dorsal and femoral fur were also shaved for hydration and injection of antibacterial agents, respectively. Hydration was performed by subcutaneously injecting 10 mL 0.9% saline solution from multiple sites before beginning surgery.

Surgical procedures

The SADI-S surgery was performed according to the protocol described by Wang et al. [(12)]. Briefly, two thirds of the stomach along with the greater curvature were removed. Secondly, we transected the duodenum about 5 mm from the pylorus, and sutured the duodenal stump using a 6-0 PDS suture (Ethicon). Thirdly, we retrogradely measured a 40-cm small intestine from the ileocecal junction and marked it with sutures. Fourthly, we performed an end-to-side anastomosis of the proximal duodenum with the marked ileal at 40-cm away from ileocecal junction. Finally, the abdomen was closed using a 4-0 non-absorbable silk suture. Rats in the sham operation group received laparotomy only.

Postoperative care

At the end of surgery, the rats were immediately placed on a heating pad in a prone position until they fully regained consciousness. They were then subcutaneously injected with 30 mL parenteral nutrition solution (20ml 50%GLU+ 10ml calcium gluconate+70ml 0.9%NaCl solution+3U insulin) daily in the first 3 postoperative days (10 mL at 7:00am,10 mL at 3pm and 10 mL at 11pm). Meanwhile, ceftazidime (90 mg/kg) was administered intramuscularly to prevent infection in the first 3 postoperative days. In terms of feeding, we gradually decreased the amount of liquid diet and increased the amount of solid diet at day 4-6 postoperatively. Full solid diet was provided on day 7 postoperatively. The postoperative food intake per day was similar in both groups.

Intraperitoneal glucose tolerance test

The IPGTT was performed before surgery and at 8 weeks after surgery. After fasting for 12 h, rats were intraperitoneally injected with 50% glucose (2g/kg). Subsequently,we measured blood glucose *via* pricking the tail vein before injection and at 15,30, 60, 120, and 180 min after injecting glucose. Finally, a blood glucose-time curve was constructed and used to calculate the area under the curve (AUC) of IPGTT.

Histological assessment

Eight weeks after surgery, the pancreas and small intestine tissue samples of rats were fixed in paraformaldehyde solution, embedded, cut into 4 μm sections, stained with immunofluorescence double-labeling staining or hematoxylin and eosin (H&E),followed by observing the pathological changes in the pancreas and small intestine using a light microscope.

Non-targeted metabolomics analysis

Sample preparation

At 8 weeks after surgery, stool samples were collected by stimulating the rats' anus with a sterile pincer. The samples were immediately placed in liquid nitrogen and stored at -80°C until use. To identify metabolites by liquid chromatography-mass spectrometry, stool samples were processed as follows: a) Stool samples were thawed on ice; b) 50 mg of stool samples and 800 μl of 80% methanol were mixed in a labeled 1.5-ml microcentrifuge tube; c) the specimens were ground at 65 HZ for 90 s, thoroughly mixed on a vortex mixer, sonicated for 30 min at 4°C, allowed to stand for 1 h at -40°C, vortexed for 30 s, allowed to stand for 30 min at 4°C, and centrifuged at 12,000 rpm at 4°C for 15 min. Next, 200 uL of the supernatant and 5 uL of the internal standard (0.14 mg/mL dichlorophenylalanine) were added into a labeled 1.5-ml microcentrifuge tube, mixed and transferred into autosampler vial.

Liquid chromatography-mass spectrometry conditions

The stool samples were subjected to LC-MS (Waters, UPLC; Thermo, Q Exactive) to separate metabolites. The chromatographic separation conditions were set as follows: Column temperature: 40°C; Flow rate: 0.3 mL/min; Mobile phase A: water +0.05% formic acid; Mobile phase B: acetonitrile; Injection volume: 5 ul; Automatic injector temperature: 4°C. The following elution program was used: 0.00-1.00 min, 0.3 mL/min, 95% A,5% B;1.00-13.50 min, 0.3 mL/min, 5% A, 95% B; 13.50-16.00 min, 0.3 mL/min, 95% A,5% B. The conditions of electrospray ionization (ESI) source were set as follows: ESI+: Heater Temp 300°C; Sheath Gas Flow rate, 45 arb; Aux Gas Flow Rate, 15 arb; Sweep Gas Flow Rate, 1arb; spray voltage, 3.0KV; Capillary Temp, 350°C; S-Lens RF Level, 30%. ESI-: Heater Temp 300°C, Sheath Gas Flow rate,45arb; Aux Gas Flow Rate, 15arb; Sweep Gas Flow Rate, 1arb; spray voltage, 3.2KV; Capillary Temp, 350°C; S-Lens RF Level, 60%.

Multivariate data processing and analysis

The R package XCMS (version 3.3.2) was used to process the raw data in terms of peak identification, filtration, and alignment. The MS2 database was used to identify the differential metabolites. The quality of data was determined based on the relative standard deviation (RSD). The data was considered to have a high quality when the proportion of characteristic peaks with RSD<30% was at least 70%. The data

were analyzed using multivariate statistical analyses, including Principal Component Analysis (PCA) and Orthogonal Projections to Latent Structures Discriminant Analysis (OPLS-DA). Clusters and differences between SADI-S group and sham operation group were determined by PCA and OPLS-DA. The R^2Y and Q^2 values were used to evaluate the stability and predictability of each model. Differential metabolites were defined as those metabolites with $P \leq 0.05$ and variable importance in the projection (VIP)≥1. A Permutations Plot was constructed to evaluate over-fitting in the PLS-DA model.

Statistical analysis

Statistical analysis was performed using SPSS 22.0 software. All data are presented as mean ± standard deviation, and differences between groups were compared using wilcoxon rank sum test. Differences were considered statistically significant at a P value less than 0.05.

Results

Surgical outcomes

Five T2DM rats died during the study. In the SADI-S group, four rats died after operation, 3 due to bleeding and 1 rat because of anastomotic leakage. Finally, 6 rats survived to 8 weeks after SADI-S surgery until they were sacrificed. In the sham operation group, one rat died due to incision rupture at day 12 postoperatively and 8 rats survived to 8 weeks after surgery until they were sacrificed.

Changes in body weight and glucose metabolism

The changes in body weight are illustrated in Figure 1A. Notably, the SADI-S surgery resulted in a significant decrease in body weight ($P<0.05$). The body weight in the sham operation group also showed decreasing trend. However it was observed that the decrease in body weight at each postoperative follow-up point was significantly higher in the SADI-S group compared with the sham operation group ($P<0.05$).

The changes in area under curve (AUC) of blood glucose during IPGTT and fasting blood glucose (FBG) before and after surgery are illustrated in Figures 1B, C. The levels of FBG and AUC values for glucose were significantly decreased after SADI-S surgery compared with the preoperative levels. In contrast, the FBG and AUC values for glucose were increased in the sham operation group. At 8 weeks after surgery, the level of glycated hemoglobin (HBA1c) in the SADI-S group was significantly lower compared with level in the sham operation group (Figure 1D).

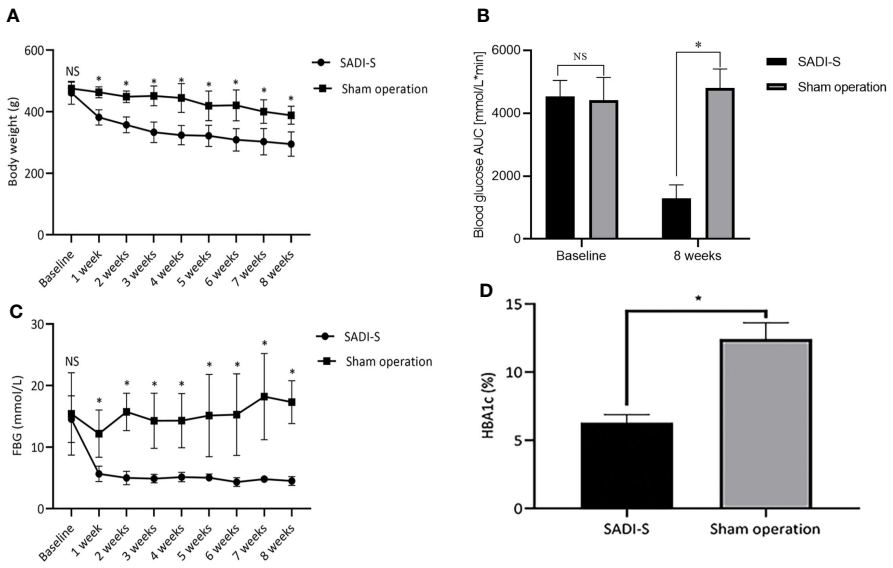

FIGURE 1
Changes in body weight **(A)**, changes in blood glucose AUC during IPGTT before and after surgery **(B)** and FBG **(C)** before and after surgery. Comparison of the HBA1c level at 8 weeks after surgery between the two groups **(D)**. All values are expressed as Mean ± SD. NS indicates no significant difference between the SADI-S group and sham operation group. * represents a significant difference between the SADI-S group and sham operation group (P< 0.05).

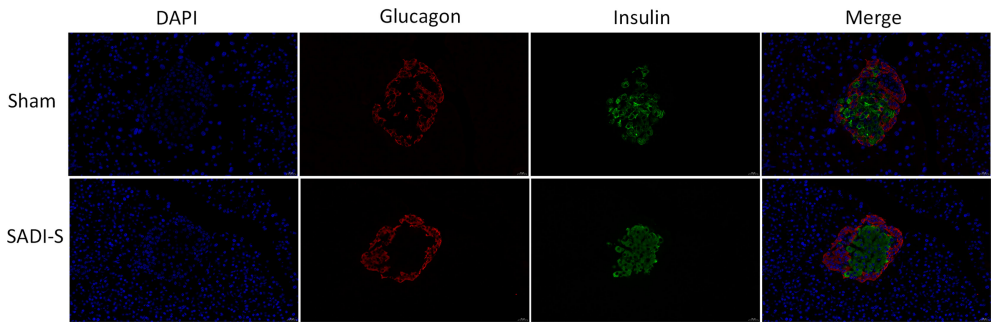

FIGURE 2
Immunofluorescence double-labeling staining images. Morphological and histological evaluation of pancreas tissues between the SADI-S group and the sham operation group. Red represents pancreatic islet α cells, green represents pancreatic islet β cells, and blue represents cell nucleus.

Histological assessment of pancreas and small intestine

The immunofluorescence double-labeling staining images of the pancreas tissue are shown in Figure 2. Significant pancreatic islet β cells damage accompanied by marked degeneration of vacuolation were observed in the sham group compared with the SADI-S group. In addition, the distribution of pancreatic islet β cells and α cells disorderly in the sham group. In contrast, the distribution pattern of β cells and morphology in the SADI-S group was uniform and there was no significant vacuolar degeneration.

The hematoxylin and eosin (H&E) staining images of the small intestine are shown in Figure 3. In the SADI-S group, the structure of the small intestinal mucosa was normal, with tall and continuous villi arranged neatly, whereas the villi of small intestine in the sham operation group,especially in the ileal, was swollen, short, thick and disorderly, some villi were necrotic, shed or disappeared.

Metabolomics analysis

Multivariate statistical analysis

The PCA, an unsupervised analysis method, was used to provide a comprehensive view of stool samples. The parameter R^2X and percent of relative standard deviation (RSD)<30% are often used to reflect the stability of the LC-MS system and the reliability of data. As shown in Figures 4A, B, the R^2X>0.5 was obtained both in the positive ion mode and the negative ion mode, and percent of RSD<30% exceeded 70% in both modes. These results indicated that the LC-MS system was highly stable for metabolomics analysis and the data were reliable. Besides, analysis of the results revealed that the metabolic profile of the SADI-S group was different from that of the sham-operated group, indicating that the metabolites in stool of T2DM rats were significantly changed after SADI-S.

OPLS-DA, a supervised analysis method, was performed to analyze differences between the SADI-S group and sham operation group. As shown in Figure 5A, the OPLS-DA score plot revealed that the metabolic profile of T2DM rats treated with SADI-S was significantly different from that of sham operation group both in the positive ion mode and in the negative ion mode, indicating that SADI-S significantly altered the metabolic profile of T2DM rats. The two classification parameters, R^2Y and Q^2, were 0.998 and 0.966 in the positive mode, 0.999 and 0.968 in the negative mode, respectively. The

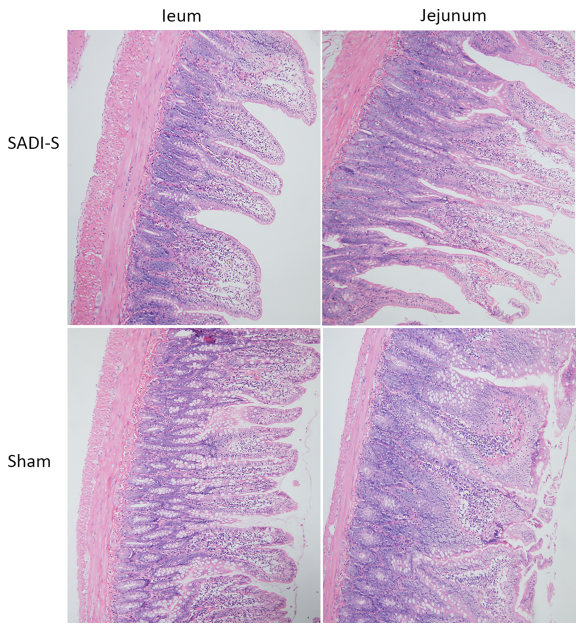

FIGURE 3
Hematoxylin and eosin (H&E) staining photographs. Morphological and histological evaluation of ileum and jejunum between the SADI-S group and the sham operation group (200×).

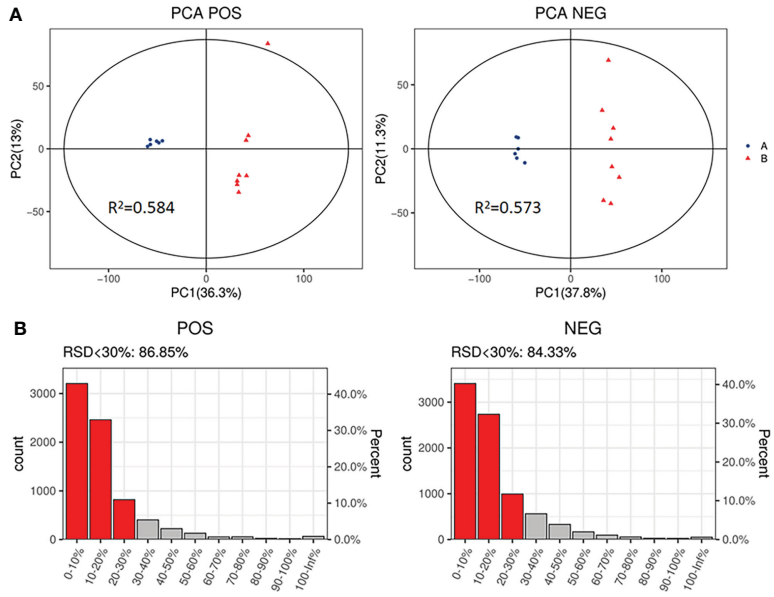

FIGURE 4
PCA score plot of SADI-S group and sham operation group in the positive ion mode and in the negative ion mode **(A)**; quality assurance in the positive ion mode and in the negative ion mode **(B)**. A=SADI-S group, B=sham operation group.

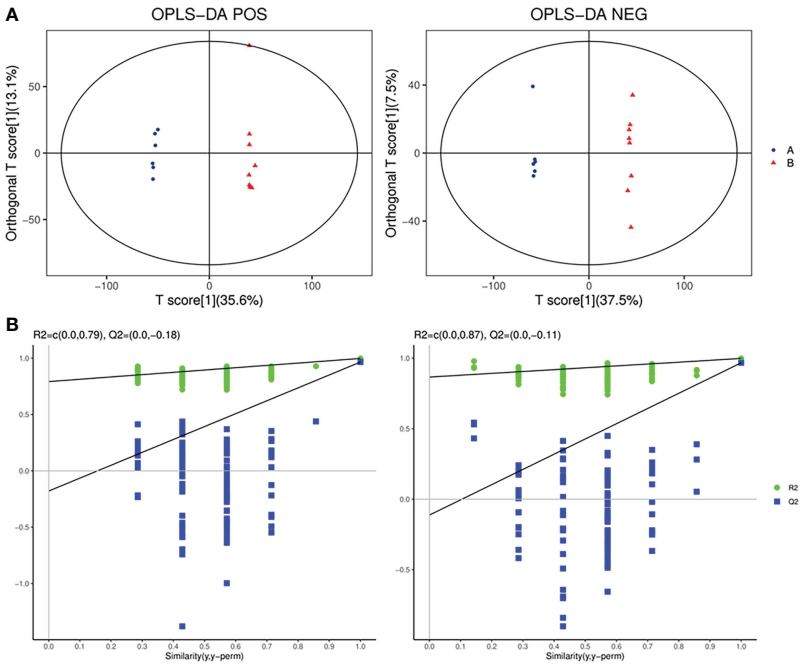

FIGURE 5
The plot of OPLS-DA score for SADI-S group and sham operation group in the positive ion mode and in the negative ion mode **(A)**; permutations plot in the positive ion mode and in the negative ion mode **(B)**. A=SADI-S group, B=sham operation group.

R^2Y and Q^2 were >0.5, suggesting that the OPLS-DA model had good stability and predictability. Analysis of the Permutations Plot shown in Figure 5B indicated that the intersection between the regression line of Q^2 point and the ordinate was negative value, implying that there was no over-fitting in the OPLS-DA model.

Identification of differential metabolites

According to the OPLS-DA model, VIP was generated to illustrate the importance of variables in explaining the X dataset and the associated Y dataset. The screening conditions of differential metabolites were as follows: VIP≥1 and p-value ≤ 0.05. The data shown in the Supplemental Table 1 indicated that 245 differential metabolites were identified, among which 81 metabolites were obtained under the positive ion model and 164 metabolites were obtained under the negative ion model. Eight of these metabolites were detectable in both modes. Therefore, a total of 237 differential metabolites were identified between the two groups. Notably, 181 metabolites were significantly higher in the SADI-S group than in the sham operation group. Moreover, 64 metabolites were significantly lower in the SADI-S group than in the sham operation group. According to the previous literature, some metabolites that may be associated with the T2DM such as branched-chain amino acids (valine), aromatic amino acid (phenylalanine), bile acid (cholic acid, lithocholic acid and b-muricholic acid), short-chain fatty acid (isobutyric acid), phospholipid lysoPE(17:0), lysoPE (20:3), and lysoPS (16:0), were also observed to have a significant changes in our study.

To explore the direct relationship between the groups, we constructed a heatmap based on the abundance value of each metabolite. The Supplemental Figure 1 and Figure 2 show the overall changes in the common features and the tendency of variation in metabolite levels in both groups. In the heatmap, the positions of metabolites with similar changes in abundance were closer and the abundance of metabolites in T2DM rats treated with SADI-S was significantly difference from that of the sham group.

Pathway analysis of differential metabolites

Kyoto Encyclopedia of Genes and Genomes (KEGG) analysis was performed to screen differential metabolic pathways based on the following conditions: pathway impact >0.1 and $P < 0.05$ (13). As shown in Figures 6A, B, the following 14 metabolic pathways were identified in SADI-S group: tryptophan metabolism; cysteine and methionine metabolism; phenylalanine metabolism; phenylalanine; tyrosine and tryptophan biosynthesis; arginine biosynthesis; alanine, aspartate and glutamate metabolism; Arginine and proline metabolism; glyoxylate and dicarboxylate metabolism; alpha-Linolenic acid metabolism; Linoleic acid metabolism; riboflavin metabolism; nicotinate and nicotinamide metabolism; pyrimidine metabolism; porphyrin and chlorophyll metabolism.

Discussion

To the best of our knowledge, the current study was the first to explore the effects of SADI-S on metabolites of stool in T2DM rats. The results of the present study showed that SADI-S significantly lowered the blood glucose level and altered the level of 245 metabolites in T2DM rats. This was evaluated using a low-dose STZ and HFD. Among the 245 metabolites, 16 of them were associated with the remission of T2DM after SADI-S.

Branched-chain amino acids (BCAAs) are correlated with the occurrence of T2DM and are significantly elevated in T2DM (14–17). Three potential mechanisms for how BCAAs lead to the occurrence of T2DM are: First, increased levels of BCAAs can result in the accumulation of toxic metabolites, which in turn

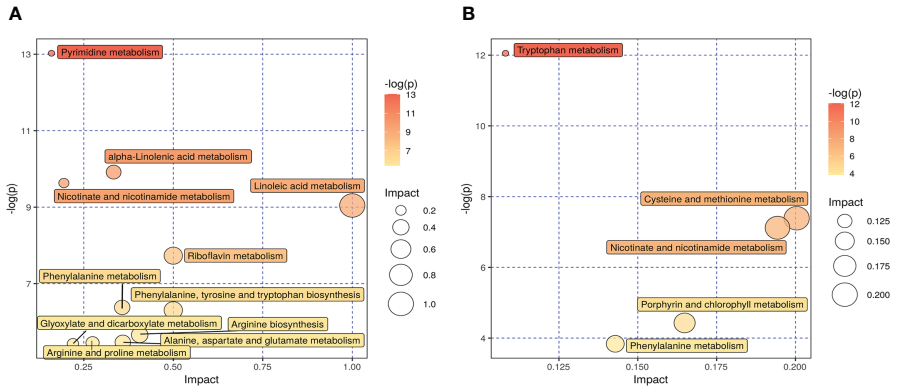

FIGURE 6
The effect of SADI-S on metabolic pathway in the negative ion mode **(A)** and in the positive ion mode **(B)**. The bigger the circle, the more significant is the enrichment. The darker the yellow, the smaller the P value.

causes mitochondrial dysfunction and a decrease in secretion of insulin in pancreatic beta cells (18, 19); second, perturbations of BCAAs can induce insulin resistance through the mTOR signaling pathway (20); third, increased levels of BCAAs can activate the rapamycin pathway, which then disturb the action of insulin and promote the degradation of insulin receptor substrates (21, 22). A previous study found that the level of valine was significantly higher in patients with T2DM as compared with healthy individuals (23). Several studies have reported that bariatric surgery can cause a significant decrease in levels of BCAAs in T2DM (24, 25). Consistent with these studies, we found that the level of Valine, a type of BCAAs, was significantly reduced in T2DM after SADI-S.

Phenylalanine is an aromatic amino acid which is involved in sugar metabolism after it is oxidized to tyrosine by phenylalanine hydroxylase (26). Previous studies have shown that the level of phenylalanine is significantly decreased in patients with diabetes (27, 28). In the current study, SADI-S caused a significant elevation in the level of phenylalanine and also remission of T2DM.

Tryptophan and its derivates, especially those from the kynurenine and serotonin pathways, are also correlated with glucose metabolism (29–32). Kynurenic acid is a metabolite of tryptophan, derived from the kynurenine pathway and is closely related with the occurrence of T2DM (33–35). Previous studies have shown that bariatric surgery causes a decrease in level of kynurenic acid accompanied with diabetes remission (36, 37). Xanthurenic acid is a metabolite of tryptophan which has been found to be conductive to development of diabetes through chelating complexes with insulin and hence inducing pathological apoptosis of pancreatic β cells (38). 5-hydroxytryptophan acid is another a kind of tryptophan derivative which forms hydrogen bonds with the key residues of the PPAR-r protein at its indole ring and carboxyl group. A separate study has shown that 5-hydroxytryptophan acid can be used as a lead compound to develop the PPAR-r agonists (39). In the present study, SADI-S showed a significant therapeutic effect in T2DM comparable to the effects noted in the previous studies. In addition, it has been shown that the levels of above-mentioned tryptophan derivatives are significantly increased after the SADI-S surgery. However, there is need for further study to evaluate the reasons for the observed difference.

Some studies have shown that low levels of glutamate and glutamine are associated with T2DM (34, 40). In the current study, it was evident that the levels of glutamate and glutamine were significantly increased after SADI-S, which were in consonance with the findings of the previous studies. It has also been found that the level of proline is decreased in patients with diabetes (18). Results of the current study showed that the level of proline was significantly lower in the sham operation group as compared with the SADI-S group. Elsewhere, it has been evident that the level of alanine is elevated after RYGB (41). Similarly, an elevated alanine levels after SADI-S was also found in the present study.

Hippuric acid is synthesized from benzoic acid and glycine in liver. An elevated level of glycine causes an increase in level of hippuric acid and a decrease in level of the branched-chain amino acid, which contribute to the restoration of the mitochondrial function. A previous study has shown that increased level of hippuric acid is accompanied by a decrease in the levels of branched-chain amino acids after Roux-en-Y gastric bypass (41). The present study also showed that the remission of diabetes after SADI-S was accompanied by an elevation in the level of hippuric acid and a decline in the level of branched-chain amino acid.

The alterations in the level of bile acid influences glucose metabolism by acting as the farnesoid X receptors (FXRs). Cholic acid, lithocholic acid, deoxycholic acid, and taurochenodeoxycholic acid are FXR agonists (42). The increased levels of the bile acids activate FXRs and then downregulate the level of blood glucose. Our results showed that the levels of cholic acid and lithocholic acid were significantly increased after SADI-S, while as the levels of deoxycholic acid and taurochenodeoxycholic acid were significantly declined.β-Muricholic acid is a FXRs antagonist (42) and an increase in its levels inhibits FXR and then increases the levels of blood sugar. Our results showed that the levels of β-Muricholic acid were significantly decreased after SADI-S.

Isobutyric acid is a short-chain fatty acid which primarily originate from the degradation of leucine, isoleucine, valine, and proline in gut bacteria (43). Previous study has shown that an elevated level of Isobutyric acid can improve diabetes (44). In agreement with this, the level of isobutyric acid, which is responsible for the diabetes remission, was significantly increased after SADI-S.

The metabolic disorder of phospholipid contributes to development of diabetes (45). It has been shown that LysoPC, lysoPE, and lysoPS are associated with diabetes-related inflammatory stress (18, 45, 46). Therefore, the levels of lysoPC, lysoPE, and lysoPS significantly decreases after diabetes remission. However, the results obtained in the present study showed that the levels of LysoPE (17:0), LysoPE (20:3), and LysoPS (16:0) decreased, whereas the levels of LysoPE (18:2), LysoPE (18:3), LysoPE (17:1) and LysoPC (14:0) were elevated. This was in agreement with the findings of the study by Marta Ugarte et al. (18).

It has been previously found alterations of urea cycle intermediates and urea cycle enzymes in diabetic rats induced by STZ and HFD (18). Ornithine is an intermediate of urea cycle which is synthesized from L-arginine in liver, and its levels are reduced in patients with diabetes (47). It promotes the release of growth hormone from the pituitary gland which plays an

important role in energy metabolism (48, 49). Therefore, the current study shows that the level of ornithine is significantly increased after SADI-S.

Although this is the first study to explore the effects of SADI-S on metabolites of stool in T2DM rats, the study also had some limitations. First,we didn't set other bariatric surgeries as control group of SADI-S surgery,so it is unclear whether other bariatric surgeries will also result in similar changes in fecal metabolomics as SADI-S surgery. Second,metabolites were only detected in feces of T2DM rats rather than serum metabolites.Third, the effects of SADI-S was not evaluated on metabolites in patients with T2DM. Therefore, there is need for further studies, especially clinical studies to be performed on the effects of SADI-S on serum metabolites in T2DM.

Conclusion

The current study shows that SADI-S can improve the disease state of T2DM rats. Mechanistically, the improvement of T2DM caused by SADI-S may be associated with the changes of pathways such as tryptophan metabolism pathway, linoleic acid metabolism pathway and so on.

Data availability statement

The original contributions presented in the study are included in the article/Supplementary Material. Further inquiries can be directed to the corresponding author.

Ethics statement

The animal study was reviewed and approved by The Animal Experiment Ethics Committee of First hospital of Jilin University.

Author contributions

LW: Conceptualization, Methodology, Software, Data Curation, Formal Analysis, Writing-Original Draft. ZW, YY, ZR, YJ, JW, and SL: Data Curation, Formal Analysis; TJ: Conceptualization, Funding Acquisition, Resources, Supervision, Writing - Review & Editing. All authors contributed to the article and approved the submitted version.

Funding

The special health research talents project of Jilin province (2020SCZ04).

Conflict of interest

The authors declare that the research was conducted in the absence of any commercial or financial relationships that could be construed as a potential conflict of interest.

Publisher's note

Supplementary material

The Supplementary Material for this article can be found online at: https://www.frontiersin.org/articles/10.3389/fendo.2022.1013959/full#supplementary-material

References

1. International Diabetes Federation. *IDF diabetes atlas. 10th edn*. Brussels, Belgium: International Diabetes Federation (2021). Available at: https://diabetesatlas.org/atlas/tenth-edition/.

2. Schauer PR, Kashyap SR, Wolski K, Brethauer SA, Kirwan JP, Pothier CE, et al. Bariatric surgery versus intensive medical therapy in obese patients with diabetes. *N Engl J Med* (2012) 366(17):1567–76. doi: 10.1056/NEJMoa1200225

3. Kashyap SR, Bhatt DL, Wolski K, Watanabe RM, Abdul-Ghani M, Abood B, et al. Metabolic effects of bariatric surgery in patients with moderate obesity and type 2 diabetes: Analysis of a randomized control trial comparing surgery with intensive medical treatment. *Diabetes Care* (2013) 36(8):2175–82. doi: 10.2337/dc12-1596

4. Mingrone G, Panunzi S, De Gaetano A, Guidone C, Iaconelli A, Capristo E, et al. Metabolic surgery versus conventional medical therapy in patients with type 2 diabetes: 10-year follow-up of an open-label, single-centre, randomised controlled trial. *Lancet* (2021) 397(10271):293–304. doi: 10.1016/S0140-6736(20)32649-0

5. Sánchez-Pernaute A, Rubio Herrera MA, Pérez-Aguirre E, García Pérez JC, Cabrerizo L, Díez Valladares L, et al. Proximal duodenal-ileal end-to-side bypass with sleeve gastrectomy: Proposed technique. *Obes Surg* (2007) 17(12):1614–8. doi: 10.1007/s11695-007-9287-8

6. Buchwald H, Estok R, Fahrbach K, Banel D, Jensen MD, Pories WJ, et al. Weight and type 2 diabetes after bariatric surgery: Systematic review and meta-analysis. *Am J Med* (2009) 122(3)248–65. doi: 10.1016/j.amjmed.2008.09.041

7. Skogar ML, Sundbom M. Weight loss and effect on co-morbidities in the long-term after duodenal switch and gastric bypass: A population-based cohort study. *Surg For Obes Related Dis Off J Am Soc For Bariatric Surg* (2020) 16(1):17–23. doi: 10.1016/j.soard.2019.09.077

8. Finno P, Osorio J, García-Ruiz-de-Gordejuela A, Casajoana A, Sorribas M, Admella V, et al. Single versus double-anastomosis duodenal switch: Single-site comparative cohort study in 440 consecutive patients. *Obes Surg* (2020) 30 (9):3309–16. doi: 10.1007/s11695-020-04566-5

9. Johnson CH, Ivanisevic J, Siuzdak G. Metabolomics: Beyond biomarkers and towards mechanisms. *Nat Rev Mol Cell Biol* (2016) 17(7):451–9. doi: 10.1038/nrm.2016.25

10. Patti GJ, Yanes O, Siuzdak G. Innovation: Metabolomics: The apogee of the omics trilogy. *Nat Rev Mol Cell Biol* (2012) 13(4):263–9. doi: 10.1038/nrm3314

11. Ha J, Kwon Y, Park S. Metabolomics in bariatric surgery: Towards identification of mechanisms and biomarkers of metabolic outcomes. *Obes Surg* (2021) 31(10):4564–74. doi: 10.1007/s11695-021-05566-9

12. Wang T, Shen Y, Qiao Z, Wang Y, Zhang P, Yu B. Comparison of diabetes remission and micronutrient deficiency in a mildly obese diabetic rat model undergoing SADI-s versus RYGB. *Obes Surg* (2019) 29(4):1174–84. doi: 10.1007/s11695-018-03630-5

13. Yu Y, Lu Q, Chen F, Wang S, Niu C, Liao J, et al. Serum untargeted metabolomics analysis of the mechanisms of evodiamine on type 2 diabetes mellitus model rats. *Food Funct* (2022) 13(12):6623–35. doi: 10.1039/d1fo04396j

14. Mihalik SJ, Michaliszyn SF, de las Heras J, Bacha F, Lee S, Chace DH, et al. Metabolomic profiling of fatty acid and amino acid metabolism in youth with obesity and type 2 diabetes: evidence for enhanced mitochondrial oxidation. *Diabetes Care* (2012) 35(3):605–11. doi: 10.2337/DC11-1577

15. Wang TJ, Larson MG, Vasan RS, Cheng S, Rhee EP, McCabe E, et al. Metabolite profiles and the risk of developing diabetes. *Nat Med* (2011) 17(4):448–53. doi: 10.1038/nm.2307

16. Zheng Y, Li Y, Qi Q, Hruby A, Manson JE, Willett WC, et al. Cumulative consumption of branched-chain amino acids and incidence of type 2 diabetes. *Int J Epidemiol* (2016) 45(5):1482–92. doi: 10.1093/ije/dyw143

17. Wang Q, Holmes MV, Davey Smith G, Ala-Korpela M. Genetic support for a causal role of insulin resistance on circulating branched-chain amino acids and inflammation. *Diabetes Care* (2017) 40(12):1779–86. doi: 10.2337/dc17-1642

18. Ugarte M, Brown M, Hollywood KA, Cooper GJ, Bishop PN, Dunn WB. Metabolomic analysis of rat serum in streptozotocin-induced diabetes and after treatment with oral triethylenetetramine (TETA). *Genome Med* (2012) 4(4):35. doi: 10.1186/gm334

19. Zhao M, Zhang H, Wang J, Shan D, Xu Q. Serum metabolomics analysis of the intervention effect of whole grain oats on insulin resistance induced by high-fat diet in rats. *Food Res Int (Ottawa Ont)* (2020) 135:109297. doi: 10.1016/j.foodres.2020.109297

20. Yan Y, Sha Y, Huang X, Yuan W, Wu F, Hong J, et al. Roux-en-Y gastric bypass improves metabolic conditions in association with increased serum bile acids level and hepatic farnesoid X receptor expression in a T2DM rat model. *Obes Surg* (2019) 29(9):2912–22. doi: 10.1007/s11695-019-03918-0

21. Arany Z, Neinast M. Branched chain amino acids in metabolic disease. *Curr Diabetes Rep* (2018) 18(10):76. doi: 10.1007/s11892-018-1048-7

22. Newgard CB. Interplay between lipids and branched-chain amino acids in development of insulin resistance. *Cell Metab* (2012) 15(5):606–14. doi: 10.1016/j.cmet.2012.01.024

23. Xu F, Tavintharan S, Sum CF, Woon K, Lim SC, Ong CN. Metabolic signature shift in type 2 diabetes mellitus revealed by mass spectrometry-based metabolomics. *J Clin Endocrinol Metab* (2013) 98(6):E1060–E5. doi: 10.1210/jc.2012-4132

24. Arora T, Velagapudi V, Pournaras DJ, Welbourn R, le Roux CW, Orešič M, et al. Roux-en-Y gastric bypass surgery induces early plasma metabolomic and lipidomic alterations in humans associated with diabetes remission. *PloS One* (2015) 10(5):e0126401. doi: 10.1371/journal.pone.0126401

25. Luo P, Yu H, Zhao X, Bao Y, Hong CS, Zhang P, et al. Metabolomics study of roux-en-Y gastric bypass surgery (RYGB) to treat type 2 diabetes patients based on ultraperformance liquid chromatography-mass spectrometry. *J Proteome Res* (2016) 15(4):1288–99. doi: 10.1021/acs.jproteome.6b00022

26. Pan L, Li Z, Wang Y, Zhang B, Liu G, Liu J. Network pharmacology and metabolomics study on the intervention of traditional Chinese medicine huanglian decoction in rats with type 2 diabetes mellitus. *J Ethnopharmacology* (2020) 258:112842. doi: 10.1016/j.jep.2020.112842

27. Huo T, Xiong Z, Lu X, Cai S. Metabonomic study of biochemical changes in urinary of type 2 diabetes mellitus patients after the treatment of sulfonylurea antidiabetic drugs based on ultra-performance liquid chromatography/mass spectrometry. *BioMed Chromatogr* (2015) 29(1):115–22. doi: 10.1002/bmc.3247

28. Yang Z, Dan W, Li Y, Zhou X, Liu T, Shi C, et al. Untargeted metabolomics analysis of the anti-diabetic effect of red ginseng extract in type 2 diabetes mellitus rats based on UHPLC-MS/MS. *Biomedicine Pharmacotherapy = Biomedecine Pharmacotherapie* (2022) 146:112495. doi: 10.1016/j.biopha.2021.112495

29. Le Floc'h N, Otten W, Merlot E. Tryptophan metabolism, from nutrition to potential therapeutic applications. *Amino Acids* (2011) 41(5):1195–205. doi: 10.1007/s00726-010-0752-7

30. Oxenkrug G. Insulin resistance and dysregulation of tryptophan-kynurenine and kynurenine-nicotinamide adenine dinucleotide metabolic pathways. *Mol Neurobiol* (2013) 48(2):294–301. doi: 10.1007/s12035-013-8497-4

31. Pedersen ER, Tuseth N, Eussen SJPM, Ueland PM, Strand E, Svingen GFT, et al. Associations of plasma kynurenines with risk of acute myocardial infarction in patients with stable angina pectoris. *Arterioscler Thromb Vasc Biol* (2015) 35 (2):455–62. doi: 10.1161/ATVBAHA.114.304674

32. Yabut JM, Crane JD, Green AE, Keating DJ, Khan WI, Steinberg GR. Emerging roles for serotonin in regulating metabolism: New implications for an ancient molecule. *Endocr Rev* (2019) 40(4):1092–107. doi: 10.1210/er.2018-00283

33. Kwon Y, Jang M, Lee Y, Ha J, Park S. Metabolomic analysis of the improvements in insulin secretion and resistance after sleeve gastrectomy: Implications of the novel biomarkers. *Obes Surg* (2021) 31(1):43–52. doi: 10.1007/s11695-020-04925-2

34. Floegel A, Stefan N, Yu Z, Mühlenbruch K, Drogan D, Joost H-G, et al. Identification of serum metabolites associated with risk of type 2 diabetes using a targeted metabolomic approach. *Diabetes* (2013) 62(2):639–48. doi: 10.2337/db12-0495

35. Roberts LD, Koulman A, Griffin JL. Towards metabolic biomarkers of insulin resistance and type 2 diabetes: Progress from the metabolome. *Lancet Diabetes Endocrinol* (2014) 2(1):65–75. doi: 10.1016/S2213-8587(13)70143-8

36. Favennec M, Hennart B, Verbanck M, Pigeyre M, Caiazzo R, Raverdy V, et al. Post-bariatric surgery changes in quinolinic and xanthurenic acid concentrations are associated with glucose homeostasis. *PloS One* (2016) 11(6): e0158051. doi: 10.1371/journal.pone.0158051

37. Christensen MHE, Fadnes DJ, Røst TH, Pedersen ER, Andersen JR, Våge V, et al. Inflammatory markers, the tryptophan-kynurenine pathway, and vitamin b status after bariatric surgery. *PloS One* (2018) 13(2):e0192169. doi: 10.1371/journal.pone.0192169

38. Krause D, Suh H-S, Tarassishin L, Cui QL, Durafourt BA, Choi N, et al. The tryptophan metabolite 3-hydroxyanthranilic acid plays anti-inflammatory and neuroprotective roles during inflammation: Role of hemeoxygenase-1. *Am J Pathol* (2011) 179(3):1360–72. doi: 10.1016/j.ajpath.2011.05.048

39. Chen K-C, Chen CY-C. *In silico* identification of potent PPAR-γ agonists from traditional Chinese medicine: A bioactivity prediction, virtual screening, and molecular dynamics study. *Evid Based Complement Alternat Med* (2014) 2014:192452. doi: 10.1155/2014/192452

40. Guasch-Ferré M, Hruby A, Toledo E, Clish CB, Martínez-González MA, Salas-Salvadó J, et al. Metabolomics in prediabetes and diabetes: A systematic review and meta-analysis. *Diabetes Care* (2016) 39(5):833–46. doi: 10.2337/dc15-2251

41. Huang W, Zhong A, Xu H, Xu C, Wang A, Wang F, et al. Metabolomics analysis on obesity-related obstructive sleep apnea after weight loss management: A preliminary study. *Front Endocrinol (Lausanne)* (2021) 12:761547. doi: 10.3389/fendo.2021.761547

42. Hu X, Bonde Y, Eggertsen G, Rudling M. Muricholic bile acids are potent regulators of bile acid synthesis *via* a positive feedback mechanism. *J Intern Med* (2014) 275(1):27–38. doi: 10.1111/joim.12140

43. Rasmussen HS, Holtug K, Mortensen PB. Degradation of amino acids to short-chain fatty acids in humans. an *in vitro* study. *Scand J Gastroenterol* (1988) 23 (2):178–82. doi: 10.3109/00365528809103964

44. Roy R, Nguyen-Ngo C, Lappas M. Short-chain fatty acids as novel therapeutics for gestational diabetes. *J Mol Endocrinol* (2020) 65(2):21–34. doi: 10.1530/JME-20-0094

45. Hu N, Zhang Q, Wang H, Yang X, Jiang Y, Chen R, et al. Comparative evaluation of the effect of metformin and insulin on gut microbiota and metabolome profiles of type 2 diabetic rats induced by the combination of streptozotocin and high-fat diet. *Front Pharmacol* (2021) 12:794103. doi: 10.3389/fphar.2021.794103

46. Gu Y, Zhang Y, Shi X, Li X, Hong J, Chen J, et al. Effect of traditional Chinese medicine berberine on type 2 diabetes based on comprehensive metabonomics. *Talanta* (2010) 81(3):766–72. doi: 10.1016/j.talanta.2010.01.015

47. Cao Y-F, Li J, Zhang Z, Liu J, Sun X-Y, Feng X-F, et al. Plasma levels of amino acids related to urea cycle and risk of type 2 diabetes mellitus in Chinese adults. *Front In Endocrinol* (2019) 10:50. doi: 10.3389/fendo.2019.00050

48. Evain-Brion D, Donnadieu M, Roger M, Job JC. Simultaneous study of somatotrophic and corticotrophic pituitary secretions during ornithine infusion test. *Clin Endocrinol (Oxf)* (1982) 17(2):119–22. doi: 10.1111/j.1365-2265.1982.tb01571.x

49. Sugino T, Shirai T, Kajimoto Y, Kajimoto O. L-ornithine supplementation attenuates physical fatigue in healthy volunteers by modulating lipid and amino acid metabolism. *Nutr Res* (2008) 28(11):738–43. doi: 10.1016/j.nutres.2008.08.008

frontiers | Frontiers in Endocrinology

TYPE Correction
PUBLISHED 28 March 2023
DOI 10.3389/fendo.2023.1128339

OPEN ACCESS

EDITED BY
Shaozhuang Liu,
Qilu Hospital, Shandong University, China

REVIEWED BY
Jiangfan Zhu,
Tongji University, China

*CORRESPONDENCE
Tao Jiang
jiangtao99@jlu.edu.cn

SPECIALTY SECTION
This article was submitted to Obesity, a section of the journal Frontiers in Endocrinology

RECEIVED 20 December 2022
ACCEPTED 01 March 2023
PUBLISHED 28 March 2023

CITATION
Wang L, Wang Z, Yu Y, Ren Z, Jia Y, Wang J, Li S and Jiang T (2023) Metabolomics analysis of stool in rats with type 2 diabetes mellitus after single-anastomosis duodenal–ileal bypass with sleeve gastrectomy. *Front. Endocrinol.* 14:1128339. doi: 10.3389/fendo.2023.1128339

Metabolomics analysis of stool in rats with type 2 diabetes mellitus after single-anastomosis duodenal–ileal bypass with sleeve gastrectomy

Lun Wang, Zeyu Wang, Yang Yu, Zhaoheng Ren, Yongheng Jia, Jinfa Wang, Shixing Li and Tao Jiang*

Department of Bariatric and Metabolic Surgery, China-Japan Union Hospital of Jilin University, Changchun, China

KEYWORDS

single-anastomosis duodenal–ileal bypass with sleeve gastrectomy, type 2 diabetes mellitus, metabolomics, bariatric surgery, SADI-S, T2DM

A corrigendum on

Metabolomics analysis of stool in rats with type 2 diabetes mellitus after single-anastomosis duodenal–ileal bypass with sleeve gastrectomy

by Wang L, Wang Z, Yu Y, Ren Z, Jia Y, Wang J, Li S and Jiang T (2022) *Front. Endocrinol.* 13:1013959. doi: 10.3389/fendo.2022.1013959

Text Correction

In the published article, there was an inappropriate description because of our limited metabolomics knowledge at the time of writing this paper. A correction has been made to **Abstract**, **Results**. This sentence previously stated:

"A total of 245 differential metabolites were identified between the two groups. Among them, 16 metabolites such as branched-chain amino acids (valine), aromatic amino acid (phenylalanine), bile acid (cholic acid, lithocholic acid, and β-muricholic acid), short-chain fatty acid (isobutyric acid), and phospholipid lysoPE(17:0), lysoPE(20:3) and lysoPS(16:0) were associated to the T2DM remission after SADI-S."

The corrected sentence appears below:

"A total of 245 differential metabolites were identified between the two groups, among which 8 metabolites were detectable under both the positive ion model and negative ion model. Therefore, a total of 237 differential metabolites were identified in our study which were mainly involved in tryptophan metabolism; cysteine and methionine metabolism; phenylalanine metabolism; phenylalanine; tyrosine and tryptophan biosynthesis; arginine biosynthesis; alanine, aspartate and glutamate metabolism; Arginine and proline metabolism; glyoxylate and dicarboxylate metabolism; alpha-Linolenic acid metabolism; Linoleic acid metabolism; riboflavin metabolism; nicotinate and nicotinamide metabolism; pyrimidine metabolism; porphyrin and chlorophyll metabolism."

Text Correction

In the published article, there was an inappropriate description because of our limited metabolomics knowledge at the time of writing this paper. Our study only found an effect of SADI-S surgery on the metabolites of stool in T2DM rats and did not further

demonstrate that these different metabolites caused by SADI-S can improve or worsen T2DM. Therefore, we could not draw a direct causal association between the metabolites and the T2DM improvement caused by SADI-S. Consequently, our previous conclusion is not scientific.

A correction has been made to the **Abstract**, **Conclusion**. This sentence previously stated:

"SADI-S improves T2DM in rats by regulating phenylalanine biosynthesis, valine, phenylalanine, alanine, glutamate, proline, bile acid, and phospholipid metabolism pathways"

The corrected sentence appears below:

"SADI-S significantly improved the glucose metabolism in T2DM rats. In addition, SADI-S significantly changed the composition of metabolites in T2DM rats which were involved in tryptophan metabolism pathway, linoleic acid metabolism pathway and so on. This may be the mechanism by which SADI-S improved T2DM."

Text Correction

In the published article, there was an inaccurate description. To supplement the description of results.

A correction has been made to **Results**, Identification of differential metabolites of Metabolomics analysis, Line 5-8 of Paragraph 1. This sentence previously stated:

"The data shown in the Supplemental Table 1 indicated that 245 differential metabolites were identified, among which 81 metabolites were obtained under the positive ion model and 164 metabolites were obtained under the negative ion model."

The corrected sentence appears below:

"The data shown in the Supplemental Table 1 indicated that 245 differential metabolites were identified, among which 81 metabolites were obtained under the positive ion model and 164 metabolites were obtained under the negative ion model. Eight of these metabolites were detectable in both modes. Therefore, a total of 237 differential metabolites were identified between the two groups."

Text Correction

In the published article, there was an inappropriate description because of our limited metabolomics knowledge at the time of writing this paper. We did not properly describe our results.

A correction has been made to the **Results**, Identification of differential metabolites of Metabolomics analysis, Line 12-17 of Paragraph. This sentence previously stated:

"Sixteen metabolites were associated to T2DM remission after SADI-S such as branched-chain amino acids (valine), aromatic amino acid (phenylalanine), bile acid (cholic acid, lithocholic acid and b-muricholic acid), short-chain fatty acid (isobutyric acid), phospholipid lysoPE(17:0), lysoPE (20:3), and lysoPS(16:0)."

The corrected sentence appears below:

"According to the previous literature, some metabolites that may be associated with the T2DM such as branched-chain amino acids (valine), aromatic amino acid (phenylalanine), bile acid (cholic acid, lithocholic acid and b-muricholic acid), short-chain fatty acid (isobutyric acid), phospholipid lysoPE(17:0), lysoPE (20:3), and lysoPS(16:0), were also observed to have a significant changes in our study."

Text Correction

In the published article, there was an inappropriate description because of our limited metabolomics knowledge at the time of writing this paper. Our study only found an effect of SADI-S surgery on the metabolites of stool in T2DM rats and did not further demonstrate that these different metabolites caused by SADI-S can improve or worsen T2DM. Therefore, we could not draw a direct causal association between the metabolites and the T2DM improvement caused by SADI-S. Consequently, our previous conclusion is not scientific.

A correction has been made to the **Conclusion**. This sentence previously stated:

"The current study shows that SADI-S can improve the disease state of T2DM rats. Mechanistically, it regulates valine metabolism, phenylalanine metabolism, phenylalanine biosynthesis, alanine and glutamate metabolism, proline metabolism, bile acid metabolism as well as the phospholipid metabolism pathways"

The corrected sentence appears below:

"The current study shows that SADI-S can improve the disease state of T2DM rats. Mechanistically, the improvement of T2DM caused by SADI-S may be associated with the changes of pathways such as tryptophan metabolism pathway, linoleic acid metabolism pathway and so on."

Error in Figure/Table

In the published article, there was an error in Figures 1B as published. We previously calculated the area under the curve (AUC) of IPGTT according to a formula described in a literature. However, at that time we did not discover that there were some differences between this literature and our research. Therefore, we used the wrong formula AUC = (G0 + G180)/2 + G15 + G30 + G60 + G120 to calculate the AUC of IPGTT. Now we calculated the AUC using the correct formula AUC=(G0 +G15)×15/2+(G15+G30)×15/2+(G30+G60)×30/2+(G60+G120)×60/2 +(G120+G180)×60/2 and redrawn the Figure 1B. The corrected Figures 1B and its caption appear below.

The authors apologize for these errors and state that they does not change the scientific conclusions of the article in any way. The original article has been updated.

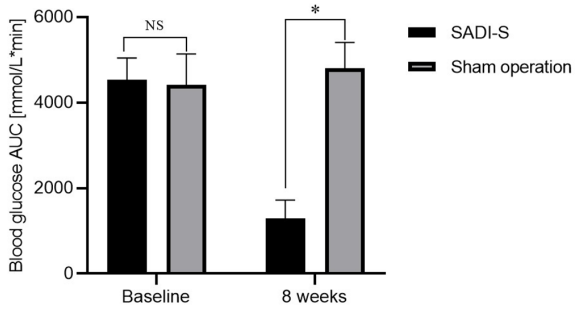

FIGURE 1B
Changes in blood glucose AUC during IPGTT before and after surgery. NS indicates no significant difference between the SADI-S group and sham operation group. * represents a significant difference between the SADI-S group and sham operation group ($P < 0.05$).

Publisher's note

frontiers | Frontiers in Endocrinology

TYPE Original Research
PUBLISHED 06 October 2022
DOI 10.3389/fendo.2022.993137

OPEN ACCESS

EDITED BY
Sanyuan Hu,
Qianfoshan Hospital, Shandong University, China

REVIEWED BY
Shiri Li,
Cornell University, United States
Wei-Hua Tang,
National Yang-Ming University, Taiwan

*CORRESPONDENCE
Jun Zhang
junzhang@tongji.edu.cn
Shen Qu
qushencn@hotmail.com

SPECIALTY SECTION
This article was submitted to Obesity, a section of the journal Frontiers in Endocrinology

RECEIVED 13 July 2022
ACCEPTED 22 September 2022
PUBLISHED 06 October 2022

CITATION
You H, Ma H, Wang X, Wen X, Zhu C, Mao W, Bu L, Zhang M, Yin J, Du L, Cheng X, Chen H, Zhang J and Qu S (2022) Association between liver-type fatty acid-binding protein and hyperuricemia before and after laparoscopic sleeve gastrectomy. *Front. Endocrinol.* 13:993137. doi: 10.3389/fendo.2022.993137

Association between liver-type fatty acid-binding protein and hyperuricemia before and after laparoscopic sleeve gastrectomy

Hui You[1,2], Huihui Ma[1], Xingchun Wang[1,2], Xin Wen[1], Cuiling Zhu[1], Wangjia Mao[1], Le Bu[1], Manna Zhang[1], Jiajing Yin[1,2], Lei Du[1], Xiaoyun Cheng[1], Haibing Chen[1], Jun Zhang[3,4]* and Shen Qu[1,2]*

[1]Department of Endocrinology and Metabolism, Shanghai Tenth People's Hospital, School of Medicine, Tongji University, Shanghai, China, [2]Shanghai Center of Thyroid Diseases, Shanghai Tenth People's Hospital, School of Medicine, Tongji University, Shanghai, China, [3]Research Center for Translational Medicine at East Hospital, Tongji University School of Medicine, Tongji University, Shanghai, China, [4]Shanghai Institute of Stem Cell Research and Clinical Translation, Shanghai, China

Background: Liver-type fatty acid-binding protein (FABP1) contributes to metabolic disorders. However, the relationship between FABP1 and hyperuricemia remains unknown. We aimed to evaluate the correlation between serum FABP1 and hyperuricemia in patients with obesity before and after laparoscopic sleeve gastrectomy (LSG).

Methods: We enrolled 105 patients (47 men and 58 women) with obesity who underwent LSG. They were divided into two groups: normal levels of uric acid (UA) (NUA, n = 44) and high levels of UA (HUA, n = 61) with matching sexes. FABP1 levels and other biochemical parameters were measured at baseline and 3, 6, and 12 months after LSG.

Results: Serum FABP1 levels were significantly higher in the HUA group than in the NUA group (34.76 ± 22.69 ng/mL vs. 25.21 ± 21.68 ng/mL, P=0.024). FABP1 was positively correlated with UA (r=0.390, P=0.002) in the HUA group. The correlation still existed after adjusting for confounding factors. Preoperative FABP1 levels were risk factors for hyperuricemia at baseline. UA and FABP1 levels decreased at 3, 6, and 12 months postoperatively. FABP1 showed a more significant decrease in the HUA group than in the NUA group at 12 months (27.06 ± 10.98 ng/mL vs. 9.54 ± 6.52 ng/mL, P=0.003). Additionally, the change in FABP1 levels positively correlated with changes in UA levels in the HUA group 12 months postoperatively (r=0.512, P=0.011).

Conclusions: FABP1 was positively associated with UA and may be a risk factor for hyperuricemia in obesity. FABP1 levels were higher but decreased more after LSG in obese patients with hyperuricemia than in those without hyperuricemia.

KEYWORDS

liver-type fatty acid-binding protein, laparoscopic sleeve gastrectomy, hyperuricemia, obesity, uric acid

Introduction

Uric acid (UA) is a final enzyme product of purine nucleotide degradation and can scavenge oxygen radicals and protect the erythrocyte membrane from lipid oxidation (1). Hyperuricemia is a metabolic disease characterized by elevated serum UA (SUA) concentration (>420 μmol/L for men and >360 μmol/L for women) (2). In the past few decades, the prevalence of hyperuricemia has been increasing rapidly worldwide (2). In addition, hyperuricemia has been traditionally considered a potential risk factor for obesity, diabetes mellitus, nonalcoholic fatty liver disease (NAFLD), and other metabolic syndromes (3, 4). However, the underlying mechanisms of hyperuricemia and its risk factors remain unclear.

Liver-type fatty acid-binding protein (FABP1) (5) is a member of the fatty acid-binding protein family and is distributed mainly in the liver, kidney, lung, and gastrointestinal tract, accounting for 3% to 5% of the total cytoplasmic protein. It mainly enhances long-chain fatty acid uptake and fatty acid metabolism, and plays a central role in the hepatic β-oxidation of unesterified fatty acids, ultimately leading to various metabolic disorders (5–8). A previous study (8) has found that FABP1 can play a negative regulatory role in the formation of very-low-density lipoproteins, which can lead to lipid metabolism disorders when combined with total cholesterol, triglycerides, and apolipoprotein B, thereby accelerating NAFLD progression. Tsai et al. (9) found increasing concentrations of FABP1 were associated independently and significantly with diabetic nephropathy. Our previous research (10) also found serum FABP1 levels were correlated closely with obesity. However, the link between FABP1 and hyperuricemia has not been reported.

Recently, laparoscopic sleeve gastrectomy (LSG) (1, 11) has become a popular procedure to assist with weight loss owing to its low damaging effects on the patient's physiology, high safety, and evident curative effect. This procedure has been shown to improve many metabolic syndromes, such as obesity, diabetes, and NAFLD, as well as hyperuricemia (12). Therefore, we aimed to evaluate the correlation between serum FABP1 and hyperuricemia in patients with obesity before and after LSG.

Methods

Patients

This retrospective, follow-up study enrolled 105 patients with obesity (body mass index [BMI], 38.39 ± 6.33 kg/m^2) aged 18 to 60 years from the Shanghai Tenth People's Hospital. Patients were divided into the following two groups according to their SUA levels (1): normal levels of UA (NUA, men ≤ 420 μmol/L, women ≤ 360 μmol/L, n = 44) and high levels of UA (HUA, men > 420 μmol/L, women > 360 μmol/L, n = 61) groups. There was no statistical difference in sex distribution between the two groups. All patients underwent LSG. Exclusion criteria were patients with: (1) a history of substance abuse or chronic mental illness; (2) psychiatric disorders; (3) previous gastrointestinal surgery; and (4) unwillingness to undergo LSG. The patients underwent follow-up at 3, 6, and 12 months after LSG (hereafter referred to as 3, 6, and 12 M post-LSG, respectively). This study was conducted in accordance with the Declaration of Helsinki and French Legislation, and all the patients provided informed consent. The study protocol was approved by the Ethics Committee of our hospital (clinical registration number ChiCTR-OCS-12002381).

Anthropometric and biochemical measurements

Demographic and clinical data, including medical history and date of birth, were analyzed. Anthropometric measurements were performed for all patients. Height and weight measurements were performed by the medical staff, with the patients clad in light clothes, using an Omron HBF-358 body fat analyzer (Q40102010L01322F, Japan). The BMI was calculated as weight in kilograms divided by height in meters squared (kg/m^2). Morning venous blood was obtained from all patients after a 12h overnight fast and centrifuged thereafter with the supernatant being used in the laboratory tests. Serum FABP1 levels were measured using an enzyme-linked immunosorbent assay (ELISA; Abcam (Cambridge), ab218261) kit. As per the manufacturer's protocol, the normal reference level of FABP1 was 6.36–19.0 ng/

mL. UA, fasting blood glucose (FBG), fasting insulin (FINS), fasting C-peptide (FCP), alanine aminotransferase (ALT), aspartate aminotransferase (AST), and γ-transaminase (γ-GT) levels were assessed using an automated biochemical analyzer.

Statistical analysis

Statistical analysis was performed using SPSS 20.0 (SPSS Inc., Chicago, IL, USA) and GraphPad Prism 8 (GraphPad Software, San Diego, USA) in Windows 10. Data are presented as means ± standard deviations (SDs) for continuous variables, and count data are expressed as the number of columns (n). Comparisons between continuous or categorical variables in two groups were tested using the Student's t test or variance analysis, whereas paired-sample t tests were used to compare the data before and after surgery. To explore the correlation between serum FABP1 levels and UA levels or other biochemical criteria, Spearman's correlation analysis was performed. To further study the relationship between serum FABP1 levels and UA levels, we performed a multiple linear regression. We then performed a binary logistic regression for Models 1, 2, and 3 to identify potential factors related to the risk of hyperuricemia in patients with obesity. Statistical significance was set at $P < 0.05$.

Results

Elevated FABP1 levels in the HUA group with obesity

We divided the patients with obesity (male, n = 47 and female, n = 58) into the NUA (n = 44) and HUA (n = 61) groups. There was no statistical difference in the sex distribution between the two groups ($P = 0.604$). The FABP1 levels were found to be significantly higher in the HUA group than in the NUA group at baseline (34.76 ± 22.69 ng/mL vs. 25.21 ± 21.68 ng/mL, $P = 0.024$). Furthermore, the FINS, FCP, ALT, AST and γ-GT levels were also significantly lower in the NUA group than in the HUA group (25.61 ± 20.99 mU/L vs. 37.50 ± 21.61 mU/L, $P = 0.015$; 3.89 ± 1.68 ng/ml vs. 4.97 ± 1.65 ng/ml, $P = 0.004$; 45.69 ± 44.99 U/L vs. 67.67 ± 62.02 U/L, $P = 0.036$; 28.67 ± 23.28 U/L vs. 44.00 ± 36.47 U/L, $P = 0.013$; 44.26 ± 32.47 U/L vs. 62.75 ± 48.00 U/L, $P = 0.034$). However, BMI and FBG levels were not statistically different between the two groups (37.58 ± 6.46 kg/m^2 vs. 38.98 ± 6.23 kg/m^2, P=0.679; 6.85 ± 3.09 mmol/L vs. 5.80 ± 2.08 mmol/L, P=0.054) (Table 1)

Correlation between serum FABP1 levels and UA levels at baseline

Since hyperuricemia and FABP1 are closely related to diabetes and liver-related metabolic disorders, we first assessed the correlation between serum FABP1 or UA levels with glucose metabolism and liver enzyme indices in the NUA and HUA groups (Figure 1). We found the serum FABP1 levels were related to the FBG, AST and γ -GT levels in the NUA group (r = 0.422, $P = 0.004$; r=0.430, $P = 0.006$; r = 0.311, $P = 045$, respectively). Moreover, the UA levels correlated with the ALT, AST, and γ-GT levels (r = 0.297, $P = 0.049$; r = 0.394, $P = 0.013$; r = 0.381, $P = 0.013$, respectively). Furthermore, in the HUA group, the serum FABP1 level was positively correlated with the UA level (r = 0.390, $P = 0.002$), and with the BMI, ALT and AST levels (r = 0.375, $P = 0.002$; r = 0.376, $P = 0.003$; r = 0.446, $P < 0.001$, respectively). In addition, the UA level were related to the BMI, FINS, FCP and ALT levels (r = 0.338, $P = 0.008$; r = 0.334, $P = 0.014$; r = 0.428, $P = 0.01$; r = 0.308, $P = 0.016$, respectively).

TABLE 1 Baseline characteristics of the study.

Parameters	Obese population			*P value*
	Total (n = 105)	NUA (n = 44)	HUA (n = 61)	
FABP1 (ng/mL)	30.76 ± 21.53	25.21 ± 21.68	34.76 ± 22.69	0.024*
UA(μmol/L)	420.79 ± 97.65	339.44 ± 49.95	479.47 ± 79.91	0.000***
Age (years)	30.79 ± 10.92	32.47 ± 11.98	29.57 ± 10.01	0.181
Sex(male/female)	47/58	21/23	26/35	0.604
BMI (kg/m^2)	38.39 ± 6.33	37.58 ± 6.46	38.98 ± 6.23	0.679
FBG (mmol/L)	6.24 ± 2.59	6.85 ± 3.09	5.80 ± 2.08	0.054
FINS(mU/L)	33.02 ± 22.03	25.61 ± 20.99	37.50 ± 21.61	0.015*
FCP(ng/ml)	4.55 ± 1.74	3.89 ± 1.68	4.97 ± 1.65	0.004**
ALT (U/L)	58.46 ± 55.71	45.69 ± 44.99	67.67 ± 62.02	0.036*
AST (U/L)	37.90 ± 32.63	28.67 ± 23.28	44.00 ± 36.47	0.013*
γ–GT (U/L)	54.82 ± 42.85	44.26 ± 32.47	62.75 ± 48.00	0.034*

Data are presented as means ± SDs.
FABP1, liver fatty acid-binding protein; UA, uric acid; BMI, body mass index; FBG, fasting blood glucose; FINS, fasting insulin; FCP, Fasting C-peptide; ALT, alanine aminotransferase; AST, aspartate aminotransferase; γ-GT, γ-transaminase; *$P < 0.05$, **$P < 0.01$, ***$P < 0.001$.

10.3389/fendo.2022.993137

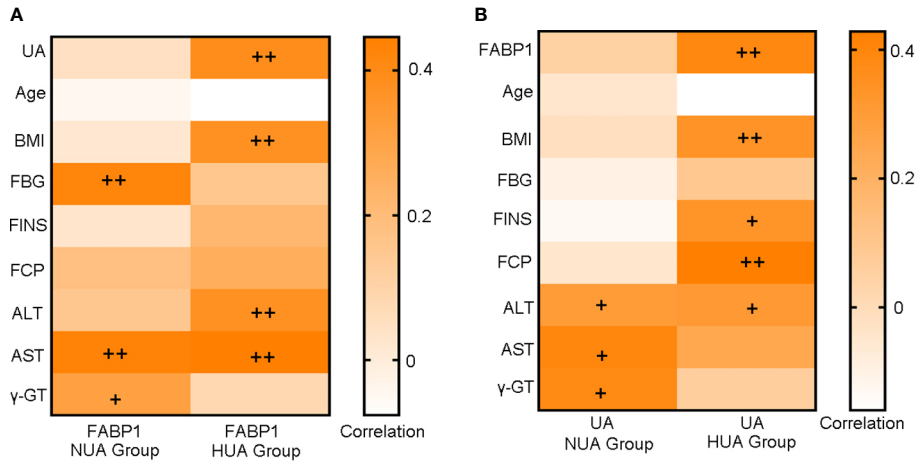

FIGURE 1
Heat map of the correlation analysis of serum FABP1 levels **(A)** or UA levels **(B)** with glucose metabolism and liver function-related indicators at baseline. +*P*<0.05; ++*P*<0.01.

To evaluate the correlation between serum UA levels and FABP1 levels, we also performed a multiple linear regression analysis on all individuals. First, Model 1 revealed a significantly positive correlation between serum UA levels and FABP1 levels (β = 0.344, *P* <0.001). Second, in Model 2, a correlation was also evident after adjusting for BMI, age, and sex (β = 0.257, *P* = 0.005). Third, in Model 3 (β = 0.280, *P* = 0.005), serum FABP1 levels were another determinant of the UA levels after adjusting for BMI, age, and the related indicators of glucose metabolism (FBG, FINS, and FCP). The same findings were observed in Model 4 (β = 0.283, *P* = 0.009) after adjusting for BMI, age, sex, and ALT, AST, and γ-GT levels (Table 2).

Preoperative FABP1 may be a risk factor for hyperuricemia

We also constructed a multivariable logistic model for the occurrence of hyperuricemia in the preoperative obese cohort (Table 3). In Model 1, with BMI and age as additional covariables, we observed a statistically significant association between serum FABP1 levels and the risk of hyperuricemia in patients with obesity (Odds ratio [OR], 95% confidence interval [CI] = 1.023, 1.001–1.046, *P* = 0.048). This association was also significant in Model 2 (OR, 95% CI = 1.045, 1.009–1.083, *P* = 0.016) with the same variables as in Model 1 and with FBG, FINS, and FCP levels as additional covariables. After further adjustment for age, BMI, sex, ALT, AST, and γ-GT levels in Model 3, there was no statistical difference in the association between FABP1 and the risk of hyperuricemia (OR, 95% CI = 1.022, 0.994–1.052, *P* = 0.125).

Correlation between the change in serum UA levels and FABP1 levels after LSG

The UA levels decreased significantly in the HUA group after LSG (from 479.47 ± 79.91 μmol/L to 429.98 ± 90.52 μmol/L at 3 M, *P* < 0.001; 396.78 ± 80.87 μmol/L at 6 M, *P* < 0.001; and

TABLE 2 Multiple Regression Modeling of the serum UA levels associated with the FABP1 levels.

Model	UA			
	R^2	β	*P* value	95% CI of β
1	0.118	0.344	0.000***	0.726-2.391
2	0.263	0.257	0.005**	0.361-1.968
3	0.423	0.280	0.005**	0.407-2.224
4	0.311	0.283	0.009**	0.373-2.508

Model 1: FABP1; Model 2: FABP1, adjusting for BMI, age, and sex; Model 3: FABP1, adjusting for BMI, age, sex, and FBG,FINS, and FCP levels; Model 4: FABP1, adjusting BMI, age, sex, and ALT,AST and γ-GT levels; FABP1, liver fatty acid-binding protein; UA, uric acid; BMI, body mass index; FBG, fasting blood glucose; FINS, fasting insulin; FCP, Fasting C-peptide; ALT, alanine aminotransferase; AST, aspartate aminotransferase; γ-GT, γ-transaminase; **$P < 0.01$, ***$P < 0.001$.

TABLE 3 Multivariable-adjusted association of serum FABP1 levels and hyperuricemia in patients with obesity.

Model	OR (95% CI)	*P* value
1	1.023 (1.001-1.046)	0.048*
2	1.045 (1.009-1.083)	0.016*
3	1.022 (0.994-1.052)	0.125

Model 1:included the serum FABP1 level, age, BMI, and sex; Model 2:included serum FABP1 level, age, BMI, sex, and FBG, FINS, and FCP levels; Model 3: included serum FABP1 level, age, BMI, sex, and ALT,AST and γ -GT levels. FABP1, liver fatty acid-binding protein; UA, uric acid; BMI, body mass index; FBG, fasting blood glucose; FINS, fasting insulin; FCP, Fasting C-peptide; ALT, alanine aminotransferase; AST, aspartate aminotransferase; γ-GT, γ-transaminase; *$P < 0.05$.

406.34 ± 93.90 μmol/L at 12 M, $P < 0.001$) (Figure 2A). Moreover, the serum FABP1 levels decreased progressively at 3, 6, and 12 months after surgery (for the NUA group: from 25.21 ± 21.68 ng/mL to 14.38 ± 11.88 ng/mL at 3M, $P = 0.142$; 11.09 ± 4.25 ng/mL at 6 M, $P = 0.015$; and 13.77 ± 9.94 ng/mL at 12 M, P=0.005; and for the HUA group: from 34.76 ± 22.69 ng/m to 16.43 ± 8.59 ng/mL at 3 M, $P < 0.001$; 20.60 ± 16.62 ng/mL at 6 M, $P = 0.012$; 11.77 ± 6.9 ng/mL at 12 M, $P < 0.001$) (Figure 2B). Furthermore, the UA levels in the HUA group showed a greater decrease than that in the NUA group (Figure 2C). Meanwhile, the serum FABP1 levels showed a more significant decrease in the HUA group than in the NUA group at 12 months (27.06 ± 10.98 ng/mL vs. 9.54 ± 6.52 ng/mL, $P = 0.003$) (Figure 2D). Table 4 shows the correlations of the changes (△) in the serum FABP1 levels and the metabolic factors in the NUA and HUA groups. The changes in the serum FABP1 levels at 12 months after surgery were positively correlated with the changes in the UA levels (r = 0.512, P = 0.011). Moreover, the changes in BMI (r = 0.399, $P = 0.048$) and ALT levels (r = 0.390, $P = 0.031$) were associated with the change in serum FABP1 levels at 12M post-LSG in the HUA group.

To evaluate the contribution of FABP1 and other metabolic factors toward UA, a multiple linear regression analysis was also performed in Table 5. After adjusting the △BMI, age, and sex, △FBG, △FINS, △FCP, △ALT, △AST and △γ-GT levels, ΔUA (at 12M post-LSG) was also significantly correlated with ΔFABP1.

Discussion

Currently, FABP1 is commonly used as a specific biomarker for liver disease and type 1 diabetes mellitus in clinical practice (13–15). However, hyperuricemia as a common metabolic disease is closely related to liver and pancreas islet function, and its relationship with FABP1 has not been reported. Our study demonstrated that serum FABP1 levels were significantly

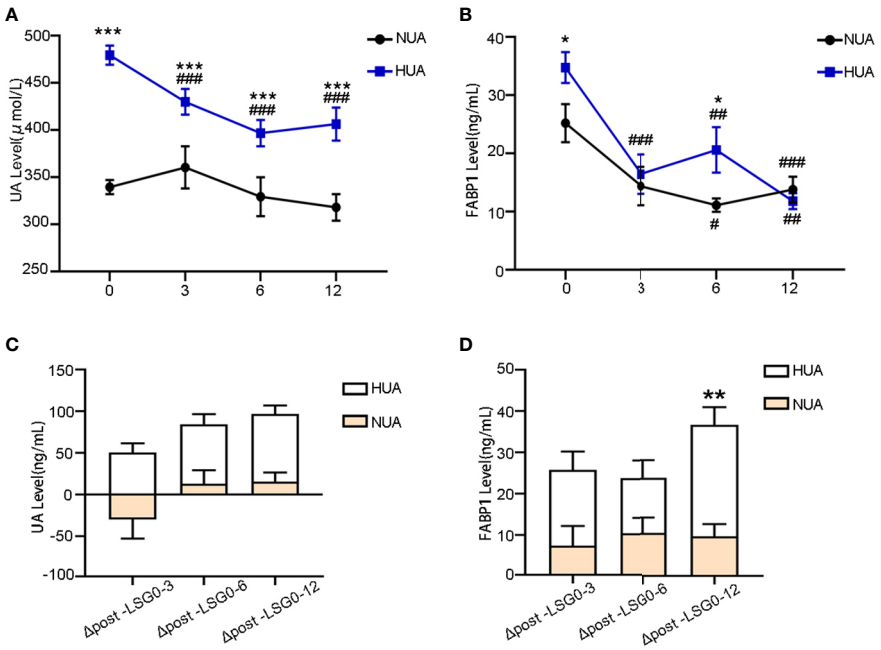

FIGURE 2
Changes in the serum FABP1 and UA levels between the NUA and HUA groups after LSG. **(A, B)** Decrease in the UA and FABP1 levels after LSG. **(C, D)** Comparison of the magnitude of the change in the UA and FABP1 levels at 3, 6, and 12 M post-LSG and baseline; Comparison of the variables between 3, 6, and 12 M post-LSG and baseline, $^{\#\#}P < 0.01$, $^{\#\#\#}P < 0.001$ Comparison of the variables between the NUA and HUA groups, *$P < 0.05$, **$P < 0.01$, ***$P < 0.001$.

TABLE 4 Correlation analysis between the improvement in the serum FABP1 levels and the clinical indices between the different UA groups after LSG.

Parameters	ΔFABP1-3		ΔFABP1-6		ΔFABP1-12	
	r	*P* value	r	*P* value	r	*P* value
NUA group						
ΔUA	-0.401	0.174	0.214	0.068	0.211	0.386
ΔBMI	0.231	0.412	-0.325	0.257	0.166	0.448
ΔFBG	0.476	0.100	0.345	0.010**	-0.094	0.670
ΔFINS	-0.248	0.414	0.398	0.159	-0.191	0.383
ΔFCP	-0.272	0.368	0.312	0.541	-0.245	0.260
ΔALT	0.021	0.946	0.421	0.134	0.180	0.460
ΔAST	0.029	0.926	0.341	0.049*	0.155	0.537
Δγ–GT	-0.148	0.683	0.378	0.135	0.123	0.639
HUA group						
ΔUA	0.198	0.304	0.318	0.214	0.512	0.011*
ΔBMI	-0.141	0.465	0.557	0.020*	0.399	0.048*
ΔFBG	0.260	0.173	0.139	0.595	0.175	0.364
ΔFINS	0.104	0.591	0.131	0.617	0.241	0.225
ΔFCP	0.171	0.376	0.235	0.364	0.223	0.254
ΔALT	0.346	0.071	0.378	0.135	0.390	0.031*
ΔAST	0.436	0.020	0.347	0.173	0.266	0.220
Δγ–GT	0.123	0.575	0.140	0.632	0.133	0.566

FABP1, liver fatty acid-binding protein; UA, uric acid; BMI, body mass index; FBG, fasting blood glucose; FINS, fasting insulin; FCP, Fasting C-peptide; ALT, alanine aminotransferase; AST, aspartate aminotransferase; γ-GT, γ-transaminase; *$P < 0.05$, **$P < 0.01$.

higher in the HUA group than in the NUA group and the positive correlativity between the change in FABP1 and UA levels at 3, 6, and 12 months after LSG. To the best of our knowledge, this is the first study to provide clinical evidence confirming the relationship between serum FABP1 levels and hyperuricemia in patients with obesity before and after LSG.

Hyperuricemia refers to a disorder of purine metabolism or decreased UA excretion, leading to increased SUA levels. Studies (16, 17) have shown that this disorder forms not only the biochemical basis for gout but can also induce major diseases, such as myocardial infarction, diabetes, coronary heart disease, metabolic syndrome, and other diseases, which ultimately deprive patients' lives. The meta-analysis (18) suggested that the OR value of hypertension risk in HUA patients was 1.48, especially in younger patients with early-onset hypertension. Besides, clinical studies (19, 20) have found that elevated SUA at baseline can predict the incidence of diabetes and insulin resistance (IR) status, suggesting that elevated SUA is an independent risk factor for IR and diabetes. Our study also found that compared with the NUA group, patients in the HUA group had relatively higher BMI and poorer pancreatic islet and liver function. These results suggest the danger of hyperuricemia and the urgency of treatment. Thus, there was an urgent need for further studies to identify the pathogenesis of hyperuricemia.

TABLE 5 Multiple linear analysis of the correlation between changes in UA and FABP1 levels at 12M post-LSG.

Model	△UA			
	R^2	β	*P* value	95% CI of β
1	0.287	0.536	0.000***	0.352-2.379
2	0.423	0.458	0.002**	0.573-2.237
3	0.436	0.470	0.002**	0.547-2.343
4	0.471	0.550	0.001**	0813-3.025

Model 1: △FABP1;
Model 2: △FABP1, adjusting for △BMI, age, and sex;
Model 3: △FABP1, adjusting for △BMI, age, sex, and △FBG, △FINS, and △FCP levels;
Model 4: △FABP1, adjusting △BMI, age, sex, and △ALT, △AST and △γ-GT levels;
FABP1, liver fatty acid-binding protein; UA, uric acid; BMI, body mass index; FBG, fasting blood glucose; FINS, fasting insulin; FCP, Fasting C-peptide; ALT, alanine aminotransferase; AST, aspartate aminotransferase; γ-GT, γ-transaminase; **$P < 0.01$,***$P < 0.001$.

FABPs (21–23) belong to the lipid-binding protein superfamily. To date, nine types of FABPs have been identified based on tissue-specific distributions: L (liver), I (intestinal), H (muscle and heart), A (adipocyte), E (epidermal), Il (ileal), B (brain), M (myelin), and T (testis) (24). The first described FABP, liver-FABP (L-FABP or FABP1), is expressed highly in the liver, as well as in the intestines and kidneys. FABP1 comprises 127 amino acids with a molecular weight of approximately 14–15 kDa, can regulate the expression of some essential genes involved in lipid metabolism, and is related closely to a variety of metabolic syndromes, such as obesity, NAFLD, and IR (25, 26). In our previous study, we also found that serum FABP1 levels positively correlated with BMI, and after performing a multiple linear regression adjusted for sex, age, ALT, and other factors, the serum FABP1 levels remained strongly correlated with BMI (10). Newberry (27) found that, compared with wild-type mice, the *FABP1*-gene knockout mice could significantly inhibit diet-induced obesity and reduce the development of fatty liver when fed a diet rich in fatty acids. This was related to the reduced absorption of fatty acids and their esterification in the intestines of mice with this gene deletion, which affects the synthesis rate of chylomicrons. Therefore, serum FABP1 levels can change a variety of metabolic factors and regulate the pathogenesis of obesity.

Furthermore, FABP1 is closely related to the occurrence and development of other metabolic syndromes. Studies have found that FABP1 plays an important role in lipid transport and cholesterol metabolism in the liver. *FABP1* expression increased significantly with the formation of fatty liver and was correlated with the degree of hepatic steatosis, proving that serum FABP1 levels play an important role in NAFLD using a mouse model of NAFLD (28). Moreover, the serum FABP1 levels are related to glucose metabolism. Shi Juan et al. (29) found that serum FABP1 levels increased in adolescents with abnormal glucose metabolism and were related to glucose and lipid metabolism but not to the function of pancreatic islet β cells. Furthermore, a previous study suggested that the serum FABP1 level in the renal tubules is associated with glomerular disease and FABP1 plays a protective role in renal tubulointerstitial injury and glomerular injury of diabetic nephropathy (30). However, the relationship between FABP1 and hyperuricemia is unknown. In this study, we also found that serum FABP1 levels were closely related to UA, liver enzyme and glucose metabolism parameters; moreover, it is worth highlighting that after adjusting for confounding factors, preoperative FABP1 level was a risk factor for hyperuricemia at baseline.

Bariatric surgery has been found to regulate BMI safely and effectively and improve metabolic markers such as blood glucose and liver function levels. In recent years, multiple pieces of evidence (31–33) have shown that bariatric surgery is effective in reducing the incidence of gout attacks and serum urate concentration in patients with hyperuricemia or gout up to 12 months of follow-up. Our results also indicated UA and FABP1 levels decreased at 3, 6, and 12 months postoperatively, and the decrease was greater in the HUA group than in the NUA group at 3, 6, and 12 months after LSG; Moreover, the changes in the serum FABP1 levels at 12 months after LSG showed a positive correlation with changes of SUA levels in the HUA group.

The current study applied a variety of statistical methods to elucidate the relationship between serum FABP1 levels and hyperuricemia before and after LSG for the first time. However, our study had certain limitations. First, owing to the observational nature of this study, we could not determine any causal relationship between the UA levels and elevated serum FABP1 levels. Moreover, this study did not investigate the mechanism in depth. In binomial logistic regression, we found that the association between serum FABP1 levels and the risk of hyperuricemia had no statistical effect after adjusting for liver enzymes. Now, a large number of studies have shown that UA levels are closely related to liver diseases, such as NAFLD (34–36), and are also positively correlated with liver enzyme indicators (37). And there is no doubt that IR must play a crucial role in this connection. FABP1 is also mainly expressed in the liver. Many studies have also proved the association between FABP1 and liver diseases (15, 38). Silencing of FABP1 can ameliorate hepatic steatosis, inflammation, and oxidative stress (38). And FABP1 can be used as a marker of liver damage after medication (15). Meanwhile, FABP1 is also positively correlated with liver enzymes levels. So we speculated that FABP1 and hyperuricemia may interact through liver function-related indicators. We will conduct further research using animal and cell experiments in the future. Second, the study had a small sample size and short follow-up durations. There was a sampling error in this study. Future studies with larger numbers of patients and longer follow-up periods are warranted to validate our findings.

Conclusions

Serum FABP1 levels were significantly higher in the HUA group than in the NUA group. In addition, serum FABP1 levels positively correlated with UA levels, and the preoperative serum FABP1 levels may be a risk factor for hyperuricemia. Moreover, the serum FABP1 levels decreased postoperatively and with a greater reduction in the HUA group than in the NUA group at 3, 6, and 12 M after LSG. Furthermore, changes in the serum FABP1 levels at 12 M after LSG showed a positive correlation with changes in the UA levels in the HUA group. Our findings may provide a basis for encouraging researchers and clinicians working on metabolic

diseases to adopt a new perspective on the role of FABP1, and endorse FABP1 as an important indicator of hyperuricemia.

Data availability statement

The original contributions presented in the study are included in the article/supplementary material. Further inquiries can be directed to the corresponding authors.

Ethics statement

The studies involving human participants were reviewed and approved by ClinicalTrial.gov ID: ChiCTR-OCS-12002381. The patients/participants provided their written informed consent to participate in this study.

Author contributions

JZ and SQ conceived and supervised the overall study. XW, CZ, WM, LB, MZ, JY, and LD performed the literature review and collected the epidemiological and clinical data. XC and HC contributed to the statistical analysis. HY, HM, and XCW drafted the manuscript. All authors contributed to the article and approved the submitted version.

Funding

This work was supported by the National Natural Science Foundation of China (grant numbers 81700752, 81970677, 82170861, 82170904), Traditional Chinese Medicine Scientific Research Project of Shanghai Municipal Health Commission (grant number 2020_JP013), and Climbing Talent Program of the 10th People's Hospital affiliated to Tongji University (2021SYPDRC059,2021SYPDRC050).

Conflict of interest

The authors declare that the research was conducted in the absence of any commercial or financial relationships that could be construed as a potential conflict of interest.

Publisher's note

References

1. Menenakos E, Doulami G, Tzanetakou IP, Natoudi M, Kokoroskos N, Almpanopoulos K, et al. The use of serum uric acid concentration as an indicator of laparoscopic sleeve gastrectomy success. *International Surgery*. (2015) 100(1):173–9. doi: 10.9738/INTSURG-D-13-00186.1

2. Li L, Zhang Y, Zeng C. Update on the epidemiology, genetics, and therapeutic options of hyperuricemia. *Am J Trans Res* (2020) 12(7):3167–81.

3. Li C, Hsieh M-C, Chang S-J. Metabolic syndrome, diabetes, and hyperuricemia. *Curr Opin In Rheumatol* (2013) 25(2):210–6. doi: 10.1097/BOR.0b013e32835d951e

4. Dehlin M, Jacobsson L, Roddy E. Global epidemiology of gout: Prevalence, incidence, treatment patterns and risk factors. *Nat Rev Rheumatol* (2020) 16 (7):380–90. doi: 10.1038/s41584-020-0441-1

5. Wang G, Bonkovsky HL, de Lemos A, Burczynski FJ. Recent insights into the biological functions of liver fatty acid binding protein 1. *J Lipid Res* (2015) 56 (12):2238–47. doi: 10.1194/jlr.R056705

6. Huang H, McIntosh AL, Martin GG, Landrock D, Chung S, Landrock KK, et al. FABP1: A novel hepatic endocannabinoid and cannabinoid binding protein. *Biochemistry* (2016) 55(37):5243–55. doi: 10.1021/acs.biochem.6b00446

7. Pi H, Liu M, Xi Y, Chen M, Tian L, Xie J, et al. Long-term exercise prevents hepatic steatosis: A novel role of FABP1 in regulation of autophagy-lysosomal machinery. *FASEB J* (2019) 33(11):11870–83. doi: 10.1096/fj.201900812R

8. Eguchi A, Iwasa M. The role of elevated liver-type fatty acid-binding proteins in liver diseases. *Pharm Res* (2021) 38(1):89–95. doi: 10.1007/s11095-021-02998-x

9. Tsai IT, Wu C-C, Hung W-C, Lee T-L, Hsuan C-F, Wei C-T, et al. FABP1 and FABP2 as markers of diabetic nephropathy. *Int J Med Sci* (2020) 17(15):2338–45. doi: 10.7150/ijms.49078

10. You H, Wen X, Zhu C, Chen M, Dong L, Zhu Y, et al. Serum FABP1 levels correlate positively with obesity in Chinese patients after laparoscopic sleeve gastrectomy: a 12-month follow-up study. *Obes Surg* (2020) 30(3):931–40. doi: 10.1007/s11695-019-04307-3

11. de Jonge C, Rensen SS, Koek GH, Joosten MF, Buurman WA, Bouvy ND, et al. Endoscopic duodenal-jejunal bypass liner rapidly improves plasma parameters of nonalcoholic fatty liver disease. *Clin Gastroenterol Hepatol* (2013) 11(11):1517–20. doi: 10.1016/j.cgh.2013.07.029

12. Chang X, Cai H, Yin K. The regulations and mechanisms of laparoscopic sleeve gastrectomy (LSG) for obesity and type 2 diabetes: A systematic review. *Surg Laparoscopy Endosc Percutaneous Techniques* (2017) 27(6):e122–6. doi: 10.1097/SLE.0000000000000468

13. Pelsers MM, Hermens WT, Glatz JF. Fatty acid-binding proteins as plasma markers of tissue injury. *Clin Chim Acta* (2005) 352(1-2):15–35. doi: 10.1016/j.cccn.2004.09.001

14. Nakamura T, Sugaya T, Kawagoe Y, Ueda Y, Osada S, Koide H. Effect of pitavastatin on urinary liver-type fatty acid-binding protein levels in patients with early diabetic nephropathy. *Diabetes Care* (2005) 28(11):2728–32. doi: 10.2337/diacare.28.11.2728

15. Karvellas CJ, Speiser JL, Tremblay M, Lee WM, Rose CF. Elevated FABP1 serum levels are associated with poorer survival in acetaminophen-induced acute liver failure. *Hepatology* (2017) 65(3):938–49. doi: 10.1002/hep.28945

16. Mandal AK, Mount DB. The molecular physiology of uric acid homeostasis. *Annu Rev Physiol* (2015) 77:323–45. doi: 10.1146/annurev-physiol-021113-170343

17. Joosten LAB, Crişan TO, Bjornstad P, Johnson RJ. Asymptomatic hyperuricaemia: A silent activator of the innate immune system. *Nat Rev Rheumatol* (2020) 16(2):75–86. doi: 10.1038/s41584-019-0334-3

18. Kim SY, Guevara JP, Kim KM, Choi HK, Heitjan DF, Albert DA. Hyperuricemia and coronary heart disease: a systematic review and meta-analysis. *Arthritis Care Res (Hoboken)* (2010) 62(2):170–80. doi: 10.1002/acr.20065

19. Spatola L, Ferraro PM, Gambaro G, Badalamenti S, Dauriz M. Metabolic syndrome and uric acid nephrolithiasis: Insulin resistance in focus. *Metabolism* (2018) 83:225–33. doi: 10.1016/j.metabol.2018.02.008

20. Han Y, Han X, Yin Y, Cao Y, Di H, Wu J, et al. Dose-response relationship of uric acid with fasting glucose, insulin, and insulin resistance in a united states cohort of 5,148 non-diabetic people. *Front Med (Lausanne)* (2022) 9:905085. doi: 10.3389/fmed.2022.905085

21. Binas B, Erol E. FABPs as determinants of myocellular and hepatic fuel metabolism. *Mol Cell Biochem* (2007) 299(1-2):75–84. doi: 10.1007/s11010-005-9043-0

22. Prinetti A, Mitro N. FABP1 in wonderland. *J Neurochem* (2016) 138(3):371–3. doi: 10.1111/jnc.13685

23. Atshaves BP, Martin GG, Hostetler HA, McIntosh AL, Kier AB, Schroeder F. Liver fatty acid-binding protein and obesity. *J Nutr Biochem* (2010) 21(11):1015–32. doi: 10.1016/j.jnutbio.2010.01.005

24. Gajda AM, Storch J. Enterocyte fatty acid-binding proteins (FABPs): Different functions of liver and intestinal FABPs in the intestine. *Prostaglandins Leukot Essent Fatty Acids* (2015) 93:9–16. doi: 10.1016/j.plefa.2014.10.001

25. Hostetler HA, McIntosh AL, Atshaves BP, Storey SM, Payne HR, Kier AB, et al. L-FABP directly interacts with PPARalpha in cultured primary hepatocytes. *J Lipid Res* (2009) 50(8):1663–75. doi: 10.1194/jlr.M900058-JLR200

26. Thumser AE, Moore JB, Plant NJ. Fatty acid binding proteins: tissue-specific functions in health and disease. *Curr Opin Clin Nutr Metab Care* (2014) 17(2):124–9. doi: 10.1097/mco.0000000000000031

27. Newberry EP, Kennedy S, Xie Y, Luo J, Jiang H, Ory DS, et al. Phenotypic divergence in two lines of l-fabp-/- mice reflects substrain differences and environmental modifiers. *Am J Physiol Gastrointest Liver Physiol* (2015) 309(8):G648–61. doi: 10.1152/ajpgi.00170.2015

28. Newberry EP, Xie Y, Kennedy SM, Luo J, Davidson NO. Protection against Western diet-induced obesity and hepatic steatosis in liver fatty acid-binding protein knockout mice. *Hepatology* (2006) 44(5):1191–205. doi: 10.1002/hep.21369

29. Shi J, Zhang Y, Gu W, Cui B, Xu M, Yan Q, et al. Serum liver fatty acid binding protein levels correlate positively with obesity and insulin resistance in Chinese young adults. *PloS One* (2012) 7(11):e48777. doi: 10.1371/journal.pone.0048777

30. Iguchi N, Uchiyama A, Ueta K, Sawa Y, Fujino Y. Neutrophil gelatinase-associated lipocalin and liver-type fatty acid-binding protein as biomarkers for acute kidney injury after organ transplantation. *J Anesth* (2015) 29(2):249–55. doi: 10.1007/s00540-014-1909-4

31. Golomb I, Ben David M, Glass A, Kolitz T, Keidar A. Long-term metabolic effects of laparoscopic sleeve gastrectomy. *JAMA Surg* (2015) 150(11):1051–7. doi: 10.1001/jamasurg.2015.2202

32. Romero-Talamás H, Daigle CR, Aminian A, Corcelles R, Brethauer SA, Schauer PR. The effect of bariatric surgery on gout: a comparative study. *Surg Obes Relat Dis* (2014) 10(6):1161–5. doi: 10.1016/j.soard.2014.02.025

33. Antozzi P, Soto F, Arias F, Carrodeguas L, Ropos T, Zundel N, et al. Development of acute gouty attack in the morbidly obese population after bariatric surgery. *Obes Surg* (2005) 15(3):405–7. doi: 10.1381/0960892053576802

34. Wan X, Xu C, Lin Y, Lu C, Li D, Sang J, et al. Uric acid regulates hepatic steatosis and insulin resistance through the NLRP3 inflammasome-dependent mechanism. *J Hepatol* (2016) 64(4):925–32. doi: 10.1016/j.jhep.2015.11.022

35. Iracheta-Vellve A, Petrasek J, Satishchandran A, Gyongyosi B, Saha B, Kodys K, et al. Inhibition of sterile danger signals, uric acid and ATP, prevents inflammasome activation and protects from alcoholic steatohepatitis in mice. *J Hepatol* (2015) 63(5):1147–55. doi: 10.1016/j.jhep.2015.06.013

36. Xu C, Wan X, Xu L, Weng H, Yan M, Miao M, et al. Xanthine oxidase in non-alcoholic fatty liver disease and hyperuricemia: One stone hits two birds. *J Hepatol* (2015) 62(6):1412–9. doi: 10.1016/j.jhep.2015.01.019

37. Molla NH, Kathak RR, Sumon AH, Barman Z, Mou AD, Hasan A, et al. Assessment of the relationship between serum uric acid levels and liver enzymes activity in Bangladeshi adults. *Sci Rep* (2021) 11(1):20114. doi: 10.1038/s41598-021-99623-z

38. Mukai T, Egawa M, Takeuchi T, Yamashita H, Kusudo T. Silencing of FABP1 ameliorates hepatic steatosis, inflammation, and oxidative stress in mice with nonalcoholic fatty liver disease. *FEBS Open Bio* (2017) 7(7):1009–16. doi: 10.1002/2211-5463.12240

frontiers | Frontiers in Endocrinology

TYPE Original Research
PUBLISHED 07 October 2022
DOI 10.3389/fendo.2022.999928

OPEN ACCESS

EDITED BY
Sanyuan Hu,
Qianfoshan Hospital, Shandong University, China

REVIEWED BY
Yanmin Wang,
California Medical Innovations Institute, United States
Yongtao Yu,
General Hospital of Ningxia Medical University, China

*CORRESPONDENCE
Xiaodong He
hxdpumch@163.com

SPECIALTY SECTION
This article was submitted to Obesity, a section of the journal Frontiers in Endocrinology

RECEIVED 21 July 2022
ACCEPTED 16 September 2022
PUBLISHED 07 October 2022

CITATION
Zhou S, Chen W, Bai X, Chen J, Xu Q, Dong L, Chen W, Qu Q and He X (2022) Upregulation of hypothalamic POMC neurons after biliary diversion in GK rats.
Front. Endocrinol. 13:999928.
doi: 10.3389/fendo.2022.999928

Upregulation of hypothalamic POMC neurons after biliary diversion in GK rats

Shengnan Zhou[1], Weijie Chen[1], Xuesong Bai[1], Jiemin Chen[2], Qiang Xu[1], Liangbo Dong[1], Wei Chen[3], Qiang Qu[1] and Xiaodong He[1]*

[1]Department of General Surgery, State Key Laboratory of Complex Severe and Rare Diseases, Peking Union Medical College Hospital, China Academy of Medical Science & Peking Union Medical College, Beijing, China, [2]Gastroenterology Department, State Key Laboratory of Complex Severe and Rare Diseases, Peking Union Medical College Hospital, China Academy of Medical Science & Peking Union Medical College, Beijing, China, [3]Clinical Nutrition Department, State Key Laboratory of Complex Severe and Rare Diseases, Peking Union Medical College Hospital, China Academy of Medical Science & Peking Union Medical College, Beijing, China

Background: Bile acids are important signaling molecules that might activate hypothalamic neurons. This study aimed to investigate possible changes in hypothalamic pro-opiomelanocortin (POMC) neurons after biliary diversion in diabetic rats.

Methods: Ten GK rats were randomly divided into the biliary diversion (BD) and sham groups. The glucose metabolism, hypothalamic POMC expression, serum bile acid profiles, and ileal bile acid-specific receptors of the two groups were analyzed.

Results: Biliary diversion improved blood glucose (P = 0.001) and glucose tolerance (P = 0.001). RNA-Seq of the hypothalamus showed significantly upregulated expression of the POMC gene (log2-fold change = 4.1, P < 0.001), which also showed increased expression at the protein (P = 0.030) and mRNA (P = 0.004) levels. The POMC-derived neuropeptide α-melanocyte stimulating hormone (α-MSH) was also increased in the hypothalamus (2.21 ± 0.11 ng/g, P = 0.006). In addition, increased taurocholic acid (TCA) (108.05 ± 20.62 ng/mL, P = 0.003) and taurodeoxycholic acid (TDCA) (45.58 ± 2.74 ng/mL, P < 0.001) were found in the BD group and induced the enhanced secretion of fibroblast growth factor-15 (FGF15, 74.28 ± 3.44 pg/ml, P = 0.001) by activating farnesoid X receptor (FXR) that was over-expressed in the ileum.

Conclusions: Hypothalamic POMC neurons were upregulated after BD, and the increased TCA, TDCA, and the downstream gut-derived hormone FGF15 might activate POMC neurons.

KEYWORDS

biliary diversion, bile acids, FGF15, POMC neurons, metabolism

Introduction

Type 2 diabetes mellitus (T2DM) is a major public health problem that causes vascular, renal, and neurologic complications (1). The number of T2DM patients is rising worldwide, although there are many treatment approaches available to control diabetes, such as sulphonylureas and metformin, exercise and diet. T2DM still causes high rates of disability and mortality year by year because of poor compliance of patients (2). Therefore, the search for new diabetes therapies is undoubtedly an active area of research and development.

Several randomized controlled trials and animal experiments have shown that bariatric surgery, including Roux-en-Y gastric bypass (RYGB) (3), sleeve gastrectomy (SG) (4) and biliopancreatic diversion (BPD) (5), is not only highly effective at producing weight loss but also results in significant improvement in T2DM (6). Moreover, many bariatric surgeries have been recommended as antidiabetes interventions for people with T2DM (7) and obesity (8), supported by the 2nd Diabetes Surgery Summit (DSS-II) guidelines (9).

The role bile acids (BAs) has been widely recognized recently (10). They are not only involved in the digestion of lipids but also act as signaling molecules that play an important role in glucose metabolism (11). It has been reported that BA levels are elevated following bariatric surgeries and could be potential mediators that contribute to metabolic homeostasis (12). In addition, biliary diversion surgery aimed at increasing enterohepatic circulation of BAs has been found to improve glucose levels (13), which supports the metabolic role of BAs. Farnesoid X receptor (FXR) and Takeda G-protein-coupled receptor 5 (TGR5) in the ileum are the BA-specific receptors that can be activated, leading to the secretion of gut-derived hormones, such as fibroblast growth factor-15 (FGF15) (14, 15) and glucagon-like peptide-1 (GLP-1) (16–18). BAs and downstream signaling molecules can activate the corresponding receptors that are present in the rat hypothalamus to regulate energy and glucose homeostasis (19, 20). Intracerebroventricular administration of FGF19 (ortholog of FGF15 in humans) has been found to increase energy expenditure and improve glucose tolerance through binding to the FGF receptor (21) stably mediated by Klotho (a transmembrane glycoprotein) (22).

The hypothalamus is critical for maintaining metabolic homeostasis. In particular, pro-opiomelanocortin (POMC) -expressing neurons (23) can produce a derived peptide, alpha-melanocyte-stimulating hormone (a-MSH) (24), leading to the activation of melanocortin 4 receptors (MC4Rs) (25) to exert a powerful effect on whole-body glucose regulation. According to Kalsbeek et al.'s reports, T2DM patients showed a decrease in the number of POMC-immunoreactive neurons (26). In addition, the prevalence of a specific heterozygous mutation in POMC was significantly higher in patients with early-onset obesity than in normal-weight controls (27), and heterozygous mutations in POMC may interfere with the effectiveness of bariatric surgeries (28). However, whether bariatric surgery leads to changes in these hypothalamic POMC neurons and the underlying mechanisms are unclear and imprecise.

Therefore, in an attempt to determine the changes in hypothalamic POMC neurons and the unique role of BA-related signaling pathways after bariatric surgery, we performed biliary diversion to the terminal ileum in Goto-Kakizaki (GK) rats.

Materials and methods

Animals

In this study, 10 GK rats (12-week-old male) weighing approximately 320 g were purchased from Junke Bioengineering Co., Ltd. (Nanjing, P.R. China). GK rats are a nonobese model of T2DM that present typical metabolic characteristics similar to those of human diabetes. The GK rats were housed in a climate-controlled environment with a 12-h light/dark cycle and were fed a standard chow diet and tap water in the laboratory animal center before being randomly allocated to the biliary diversion (BD) group (5 rats) or the sham group (5 rats). In addition, because rats are coprophagic animals and feces contain considerable amounts of bile acids, the rats were individually housed in metabolic cages during the study (Supplementary Figure 1). All experiments and surgical preparations were performed according to protocols approved by the Experimental Animal Welfare Ethics Committee.

Operations

The rats were fasted overnight (12 hours) and anesthetized by peritoneal injection of pentobarbital sodium that suited for experiments that focus on measurement of metabolic parameters (29) (the pentobarbital sodium concentration was 1%, and the injection dose was 35-40 mg per kilogram body weight). The biliary diversion operation is to transfer the bile in the common bile duct to the distal ileum (4 cm proximal to the ileocaecal valve) through a sterilized polytetrafluoroethylene (PTFE) tube with an inner diameter of 0.3 mm and outer diameter of 0.6 mm (Figure 1A). The abdominal wall was closed using simple, interrupted 3-0 polypropylene sutures. The sham operation involved the same procedures except that the distal end of the tube was fixed to the duodenum (parallel to the level of the ampulla of Vater) so that these rats also experienced surgical stress without physiologic biliary diversion (Figure 1B). All rats were fasted and deprived of water within 12 hours after surgery. The rats started to drink 12 hours after surgery and were fed enteral nutrient solution

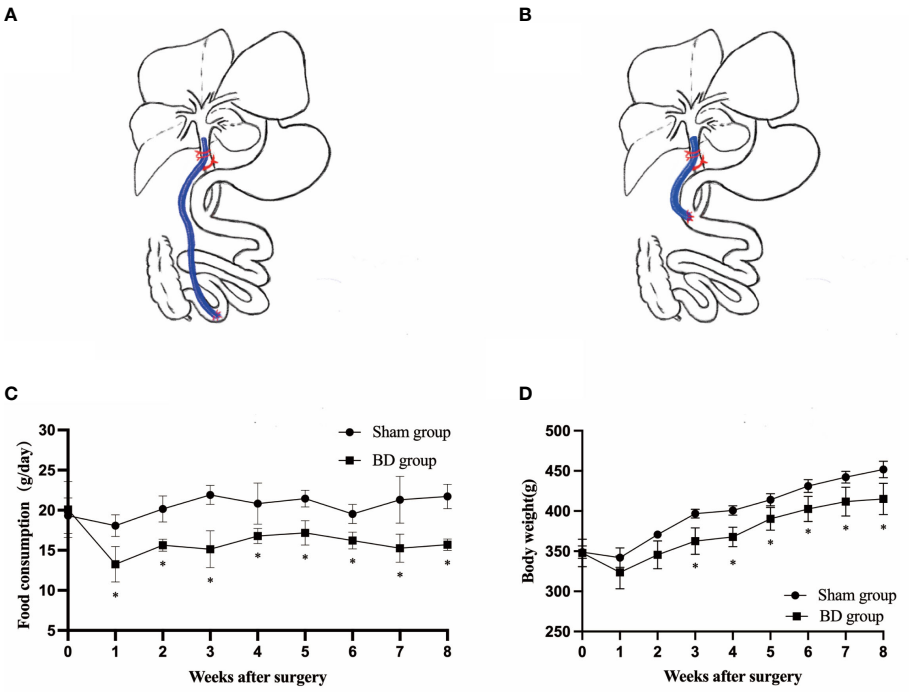

FIGURE 1
Surgical schematic and effects on body weight and food intake. **(A)** Sketch of biliary diversion of the common bile duct to the distal ileum. **(B)** Sketch of sham surgery with biliary diversion to the duodenum. **(C)** Average daily food intake in the two groups. **(D)** The body weight of the two groups. *P < 0.05.

(10% ENSURE® Enteral Nutritional Powder (TP), ABBOTT LABORATORIES B.V.) from 24 hours after surgery to the third postoperative day. The surviving rats were maintained on a regular chow diet and water after surgery until the endpoint measurements.

Food consumption and body weight

Rats were pair-fed to maintain the same food intake between the two groups and reduce the potential impact of food on glucose metabolism. The maximum food intake for 24 hours was measured without restriction from 8 am to 8 am the next day. Body weight was measured at 8 am after an overnight fast using an electronic scale.

Glucose metabolism

Random blood glucose (RBG) levels in blood from the caudal vein were tested using a glucometer (Roche, Mannheim, Germany) at any time on any two days a week from 1 week before surgery to 8 weeks after surgery. Intraperitoneal glucose tolerance tests (IPGTT) were conducted before surgery and at 2, 4, 6, and 8 weeks after surgery. After fasting overnight (12 hours), the blood glucose levels of all rats were measured 0, 30, 60, 90 and 120 min using a glucometer after an intraperitoneal injection of dextrose (50%) at 2.0 mg/g body weight (30). The trapezoidal rule was used to determine the area under the curve (AUC) for the IPGTT (AUCIPGTT).

RNA-sequencing of the hypothalamus

The rats were euthanized by anesthesia overdose at 8 postoperative weeks after an overnight fast to obtain the hypothalamus. Total ribonucleic acid was extracted from hypothalamus samples using TRIzol reagent (Invitrogen, CA, USA) according to the manufacturer's instructions. Transcriptional sequencing was implemented based on Illumina methods. An Agilent 2100 bioanalyzer was used to determine the quality and quantity of the extracted RNA from the samples. Briefly, cDNA libraries were prepared using a NEBNext® UltraTM Directional RNA Library ep Kit for Illumina®, and paired-end sequencing was performed on an Illumina HiSeq2000 sequencer. Clean read data for subsequent analysis were obtained after filtration of the raw data, a

sequencing error rate check and a GC content distribution check. The clean sequence reads were aligned to the rat genome (Rnor 6.0.104) using HISAT2 2.1.0. Differentially expressed genes (DEGs) were identified using featureCounts (2.0.1) and the DESeq2 package (1.34.0) and judged by log2 (fold-change) ≥ 1 or log2 (fold-change) ≤ −1 and a P-adjusted value of < 0.05. Kyoto Encyclopedia of Genes and Genomes (KEGG) pathway analysis was performed using the R package (v4.1.0). RNA-Seq clean data were uploaded to the National Center for Biotechnology Information Gene Expression Omnibus database with the accession number PRJNA795651.

Bile acid profiles

To identify the alteration in the bile acid profiles induced by biliary diversion, we measured and identified 18 bile acids in plasma samples collected from GK rats before surgery and 8 weeks postoperatively through targeted metabolomics analysis. At postoperative week 8, all rats were gavaged with 10% ENSURE® (1 ml/100 g body weight (31)) after fasting for 12 h. Blood was then collected from the angular vein at 2 hours after gavage. Targeted quantitative detection of serum bile acid was performed on an ultra-performance liquid chromatography-tandem mass spectrometry (UPLC–MS) platform (Waters Corporation, Milford, MA, USA) using the Waters ACQUITY UPLC I-class ULTRA high-performance liquid chromatography system combined with the Waters XEVO TQ-S tandem quadrupole mass spectrometry system. Data acquisition was carried out with MassLynx v 4.1 software (Waters Corporation, Milford, MA, USA).

Biochemical tests

Serum insulin and glucagon levels were analyzed using enzyme-linked immunosorbent assay (ELISA) kits (Solarbio Life Science, Beijing, P. R. China). Serum FGF15 was evaluated using a Rat FGF15 ELISA Kit (Solarbio Life Science, Beijing, P. R. China), and serum GLP-1 was analyzed using a Rat GLP-1 ELISA Kit (CUSABIO, Wuhan, P. R. China). Serum and hypothalamus (1 mg of tissue in 9 ml of phosphate-buffered saline) α-MSH levels were assessed using a Rat α-MSH ELISA Kit (FineTest, Wuhan, China). All kits were used according to the manufacturers' guidelines.

Western blotting

The hypothalamus and distal ileum were collected 8 weeks postsurgery and lysed in radioimmunoprecipitation assay buffer. Protein concentrations of the supernatant were quantified using the BCA Protein Assay Kit (Solarbio Life Science, Beijing, P. R. China), and equivalent amounts of protein were subjected to 10% sodium dodecyl sulfate–polyacrylamide gel electrophoresis and transferred to a 0.2 μm aperture polyvinylidene fluoride membrane. The membranes were blocked in 5% bovine serum albumin liquid and incubated with primary TGR5 (Abcam, Cambridge, UK), FXR (ABclonal, Wuhan, P.R. China), MC4R (ABclonal, Wuhan, P.R. China), Klotho (Proteintech, Wuhan, P.R. China), POMC (Wuhan, P.R. China) and β-actin (Cell Signaling Technology, Danvers, MA, USA) antibodies at 4 °C overnight. The membranes were washed three times with Tris-buffered saline and Tween 20, goat anti-rabbit (ABclonal, Wuhan, P.R. China) and goat anti-mouse (ABclonal, Wuhan, P.R. China) were incubated at room temperature for 1 hour with shaking. After three rinses with TBST solution, the membrane was scanned. The relative concentration of protein was quantified by densitometry using the Tanon Imaging System and ImageJ software.

Real-time qPCR

Complementary DNA (cDNA) was synthesized in a TaqMan-based assay from 5 μg of extracted total RNA. The primer sequences are listed in Table 1. Real-time quantitative polymerase chain reaction (qPCR) analysis was performed using SYBR Green (Roche) on a LightCycler® 480 instrument (Roche, Germany). The mRNA expression of GAPDH was used for normalization, and 2^-△△Ct values were analyzed to determine the relative mRNA expression levels.

Immunohistochemistry

Hypothalamic tissue was fixed in 4% paraformaldehyde for 24 hours. Then, these tissues were embedded in paraffin and cut into 4-μm slices. For immunohistochemistry (IHC), the slides

TABLE 1 Primer sequences Real-time qPCR.

Name	Sequences (5'→3')
TGR5 Forward	TACTCACAGGGTTGGCACTG
TGR5 Reverse	GTACCATTACAACGCGCTCAC
FXR Forward	GTACCATTACAACGCGCTCAC
FXR Reverse	AATTTCAGTTAACAAACATTCAGCC
MC4R Forward	TTGCTCGCATCCATTTGCAG
MC4R Reverse	TGCAAGCTGCCCAGATACAA
POMC Forward	TTCTGCTACAGTCGCTCAGG
POMC Reverse	GGATGCAAGCCAGCAGGT
Klotho Forward	TGGATCACCATTGACAACCC
Klotho Reverse	TTGGCGTGAGCCAAAAGTA
GAPDH Forward	GTCGGTGTGAACGGATTTGG
GAPDH Reverse	TCCCGTTGATGACCAGCTTC

were incubated with antibodies against POMC, MC4R and Klotho and goat anti-rabbit and goat anti-mouse antibodies. Images were acquired and analyzed using a microscope and Case Viewer 2.4 software.

Statistical analysis

The statistical analyses were performed using SPSS statistics software (version 25.0, IBM, Armonk, NY, USA) and Prism version 9 (GraphPad Prism, La Jolla, CA, USA). All quantitative data are expressed as the mean ± standard deviation. Student's t test (unpaired, two-tailed) and analysis of variance (ANOVA) test were used to compare the difference between the biliary diversion group and the sham group. The threshold for statistical significance was set at $P < 0.05$.

Results

Rat models

Biliary diversion and sham surgery were performed successfully in rat models. A BD rat died at postoperative week 2 because of intestinal obstruction due to abdominal adhesions, and a sham rat died at postoperative week 1 because of bile leakage. No other severe complications were observed.

Food intake and body weight

Before surgery, the daily food intake (20.10 ± 3.49 g vs. 19.33 ± 2.20 g, P = 0.722) and body weight (347.75 ± 17.24 g vs. 348.88 ± 7.77 g, P = 0.911) were not significantly different between the BD group (4 rats) and sham group (4 rats). The consumption in the BD group remained significantly lower than that in the sham group at postoperative week 8 (15.60 ± 0.59 g vs. 21.73 ± 1.52 g, P = 0.007, Figure 1C). The body weight of the BD group and the sham group was not statistically significant until the third week after surgery (362.50 ± 16.52 g vs. 396.75 ± 5.50 g, P = 0.020) Figure 1D and the difference between the two groups on food intake (P = 0.013) and body weight (P < 0.001) was also statistically significant over time through ANOVA test.

Effect on glucose metabolism

The RBG and the IPGTT were measured to evaluate the effects of biliary diversion on glucose homeostasis. The RBG levels in the BD group were significantly lower than those in the sham group (9.25 ± 0.72 mmol/L vs. 12.73 ± 0.84 mmol/L, P = 0.001) at postoperative week 8 (Figure 2A). The BD group also

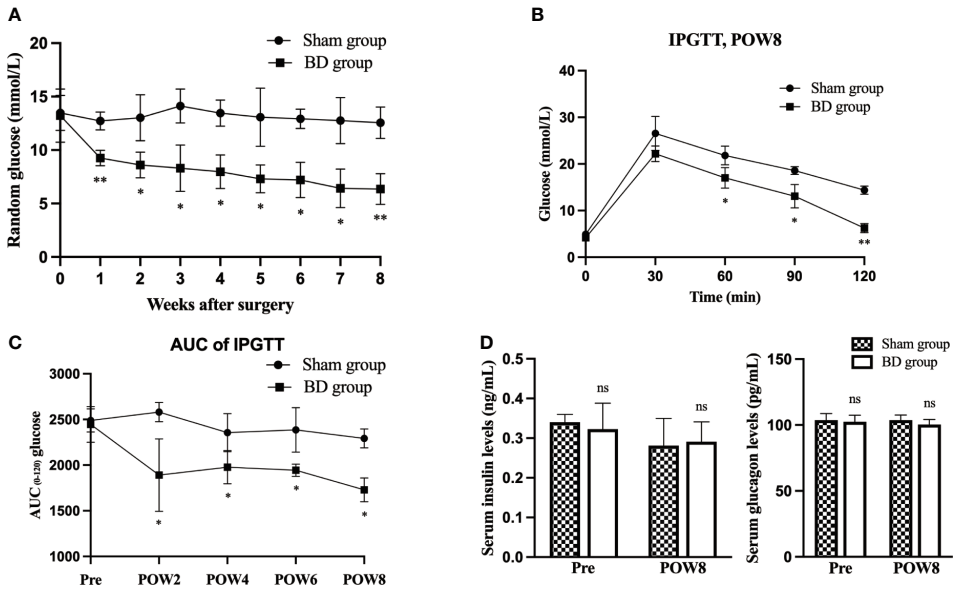

FIGURE 2
BD improved glucose homeostasis. **(A)** Random blood glucose (RBG) curves of the two groups presurgery and within 8 weeks after surgery. **(B)** Glycemic curves of intraperitoneal glucose tolerance tests (IPGTT) 8 weeks after surgery. **(C)** Area under the curve (AUC) measurements between 0 and 120 min in the IPGTT were calculated and compared between the two groups. **(D)** Serum insulin and glucagon levels in the two groups at presurgery and 8 weeks after surgery. *P < 0.05 and **P < 0.01. ns, not significant. POW, postoperative week. Pre, preoperation.

displayed improved glucose tolerance at 8 weeks postsurgery compared to the sham group (Figure 2B). In addition, the AUCIPGTT at 8 weeks (1729.00 ± 130.24 vs. 2292.00 ± 104.11, P = 0.001) postsurgery was significantly lower in the BD group than that in the sham group (Figure 2C), and the differences in RBG (P < 0.001) and AUCIPGTT (P < 0.001) between the two groups were also statistically significant over time. Moreover, the serum levels of insulin (0.29 ± 0.05 ng/ml vs. 0.28 ± 0.07 ng/ml, P = 0.823) and glucagon (100.26 ± 3.39 pg/ml vs. 103.63 ± 3.90 pg/ml, P = 0.269) did not differ significantly between the BD and sham groups (Figure 2D).

Changes in hypothalamic POMC neurons

Through RNA-seq of the hypothalamus (Figure 3A), we found that the POMC gene was significantly upregulated (log2-fold change = 4.1, P < 0.001) in the BD group compared to the sham group. According to KEGG pathway enrichment analysis (Figure 3A), the top four canonical pathways most increased in the BD group versus the sham group included cortisol synthesis and secretion, GABAergic synapse, aldosterone synthesis and secretion, and neuroactive ligand–receptor interaction signaling pathway.

The expression of POMC in the hypothalamus was measured by Western blotting. The relative expression level of hypothalamic POMC in the BD group (2.17 ± 0.45) was significantly higher than that in the sham group (1.18 ± 0.53, P = 0.030), and IHC also showed that the number of neuronal cells expressing POMC increased. For the BD group, RT–qPCR showed increased expression of the POMC gene in the hypothalamus (6.34 ± 1.29 vs. 1.03 ± 0.21, P = 0.004, Figure 3B). In addition, the concentrations of α-MSH, a POMC-derived neuropeptide, within the hypothalamus (2.21 ± 0.11 ng/g vs. 1.98 ± 0.03 ng/g, P = 0.006) and peripheral blood at 8 weeks postsurgery (4.20 ± 0.35 ng/mL vs. 2.91 ± 0.32 ng/mL, P = 0.002) were also significantly increased in the BD group (Figure 3C). The receptor of α-MSH in the hypothalamus-MC4R was also upregulated at the protein (1.43 ± 0.22 vs. 0.75 ± 0.19, P = 0.003) and mRNA levels (1.54 ± 0.31 vs. 1.00 ± 0.04, P = 0.038, Figure 3D).

Bile acid alteration and its effects on the ileum

The levels of serum total BA and 18 bile acid subclasses were not significantly different between the sham group and the BD group before surgery (Table 2). At 8 weeks after surgery, the levels of taurocholic acid (TCA, P = 0.003), taurodeoxycholic acid (TDCA, P < 0.001), and total bile acids (TBA, P = 0.035) were significantly higher in the BD group than in the sham group (Figure 4A).

The expression of the bile acid-specific receptors FXR and TGR5 in the ileum was measured by Western blotting and RT–qPCR. The expression of FXR at the protein level (0.98 ± 0.07 vs. 0.57 ± 0.15, P = 0.002) and mRNA level (2.65 ± 0.52 vs. 0.98 ± 0.25, P = 0.004) in the BD group increased, whereas that of TGR5 showed no significant change at the protein level (0.85 ± 0.13 vs. 0.95 ± 0.06, P = 0.209) and mRNA level (1.02 ± 0.27 vs. 1.01 ± 1.32, P = 0.956, Figure 4B). In addition, the BD group displayed increased serum levels of FGF15 (74.28 ± 3.44 pg/ml vs. 53.19 ± 4.72 pg/ml, P = 0.001), which is a gut-derived hormone induced by FXR agonists, compared to the sham group. However, the serum GLP-1 concentration showed no significant differences between the two groups (0.75 ± 0.04 pg/ml vs. 0.75 ± 0.05 pg/ml, P = 0.981, Figure 4C).

BAs-related receptors in the hypothalamus

Given the increased level of bile acids and upregulation of POMC genes, bile acid signaling proteins in the hypothalamus were measured. The expression of BA-specific receptors FXR and TGR5 in the hypothalamus at the protein level (0.78 ± 0.01 vs. 0.82 ± 0.04, P = 0.570; 0.84 ± 0.06 vs. 0.87 ± 0.08, P = 0.059) and mRNA level (0.81 ± 0.23 vs. 0.94 ± 0.21, P = 0.413; 0.97 ± 0.23 vs. 0.98 ± 0.17, P = 0.949) was not significantly changed between the BD group and the sham group (Figure 5A). In addition, there was also no change in the expression of these two receptors at the gene level, which refuted the hypothesis that specific bile acids that crossed the blood–brain barrier act directly on the hypothalamus.

The BD group displayed significantly increased levels of FGF15 in serum (Figure 4C) and brain (110.91 ± 15.69 pg/g vs. 78.21 ± 4.58 pg/g, P = 0.007, Figure 5B), which could bind to the coreceptor Klotho in the hypothalamus. In view of the results of RNA-Seq that Klotho did not show a significant difference between the two groups, we detected the expression of Klotho through WB and RT–qPCR. Compared with the sham group, the BD group showed significantly increased expression of Klotho at the protein (5.22 ± 1.25 vs. 2.39 ± 0.97, P = 0.012) and mRNA levels (4.87 ± 0.56 vs. 1.03 ± 0.20, P < 0.001, Figure 5C). Moreover, IHC staining also showed that the expression of Klotho was increased in hypothalamic cells in the BD group compared with the sham group.

Discussion

Biliary diversion resulted in improvements in glucose homeostasis and reduced food consumption and body weight of GK rats, which agreed with previous findings (32, 33). The levels of RBG and AUCIPGTT in the BD group decreased significantly after surgery and were lower than those in the

10.3389/fendo.2022.999928

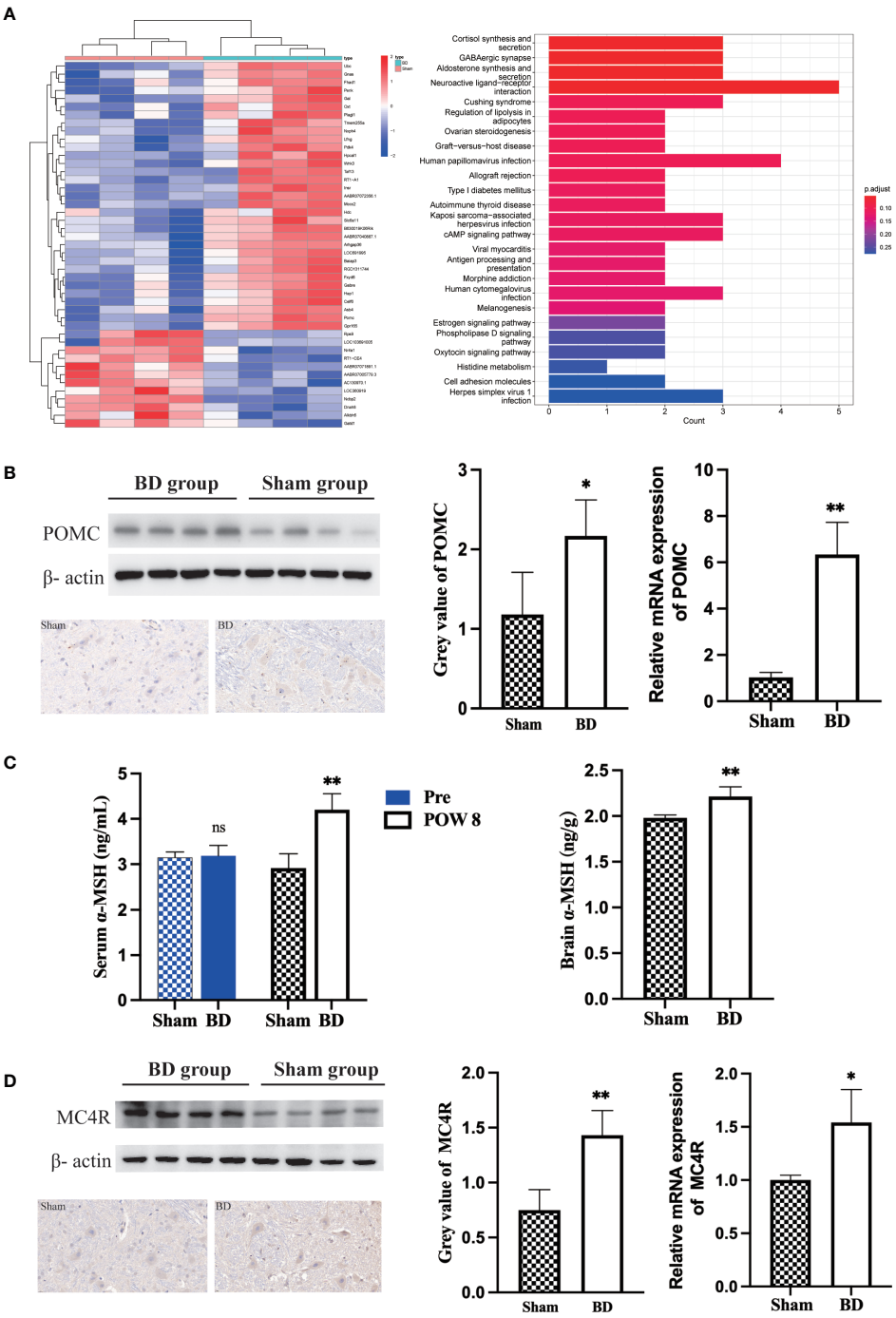

FIGURE 3
Biliary diversion altered hypothalamic gene expression and the related signaling pathway. **(A)** Left, clustered heatmap of the hypothalamic differentially expressed genes between the two groups. Right, the 25 most differentially expressed pathways between the two groups through KEGG analysis. **(B)** Western blots, IHC and RT–qPCR of POMC in the hypothalamus 8 weeks after surgery. **(C)** The concentration of α-MSH in the serum and hypothalamus 8 weeks after surgery in the two groups. **(D)** Western blots, IHC and RT–qPCR of MC4R in the hypothalamus 8 weeks after surgery. *P < 0.05. **P < 0.01. Scale bar = 10 μm. Sham, Sham group. BD, biliary diversion group.

10.3389/fendo.2022.999928

TABLE 2 Serum bile acid species and levels (ng/ml) detected by targeted metabolomics.

Items	Before surgery			After surgery		
	Sham group (n=5)	BD group (n=5)	P value	Sham group (n=4)	BD group (n=4)	P value
TCA	53.15 ± 2.72	52.30 ± 3.51	0.679	55.71 ± 4.72	108.05 ± 20.62	0.003
TUDCA	15.34 ± 4.40	12.49 ± 2.13	0.228	13.31 ± 3.92	12.93 ± 2.52	0.874
THDCA	55.35 ± 5.76	56.32 ± 6.13	0.803	52.27 ± 2.68	51.49 ± 8.82	0.871
TDCA	21.81 ± 2.44	22.49 ± 2.23	0.656	25.20 ± 1.45	45.58 ± 2.74	0.000
GUDCA	1.62 ± 0.33	1.41 ± 0.26	0.275	1.29 ± 0.07	1.73 ± 0.93	0.379
GCDCA	5.95 ± 0.37	5.95 ± 0.37	0.990	6.55 ± 0.91	7.15 ± 1.11	0.435
GDCA	4.30 ± 1.18	5.28 ± 0.75	0.163	4.58 ± 0.41	4.66 ± 0.64	0.826
GCA	61.77 ± 13.94	60.37 ± 15.30	0.884	62.46 ± 16.87	67.00 ± 14.48	0.697
HDCA	22.32 ± 8.01	25.44 ± 6.23	0.511	25.06 ± 16.87	22.82 ± 11.83	0.769
αMCA	132.58 ± 38.37	123.59 ± 27.58	0.682	123.55 ± 29.77	131.71 ± 38.66	0.749
βMCA	234.86 ± 30.51	223.60 ± 37.89	0.619	248.21 ± 39.35	236.34 ± 40.87	0.691
CA	235.10 ± 40.85	238.38 ± 29.08	0.888	237.68 ± 12.06	259.32 ± 77.04	0.599
TLCA	0.28 ± 0.06	0.29 ± 0.07	0.902	0.20 ± 0.08	0.22 ± 0.06	0.722
DCA	148.20 ± 32.86	154.40 ± 32. 46	0.772	157.53 ± 20.81	143.13 ± 42.03	0.562
CDCA	68.71 ± 5.87	66.70 ± 6.22	0.613	67.33 ± 2.92	67.90 ± 6.69	0.882
LCA	8.34 ± 0.88	8.48 ± 0.96	0.811	7.73 ± 0.76	8.63 ± 1.62	0.238
TαMCA+TβMCA	118.13 ± 18.70	113.10 ± 18.03	0.676	103.35 ± 12.04	287.98 ± 176.69	0.128
TBA	1187.81 ± 86.57	1170.57 ± 47.33	0.706	1192.01 ± 35.17	1456.64 ± 150.22	0.035

TCA, taurocholic acid; TUDCA, tauroursodeoxycholic acid; THDCA, taurohyodeoxycholic acid.
TDCA, taurodeoxycholic acid; GUDCA, glycoursodeoxycholic acid; GCDCA, glycochenodeoxycholic acid.
GDCA, glycodeoxycholic acid; GCA, glycocholic acid; HDCA, hyodeoxycholic acid.
αMCA, alpha-muricholic acid; βMCA, beta-muricholic acid; CA, cholic acid.
TLCA, Taurolithocholic acid; DCA, deoxycholic acid.
CDCA, chenodeoxycholic acid; LCA, Lithocholic acid; TαMCA, tauro-alpha-muricholic acid.
TβMCA, tauro-beta-muricholic acid; TBA, total bile acids.

sham group at postoperative week 8. The model procedure eliminated other factors that may affect metabolism, such as stomach capacity (34), alimentary path and pancreatic juice.

The hypothalamus is an appetite regulation center, and we found that anorexigenic (appetite-reducing) POMC neurons were upregulated at the gene, mRNA and protein levels through RNA-seq, RT–qPCR, WB and IHC. Over the years, the recognition of the importance of the hypothalamus in glucose metabolism and appetite regulation has inspired a new wave of research on neural pathways (35). POMC neurons, as one of the most intensively studied populations of hypothalamic neurons, have been found to express receptors corresponding to different circulatory factors, such as leptin (36), insulin (37), PYY (38) and GLP-1/2 (39). Some animal and clinical studies have focused on the abovementioned gut hormones and reported related alterations caused by bariatric surgery (40) (41). Our results showed that the serum levels of GLP-1, its upstream receptor TGR5, and its downstream molecule insulin were not significantly changed in the BD group, which may be because biliary diversion to the ileum did not change the rate of nutrient entry into the intestine (42), which suggests that there are other signaling molecules and pathways responsible for the upregulation of the POMC gene, such as the bile acids that have significantly changed after bariatric surgery.

Several studies have identified the metabolic benefit of increased bile acid through FXR and TGR5 in bariatric surgery. Through bile acid-targeted metabolomics, the serum concentrations of TCA and TDCA were found to be significantly increased in the BD group (43). TCA and TDCA were identified as FXR agonists (44), and the activation of FXR signaling potently induced gut-derived hormone secretion and improved glucose homeostasis in subjects who received RYGB (45) and SG (46). The expression of FXR in the distal ileum was significantly increased in the BD group. In addition, the serum concentrations of FGF15, which is secreted from the intestine into the blood induced by the activation of FXR, were also increased. This proved that elevated TCA and TDCA levels upregulated the intestinal FXR-FGF15 signaling pathway. However, among the two identified bile acid subtypes of FXR agonists, which subtype acts as the determinant in the regulation of glucose metabolism was not determined. Thus, the effect of altered bile acids observed in the BD group was predominantly on the bile acid-specific receptor FXR and the downstream of the intestinal endogenous molecule FGF15.

FGF15/19, as an intestinal hormone, has been shown to regulate glucose homeostasis (47) by binding to FGF receptors and the coreceptor Klotho, which are located in different tissues, such as the liver (48), adipose tissue (49), and the brain (50).

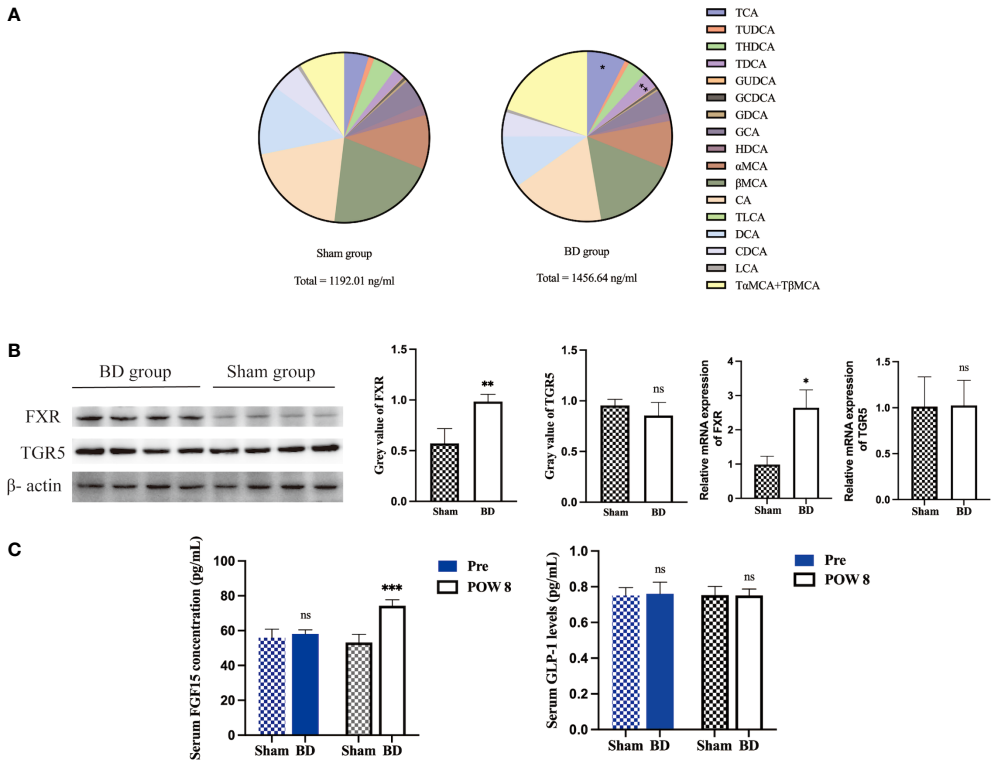

FIGURE 4
Altered bile acid pools and related signaling in the ileum after surgery. **(A)** Bile acid abundance and composition in the two groups 8 weeks after surgery. **(B)** Western blots and RT–qPCR of FXR and TGR5 in ileum tissue harvested from the two groups 8 weeks after surgery. **(C)** Serum FGF15 and GLP-1 concentrations presurgery and 8 weeks after surgery. *P < 0.05, **P < 0.01 and ***P < 0.001. ns, not significant. POW, postoperative week. Pre, preoperation. Sham, Sham group. BD, biliary diversion group.

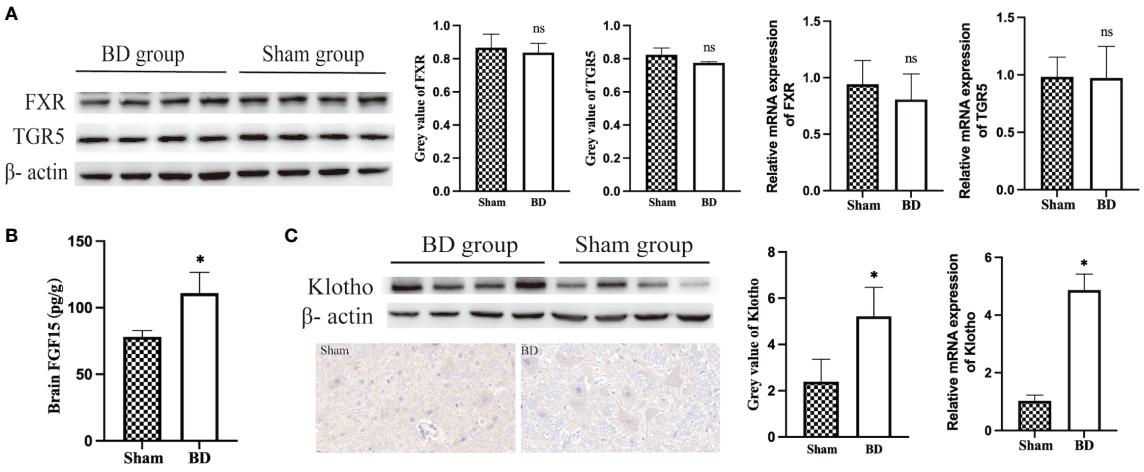

FIGURE 5
Bile acids and FGF15 receptors in the hypothalamus. **(A)** Western blots and RT–qPCR of bile acid receptors in the hypothalamus harvested from the two groups 8 weeks after surgery. **(B)** FGF15 concentration in brain tissue. **(C)** Western blots, IHC and RT–qPCR of Klotho in the hypothalamus harvested from the two groups 8 weeks after surgery. *P < 0.05. ns, not significant. Scale bar = 10 μm. Sham, Sham group. BD, biliary diversion group.

Some studies have reported that FGF19 exerts insulin-like activity that increases protein and glycogen synthesis independent of insulin through the FGF19-βKlotho axis in the liver (51, 52). Recent studies focused on the mechanism of the metabolic benefits of FGF15 indicated that FGF15 suppressed glucagon secretion (53) and silenced hypothalamic AGRP/NPY neurons (54), and the beneficial metabolic effects of FGFs on body weight and insulin sensitivity were absent in mice lacking Klotho in the nervous system (55). Our results showed that the level of FGF15 was significantly increased and that the coreceptor Klotho was also highly expressed in the hypothalamus. Therefore, it is reasonable to assume that the increased FGF15 was associated with the upregulation of POMC neurons.

POMC-derived peptide, α-MSH, is a well-known regulator of the central nervous system that can bind to and activate MC4R neurons (56), which leads to appetite inhibition and body weight loss (56) and is responsible for improved glucose homeostasis (57). Our results suggest that bile diversion may related to the activated hypothalamic POMC-α-MSH-MC4R signaling pathway, which exerts appetite-reducing effects that have been well accepted. In addition, BD not only increased the concentration of α-MSH in hypothalamic tissues but also increased α-MSH levels in the peripheral circulatory system. Peripheral α-MSH increases glucose uptake in skeletal muscles and enhances glucose clearance by activating muscle MC5R and protein kinase A (58). Subsequently, Rodrigues AR et al. (59) found that α-MSH promoted white adipose tissue (WAT) browning and upregulated insulin-dependent glucose transporter type 4 (GLUT4) in WAT, which also increased glucose clearance.

There are a few limitations in our study. One major limitation is that our animal and molecular studies do not allow us to identify the causal relation of increased BAs, FGF15 and the upregulation of the POMC gene in the hypothalamus. More studies are needed to investigate the underlying neuronal circuitry engaged by FGF15, such as the antagonism of FGF receptors or BAs. In addition, the other limitations of animal experiments is species differences and the small sample size. Thus, predicting the potential pathways in humans based on the results of GK rats is complicated, and more research and additional data are needed to prove the underlying glucose homeostatic mechanism of bariatric surgery in the future on the basis of an enlarged sample size.

In conclusion, biliary diversion to the distal ileum led to decreased appetite and weight loss, as well as sustained hyperglycemia improvements in GK rats. POMC neurons are significantly overexpressed in the hypothalamus and might be activated by increased TCA, TDCA, and FGF15 levels after BD.

Data availability statement

The original contributions presented in the study are included in the article/Supplementary Material, further inquiries can be directed to the corresponding author. The datasets of RNA-Seq in this study can be found in online repositories. The names of the repository/repositories and accession number(s) can be found below: https://dataview.ncbi.nlm.nih.gov/object/PRJNA795651.

Ethics statement

The animal study was reviewed and approved by Experimental Animal Welfare Ethics Committee of Peking Union Medical College Hospital.

Author contributions

SZ, WJC, and XH contributed to conception and design of the study. SZ, XB, QX, JC, and LD organized the database and performed the statistical analysis. SZ wrote the first draft of the manuscript. WC and QQ wrote sections of the manuscript. All authors contributed to the article and approved the submitted version.

Funding

This work was supported by the Program Focus Health of Liver and Gallbladder in Elder (ZYJ201912), China Academy of Medical Science Innovation Fund for Medical Sciences (2021-1-I2M-022) and National Natural Science Foundation of China (81970763).

Acknowledgments

We would like to thank Dr Kegong Tang and his colleagues, State Key Laboratory of Medical Molecular Biology, Institute of Basic Medical Sciences, Chinese Academy of Medical Sciences, Department of Biochemistry, Peking Union Medical College, for their invaluable technical efforts related to this project and the usage of the basic experimental facilities.

Conflict of interest

The authors declare that the research was conducted in the absence of any commercial or financial relationships that could be construed as a potential conflict of interest.

Publisher's note

Supplementary material

The Supplementary Material for this article can be found online at: https://www.frontiersin.org/articles/10.3389/fendo.2022.999928/full#supplementary-material

SUPPLEMENTARY FIGURE 1
Metabolic cages used for housing GK rats.

References

1. Vijan S. Type 2 diabetes. *Ann Intern Med* (2019) 171:ITC65–80. doi: 10.7326/AITC201911050

2. Nauck MA, Wefers J, Meier JJ. Treatment of type 2 diabetes: challenges, hopes, and anticipated successes. *Lancet Diabetes Endocrinol* (2021) 9:525–44. doi: 10.1016/S2213-8587(21)00113-3

3. Osto E, Doytcheva P, Corteville C, Bueter M, Dorig C, Stivala S, et al. Rapid and body weight-independent improvement of endothelial and high-density lipoprotein function after roux-en-Y gastric bypass: role of glucagon-like peptide-1. *Circulation* (2015) 131:871–81. doi: 10.1161/CIRCULATIONAHA.114.011791

4. Jahansouz C, Xu H, Hertzel AV, Serrot FJ, Kvalheim N, Cole A, et al. Bile acids increase independently from hypocaloric restriction after bariatric surgery. *Ann Surg* (2016) 264:1022–8. doi: 10.1097/SLA.0000000000001552

5. Ferrannini E, Camastra S, Astiarraga B, Nannipieri M, Castro-Perez J, Xie D, et al. Increased bile acid synthesis and deconjugation after biliopancreatic diversion. *Diabetes* (2015) 64:3377–85. doi: 10.2337/db15-0214

6. Mingrone G, Panunzi S, De Gaetano A, Guidone C, Iaconelli A, Nanni G, et al. Bariatric-metabolic surgery versus conventional medical treatment in obese patients with type 2 diabetes: 5 year follow-up of an open-label, single-centre, randomised controlled trial. *Lancet* (2015) 386:964–73. doi: 10.1016/S0140-6736(15)00075-6

7. Syn NL, Cummings DE, Wang LZ, Lin DJ, Zhao JJ, Loh M, et al. Association of metabolic-bariatric surgery with long-term survival in adults with and without diabetes: a one-stage meta-analysis of matched cohort and prospective controlled studies with 174 772 participants. *Lancet* (2021) 397:1830–41. doi: 10.1016/S0140-6736(21)00591-2

8. Mingrone G, Panunzi S, De Gaetano A, Guidone C, Iaconelli A, Capristo E, et al. Metabolic surgery versus conventional medical therapy in patients with type 2 diabetes: 10-year follow-up of an open-label, single-centre, randomised controlled trial. *Lancet* (2021) 397:293–304. doi: 10.1016/S0140-6736(20)32649-0

9. Rubino F, Nathan DM, Eckel RH, Schauer PR, Alberti KG, Zimmet PZ, et al. Metabolic surgery in the treatment algorithm for type 2 diabetes: A joint statement by international diabetes organizations. *Diabetes Care* (2016) 39:861–77. doi: 10.2337/dc16-0236

10. Ahlin S, Cefalo C, Bondia-Pons I, Capristo E, Marini L, Gastaldelli A, et al. Bile acid changes after metabolic surgery are linked to improvement in insulin sensitivity. *Br J Surg* (2019) 106:1178–86. doi: 10.1002/bjs.11208

11. Browning MG, Pessoa BM, Khoraki J, Campos GM. Changes in bile acid metabolism, transport, and signaling as central drivers for metabolic improvements after bariatric surgery. *Curr Obes Rep* (2019) 8:175–84. doi: 10.1007/s13679-019-00334-4

12. Albaugh VL, Banan B, Ajouz H, Abumrad NN, Flynn CR. Bile acids and bariatric surgery. *Mol Aspects Med* (2017) 56:75–89. doi: 10.1016/j.mam.2017.04.001

13. Flynn CR, Albaugh VL, Cai S, Cheung-Flynn J, Williams PE, Brucker RM, et al. Bile diversion to the distal small intestine has comparable metabolic benefits to bariatric surgery. *Nat Commun* (2015) 6:7715. doi: 10.1038/ncomms8715

14. Ryan PM, Hayward NE, Sless RT, Garwood P, Rahmani J. Effect of bariatric surgery on circulating FGF-19: A systematic review and meta-analysis. *Obes Rev* (2020) 21:e13038. doi: 10.1111/obr.13038

15. Bozadjieva N, Heppner KM, Seeley RJ, Targeting FXR. And FGF19 to treat metabolic diseases-lessons learned from bariatric surgery. *Diabetes* (2018) 67:1720–8. doi: 10.2337/dbi17-0007

16. Chaudhari SN, Luo JN, Harris DA, Aliakbarian H, Yao L, Paik D, et al. A microbial metabolite remodels the gut-liver axis following bariatric surgery. *Cell Host Microbe* (2021) 29:408–424 e7. doi: 10.1016/j.chom.2020.12.004

17. Chaudhari SN, Harris DA, Aliakbarian H, Luo JN, Henke MT, Subramaniam R, et al. Bariatric surgery reveals a gut-restricted TGR5 agonist with anti-diabetic effects. *Nat Chem Biol* (2020) 17(1):20–9. doi: 10.1101/2020.01.10.902346

18. Scholtz S, Miras AD, Chhina N, Prechtl CG, Sleeth ML, Daud NM, et al. Obese patients after gastric bypass surgery have lower brain-hedonic responses to food than after gastric banding. *Gut* (2014) 63:891–902. doi: 10.1136/gutjnl-2013-305008

19. Castellanos-Jankiewicz A, Guzman-Quevedo O, Fenelon VS, Zizzari P, Quarta C, Bellocchio L, et al. Hypothalamic bile acid-TGR5 signaling protects from obesity. *Cell Metab* (2021) 33(7):1483–1492.e10. doi: 10.1016/j.cmet.2021.04.009

20. Fortin SM, Lipsky RK, Lhamo R, Chen J, Kim E, Borner T, et al. GABA neurons in the nucleus tractus solitarius express GLP-1 receptors and mediate anorectic effects of liraglutide in rats. *Sci Transl Med* (2020) 12(533):eaay8071. doi: 10.1126/scitranslmed.aay8071

21. Ryan KK, Kohli R, Gutierrez-Aguilar R, Gaitonde SG, Woods SC, Seeley RJ. Fibroblast growth factor-19 action in the brain reduces food intake and body weight and improves glucose tolerance in male rats. *Endocrinology* (2013) 154:9–15. doi: 10.1210/en.2012-1891

22. Jackson TC, Janesko-Feldman K, Carlson SW, Kotermanski SE, Kochanek PM. Robust RBM3 and beta-klotho expression in developing neurons in the human brain. *J Cereb Blood Flow Metab* (2019) 39:2355–67. doi: 10.1177/0271678X19878889

23. Harno E, Gali Ramamoorthy T, Coll AP, White A. POMC: The physiological power of hormone processing. *Physiol Rev* (2018) 98:2381–430. doi: 10.1152/physrev.00024.2017

24. Jais A, Bruning JC. Arcuate nucleus-dependent regulation of metabolism - pathways to obesity and diabetes mellitus. *Endocr Rev* (2021) 43(2):314–28. doi: 10.1210/endrev/bnab025

25. Krashes MJ, Lowell BB, Garfield AS. Melanocortin-4 receptor-regulated energy homeostasis. *Nat Neurosci* (2016) 19:206–19. doi: 10.1038/nn.4202

26. Kalsbeek MJ, Wolff SE, Korpel NL, la Fleur SE, Romijn JA, Fliers E, et al. The impact of antidiabetic treatment on human hypothalamic infundibular neurons and microglia. *JCI Insight 5* (2020) 5(16):e133868. doi: 10.1172/jci.insight.133868

27. Challis BG, Pritchard LE, Creemers JW, Delplanque J, Keogh JM, Luan J, et al. A missense mutation disrupting a dibasic prohormone processing site in pro-opiomelanocortin (POMC) increases susceptibility to early-onset obesity through a novel molecular mechanism. *Hum Mol Genet* (2002) 11:1997–2004. doi: 10.1093/hmg/11.17.1997

28. Poitou C, Puder L, Dubern B, Krabusch P, Genser L, Wiegand S, et al. Long-term outcomes of bariatric surgery in patients with bi-allelic mutations in LEPR, and MC4R genes. *Surg Obes Relat Dis* (2021) 17:1449–56. doi: 10.1016/j.soard.2021.04.020

29. Sano Y, Ito S, Yoneda M, Nagasawa K, Matsuura N, Yamada Y, et al. Effects of various types of anesthesia on hemodynamics, cardiac function, and glucose and lipid metabolism in rats. *Am J Physiol Heart Circ Physiol* (2016) 311:H1360–6. doi: 10.1152/ajpheart.00181.2016

30. Andrikopoulos S, Blair AR, Deluca N, Fam BC, Proietto J. Evaluating the glucose tolerance test in mice. *Am J Physiol Endocrinol Metab* (2008) 295:E1323–32. doi: 10.1152/ajpendo.90617.2008

31. Wei M, Shao Y, Liu QR, Wu QZ, Zhang X, Zhong MW, et al. Bile acid profiles within the enterohepatic circulation in a diabetic rat model after bariatric surgeries. *Am J Physiol Gastrointest Liver Physiol* (2018) 314:G537–46. doi: 10.1152/ajpgi.00311.2017

32. Poland JC, Schrimpe-Rutledge AC, Sherrod SD, Flynn CR, McLean JA. Utilizing untargeted ion mobility-mass spectrometry to profile changes in the gut metabolome following biliary diversion surgery. *Anal Chem* (2019) 91:14417–23. doi: 10.1021/acs.analchem.9b02924

33. Ray K. Surgery: Bile diversion comparable to bariatric surgery in mice. *Nat Rev Gastroenterol Hepatol* (2015) 12:488. doi: 10.1038/nrgastro.2015.130

34. Zhang X, Yu B, Yang D, Qiao Z, Cao T, Zhang P. Gastric volume reduction is essential for the remission of type 2 diabetes mellitus after bariatric surgery in nonobese rats. *Surg Obes Relat Dis* (2016) 12:1569–76. doi: 10.1016/j.soard.2016.04.018

35. Kim KS, Seeley RJ, Sandoval DA. Signalling from the periphery to the brain that regulates energy homestasis. *Nat Neurosci*. (2018) 19(4):185–96. doi: 10.1038/nrn.2018.8

36. da Silva AA, do Carmo JM, Hall JE. CNS regulation of glucose homeostasis: Role of the leptin-melanocortin system. *Curr Diabetes Rep* (2020) 20:29. doi: 10.1007/s11892-020-01311-1

37. Dodd GT, Decherf S, Loh K, Simonds SE, Wiede F, Balland E, et al. Leptin and insulin act on POMC neurons to promote the browning of white fat. *Cell* (2015) 160:88–104. doi: 10.1016/j.cell.2014.12.022

38. Batterham RL, Cowley MA, Small CJ, Herzog H, Cohen MA, Dakin CL, et al. Gut hormone PYY(3-36) physiologically inhibits food intake. *Nature* (2002) 418:650–4. doi: 10.1038/nature00887

39. Shi X, Zhou F, Li X, Chang B, Li D, Wang Y, et al. Central GLP-2 enhances hepatic insulin sensitivity *via* activating PI3K signaling in POMC neurons. *Cell Metab* (2013) 18:86–98. doi: 10.1016/j.cmet.2013.06.014

40. Tsoli M, Chronaiou A, Kehagias I, Kalfarentzos F, Alexandrides TK. Hormone changes and diabetes resolution after biliopancreatic diversion and laparoscopic sleeve gastrectomy: a comparative prospective study. *Surg Obes Relat Dis* (2013) 9:667–77. doi: 10.1016/j.soard.2012.12.006

41. Kawasaki T, Ohta M, Kawano Y, Masuda T, Gotoh K, Inomata M, et al. Effects of sleeve gastrectomy and gastric banding on the hypothalamic feeding center in an obese rat model. *Surg Today* (2015) 45:1560–6. doi: 10.1007/s00595-015-1135-1

42. Douros JD, Tong J, D'Alessio DA. The effects of bariatric surgery on islet function, insulin secretion, and glucose control. *Endocr Rev* (2019) 40:1394–423. doi: 10.1210/er.2018-00183

43. So SSY, Yeung CHC, Schooling CM, El-Nezami H. Targeting bile acid metabolism in obesity reduction: A systematic review and meta-analysis. *Obes Rev* (2020) 21:e13017. doi: 10.1111/obr.13017

44. Monteiro-Cardoso VF, Corliano M, Singaraja RR. Bile acids: A communication channel in the gut-brain axis. *Neuromol Med* (2021) 23:99–117. doi: 10.1007/s12017-020-08625-z

45. Li K, Zou J, Li S, Guo J, Shi W, Wang B, et al. Farnesoid X receptor contributes to bidy weight-independent improvements in glycemic control after Roux-en-Y gastric bypass surgery in diet-induced obese mice. *Mol Metab*. 37:100980. doi: 10.016/j.molmet.2020.100980

46. McGavigan AK, Garibay D, Henseler ZM, Chen J, Bettaieb A, Haj FG, et al. TGR5 contributes to glucoregulatory improvements after vertical sleeve gastrectomy in mice. *Gut* (2017) 66:226–34. doi: 10.1136/gutjnl-2015-309871

47. Degirolamo C, Sabba C, Moschetta A. Therapeutic potential of the endocrine fibroblast growth factors FGF19, FGF21 and FGF23. *Nat Rev Drug Discovery* (2016) 15:51–69. doi: 10.1038/nrd.2015.9

48. Potthoff MJ, Boney-Montoya J, Choi M, He T, Sunny NE, Satapati S, et al. FGF15/19 regulates hepatic glucose metabolism by inhibiting the CREB-PGC-1alpha pathway. *Cell Metab* (2011) 13:729–38. doi: 10.1016/j.cmet.2011.03.019

49. Moron-Ros S, Uriarte I, Berasain C, Avila MA, Sabater-Masdeu M, Moreno-Navarrete JM, et al. FGF15/19 is required for adipose tissue plasticity in response to thermogenic adaptations. *Mol Metab* (2021) 43:101113. doi: 10.1016/j.molmet.2020.101113

50. Morton GJ, Matsen ME, Bracy DP, Meek TH, Nguyen HT, Stefanovski D, et al. FGF19 action in the brain induces insulin-independent glucose lowering. *J Clin Invest* (2013) 123:4799–808. doi: 10.1172/JCI70710

51. Kir S, Beddow SA, Samuel VT, Miller P, Previs SF, Suino-Powell K, et al. FGF19 as a postprandial, insulin-independent activator of hepatic protein and glycogen synthesis. *Science* (2011) 331:1621–4. doi: 10.1126/science.1198363

52. Kuro OM. The klotho proteins in health and disease. *Nat Rev Nephrol* (2019) 15:27–44. doi: 10.1038/s41581-018-0078-3

53. Picard A, Metref S, Tarussio D, Dolci W, Berney X, Croizier S, et al. Fgf15 neurons of the dorsomedial hypothalamus control glucagon secretion and hepatic gluconeogenesis. *Diabetes* (2021) 70:1443–57. doi: 10.2337/db20-1121

54. Liu S, Marcelin G, Blouet C, Jeong JH, Jo YH, Schwartz GJ, et al. A gut-brain axis regulating glucose metabolism mediated by bile acids and competitive fibroblast growth factor actions at the hypothalamus. *Mol Metab* (2018) 8:37–50. doi: 10.1016/j.molmet.2017.12.003

55. Owen BM, Mangelsdorf DJ, Kliewer SA. Tissue-specific actions of the metabolic hormones FGF15/19 and FGF21. *Trends Endocrinol Metab* (2015) 26:22–9. doi: 10.1016/j.tem.2014.10.002

56. Israeli H, Degtjarik O, Fierro F, Chunilal V, Gill AK, Roth NJ, et al. Structure reveals the activation mechanism of the MC4 receptor to initiate satiation signaling. *Science* (2021) 372:808–14. doi: 10.1126/science.abf7958

57. Zechner JF, Mirshahi UL, Satapati S, Berglund ED, Rossi J, Scott MM, et al. Weight-independent effects of roux-en-Y gastric bypass on glucose homeostasis *via* melanocortin-4 receptors in mice and humans. *Gastroenterology* (2013) 144:580–590 e7. doi: 10.1053/j.gastro.2012.11.022

58. Enriori PJ, Chen W, Garcia-Rudaz MC, Grayson BE, Evans AE, Comstock SM, et al. Alpha-melanocyte stimulating hormone promotes muscle glucose uptake *via* melanocortin 5 receptors. *Mol Metab* (2016) 5:807–22. doi: 10.1016/j.molmet.2016.07.009

59. Rodrigues AR, Salazar MJ, Rocha-Rodrigues S, Goncalves IO, Cruz C, Neves D, et al. Peripherally administered melanocortins induce mice fat browning and prevent obesity. *Int J Obes (Lond)* (2019) 43:1058–69. doi: 10.1038/s41366-018-0155-5

frontiers | Frontiers in Endocrinology

TYPE Original Research
PUBLISHED 03 November 2022
DOI 10.3389/fendo.2022.1015819

OPEN ACCESS

EDITED BY
Wah Yang,
The First Affiliated Hospital of Jinan University, China

REVIEWED BY
Yanmin Wang,
California Medical Innovations Institute, United States
Jason Widjaja,
Fudan UniversityChina
Cunchuan Wang,
First Affiliated Hospital of Jinan University, China

*CORRESPONDENCE
Guangyong Zhang
guangyongzhang@hotmail.com

SPECIALTY SECTION
This article was submitted to Obesity, a section of the journal Frontiers in Endocrinology

RECEIVED 10 August 2022
ACCEPTED 19 October 2022
PUBLISHED 03 November 2022

CITATION
Ding H, Liu C, Zhang S, Li B, Xu Q, Shi B, Li S, Dong S, Ma X, Zhang Y, Zhong M and Zhang G (2022) Sleeve gastrectomy attenuated diabetes-related cognitive decline in diabetic rats. *Front. Endocrinol.* 13:1015819. doi: 10.3389/fendo.2022.1015819

Sleeve gastrectomy attenuated diabetes-related cognitive decline in diabetic rats

Huanxin Ding[1], Chuxuan Liu[1], Shuo Zhang[2], Bingjun Li[3], Qian Xu[3], Bowen Shi[1], Songhan Li[4], Shuohui Dong[1], Xiaomin Ma[3], Yun Zhang[3], Mingwei Zhong[3] and Guangyong Zhang[1*]

[1]Department of General Surgery, Shandong Provincial Qianfoshan Hospital, Cheeloo College of Medicine, Shandong University, Jinan, China, [2]Medical Research Center, Shandong Provincial Qianfoshan Hospital, Cheeloo College of Medicine, Shandong University, Jinan, China, [3]Department of General Surgery, The First Affiliated Hospital of Shandong First Medical University, Jinan, Shandong, China, [4]Department of Breast Disease, Peking University People's Hospital, Beijing, China

Objective: To investigate the effects of sleeve gastrectomy (SG) on diabetes-related cognitive decline (DCD) in rats with diabetic mellitus (DM).

Methods and methods: Forty Wistar rats were randomly divided into control (CON) group (n=10), diabetes mellitus (DM) group (n=10), sham operation (SHAM) group (n=10) and SG group (n=10). DM model was established by high-fat diet (HFD) combined with intraperitoneal injection of streptozocin (STZ). Behavioral evaluation was given using Morris water maze test and Y-maze. In addition, PET-CT, TUNEL assay, histological analysis, transmission electron microscopy (TEM), immunohistochemistry (IHC) and Western blot analysis were used to evaluate the alleviating effects and potential mechanisms of SG on DCD in DM rats.

Results: Compared with the sham group, SG induced significant improvement in the metabolic indices such as blood glucose and body weight. Besides, it could attenuate the insulin resistance compared with SHAM group. In addition, SG could improve the cognitive function of DM rats, which were featured by significant decrease in the escape latency ($P<0.05$), and significant increase in the time in target quadrant and platform crossings ($P<0.05$) compared with the SHAM group. SG induced significant elevation in the spontaneous alternation compared with SHAM group ($P<0.05$). Moreover, SG could improve the arrangement and biosynthesis of hippocampus neuron. Moreover, SG triggered the inhibition of apoptosis of hippocampus neurons, and Western blot analysis showed SG induced significant increase in the ratios of Bcl-2/Bax and Caspase3/cleaved Caspase 3. TEM demonstrated SG could significantly improve the microstructure of hippocampus neurons compared with the SHAM group. Western blot and IHC confirmed the significant decrease in the phosphorylation of tau at Ser404 and Ser396 sites in the SG group. Furthermore, SG activated the PI3K signaling pathway by elevating the phosphorylation of PI3K and Akt and GSK3β compared with the SHAM group.

10.3389/fendo.2022.1015819

Conclusion: SG attenuated the DCD in DM rats, which may be related to the activation of PI3K signaling pathway.

KEYWORDS

diabetes-related cognitive decline, sleeve gastrectomy, PI3K, tau, neuronal apoptosis

Introduction

Diabetes mellitus (DM), with a sharp increase in the prevalence in the last three decades, is considered the ninth leading cause of death worldwide (1). Patients with DM usually show involvement of the nervous system, resulting in cognitive decline (2, 3). As a major complication of DM, the diabetes-related cognitive decline (DCD) is characterized by abnormalities in learning, memory, attention and speed of information processing (4). To date, impairment of hippocampus has been closely associated with the learning and memory loss, while in animals with DCD, the main pathological features of the hippocampus are neurogenic fibrillary tangles due to tau hyperphosphorylation and neuronal apoptosis (5).

Bariatric surgery, initially utilized for treating morbid obesity, is later reported to show a moderate effect on DM and its complications (6, 7). Bariatric surgery can ameliorate hyperglycemia (8) and reduce the body weight (9). In addition, patients underwent such type of surgery showed significant improvement in the cognitive function (10).

PI3K/Akt signaling pathway plays a key role in the pathogenesis of DCD (11, 12), which mediates biological growth and crucial cellular metabolic processes, such as glucose homeostasis, lipid metabolism, protein synthesis and cell proliferation and survival (13). In diabetic rats or glucose-induced hippocampal neuronal impairments, there was decrease in the phosphorylation of AKT, resulting in a decrease in the phosphorylation level of glycogen synthase kinase 3β (GSK3β) (14, 15), serving as a key enzyme that inhibits glycogen synthesis and one of the key kinases for tau phosphorylation (16). Physiologically, activation of the PI3K insulin signaling pathway could inhibit the hippocampal neuronal apoptosis. In addition, it could ensure that tau phosphorylation is maintained at a normal level by inactivating GSK3β (17).

Sleeve gastrectomy (SG) serving as one of the most popular bariatric surgeries for obesity has been reported to improve the cognitive function among the obesity patients (18, 19). However, little is known about the exact mechanisms for this process. In this study, a DM rat model was established in order to investigate how SG improved the cognitive function, and at the same time, we determined the activity of PI3K/AKT signaling pathway, with an aim to illustrate its roles in this process.

Materials and methods

Animals

Forty male Wistar rats (90–110g; 6-week-old), purchased from Vital River Laboratory Animal Technology (Beijing, China), were housed in the animal laboratory of Shandong Provincial Qianfoshan Hospital of Shandong University, under specific pathogen-free housing conditions at 20–26°C in a humidity of 50–60%. All animals were fed on a standard diet containing 15% of fat for 1 week for acclimatization. This animal study was approved by the Institutional Animal Care and Use Committee of Shandong Qianfoshan Hospital, Shandong University.

Grouping

The animals were randomly divided into the following four groups: (i) control (CON) group (n=10), rats subject to a standard diet; (ii) DM group (n=10), rats subject to DM induction; (iii) sham operation (SHAM) group (n = 10), and (iv) SG group (n=10). One week before the surgical intervention in the SG and SHAM groups, Y-maze test was performed to confirm the differences in cognitive ability among the groups (Figure S1). Animals in the SG group were subject to SG after a 12 hrs fast. Animals in the SHAM group were subject to DM induction, followed by operations that were the same as the above surgery before occlusion of gastric blood vessels. There were no interventions in the SHAM group except exposure of abdominal organs such as the stomach, small intestine, and liver. The flowchart of the study was shown in Figure 1.

DM induction

Animals were given a 4-week high fiber diet (HFD, 40% fat; Xietong Pharmaceutical Bio-engineering, Nanjing, China),

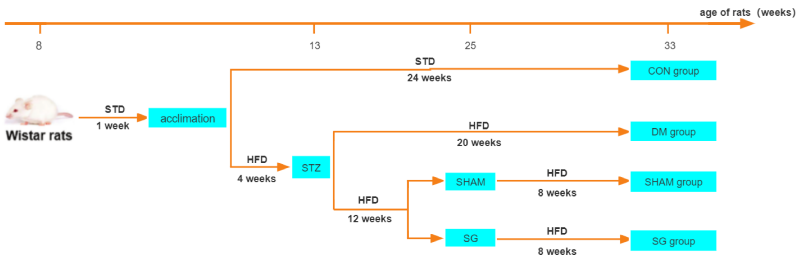

FIGURE 1
Flowchart of animal experiments. N = 10 for each group. STD, standard diet; HFD, high-fat diet; STZ, streptozotocin; CON, control group; DM, diabetes mellitus; SHAM, sham operation; SG, sleeve gastrectomy.

followed by a 12 hrs fast. Then the rats received a single intraperitoneal injection of streptozocin (STZ, 35 mg/kg, Sigma-Aldrich, St. Louis, MO, US). Three days after STZ injection, random blood glucose was measured 3 times consecutively, and a glucose level of ≥ 16.7 mmol/L was considered a successful model (20).

SG procedures

The procedures of SG were performed as previously reported (21). All rats were fasted for 12 hrs before surgery and then anesthetized by continuous inhalation of 2% isoflurane gas using a mask. First, a 4 cm incision was made in the middle of the upper abdomen. Then, the stomach was separated until a clear distinguish of the gastric blood vessels. The blood vessels of the fundus and the greater curvature of the stomach were ligated with a 7-0 thread (Chenghe Microsurgical Instruments, Ningbo, China), and then cut off after ligation. Subsequently, an incision of about 0.5 cm parallel to the greater curvature of the stomach was made in the fundus to remove the gastric contents. The fundus and most of the gastric body on the greater curvature of the stomach were removed, and the remaining part was sutured with 5-0 sutures (Cheng-He Microsurgical Instruments Factory, Ningbo, China). No active bleeding was confirmed and the anatomical position of the abdominal organs was restored. Finally, close the abdominal wall layer by layer with 3-0 sutures (Chenghe Microsurgical Instruments, Ningbo, China).

Body weight and food intake measurement

For the animals in each group, we measured the baseline body weight and food intake. Then the body weight and food intake were measured at 2, 4, 6, and 8 weeks afterwards.

Homeostasis model assessment of insulin resistance

Upon fasting for 12 hrs, the blood samples were collected from the tail vein after anesthesia, and centrifuged at 3,000 rpm for 8 min. Fasting blood glucose (FBG) was measured using a blood glucose meter (One Touch Ultra, Johnson & Johnson, CA, USA). Then serum insulin was detected with EZRMI-13K kit (One Touch Ultra, Johnson & Johnson, CA, USA). Finally, the Homeostasis Model Assessment of Insulin Resistance (HOMA-IR) was calculated to assess the degree of insulin resistance, using the following formula: HOMA-IR=fasting serum insulin (mIU/L)×FBG (mmol/L)/22.5 (22).

Oral glucose tolerance test and insulin tolerance Test

For the OGTT, glucose (1 g/kg) was given to each rat *via* intragastrical administration. Then the blood glucose was measured at 0, 10, 30, 60, and 120 min, respectively. About 24 hrs after OGTT, ITT was performed after a 12-hour fast. The rats were intraperitoneally injected with insulin (0.5 IU/kg, Tonghua Dongbao Pharmacy. Gansu, China), and then the blood glucose was measured at 0, 10, 30, 60, and 120 min, respectively. Finally, the area under the curve (AUC) of OGTT and ITT was calculated with the trapezoidal method according to the previous description (23, 24).

Morris water maze test

MWM test was used to measure hippocampus-dependent cognitive function as previously described (25). All behavioral tests were performed during the active period of the photoperiod. A video analysis system (Calvin Biotech, Nanjing, China) was utilized to record the swimming patterns

of each rat. The pool was filled with water at a constant temperature of 20°C. An escape platform with a diameter of 4.5 cm was placed in the swimming pool. The top of the platform was approximately 1.5 cm below the water surface.

The 5-day hidden platform test was used to detect the learning ability of rats. Rats were trained for 5 days. Animals failed to find the platform within 120 sec were placed on the platform for 10 sec. Spatial memory for each rat was determined based on the probe trial. Hidden platforms in the target quadrant were removed after training for 5 days. On day 6, a probe trial was performed and the rats were allowed to swim freely in the pool for 2 min.

Y-maze test

Spatial memory status in rats was tested by measuring the percentage of alternation in Y-maze test according to the previous description (26). The test device consisted of three equal-length arms (50×18×35 cm) in a Y-shape and an intermediate region. Rats were placed at the end of either arm, and were allowed to explore freely for 8 min. Subsequently, the total number and sequence of entries into each arm were recorded. The percentage of alternations was determined based on the following equation: (spontaneous alternations)/(total number of arm entries-2).

Positron-emission tomography and image processing

Before euthanasia, rats fasted for 12 h were maintained under anesthesia with 1.5% isoflurane for PET. After intravenous injection of 18F-FDG (800 μCi, 29.6 MBq), the entire body of the rat was continuously scanned for 21 min with a PET scanner (Metis 1800, Madic Technology, Linyi, China) in the coronal, sagittal and transverse dimensions, followed by a focused scan of the brain for 15 min, especially the hippocampus. The brain glucose uptake was analyzed by measuring the mean standard uptake values (SUV_{Mean}) using PMOD 4.1 software (PMOD Technology, Zurich, Switzerland).

Histological analysis

Hippocampal tissues were fixed with 4% paraformaldehyde and embedded in paraffin. Paraffin sections (5 μm) were stained with hematoxylin-eosin to evaluate the structure of four vital sub-regions of the hippocampus. After dewaxing, the sections were stained with hematoxylin staining solution (G1004, ServiceBio, Wuhan, China) for 5 min, and then stained with eosin staining solution (G1001, Wuhan, China, ServiceBio, Wuhan, China) for 5 min. In addition, Nissl staining was performed on the sections to evaluate the neuronal damage. The samples were processed in the same way as H&E staining, then stained with Nissl's staining solution (G1036, ServiceBio, Wuhan, China) for 5 min, and finally sealed with neutral resin. Digital slides were prepared by a Pannorama digital slide scanner (Pannoramic DESK, P-MIDI, P250, and P1000, 3DHISTECH, Budapest, Hungary).

TUNEL assay

Apoptosis in the hippocampus tissues was detected by commercial TUNEL Apoptosis kit (C1086, Beyotime Biotechnology, Shanghai, China), according to the manufacturer's instructions. The positive cells in each group were counted under a microscope. Apoptotic cells were stained in green color.

Transmission electron microscopy

Tissue squares (1 mm×1 mm×1 mm) were fixed with electron microscopy fixative (G1102, ServiceBio, Wuhan, China) for 2-4 hrs at 4°C, and then were post-treated in 1% osmium tetroxide for 2 hrs at 4°C. Subsequently, the samples were dehydrated through an ethanol series and infiltrated using acetone and 812 embedding medium (905529-77-4, SPI). After complete polymerization, the sections were observed under the TEM (Hitachi, HT-7700, Japan).

Immunohistochemistry

Paraffin sections (5 μm) were deparaffinized, and washed 3 times with PBS (G0002-2L, Servicebio, Wuhan, China). The antigens were retrieved in a microwave oven with citrate buffered saline (C1032, Solarbio, Beijing, China). Sections were incubated overnight with primary antibodies including p-tau (Ser404) (1:200, ab92676, Abcam, Cambridge, USA) and p-tau (Ser396) (1:4000, ab109390, Abcam, Cambridge, USA), followed by washing three times with PBS. Sections were then incubated with a universal two-step detection kit (PV-9000, ZSGB-BIO, Beijing, China) following the manufacturer's instructions. After washing 3 times with PBS, the sections were stained with diaminobenzidine (DAB, ZLI-9017, ZSGB-BIO, Beijing, China) and hematoxylin. Finally, the sealed sections were made into digital slides by a panoramic digital slide scanner (Panorama Desk, P-MIDI, P250 and P1000, 3DHISTECH).

Western blot analysis

Hippocampal tissues were homogenized in RIPA cold buffer (89901; Thermofisher, USA) containing protease inhibitor

(ST506, Beyotime Biotech, Shanghai, China). Protein samples were quantified using the BCA protein assay kit (E-BC-K318-M, Elabscience, Wuhan, China). Protein samples (50 μg) were separated by SDS-PAGE gel (PG212, EpiZyme, Shanghai, China) and then transferred to a polyvinylidene fluoride (PVDF) membrane. PVDF membranes were blocked with 5% nonfat dry milk for 1 h, and incubated with primary antibody overnight at 4°C [p-tau (Ser404), 1:2000, ab92676, Abcam, USA; p-tau(Ser396), 1:50000, ab109390, Abcam, USA; Tau, 1:10000, sc-32274, Santa Cruz Biotechnology, Beijing; p-PI3K, 1:1000, 13857S, Cell Signaling Technology, USA; PI3K, 1:1000, 3358S, Cell Signaling Technology, USA; Akt, 1: 1000, 4685S, Cell Signaling Technology, USA; p-Akt, 1:2000, 4060S, Cell Signaling Technology; GSK3β, 1:1000, 9315S, Cell Signaling Technology, USA; p-GSK3β, 1:1000, 9315S, Cell Signaling Technology, USA; Bcl-2, 1:5000, 60178-1-Ig, Proteintech, China; Bax, 1:10000, 50599-1-Ig, Proteintech, China; Caspase 3, 1:1000, 9662S, Cell Signaling Technology, USA; cleaved Caspase 3, 1:1000, 9664S, Cell Signaling Technology, USA; β actin, 1:20000, 66009-1-Ig, Proteintech, China]. Then, the membrane was washed and incubated with secondary antibodies (goat anti-mouse IgG, 1:10000, ab216776, Abcam; goat anti-rabbit IgG, 1:10000, ab6721, Abcam). Protein bands were visualized by ECL (Millipore) and quantified using ImageJ software (National Institutes of Health).

Statistical analysis

Data were analyzed using Graph Pad Prism 8.0 (San Diego, CA, USA). Data were presented as mean ± standard error of mean. One-way ANOVA was utilized to compare the differences between groups, together with Tukey's multiple comparison test. Statistical outliers were determined using the Grubbs test. $P < 0.05$ was considered to be statistically significant.

Results

SG improved basic metabolic parameters in diabetic rats

The body weight and food intake were significantly higher in the DM group than these of the CON group. Compared with the DM group, significant decrease was noticed in the body weight and food intake of rats in SG group (Figures 2A, B). In addition, compared with the SHAM group, the FBG showed significant decrease in the SG group within 2 weeks after surgery (Figure 2C). By recording FBG and serum insulin levels for HOMA-IR assessment, we found a significant decrease in insulin resistance in the SG group compared to the sham group (Figures 2C-2E). Consistently, AUC_{OGTT} and AUC_{ITT} further validated the improvement in insulin resistance in the SG group (Figures 2F, G). All these indicated that SG could significantly improve the basic metabolic parameters in diabetic obese rats.

SG ameliorated cognitive function in diabetic rats

The escape latency of the rats in the DM group and the SHAM group was significantly longer than that of the control (Figure 3A). The escape latency in the SG group was significantly shorter than that of the DM group (Figure 3A). Meanwhile, there was no statistical difference in the swimming speed of the rats in each group (Figure 3B). The travelled distance of rats in each group showed gradual decrease in a time-dependent manner. The travelled distance in the SG group was significantly shorter than the SHAM group on day 4 and 5 (Figure 3C). Compared with normal rats, the percentage of time in target quadrant (Figure 3D) and the number of platform crossing (Figure 3E) were significantly shortened in the DM and SHAM groups. In contrast, the percentage of time and number of platform crossings in SG group showed significant increase compared with the SHAM group (Figures 3D, E). These indicated that SG significantly improved spatial memory and learning ability in diabetic rats. In addition, the Y-maze test showed that the percentage of spontaneous alternation in the DM group was lower than that in the control group, while the percentage of spontaneous alternation in the SG group was significantly different compared to the SHAM group (Figure 3F), with no significant changes in total arm entries (Figure 3G). This suggested that SG may improve the ability of diabetic rats to recognize novel environment, and could partially improve the DCD.

SG significantly improved cerebral glucose uptake in diabetic rats

We evaluated glucose uptake in brain tissues using a PET scanner (Figure 3H). The SUV_{mean} of the control group and SG group was significantly higher than that of the DM group and sham group, respectively (Figure 3I). These results suggested that SG improved the diabetes-induced obstruction of cerebral glucose uptake.

SG significantly reversed hippocampal histopathology in diabetic rats

Changes in the hippocampus tissue underlie cognitive decline as central nervous system diseases and diabetes progress (27, 28). Compared with the CON group, the number of neurons in the hippocampal cornu ammonis (CA)1, CA2, CA3, and dentate gyrus (DG) regions of the DM group showed

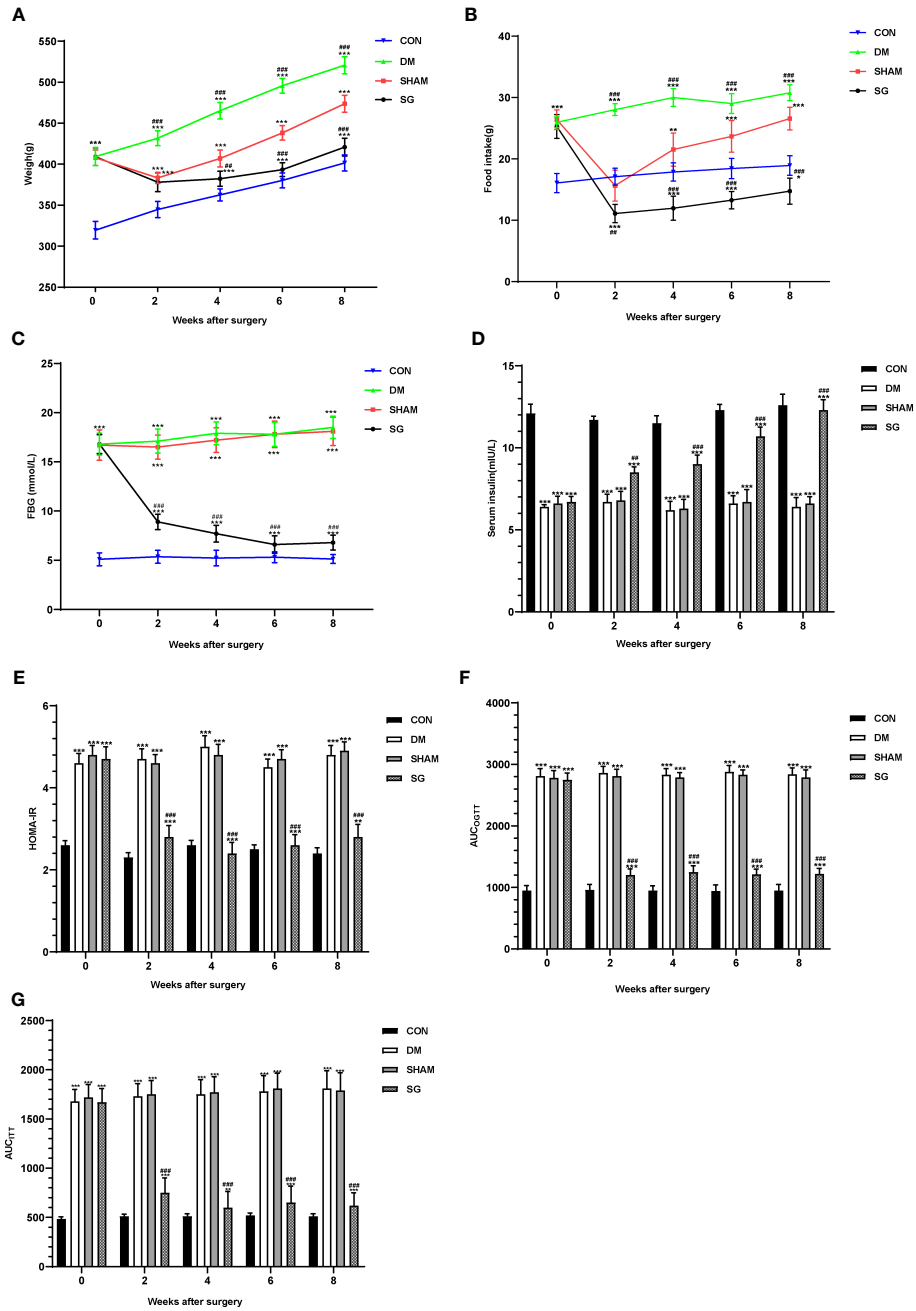

FIGURE 2
Changes of metabolic parameters including body weight **(A)**, food intake **(B)**, FBG **(C)**, serum insulin **(D)**, HOMA-IR **(E)**, AUC_{OGTT} **(F)**, and AUC_{ITT} **(G)** before and after surgery. Data were expressed as means ± SEM for n = 10 per group. $^{**}p < 0.01$ vs. CON group, $^{***}p < 0.001$ vs. CON group; $^{\#\#}p < 0.01$ vs. SHAM group, $^{\#\#\#}p < 0.001$ vs. SHAM group. FBG, fasting blood glucose; HOMA-IR, homeostasis model assessment of insulin resistance; AUCOGTT, the area under the curve of the oral glucose tolerance test; AUCITT, the area under the curve of the insulin tolerance test; CON, control; DM, diabetes mellitus; SHAM, sham operation; SG, sleeve gastrectomy.

significant decrease, which were featured by presence of swollen cells, nuclear fragmented or disappearance, and irregular arrangement of cell. Notably, SG significantly improved these changes (Figure 4A). To assess the damage of hippocampal neurons, the hippocampus of each group was analyzed using Nissl staining. DM resulted in the reduction of Nissl bodies in the CA1, CA3 and DG regions of the hippocampus, indicating significant neuronal damage. Whereas, the number of Nissl bodies in the SG group showed significant increase compared with SHAM group (Figure 4B). In conclusion, SG ameliorated

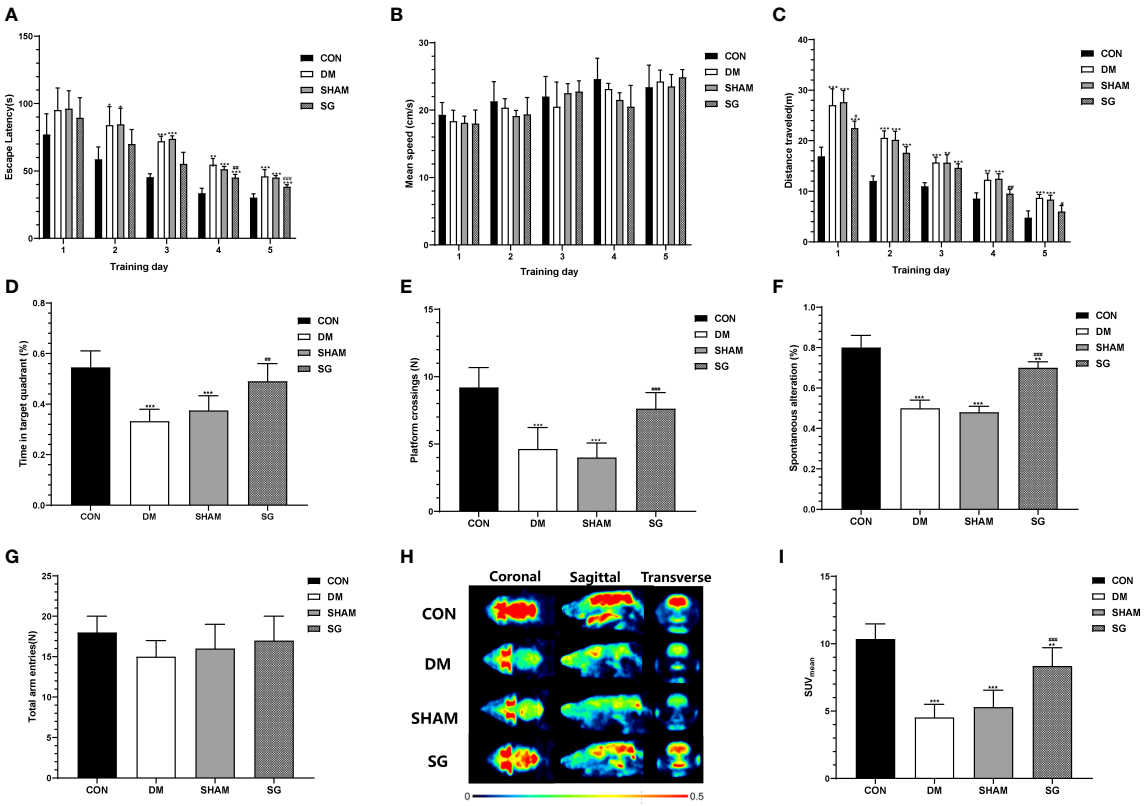

FIGURE 3
SG induced significant improvement in the animal behaviors in the Morris water maze test **(A-E)** and Y-maze test **(F, G)**, and PET imaging system validated the improvement of glucose uptake in brain **(H, I)**. Data were expressed as means ± SEM for n = 10 per group. *$p < 0.05$ vs. CON group, **$p < 0.01$ vs. CON group, ***$p < 0.001$ vs. CON group; $^{\#}p < 0.05$ vs. SHAM group, $^{\#\#}p < 0.01$ vs. SHAM group, $^{\#\#\#}p < 0.001$ vs. SHAM group. PET, positron-emission tomography; SUV_{Mean}, the average standard uptake value; CON, control; DM, diabetes mellitus; SHAM, sham operation; SG, sleeve gastrectomy.

the histological changes in the hippocampus induced by diabetes.

SG alleviated hippocampal neuronal apoptosis in diabetic rats

In DM group, there was a significant increase in the number of positive neurons in the hippocampus, indicating significant increase in the apoptosis compared with the CON group. In contrast, SG alleviated the situation of neuronal apoptosis (Figure 4C). Western blot analysis showed that Bcl-2 and Caspase 3 were down-regulated in DM group and SHAM group compared with these of the CON group, while significant up-regulation was seen in the expressions of Bax and cleaved Caspase 3 in DM group (Figures 4D, F). The ratio of Bcl-2 to Bax and Caspase 3 to cleaved Caspase 3 in the SG group showed significant increase compared with that of SHAM group (Figures 4E, G). Taken together, we concluded that SG can ameliorate diabetes-induced apoptosis of hippocampal neurons.

SG significantly improved the fine structure of hippocampal neurons

TEM indicated pyknosis, severe edema, condensed cell matrix, obvious swelling of organelles in the hippocampal neurons in the DM group and SHAM group (Figure 4H), together with obvious vacuolar degeneration. In CON group and the SG group, the nuclear membrane was intact. In addition, the chromatin was uniform, and the cell membrane was intact. Moreover, the intracellular matrix was abundant and evenly distributed. It was worth noting that the mitochondria in the SG group were slightly swollen, and the cristae were fragmented and reduced, but not as severe as the SHAM group.

SG inhibited tau phosphorylation in the hippocampus of diabetic rats

There was increased phosphorylation of tau at Ser404 and Ser396 in the hippocampus of DM and SHAM group compared

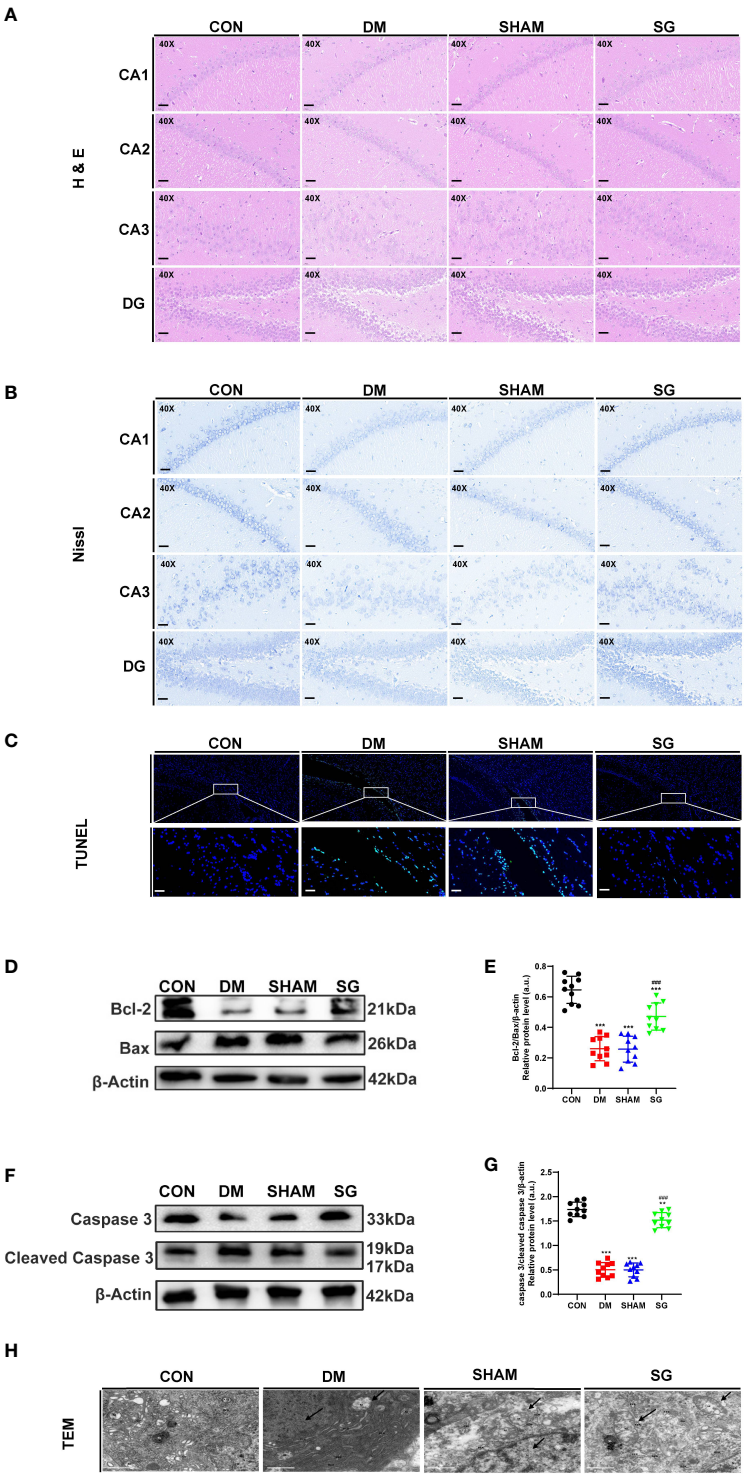

FIGURE 4
SG reversed the histological features **(A)**, induce the increase of Nissl's bodies **(B)**, and inhibited the apoptosis of hippocampus neurons **(C-G)**, and improved the microstructure of hippocampus neurons under TEM **(H)**. The scale bar for A-C was 100 μm, while that for H was 1 μm. Data were expressed as means ± SEM for n = 10 per group. $^{**}p < 0.01$ vs. CON group, $^{***}p < 0.001$ vs. CON group; $^{\#\#\#}p < 0.001$ vs. SHAM group. H&E, hematoxylin and eosin; TUNEL, terminal deoxynucleotidyl transferase-mediated dUTP nick end labeling; CA1, cornu ammonis1; CA2, cornu ammonis2; CA3, cornu ammonis3; DG, dentate gyrus; M, mitochondrion; N, nucleus; RER, rough endoplasmic reticulum; GO, Golgi apparatus; CON, control; DM, diabetes mellitus; SHAM, sham operation; SG, sleeve gastrectomy.

with CON group (Figure 5A). In contrast, SG decreased the phosphorylation of these two tau sites (Figures 5B, C), which was verified by IHC results (Figure 5D). Thus, SG alleviated hyperphosphorylation of tau in the hippocampus of diabetic rats.

Effects of SG on PI3K signaling pathways

Compared with the CON group, the hippocampal expression of p-PI3K, p-Akt, and p-GSK3β showed significant decrease in both DM and SHAM groups, while SG induced significant increase in their expression (Figure 5E). The ratios of p-PI3K to total PI3K, p-Akt to total Akt and p-GSK3β to total GSK3β were consistent with the above results (Figures 5F-5H).

In conclusion, we infer that SG partially ameliorated diabetes-induced cognitive impairment, which was associated with activation of the PI3K signaling pathway.

Discussion

DM and its complications were indeed a serious threat to global health. On this basis, there has been widespread interests in the treatment of diabetes (1). DCD has been more and more widely recognized as a serious complication for DM (29). Slowly progressive DCD occurs in all age groups, not limited to the aged population (30). The main pathological features of DCD include hyperphosphorylation of tau and apoptosis of hippocampal neurons, leading to progressive impairment of hippocampal

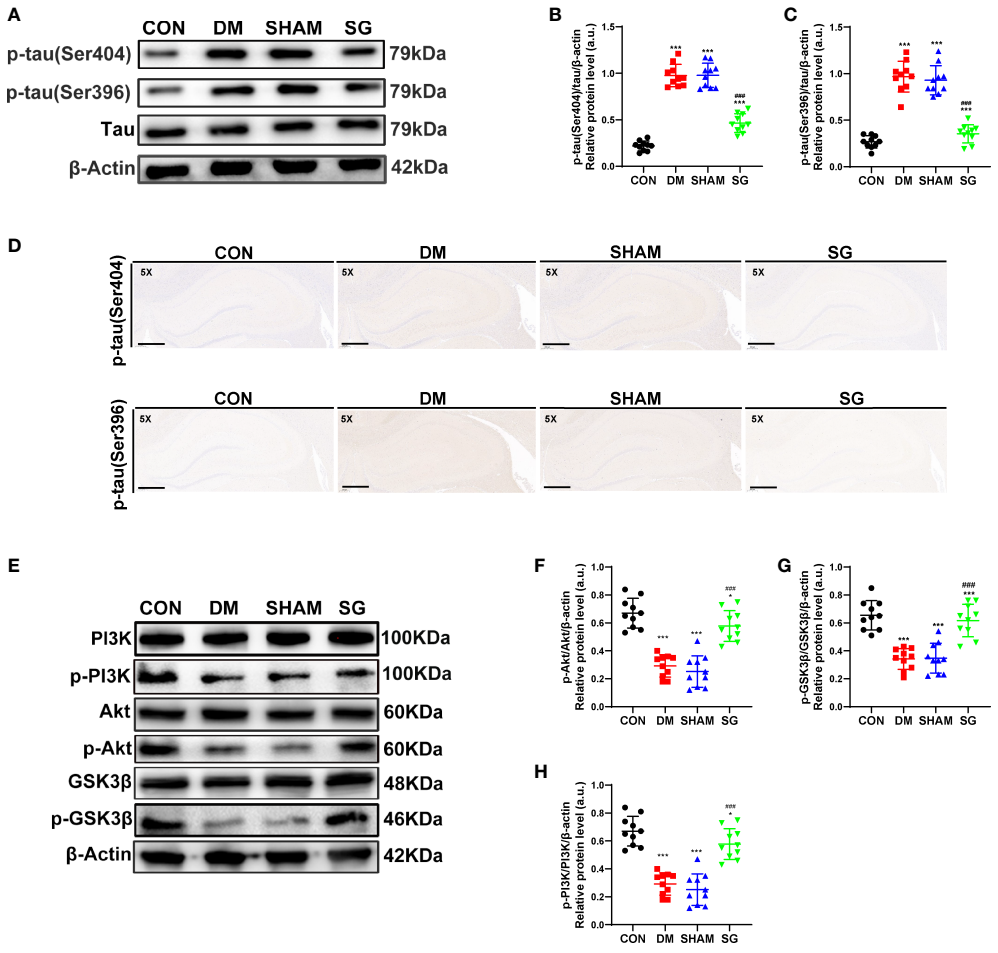

FIGURE 5
SG inhibited the phosphorylation of tau **(A-D)** and activated the PI3K signaling pathway **(E-H)**. The scale bar for D was 800 μm. Data were expressed as means ± SEM for each group (n = 10). *$p < 0.05$ vs. CON group, ***$p < 0.001$ vs. CON group; $^{###}p < 0.001$ vs. SHAM group. CON, control; DM, diabetes mellitus; SHAM, sham operation; SG, sleeve gastrectomy.

function (31–33). A large number of DCD patients are more likely to present mild cognitive impairment (MCI) or dementia, showing a poor prognosis even after treatment (33, 34). Conventional treatment options for DCD include measurements for lowering blood glucose, lifestyle interventions, and cognitive rehabilitation training. In addition, delivery of insulin to targeted brain tissues has been proposed as a potential strategy for treating cognitive impairment in DM patients (35). Unfortunately, this strategy is not universally effective due to poor adherence and individual variability (36). Therefore, it is urgently to develop more effective treatment options for these patients.

In the 1990s, bariatric surgery began to be recognized as a form of inducing weight loss, which may improve the symptoms of DM and its complications (37). Recently, it has gradually considered as the best treatment strategy for DM and obesity, with the advances in the surgical safety (38). In terms of animal models, due to the similarity of metabolic characteristics, the most commonly used diabetes model is the DM rodent model, which is used to investigate the pathogenesis and treatment of DM (39). In this study, such model was used to investigate the therapeutic effects of SG on DCD and its associated mechanisms. According to the previous studies, cognitive decline was sufficiently induced in this model about 8-9 weeks after induction of DM (40, 41). Our data showed that the cognitive function of rats was significantly impaired at week 12 after DM. Meanwhile, SG showed significant effects on reducing body weight, together with improving hyperglycemia and reversing insulin resistance. However, some rats showed signs of rebound in body weight and blood sugar after surgery, which we consider to be caused by maintaining a high-fat diet during the experiments. The CA1, CA3 and DG regions of the hippocampus were crucial for learning and spatial memory, and there was a unidirectional tri-synaptic pathway between these regions (42). In this study, we found that cognitive function decreased. HE and Nissl staining revealed neuronal damage in the CA1, CA3, and DG regions in DM rats. Interestingly, these negative effects were improved to varying degrees after SG. The above notion was further supported by the changes in neuronal microstructure under TEM. Taken together, SG could improve the symptoms in diabetic rats with DCD.

PET, employing molecules labeled with positron-emitting radioisotopes to provide direct and specific measurements of biochemical processes in regions of interest, has been used to gain a deeper understanding on the neural mechanisms underlying behavioral and cognitive processes (43). In cognition-related regions, there is an association between insulin resistance and reduced brain glucose metabolism (44). Therefore, PET scans of rat brains were performed and SUV was utilized to assess glucose uptake in brain, particularly the hippocampus. PET scan showed significant increase in the SUV in SG group, but it did not reach the level of the CON group. And confirmed that SG significantly reversed cerebral glucose uptake in diabetic rats.

Pathological alternations of hippocampus are closely associated with the pathogenesis of DCD with the main pathological manifestations as hyperphosphorylation of tau and increased neuronal apoptosis (45). These pathological changes would trigger the inhibition of PI3K/Akt signaling pathway (46). Previous study indicated that many Tau sites can be phosphorylated and inactivated, including Ser404, Ser396, Ser202 and Thr205 (47). In our study, Western blot analysis and IHC showed that the expression of p-tau (Ser404) and p-tau (Ser396) showed significant up-regulation in the DM group and SHAM group compared with those of the CON group. According to the previous studies, DM could mediate the increased apoptosis of hippocampal neurons by inhibiting the PI3K pathway (48, 49). Consistently, our TUNEL assay indicated the increased expression of apoptosis-related proteins in hippocampus. Therefore, we concluded that SG could improve the pathological changes. Additionally, our data provided solid evidence for the neuroprotective effects of bariatric surgery by inhibiting neuronal apoptosis and tau phosphorylation.

PI3K signaling pathway plays crucial roles in several biological processes, such as glucose homeostasis, cell growth and proliferation (50). The activation of Akt and inactivation of GSK3β was highly depending on phosphorylation of corresponding serine residues, which functioned as serine/threonine kinases (51, 52). PI3K was activated by direct interaction with insulin receptor substrate 1 (IRS-1), and then the Akt was phosphorylated, which in turn induced the phosphorylation of GSK3β and ultimately promoted the balance of blood glucose (53). It has been assumed that there is a potential link between PI3K signaling pathway and the pathogenesis of DM or Alzheimer's disease (AD) as there is confirmed impairment of PI3K signaling pathway in the DM. Inhibition of glycogen synthesis and inactivation of tau have been reported to trigger hyperglycemia and cognitive decline, respectively (54). Meanwhile, increased ratio of GSK3β to p-GSK3β resulted in increased apoptosis of hippocampal neurons in DM rats (55). Notably, the expression of p-PI3K, p-Akt, and p-GSK3β was significantly up-regulated after SG, which suggested that the activation of PI3K signaling pathway may play an important role in the attenuation of DCD mediated by SG (Figure 6).

Indeed, our study has some limitations. Some patients may present rebounding of blood glucose and weight even after bariatric surgery (56). It is still difficult to predict the state of diabetes-induced cognitive impairment following re-elevation of blood glucose and weight. Therefore, it is necessary to extend the observation time in the following studies to discuss the long-term effects of SG on diabetes-induced cognitive impairment. In

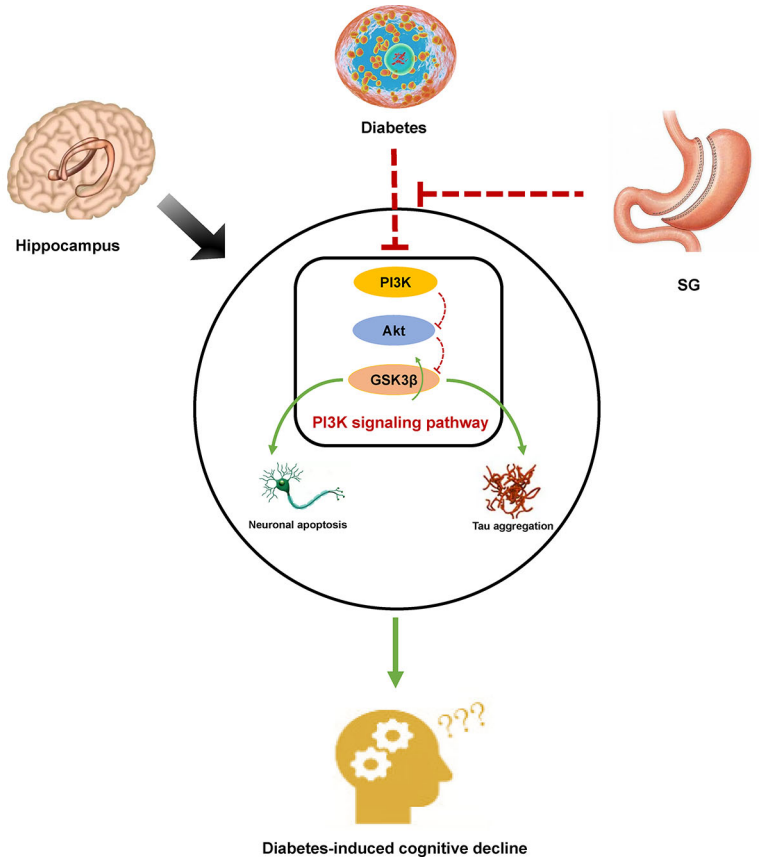

FIGURE 6
Diagram of a possible mechanism by which SG improved DCD. In DM rats, inhibition of PI3K signaling resulted in histological changes in the hippocampus by promoting tau phosphorylation and inducing apoptosis of hippocampal neurons. Activation of PI3K signaling pathway was associated with SG-induced amelioration of DCD.

addition, both glycemic control and weight loss have positive effects on metabolic status. Thus, it is not clear which is the crucial factor in the improvement of cognitive decline in SG-induced diabetes. On this basis, further studies are required to illustrate the exact mechanism of diabetes-induced cognitive impairment improvement. Finally, to further elucidate the mechanism by which SG attenuated the diabetes-induced cognitive impairment, we need to explore the interaction between GSK3β, Tau and neuronal apoptosis.

In conclusion, SG could reverse the tissue morphology of the hippocampus, decrease of glucose uptake in the hippocampus, and attenuate cognitive dysfunction induced by hippocampal neuronal apoptosis and hyperphosphorylation of Tau in DM rats. Additionally, the SG could reverse the inhibition of PI3K signaling pathway in rats with DCD. The reduction of diabetes-induced cognitive function by SG was associated with reactivation of the PI3K signaling pathway. In the future, inhibition of PI3K signaling may be a potential target for treating patients with DCD.

Data availability statement

The raw data supporting the conclusions of this article will be made available by the authors, without undue reservation.

Ethics statement

The animal study was reviewed and approved by Institutional Animal Care and Use Committee of Shandong Qianfoshan Hospital, Shandong University.

Author contributions

GZ and MZ contributed to conception and design of the study. Material preparation and data collection were performed by HD, CL, SZ, BL, QX and BS. Data analysis was performed by SL, SD, XM and YZ. HD, CL and SZ wrote the first draft of the

manuscript. BL, QX, BS, SL, SD, XM and YZ wrote sections of the manuscript. GZ and MZ provided critical review of the article. All authors contributed to manuscript revision, read, and approved the submitted version.

Funding

This project was supported by the National Natural Science Foundation of China (Grant No. 81873647) and Major Basic Research Project of Natural Science Foundation of Shandong Province (Grant No. ZR2020ZD15).

Conflict of interest

The authors declare that the research was conducted in the absence of any commercial or financial relationships that could be construed as a potential conflict of interest.

Publisher's note

Supplementary material

The Supplementary Material for this article can be found online at: https://www.frontiersin.org/articles/10.3389/fendo.2022.1015819/full#supplementary-material

SUPPLEMENTARY FIGURE 1
DM induced significant impairment in the animal behaviors in the Y-maze test (A, B). Data were expressed as means ± SEM for n = 10 per group. $^{*}p < 0.05$ vs. CON group, $^{**}p < 0.01$ vs. CON group, $^{***}p < 0.001$ vs. CON group. CON, control; DM, diabetes mellitus; SHAM, sham operation; SG, sleeve gastrectomy.

References

1. Zheng Y, Ley SH, Hu FB. Global aetiology and epidemiology of type 2 diabetes mellitus and its complications. *Nat Rev Endocrinol* (2018) 14(2):88–98. doi: 10.1038/nrendo.2017.151

2. Zilliox LA, Chadrasekaran K, Kwan JY, Russell JW. Diabetes and cognitive impairment. *Curr Diabetes Rep* (2016) 16(9):87. doi: 10.1007/s11892-016-0775-x

3. Moheet A, Mangia S, Seaquist ER. Impact of diabetes on cognitive function and brain structure. *Ann New York Acad Sci* (2015) 1353:60–71. doi: 10.1111/nyas.12807

4. Biessels GJ, Nobili F, Teunissen CE, Simó R, Scheltens P. Understanding multifactorial brain changes in type 2 diabetes: A biomarker perspective. *Lancet Neurol* (2020) 19(8):699–710. doi: 10.1016/s1474-4422(20)30139-3

5. Dutta BJ, Singh S, Seksaria S, Das Gupta G, Singh A. Inside the diabetic brain: Insulin resistance and molecular mechanism associated with cognitive impairment and its possible therapeutic strategies. *Pharmacol Res* (2022) 182:106358. doi: 10.1016/j.phrs.2022.106358

6. Goldberg I, Nie L, Yang J, Docimo S, Obici S, Talamini M, et al. Impact of bariatric surgery on the development of diabetic microvascular and macrovascular complications. *Surg Endosc* (2021) 35(7):3923–31. doi: 10.1007/s00464-020-07848-2

7. Xiong Y, Zhu W, Xu Q, Ruze R, Yan Z, Li J, et al. Sleeve gastrectomy attenuates diabetic nephropathy by upregulating nephrin expressions in diabetic obese rats. *Obes Surg* (2020) 30(8):2893–904. doi: 10.1007/s11695-020-04611-3

8. Via MA, Mechanick JI. The role of bariatric surgery in the treatment of type 2 diabetes: Current evidence and clinical guidelines. *Curr Atheroscl Rep* (2013) 15 (11):366. doi: 10.1007/s11883-013-0366-0

9. Pareek M, Schauer PR, Kaplan LM, Leiter LA, Rubino F, Bhatt DL. Metabolic surgery: Weight loss, diabetes, and beyond. *J Am Coll Cardiol* (2018) 71(6):670–87. doi: 10.1016/j.jacc.2017.12.014

10. Morledge MD, Pories WJ. Bariatric surgery and cognitive impairment. *Obes (Silver Spring Md)* (2021) 29(8):1239–41. doi: 10.1002/oby.23187

11. Yang W, Liu Y, Xu QQ, Xian YF, Lin ZX. Sulforaphene ameliorates neuroinflammation and hyperphosphorylated tau protein *Via* regulating the Pi3k/Akt/Gsk-3β pathway in experimental models of alzheimer's disease. *Oxid Med Cell Longev* (2020) 2020:4754195. doi: 10.1155/2020/4754195

12. Wang BN, Wu CB, Chen ZM, Zheng PP, Liu YQ, Xiong J, et al. Dl-3-N-Butylphthalide ameliorates diabetes-associated cognitive decline by enhancing Pi3k/Akt signaling and suppressing oxidative stress. *Acta Pharmacol Sin* (2021) 42(3):347–60. doi: 10.1038/s41401-020-00583-3

13. Abeyrathna P, Su Y. The critical role of akt in cardiovascular function. *Vasc Pharmacol* (2015) 74:38–48. doi: 10.1016/j.vph.2015.05.008

14. Manning BD, Toker A. Akt/Pkb signaling: Navigating the network. *Cell* (2017) 169(3):381–405. doi: 10.1016/j.cell.2017.04.001

15. Wang S, He B, Hang W, Wu N, Xia L, Wang X, et al. Berberine alleviates tau hyperphosphorylation and axonopathy-associated with diabetic encephalopathy *Via* restoring Pi3k/Akt/Gsk3β pathway. *J Alzheimer's Dis JAD* (2018) 65(4):1385–400. doi: 10.3233/jad-180497

16. De Simone A, Tumiatti V, Andrisano V, Milelli A. Glycogen synthase kinase 3β: A new gold rush in anti-alzheimer's disease multitarget drug discovery? *J Med Chem* (2021) 64(1):26–41. doi: 10.1021/acs.jmedchem.0c00931

17. Tang SS, Ren Y, Ren XQ, Cao JR, Hong H, Ji H, et al. Erα and/or erβ activation ameliorates cognitive impairment, neurogenesis and apoptosis in type 2 diabetes mellitus mice. *Exp Neurol* (2019) 311:33–43. doi: 10.1016/j.expneurol.2018.09.002

18. Hornack SE, Nadler EP, Wang J, Hansen A, Mackey ER. Sleeve gastrectomy for youth with cognitive impairment or developmental disability. *Pediatrics* (2019) 143(5):2. doi: 10.1542/peds.2018-2908

19. Li P, Shan H, Liang S, Nie B, Liu H, Duan S, et al. Sleeve gastrectomy recovering disordered brain function in subjects with obesity: A longitudinal fmri study. *Obes Surg* (2018) 28(8):2421–8. doi: 10.1007/s11695-018-3178-z

20. Zhang KQ, Tian T, Hu LL, Wang HR, Fu Q. Effect of probucol on autophagy and apoptosis in the penile tissue of streptozotocin-induced diabetic rats. *Asian J Androl* (2020) 22(4):409–13. doi: 10.4103/aja.aja_89_19

21. Bruinsma BG, Uygun K, Yarmush ML, Saeidi N. Surgical models of roux-En-Y gastric bypass surgery and sleeve gastrectomy in rats and mice. *Nat Protoc* (2015) 10(3):495–507. doi: 10.1038/nprot.2015.027

22. Ozmen MM, Guldogan CE, Gundogdu E. Changes in homa-ir index levels after bariatric surgery: Comparison of single anastomosis duodenal switch-proximal approach (Sads-p) and one anastomosis gastric bypass-mini gastric bypass (Oagb-mgb). *Int J Surg (London England)* (2020) 78:36–41. doi: 10.1016/j.ijsu.2020.04.008

23. Dolo PR, Huang K, Widjaja J, Li C, Zhu X, Yao L, et al. Distal gastric mucosa ablation induces significant weight loss and improved glycemic control in type 2 diabetes sprague-dawley rat model. *Surg Endosc* (2020) 34(10):4336–46. doi: 10.1007/s00464-019-07200-3

24. Harris MI, Hadden WC, Knowler WC, Bennett PH. International criteria for the diagnosis of diabetes and impaired glucose tolerance. *Diabetes Care* (1985) 8 (6):562–7. doi: 10.2337/diacare.8.6.562

25. Ozkan A, Aslan MA, Sinen O, Munzuroglu M, Derin N, Parlak H, et al. Effects of adropin on learning and memory in rats tested in the morris water maze. *Hippocampus* (2022) 32(4):253–63. doi: 10.1002/hipo.23403

26. Lamtai M, Azirar S, Zghari O, Ouakki S, El Hessni A, Mesfioui A, et al. Melatonin ameliorates cadmium-induced affective and cognitive impairments and hippocampal oxidative stress in rat. *Biol Trace Elem Res* (2021) 199(4):1445–55. doi: 10.1007/s12011-020-02247-z

27. Rorabaugh JM, Chalermpalanupap T, Botz-Zapp CA, Fu VM, Lembeck NA, Cohen RM, et al. Chemogenetic locus coeruleus activation restores reversal learning in a rat model of alzheimer's disease. *Brain* (2017) 140(11):3023–38. doi: 10.1093/brain/awx232

28. Zhang S, Li H, Zhang L, Li J, Wang R, Wang M. Effects of troxerutin on cognitive deficits and glutamate cysteine ligase subunits in the hippocampus of streptozotocin-induced type 1 diabetes mellitus rats. *Brain Res* (2017) 1657:355–60. doi: 10.1016/j.brainres.2016.12.009

29. Biessels GJ, Despa F. Cognitive decline and dementia in diabetes mellitus: Mechanisms and clinical implications. *Nat Rev Endocrinol* (2018) 14(10):591–604. doi: 10.1038/s41574-018-0048-7

30. McCrimmon RJ, Ryan CM, Frier BM. Diabetes and cognitive dysfunction. *Lancet (London England)* (2012) 379(9833):2291–9. doi: 10.1016/s0140-6736(12)60360-2

31. Hanyu H. Diabetes-related dementia. *Adv Exp Med Biol* (2019) 1128:147–60. doi: 10.1007/978-981-13-3540-2_8

32. Jash K, Gondaliya P, Kirave P, Kulkarni B, Sunkaria A, Kalia K. Cognitive dysfunction: A growing link between diabetes and alzheimer's disease. *Drug Dev Res* (2020) 81(2):144–64. doi: 10.1002/ddr.21579

33. Ehtewish H, Arredouani A, El-Agnaf O. Diagnostic, prognostic, and mechanistic biomarkers of diabetes mellitus-associated cognitive decline. *Int J Mol Sci* (2022) 23(11):9. doi: 10.3390/ijms23116144

34. Ryan CM, van Duinkerken E, Rosano C. Neurocognitive consequences of diabetes. *Am Psychol* (2016) 71(7):563–76. doi: 10.1037/a0040455

35. Novak V, Gomez F, Dias AC, Pimentel DA, Alfaro FJ. Diabetes-related cognitive decline, a global health issue, and new treatments approaches. *Int J Priv Health Inf Manage* (2017) 5(2):58–70. doi: 10.4018/ijphim.2017070104

36. Kravitz E, Schmeidler J, Schnaider Beeri M. Type 2 diabetes and cognitive compromise: Potential roles of diabetes-related therapies. *Endocrinol Metab Clinics North America* (2013) 42(3):489–501. doi: 10.1016/j.ecl.2013.05.009

37. Pories WJ, Swanson MS, MacDonald KG, Long SB, Morris PG, Brown BM, et al. Who would have thought it? an operation proves to be the most effective therapy for adult-onset diabetes mellitus. *Ann Surg* (1995) 222(3):339–50. doi: 10.1097/00000658-199509000-00011

38. Affinati AH, Esfandiari NH, Oral EA, Kraftson AT. Bariatric surgery in the treatment of type 2 diabetes. *Curr Diabetes Rep* (2019) 19(12):156. doi: 10.1007/s11892-019-1269-4

39. Gheibi S, Kashfi K, Ghasemi A. A practical guide for induction of type-2 diabetes in rat: Incorporating a high-fat diet and streptozotocin. *BioMed Pharmacother* (2017) 95:605–13. doi: 10.1016/j.biopha.2017.08.098

40. Yang H, Tang L, Qu Z, Lei SH, Li W, Wang YH. Hippocampal insulin resistance and the sirtuin 1 signaling pathway in diabetes-induced cognitive dysfunction. *Neural Regen Res* (2021) 16(12):2465–74. doi: 10.4103/1673-5374.313051

41. Ye T, Meng X, Zhai Y, Xie W, Wang R, Sun G, et al. Gastrodin ameliorates cognitive dysfunction in diabetes rat model *Via* the suppression of endoplasmic reticulum stress and Nlrp3 inflammasome activation. *Front Pharmacol* (2018) 9:1346. doi: 10.3389/fphar.2018.01346

42. Alkadhi KA. Cellular and molecular differences between area Ca1 and the dentate gyrus of the hippocampus. *Mol Neurobiol* (2019) 56(9):6566–80. doi: 10.1007/s12035-019-1541-2

43. Guzzardi MA, Iozzo P. Brain functional imaging in obese and diabetic patients. *Acta Diabetol* (2019) 56(2):135–44. doi: 10.1007/s00592-018-1185-0

44. Baker LD, Cross DJ, Minoshima S, Belongia D, Watson GS, Craft S. Insulin resistance and Alzheimer-like reductions in regional cerebral glucose metabolism for cognitively normal adults with prediabetes or early type 2 diabetes. *Arch Neurol* (2011) 68(1):51–7. doi: 10.1001/archneurol.2010.225

45. Hamed SA. Brain injury with diabetes mellitus: Evidence, mechanisms and treatment implications. *Expert Rev Clin Pharmacol* (2017) 10(4):409–28. doi: 10.1080/17512433.2017.1293521

46. Gao C, Liu Y, Jiang Y, Ding J, Li L. Geniposide ameliorates learning memory deficits, reduces tau phosphorylation and decreases apoptosis *Via* Gsk3β pathway in streptozotocin-induced Alzheimer rat model. *Brain Pathol (Zurich Switzerland)* (2014) 24(3):261–9. doi: 10.1111/bpa.12116

47. Xu W, Liu J, Ma D, Yuan G, Lu Y, Yang Y. Capsaicin reduces Alzheimer-associated tau changes in the hippocampus of type 2 diabetes rats. *PloS One* (2017) 12(2):e0172477. doi: 10.1371/journal.pone.0172477

48. Li H, Tang Z, Chu P, Song Y, Yang Y, Sun B, et al. Neuroprotective effect of phosphocreatine on oxidative stress and mitochondrial dysfunction induced apoptosis in vitro and in vivo: Involvement of dual Pi3k/Akt and Nrf2/Ho-1 pathways. *Free Radical Biol Med* (2018) 120:228–38. doi: 10.1016/j.freeradbiomed.2018.03.014

49. Wang G, Fang H, Zhen Y, Xu G, Tian J, Zhang Y, et al. Sulforaphane prevents neuronal apoptosis and memory impairment in diabetic rats. *Cell Physiol Biochem* (2016) 39(3):901–7. doi: 10.1159/000447799

50. Maffei A, Lembo G, Carnevale D. Pi3kinases in diabetes mellitus and its related complications. *Int J Mol Sci* (2018) 19(12):10. doi: 10.3390/ijms19124098

51. Jayaraj RL, Azimullah S, Beiram R. Diabetes as a risk factor for alzheimer's disease in the middle East and its shared pathological mediators. *Saudi J Biol Sci* (2020) 27(2):736–50. doi: 10.1016/j.sjbs.2019.12.028

52. Deng S, Dai G, Chen S, Nie Z, Zhou J, Fang H, et al. Dexamethasone induces osteoblast apoptosis through ros-Pi3k/Akt/Gsk3β signaling pathway. *BioMed Pharmacother* (2019) 110:602–8. doi: 10.1016/j.biopha.2018.11.103

53. Huang X, Liu G, Guo J, Su Z. The Pi3k/Akt pathway in obesity and type 2 diabetes. *Int J Biol Sci* (2018) 14(11):1483–96. doi: 10.7150/ijbs.27173

54. Zhang Y, Huang NQ, Yan F, Jin H, Zhou SY, Shi JS, et al. Diabetes mellitus and alzheimer's disease: Gsk-3β as a potential link. *Behav Brain Res* (2018) 339:57–65. doi: 10.1016/j.bbr.2017.11.015

55. Sun LJ, Hou XH, Xue SH, Yan F, Dai YJ, Zhao CH, et al. Fish oil modulates glycogen synthase kinase-3 signaling pathway in diabetes-induced hippocampal neurons apoptosis. *Brain Res* (2014) 1574:37–49. doi: 10.1016/j.brainres.2014.05.050

56. Seki Y, Kasama K, Haruta H, Watanabe A, Yokoyama R, Porciuncula JP, et al. Five-Year-Results of laparoscopic sleeve gastrectomy with duodenojejunal bypass for weight loss and type 2 diabetes mellitus. *Obes Surg* (2017) 27(3):795–801. doi: 10.1007/s11695-016-2372-0

frontiers | Frontiers in Endocrinology

TYPE Mini Review
PUBLISHED 10 November 2022
DOI 10.3389/fendo.2022.1014901

OPEN ACCESS

EDITED BY
Wah Yang,
The First Affiliated Hospital of Jinan University, China

REVIEWED BY
Angelo Di Vincenzo,
University of Padua, Italy

*CORRESPONDENCE
Yan Gu
yangu@shsmu.edu.cn

SPECIALTY SECTION
This article was submitted to Obesity, a section of the journal Frontiers in Endocrinology

RECEIVED 09 August 2022
ACCEPTED 24 October 2022
PUBLISHED 10 November 2022

CITATION
Widjaja J, Chu Y, Yang J, Wang J and Gu Y (2022) Can we abandon foregut exclusion for an ideal and safe metabolic surgery?
Front. Endocrinol. 13:1014901.
doi: 10.3389/fendo.2022.1014901

Can we abandon foregut exclusion for an ideal and safe metabolic surgery?

Jason Widjaja[1], Yuxiao Chu[2], Jianjun Yang[1], Jian Wang[2] and Yan Gu[1*]

[1]Department of General Surgery, Fudan University Affiliated Huadong Hospital, Shanghai, China, [2]Department of Gastrointestinal Surgery, Affiliated Hospital of Xuzhou Medical University, Xuzhou, Jiangsu, China

Foregut (foregut exclusions) and hindgut (rapid transit of nutrients to the distal intestine) theories are the most commonly used explanations for the metabolic improvements observed after metabolic surgeries. However, several procedures that do not comprise duodenal exclusions, such as sleeve with jejunojejunal bypass, ileal interposition, and transit bipartition and sleeve gastrectomy were found to have similar diabetes remission rates when compared with duodenal exclusion procedures, such as gastric bypass, biliopancreatic diversion with duodenal switch, and diverted sleeve with ileal interposition. Moreover, the complete exclusion of the proximal intestine could result in the malabsorption of several important micronutrients. This article reviews commonly performed procedures, with and without foregut exclusion, to better comprehend whether there is a critical need to include foregut exclusion in metabolic surgery.

KEYWORDS

foregut hypothesis, micronutrient, type-2 diabetes, bariatric surgery, metabolic surgery

Introduction

Bariatric and metabolic surgeries have resulted in significant improvements and remissions in type 2 diabetes mellitus and other metabolic comorbidities (1, 2). However, the mechanisms underlying these effects remain unclear. The foregut (proximal intestine exclusions) and hindgut theories are the classic and most commonly used explanations for the resolution of type 2 diabetes mellitus observed after metabolic surgeries (3). While the hindgut theory (rapid transit of nutrients to the distal intestine) has been widely accepted, the foregut theory is not (4, 5). Several procedures that do not comprise duodenal exclusions, such as sleeve with jejunojejunal bypass/SG-JJB, sleeve with ileal interposition/SG-II, sleeve with transit bipartition/SG-TB, and standalone sleeve gastrectomy/SG (Figure 1), have similar

diabetes remission outcomes when compared with procedures comprising duodenal exclusions, such as gastric bypass/GB, biliopancreatic diversion with duodenal switch/DS, and diverted sleeve with ileal interposition/DSG-II (Figure 2) (6–13). Furthermore, the complete exclusion of the proximal intestine may result in significant micronutrient malabsorption. Thus, while being a safe metabolic procedure, the need for foregut exclusion to achieve ideal metabolic outcomes is questioned.

In this article, we briefly review the commonly performed metabolic procedures with and without foregut exclusion, with the hope to create a research direction to further comprehend the mechanisms of bariatric and metabolic surgeries.

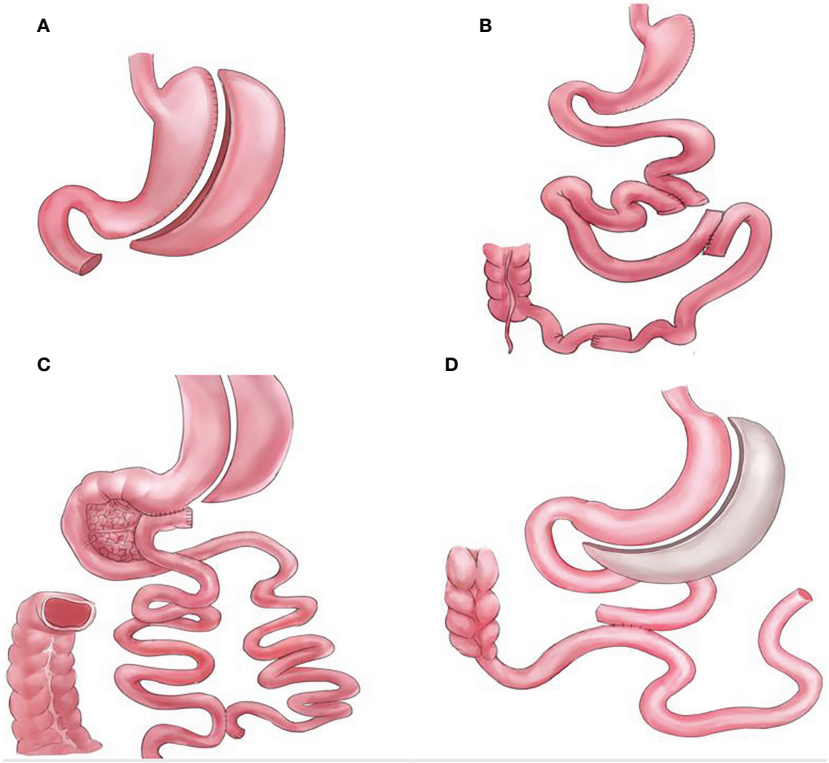

FIGURE 1
Graphical illustrations for procedures that do not bypass the foregut, **(A)** standalone sleeve gastrectomy (SG), **(B)** sleeve with ileal interposition (SG-II), **(C)** sleeve with transit bipartition (SG-TB), and **(D)** sleeve with jejunojejunal bypass (SG-JJB).

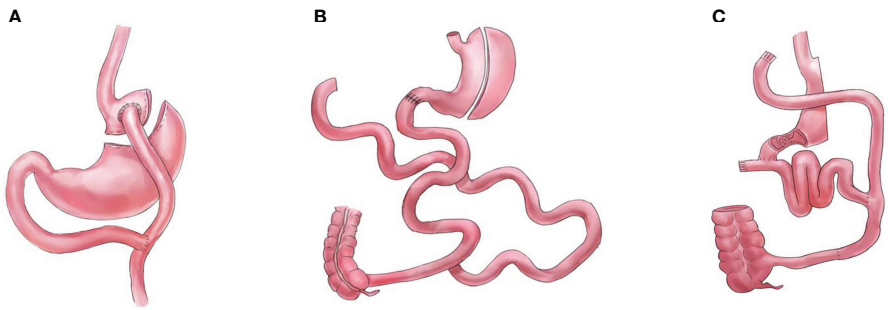

FIGURE 2
Graphical illustrations for procedures that completely bypass the foregut, **(A)** gastric bypass (GB), **(B)** biliopancreatic diversion with duodenal switch (DS), and **(C)** diverted sleeve with ileal interposition (DSG-II).

Foregut hypothesis

The foregut hypothesis is one of the classic explanations for the diabetes remission observed after bariatric surgery. This hypothesis proposes that the exclusion of the proximal small intestine (duodenum and proximal jejunum) from the transit of nutrients may prevent the secretion of a "factor" that promotes insulin resistance and type 2 diabetes mellitus (3, 14, 15). However, the foregut hypothesis fails to explain how several other bariatric procedures that did not comprise duodenal exclusion, such as SG-JJB, SG-II, SG-TB, and standalone SG, still achieved excellent diabetes remission results (6, 7, 10–12). Furthermore, we are yet to identify the foregut "factor" that affects the glucose homeostasis. If the exclusion of the foregut is not required to achieve metabolic improvements, then complete exclusion of the foregut may be abandoned to achieve the ideal metabolic procedure.

Importance of foregut inclusion in bariatric and metabolic surgeries

There are significant drawbacks of excluding the foregut from nutrient transit. The proximal intestine is a major site of absorption of several important vitamins and micronutrients. For example, the risk of vitamin B12 deficiency is higher following GB than after SG and is attributable to the duodenal exclusion in gastric bypass (16). Procedures that exclude the proximal intestine, where most iron absorption occurs, are expected to increase the risk of iron deficiency (17). Reduced calcium absorption and vitamin D deficiency were also frequently observed in procedures that excluded the proximal intestine, which has the highest concentration of calcium transporters (18). Furthermore, the proximal intestine is also indirectly involved in the absorption of liposoluble vitamins and micronutrients. Procedures that bypass the proximal intestine result in the reduction of pancreatic enzyme secretion and alteration in bile salts, leading to alterations in fat assimilation (19–21).

Procedures that completely bypass the foregut

GB, DS, and DSG-II are the procedures that are normally performed according to the foregut hypothesis (bypassing the foregut). These procedures can incorporate modifications of the "one-anastomosis reconstruction"; however, such modifications do not alter the foregut exclusion components.

Multiple randomized controlled trials (RCT) have compared the efficacy of GB with procedures that do not comprise foregut exclusion. A meta-analysis of RCTs comparing the outcomes of GB and SG found that GB resulted in a superior loss of body mass index (BMI), which persisted at 3 years postoperatively (22). Interestingly, the study did not find differences in diabetes remission, hemoglobin A1c (HbA1c) level, and homeostatic model assessment of insulin resistance levels. Similarly, three RCTs (Stampede, SM-BOSS, and SLEEVE-PASS trials) found no difference between GB and SG regarding HbA1c levels and rate of diabetes remission at 5 years postoperatively (12, 13, 23). However, GB is associated with a higher risk of nutritional deficiencies than SG (16, 24). Studies have reported that reconnecting the foregut back to the configuration can solve the malnutrition issue in GB without compromising the bariatric and metabolic outcomes (25, 26).

Another classic bariatric and metabolic procedure is DS, which is regarded as the most effective procedure (27). An RCT reported that at 5 years postoperatively, DS resulted in superior weight loss and glucose improvements compared to those of GB; however, DS is associated with more nutritional complications (28). Long-term studies (10 years) have also reported the nutritional issues associated with DS, particularly with fat-soluble vitamins (29, 30). Thus, although the effectiveness of DS is undisputed, it is not commonly performed owing to the high prevalence of complications (2, 31).

DSG-II and SG-II are among the most complex procedures, as they require more anastomosis than most metabolic surgeries (32). Unlike DSG-II, which bypasses the foregut and creates malabsorption, the SSG-II procedure ensures that there is no malabsorption. However, limited data are available regarding the prevalence of nutritional deficiency between the DSG-II and SG-II procedures. However, DSG-II and SG-II resulted in similar glucose control improvements, which further questions the need for foregut exclusion (7, 33, 34). Ileal interposition procedures are not commonly performed because of their complexity and the need for a high number of anastomoses, and because a higher number of mesenteric defects are created in these procedures (32).

Procedures that do not bypass the foregut

SG, SG-TB, SG-II, and SG-JJB are the procedures that are not normally performed according to the foregut hypothesis. Similar to the GB and DS, some of these procedures can incorporate modifications of the "one-anastomosis reconstruction"; however, such modifications do not alter the foregut inclusion components.

SG can be considered the foundation of most bariatric and metabolic surgeries, as many of the procedures consist of SG. Standalone SG is currently the most commonly performed procedure worldwide, with excellent results (2, 31). As mentioned previously, when compared with GB, SG was found to be comparable regarding metabolic improvements as well as

having a lower risk of nutritional deficiency (12, 13, 16, 23, 24). However, in the longer term, SG is complicated by several issues, such as weight regain, diabetes relapse, and reflux (35). Therefore, revisional surgery after SG is becoming a common practice.

SG-TB is a procedure that has been gaining significant attention in recent years (particularly its one-anastomosis form, the single-anastomosis sleeve ileal bypass/SASI). Proposed as a modification of the DS procedure, SG-TB eliminates the need to completely bypass the duodenum. The 5 year result of SG-TB was reported to be 74% excess BMI loss and 86% diabetes remission (5). SG-TB has been shown to have comparable weight loss and diabetes remission results, while having lesser risks for nutritional deficiencies when compared to GB (11, 36). When compared with DS, SG-TB was reported to have lesser weight loss results; however, there was no difference in the rate of diabetes remission (10). The authors further noted that SG-TB showed real benefits in reducing the side effects and malnutrition risks compared with DS (10). When compared with DSG-II, SG-TB showed similar weight loss and diabetes remission results; however, the differences in nutritional deficiencies between the two procedures has not been reported (9).

The SG-II procedure has been described and discussed in the previous section. Moreover, in the case of severe malnutrition after the DS procedure, conversion to SG-II (without bypassing the foregut) solved the malnutrition issues without compromising the bariatric and metabolic results (37). In conclusion, although more studies are needed, the SG-II and DSG-II demonstrated comparable weight loss and diabetes remission results; thus, questioning the need for foregut exclusion.

Other procedures that do not bypass the foregut have been reported. SG-JJB was reported to have comparable weight loss and diabetes remission rates to GB (6). A rodent model of jejunal-ileal loop bipartition has also been described, showing its effectiveness in improving glucose control (38).

SG-TB, SG-JJB, and SG-II procedures are still lacking comparative studies as well as RCTs; thus, further studies are warranted in this regard in the future. However, the results to date have been promising with regard to the notion of abandoning foregut exclusion.

Mechanisms related to the effect of bariatric surgery

Glucagon-like peptide-1 (GLP-1) is secreted by intestinal enteroendocrine L-cells and several brain cells in the brainstem following food consumption (39). GLP-1 is an incretin having the ability to enhance insulin secretion. In the brain and the stomach, GLP-1 also can promote satiety, reducing food intake. Per the hindgut theory (rapid transit of nutrients to the distal intestine), bariatric procedures that resulted in the rapid transient of nutrients showed significantly elevated GLP-1 levels following food consumption (39). A recent meta-analysis reported that postprandial GLP-1 levels were also increased following SG, possibly due to increased gastric emptying (40).

Similarly, peptide YY (PYY) was also reported to be elevated in bariatric procedures with or without duodenal exclusion (40). PYY is also secreted by the L-cells and has the ability to reduce appetite and promote satiety.

After bariatric surgery, several studies have shown that the increased level of bile acids can promote insulin secretion, increase energy expenditure, and alter the gut microbiota (41). Bile acids play a role in metabolic regulation mediated through several receptors, such as the farnesoid X receptor (FXR) and G protein-coupled bile acid receptor 1 (also known as TGR5) (41). Stimulation of FXR in insulin-resistant obese mice was shown to reduce hyperinsulinemia and improved glucose control (42). In response to bile acids, TGR5 activation promotes GLP-1 secretion in animal and human studies (43, 44). Increased bile acids can increase energy expenditure through TGR5 in the skeletal muscle and brown adipose tissue (45, 46). Bile acids and gut microbiota are affected and altered by bariatric surgery. Increased bile acid concentrations can kill and promote certain gut bacteria strains (41).

Individuals with obesity exhibit an altered gut microbiota as compared to lean controls, comprising of a decline in Bacteroidetes and an increase in Firmicutes in obese individuals (47). On the other hand, bariatric surgery resulted in the alteration of gut microbiota composition (decrease of Firmicutes/Bacteroidetes ratio), which contributes to fat mass regulation and reduced utilization of carbohydrates as energy fuel (48).

Several studies have shown that bariatric surgery induces changes in adipose tissue and improves systemic inflammation (49). Bariatric surgery induces changes in the levels of several microRNAs from the adipocyte-derived exosomes, which are correlated to the improved insulin signaling following the surgery. Several inflammatory factors, such as C-reactive protein, tumor necrosis factor-α, and interleukin-6, the hallmark for the initiation of insulin resistance, were also reduced following bariatric surgery.

Several other hypotheses explaining the mechanisms of bariatric surgery exist (41). However, all of these hypotheses can be justified through the anatomical changes leading to the distal intestine or as changes in general after bariatric surgery, further questioning the foregut hypothesis.

Discussion

The era of bariatric and metabolic surgeries has been evolving continuously. In the past, malabsorption and restriction were the primary targets of bariatric surgery for

achieving an ideal healthy weight (50). However, in recent years, the era of pure metabolic surgery has been initiated, focusing on improving the metabolic potency of bariatric surgery, hence the name "metabolic surgery" (51–53). To improve the metabolic potency of a procedure, we must comprehend the mechanism of the metabolic improvements observed following metabolic procedures. However, metabolic surgery appears to have a highly complex mechanism, and more time may be needed to better understand it. Moreover, recent surgical innovations have provided us with the knowledge that could be used to improve the safety of metabolic surgery.

Classic and significant metabolic procedures, such as GB and DS, resulted in excellent metabolic outcomes (54–57). However, they also resulted in unwanted effects, such as excessive nutrient malabsorption (58). In contrast, several metabolic procedures (such as SG-JJB, SG-II, SG-TB, and SG) that maintain the foregut (either completely or partially) have been demonstrated to have efficacy that is not inferior to foregut exclusion procedures (6–13). It is imperative to acknowledge that the SG procedure has been the most performed bariatric procedure worldwide in recent years, surpassing RYGB (31). Furthermore, several RCTs have shown that SG (without duodenal exclusion) could result in comparable bariatric and metabolic outcomes compared to RYGB (with duodenal exclusion) (12, 13, 23).

Although procedures such as SG-JJB, SG-II, and SG-TB, differ in intestinal reconfiguration, they have common consequences: 1) foregut inclusion and 2) expediting nutrient flow to the distal intestine (hindgut theory). It has been recently proposed that foregut exclusions may not be necessary as long as strong stimulus to the ileum is provided (59). However, we need better comparative studies to understand not only the metabolic efficacy but also the safety of these foregut inclusion procedures.

With the foregut hypothesis being the focus of this article, it is imperative to discuss the use of duodenal-jejunal bypass liner as a treatment alternative for metabolic diseases. While it has been reported that the duodenal-jejunal bypass liner resulted in significant improvements in type 2 diabetes, the underlying mechanisms remain elusive (60). In contrast to foregut exclusion, a previous study showed that preserving foregut transit in GB and DS models still resulted in significant weight loss and glucose control improvements (25, 26, 37). Therefore, these findings created another notion, "Is bypassing the foregut necessary? Or as long as there is enough exclusion, regardless of the site of exclusion, would we still observe excellent metabolic improvements?" The goal of bariatric and metabolic surgery should be to improve the patients' quality of life as well as improving their weight status and comorbidities, i.e. not to focus solely on the weight loss outcomes.

In conclusion, with the available studies, we cannot deny the credibility of foregut exclusion for excellent metabolic outcomes. However, the idea of abandoning complete foregut exclusion has some credibility, and more comparative studies are needed to prove this idea. Such studies should focus mainly on whether: 1) foregut inclusion resulted in non-inferior metabolic outcomes than after foregut exclusion and 2) foregut inclusion delivers better safety regarding micronutrient malabsorption than that following foregut exclusion.

Author contributions

JaW and YG propose the topic and design the manuscript flows. JaW and JY draft the manuscript. YC and JiW collect and analyse the materials for the manuscript. JW, YC, JY, JiW, and YG reviewed the manuscript. All authors contributed to the article and approved the submitted version.

Conflict of interest

The authors declare that the research was conducted in the absence of any commercial or financial relationships that could be construed as a potential conflict of interest.

Publisher's note

References

1. Frühbeck G. Bariatric and metabolic surgery: a shift in eligibility and success criteria. *Nat Rev Endocrinol* (2015) 11(8):465–77. doi: 10.1038/nrendo.2015.84

2. Welbourn R, Hollyman M, Kinsman R, Dixon J, Cohen R, Morton J, et al. Bariatric-metabolic surgery utilisation in patients with and without diabetes: Data from the IFSO global registry 2015-2018. *Obes Surg* (2021) 31(6):2391–400. doi: 10.1007/s11695-021-05280-6

3. Mingrone G, Castagneto-Gissey L. Mechanisms of early improvement/resolution of type 2 diabetes after bariatric surgery. *Diabetes Metab* (2009) 35(6 Pt 2):518–23. doi: 10.1016/S1262-3636(09)73459-7

4. Patriti A, Aisa MC, Annetti C, Sidoni A, Galli F, Ferri I, et al. How the hindgut can cure type 2 diabetes. ileal transposition improves glucose metabolism and beta-cell function in goto-kakizaki rats through an enhanced proglucagon gene expression and l-cell number. *Surgery* (2007) 142(1):74–85. doi: 10.1016/j.surg.2007.03.001

5. Santoro S, Castro LC, Velhote MC, Malzoni CE, Klajner S, Castro LP, et al. Sleeve gastrectomy with transit bipartition: a potent intervention for metabolic syndrome and obesity. *Ann Surg* (2012) 256(1):104–10. doi: 10.1097/SLA.0b013e31825370c0

6. Lin S, Li C, Guan W, Liang H. Three-year outcomes of sleeve gastrectomy plus jejunojejunal bypass: a retrospective case-matched study with sleeve gastrectomy and gastric bypass in Chinese patients with BMI ≥35 kg/m2. *Obes Surg* (2021) 31(8):3525–30. doi: 10.1007/s11695-021-05411-z

7. DePaula AL, Macedo AL, Schraibman V, Mota BR, Vencio S. Hormonal evaluation following laparoscopic treatment of type 2 diabetes mellitus patients with BMI 20-34. *Surg Endosc* (2009) 23(8):1724–32. doi: 10.1007/s00464-008-0168-6

8. Ugale S, Gupta N, Modi KD, Kota SK, Satwalekar V, Naik V, et al. Prediction of remission after metabolic surgery using a novel scoring system in type 2 diabetes - a retrospective cohort study. *J Diabetes Metab Disord* (2014) 13(1):89. doi: 10.1186/s40200-014-0089-y

9. Yormaz S, Yılmaz H, Ece I, Sahin M. Laparoscopic ileal interposition with diverted sleeve gastrectomy versus laparoscopic transit bipartition with sleeve gastrectomy for better glycemic outcomes in T2DM patients. *Obes Surg* (2018) 28(1):77–86. doi: 10.1007/s11695-017-2803-6

10. Topart P, Becouarn G, Finel JB. Is transit bipartition a better alternative to biliopancreatic diversion with duodenal switch for superobesity? comparison of the early results of both procedures. *Surg Obes Relat Dis* (2020) 16(4):497–502. doi: 10.1016/j.soard.2019.12.019

11. Topart P, Becouarn G, Finel JB. Comparison of 2-year results of roux-en-Y gastric bypass and transit bipartition with sleeve gastrectomy for superobesity. *Obes Surg* (2020) 30(9):3402–7. doi: 10.1007/s11695-020-04691-1

12. Salminen P, Helmiö M, Ovaska J, Juuti A, Leivonen M, Peromaa-Haavisto P, et al. Effect of laparoscopic sleeve gastrectomy vs laparoscopic roux-en-Y gastric bypass on weight loss at 5 years among patients with morbid obesity: The SLEEVEPASS randomized clinical trial. *JAMA* (2018) 319(3):241–54. doi: 10.1001/jama.2017.20313

13. Peterli R, Wölnerhanssen BK, Peters T, Vetter D, Kröll D, Borbély Y, et al. Effect of laparoscopic sleeve gastrectomy vs laparoscopic roux-en-Y gastric bypass on weight loss in patients with morbid obesity: The SM-BOSS randomized clinical trial. *JAMA* (2018) 319(3):255–65. doi: 10.1001/jama.2017.20897

14. Ramos AC, Galvao Neto MP, de Souza YM, Galvao M, Murakami AH, Silva AC, et al. Laparoscopic duodenal-jejunal exclusion in the treatment of type 2 diabetes mellitus in patients with BMI < 30 kg/m2 (LBMI). *Obes Surg* (2009) 19:307–12. doi: 10.1007/s11695-008-9759-5

15. Rubino F, Marescaux J. Effect of duodenal-jejunal exclusion in a non-obese animal model of type 2 diabetes: a new perspective for an old disease. *Ann Surg* (2004) 239:1–11. doi: 10.1097/01.sla.0000102989.54824.fc

16. Alexandrou A, Armeni E, Kouskouni E, Tsoka E, Diamantis T, Lambrinoudaki I. Cross-sectional long-term micronutrient deficiencies after sleeve gastrectomy versus roux-en-Y gastric bypass: a pilot study. *Surg Obes Relat Dis* (2014) 10(2):262–8. doi: 10.1016/j.soard.2013.07.014

17. Ruz M, Carrasco F, Rojas P, Codoceo J, Inostroza J, Basfi-Fer K, et al. Heme- and nonheme-iron absorption and iron status 12 mo after sleeve gastrectomy and roux-en-Y gastric bypass in morbidly obese women. *Am J Clin Nutr* (2012) 96 (4):810–7. doi: 10.3945/ajcn.112.039255

18. Saad R, Habli D, El Sabbagh R, Chakhtoura M. Bone health following bariatric surgery: An update. *J Clin Densitom* (2020) 23(2):165–81. doi: 10.1016/j.jocd.2019.08.002

19. Shikora SA, Kim JJ, Tarnoff ME. Nutrition and gastrointestinal complications of bariatric surgery. *Nutr Clin Pract* (2007) 22(1):29–40. doi: 10.1177/011542650702200129

20. Saltzman E, Philip Karl J. Nutrient deficiencies after gastric bypass surgery. *Ann Rev Nutr* (2013) 33:183–203. doi: 10.1146/annurev-nutr-071812-161225

21. Shankar P, Boylan M, Sriram K. Micronutrient deficiencies after bariatric surgery. *Nutrition* (2010) 26(11):1031–7. doi: 10.1016/j.nut.2009.12.003

22. Lee Y, Doumouras AG, Yu J, Aditya I, Gmora S, Anvari M, et al. Laparoscopic sleeve gastrectomy versus laparoscopic roux-en-Y gastric bypass: A systematic review and meta-analysis of weight loss, comorbidities, and biochemical outcomes from randomized controlled trials. *Ann Surg* (2021) 273(1):66–74. doi: 10.1097/SLA.0000000000003671

23. Schauer PR, Bhatt DL, Kirwan JP, Wolski K, Aminian A, Brethauer SA, et al. Bariatric surgery versus intensive medical therapy for diabetes - 5-year outcomes. *N Engl J Med* (2017) 376(7):641–51. doi: 10.1056/NEJMoa1600869

24. Gu L, Fu R, Chen P, Du N, Chen S, Mao D, et al. In terms of nutrition, the most suitable method for bariatric surgery: Laparoscopic sleeve gastrectomy or roux-en-Y gastric bypass? a systematic review and meta-analysis. *Obes Surg* (2020) 30(5):2003–14. doi: 10.1007/s11695-020-04488-2

25. Ceneviva R, Salgado Júnior W, Marchini JS. A new revisional surgery for severe protein-calorie malnutrition after roux-en-Y gastric bypass: successful duodenojejunal reconstruction using jejunal interposition. *Surg Obes Relat Dis* (2016) 12(2):e21–3. doi: 10.1016/j.soard.2015.09.020

26. Dolo PR, Yao L, Li C, Zhu X, Shi L, Widjaja J. Preserving duodenal-jejunal (Foregut) transit does not impair glucose tolerance and diabetes remission following gastric bypass in type 2 diabetes sprague-dawley rat model. *Obes Surg* (2018) 28(5):1313–20. doi: 10.1007/s11695-017-2985-y

27. O'Brien PE, Hindle A, Brennan L, Skinner S, Burton P, Smith A, et al. Long-term outcomes after bariatric surgery: a systematic review and meta-analysis of weight loss at 10 or more years for all bariatric procedures and a single-centre review of 20-year outcomes after adjustable gastric banding. *Obes Surg* (2019) 29 (1):3–14. doi: 10.1007/s11695-018-3525-0

28. Risstad H, Søvik TT, Engström M, Aasheim ET, Fagerland MW, Olsén MF, et al. Five-year outcomes after laparoscopic gastric bypass and laparoscopic duodenal switch in patients with body mass index of 50 to 60: a randomized clinical trial. *JAMA Surg* (2015) 150(4):352–61. doi: 10.1001/jamasurg.2014.3579

29. Ballesteros-Pomar MD, González de Francisco T, Urioste-Fondo A, González-Herraez L, Calleja-Fernández A, Vidal-Casariego A, et al. Biliopancreatic diversion for severe obesity: Long-term effectiveness and nutritional complications. *Obes Surg* (2016) 26(1):38–44. doi: 10.1007/s11695-015-1719-2

30. Topart P, Becouarn G, Delarue J. Weight loss and nutritional outcomes 10 years after biliopancreatic diversion with duodenal switch. *Obes Surg* (2017) 27 (7):1645–50. doi: 10.1007/s11695-016-2537-x

31. Welbourn R, Hollyman M, Kinsman R, Dixon J, Liem R, Ottosson J, et al. Bariatric surgery worldwide: Baseline demographic description and one-year outcomes from the fourth IFSO global registry report 2018. *Obes Surg* (2019) 29 (3):782–95. doi: 10.1007/s11695-018-3593-1

32. Gagner M. Surgical treatment of nonseverely obese patients with type 2 diabetes mellitus: sleeve gastrectomy with ileal transposition (SGIT) is the same as the neuroendocrine brake (NEB) procedure or ileal interposition associated with sleeve gastrectomy (II-SG), but ileal interposition with diverted sleeve gastrectomy (II-DSG) is the same as duodenal switch. *Surg Endosc* (2011) 25(2):655–6. doi: 10.1007/s00464-010-1221-9

33. De Paula AL, Stival AR, Macedo A, Ribamar J, Mancini M, Halpern A, et al. Prospective randomized controlled trial comparing 2 versions of laparoscopic ileal interposition associated with sleeve gastrectomy for patients with type 2 diabetes with BMI 21-34 kg/m(2). *Surg Obes Relat Dis* (2010) 6(3):296–304. doi: 10.1016/j.soard.2009.10.005

34. DePaula AL, Stival AR, DePaula CC, Halpern A, Vencio S. Surgical treatment of type 2 diabetes in patients with BMI below 35: mid-term outcomes of the laparoscopic ileal interposition associated with a sleeve gastrectomy in 202 consecutive cases. *J Gastrointest Surg* (2012) 16(5):967–76. doi: 10.1007/s11605-011-1807-0

35. Nudotor RD, Prokopowicz G, Abbey EJ, Gonzalez A, Canner JK, Steele KE. Comparative effectiveness of roux-en y gastric bypass versus vertical sleeve gastrectomy for sustained remission of type 2 diabetes mellitus. *J Surg Res* (2021) 261:407–16. doi: 10.1016/j.jss.2020.12.024

36. Ece I, Yilmaz H, Yormaz S, Çolak B, Calisir A, Sahin M. The short-term effects of transit bipartition with sleeve gastrectomy and distal-Roux-en-Y gastric bypass on glycemic control, weight loss, and nutritional status in morbidly obese and type 2 diabetes mellitus patients. *Obes Surg* (2021) 31(5):2062–71. doi: 10.1007/s11695-020-05212-w

37. Almahmeed T, Pomp A, Gagner M. Laparoscopic reversal of biliopancreatic diversion with duodenal switch. *Surg Obes Relat Dis* (2006) 2(4):468–71. doi: 10.1016/j.soard.2006.03.023

38. Zhang X, Shen Y, Cao T, Wang Y, Qiao Z, Zhang Z, et al. A rodent model of jejunal-ileal loop bipartition (JILB): a novel malabsorptive operation. *Obes Surg* (2021) 31(3):1361–8. doi: 10.1007/s11695-020-05163-2

39. D'Alessio D. Is GLP-1 a hormone: Whether and when? *J Diabetes Investig* (2016) 7 Suppl 1(Suppl 1):50–5. doi: 10.1111/jdi.12466

40. McCarty TR, Jirapinyo P, Thompson CC. Effect of sleeve gastrectomy on ghrelin, GLP-1, PYY, and GIP gut hormones: A systematic review and meta-analysis. *Ann Surg* (2020) 272(1):72–80. doi: 10.1097/SLA.0000000000003614

41. Wang W, Cheng Z, Wang Y, Dai Y, Zhang X, Hu S. Role of bile acids in bariatric surgery. *Front Physiol* (2019) 10:374. doi: 10.3389/fphys.2019.00374

42. Cariou B, van Harmelen K, Duran-Sandoval D, van Dijk TH, Grefhorst A, Abdelkarim M, et al. The farnesoid X receptor modulates adiposity and peripheral insulin sensitivity in mice. *J Biol Chem* (2006) 281(16):11039–49. doi: 10.1074/jbc.M510258200

43. Thomas C, Gioiello A, Noriega L, Strehle A, Oury J, Rizzo G, et al. TGR5-mediated bile acid sensing controls glucose homeostasis. *Cell Metab* (2009) 10 (3):167–77. doi: 10.1016/j.cmet.2009.08.001

44. Wu T, Bound MJ, Standfield SD, Gedulin B, Jones KL, Horowitz M, et al. Effects of rectal administration of taurocholic acid on glucagon-like peptide-1 and peptide YY secretion in healthy humans. *Diabetes Obes Metab* (2013) 15(5):474–7. doi: 10.1111/dom.12043

45. Kohli R, Bradley D, Setchell KD, Eagon JC, Abumrad N, Klein S. Weight loss induced by roux-en-Y gastric bypass but not laparoscopic adjustable gastric banding increases circulating bile acids. *J Clin Endocrinol Metab* (2013) 98(4): E708–12. doi: 10.1210/jc.2012-3736

46. Broeders EP, Nascimento EB, Havekes B, Brans B, Roumans KH, Tailleux A, et al. The bile acid chenodeoxycholic acid increases human brown adipose tissue activity. *Cell Metab* (2015) 22(3):418–26. doi: 10.1016/j.cmet.2015.07.002

47. Ciobârcă D, Cătoi AF, Copăescu C, Miere D, Crişan G. Bariatric surgery in obesity: Effects on gut microbiota and micronutrient status. *Nutrients* (2020) 12 (1):235./ doi: 10.3390/nu12010235

48. Tremaroli V, Karlsson F, Werling M, Ståhlman M, Kovatcheva-Datchary P, Olbers T, et al. Roux-en-Y gastric bypass and vertical banded gastroplasty induce long-term changes on the human gut microbiome contributing to fat mass regulation. *Cell Metab* (2015) 22(2):228–38. doi: 10.1016/j.cmet.2015.07.009

49. Xu G, Song M. Recent advances in the mechanisms underlying the beneficial effects of bariatric and metabolic surgery. *Surg Obes Relat Dis* (2021) 17(1):231–8. doi: 10.1016/j.soard.2020.08.028

50. Buchwald H. The evolution of metabolic/bariatric surgery. *Obes Surg* (2014) 24(8):1126–35. doi: 10.1007/s11695-014-1354-3

51. Pareek M, Schauer PR, Kaplan LM, Leiter LA, Rubino F, Bhatt DL. Metabolic surgery: Weight loss, diabetes, and beyond. *J Am Coll Cardiol* (2018) 71(6):670–87. doi: 10.1016/j.jacc.2017.12.014

52. Buchwald H, Buchwald JN. Metabolic (Bariatric and nonbariatric) surgery for type 2 diabetes: A personal perspective review. *Diabetes Care* (2019) 42(2):331–40. doi: 10.2337/dc17-2654

53. Wilson R, Aminian A, Tahrani AA. Metabolic surgery: A clinical update. *Diabetes Obes Metab* (2021) 23 Suppl 1:63–83. doi: 10.1111/dom.14235

54. Quevedo MDP, Palermo M, Serra E, Ackermann MA. Metabolic surgery: gastric bypass for the treatment of type 2 diabetes mellitus. *Transl Gastroenterol Hepatol* (2017) 2:58. doi: 10.21037/tgh.2017.05.10

55. Maclellan WC, Johnson JM. Laparoscopic gastric bypass: Still the gold standard? *Surg Clin North Am* (2021) 101(2):161-75. doi: 10.1016/j.suc.2020.12.013

56. Hess DS, Hess DW, Oakley RS. The biliopancreatic diversion with the duodenal switch: results beyond 10 years. *Obes Surg* (2005) 15(3):408–16. doi: 10.1381/0960892053576695

57. Sorribas M, Casajoana A, Sobrino L, Admella V, Osorio J, Pujol-Gebellí J. Experience in biliopancreatic diversion with duodenal switch: results at 2, 5 and 10 years. *Cir Esp (Engl Ed)* (2021) 100(4):202–8. doi: 10.1016/j.ciresp.2021.01.008

58. Bal BS, Finelli FC, Shope TR, Koch TR. Nutritional deficiencies after bariatric surgery. *Nat Rev Endocrinol* (2012) 8(9):544–56. doi: 10.1038/nrendo.2012.48

59. Santoro S, Aquino CGG, Mota FC. Exclusions may be dismissed if the ileum is early and potently stimulated. *Obes Surg* (2021) 31(11):5049–50. doi: 10.1007/s11695-021-05526-3

60. Jirapinyo P, Haas AV, Thompson CC. Effect of the duodenal-jejunal bypass liner on glycemic control in patients with type 2 diabetes with obesity: A meta-analysis with secondary analysis on weight loss and hormonal changes. *Diabetes Care* (2018) 41(5):1106–15. doi: 10.2337/dc17-1985

frontiers | Frontiers in Endocrinology

TYPE Original Research
PUBLISHED 18 November 2022
DOI 10.3389/fendo.2022.1041889

OPEN ACCESS

EDITED BY
Peng Zhang,
Affiliated Beijing Friendship Hospital, Capital Medical University, China

REVIEWED BY
Francesca Abbatini,
Azienda Sanitaria Locale Roma 6, Italy
Michel Vix,
Hôpitaux Universitaires de Strasbourg, France
Vivek Bindal,
Max Super Speciality Hospital, India

*CORRESPONDENCE
Kelimu Abudureyimu
klm6075@163.com

†These authors have contributed equally to this work

SPECIALTY SECTION
This article was submitted to Obesity, a section of the journal Frontiers in Endocrinology

RECEIVED 11 September 2022
ACCEPTED 24 October 2022
PUBLISHED 18 November 2022

CITATION
Aili A, Maimaitiming M, Maimaitiyusufu P, Tusuntuoheti Y, Li X, Cui J and Abudureyimu K (2022) Gastroesophageal reflux related changes after sleeve gastrectomy and sleeve gastrectomy with fundoplication: A retrospective single center study. *Front. Endocrinol.* 13:1041889. doi: 10.3389/fendo.2022.1041889

Gastroesophageal reflux related changes after sleeve gastrectomy and sleeve gastrectomy with fundoplication: A retrospective single center study

Aikebaier Aili[1,2,3,4†], Maimaitiaili Maimaitiming[1,2,3†], Pierdiwasi Maimaitiyusufu[1,2,3,4], Yusujiang Tusuntuoheti[1,4], Xin Li[1,4], Jianyu Cui[1,4] and Kelimu Abudureyimu[1,2,3,4*]

[1]Department of Minimally Invasive Surgery, Hernias and Abdominal Wall Surgery, People's Hospital of Xinjiang Uygur Autonomous Region, Urumqi, Xinjiang Uygur Autonomous Region, China, [2]Xinjiang Clinical Research Center for Gastroesophageal Reflux Disease and Bariatric Metabolic Surgery, Urumqi, Xinjiang Uygur Autonomous Region, China, [3]Research Institute of General and Minimally Invasive Surgery, Urumqi, Xinjiang Uygur Autonomous Region, China, [4]The Graduate Student Institute of Xinjiang Medical University, Urumqi, Xinjiang Uygur Autonomous Region, China

Background: The worsening of gastroesophageal reflux disease (GERD) and "*de novo*" GERD after laparoscopic sleeve gastrectomy (LSG) is a major concern as it affects the patient's quality of life; the incidence of GERD after LSG is up to 35%. Laparoscopic sleeve gastrectomy with fundoplication (LSGFD) is a new procedure which is considered to be better for patients with morbid obesity and GERD, but there is a lack of objective evidence to support this statement. This study aimed to assess the effectiveness, safety, and results of LSG and LSGFD on patients who were morbidly obese with or without GERD over an average of 34 months follow-up.

Methods: Fifty-six patients who were classified as obese underwent surgery from January 2018 to January 2020. Patients who were obese and did not have GERD underwent LSG and patients who were obese and did have GERD underwent LSFGD. The minimum follow-up time was 22 months and there were 11 cases lost during the follow-up period. We analyzed the short-term complications and medium-term results in terms of weight loss, incidence of *de novo* GERD/resolution of GERD, and remission of co-morbidities with follow-up.

Results: A total of 45 patients completed the follow-up and a questionnaire-based evaluation (GERD-Q), of whom 23 patients underwent LSG and 22 patients underwent LSGFD. We had 1 case of leak after LSGFD.No medium or long- term complications. The patient's weight decreased from an average of 111.6 ± 11.8 Kg to 79.8 ± 12.2 Kg (P = 0.000) after LSG and from 104.3 ± 17.0 Kg to 73.7 ± 13.1 Kg (P = 0.000) after LSGFD. The GERD-Q scores increased from 6.70 ± 0.5 to 7.26 ± 1.7 (P = 0.016) after LSG and decreased from 8.86 ±

1.3 to 6.45 ± 0.8 (P = 0.0004) after LSGFD. The incidence of *de novo* GERD after LSG was 12 (52.2%) at the 12 month follow-up and 7 (30.4%) at the mean 34 (22–48) month follow-up. The remission of reflux symptoms, for patients who underwent LSGFD, was seen in 19 (86.4%) of 22 patients at 12 months and 20 (90.9%) of 22 patients at the mean 34 (22-48) month follow-up. The two groups did not have any significant difference in the effect of weight reduction and comorbidity resolution.

Conclusion: The incidence of *de novo* GERD after LSG is high,LSG resulted in the same weight loss and comorbidity resolution as LSGFD, in patients who are morbidly obese and experience GERD, and LFDSG prevent the occurrence and development of GERD, combination of LSG with fundoplication (LSGFD) is a feasible and safe procedure with good postoperative results,which worthy of further clinical application.

KEYWORDS

gastroesophageal reflux disease (GERD), laparoscopic sleeve gastrectomy (LSG), laparoscopic sleeve gastrectomy with fundoplication, *de novo* GERD after sleeve gastrectomy, GERD after bariatric surgery

Introduction

Obesity has become a serious public health problem (1). Recent statistics show that overweight/obesity continues to rise globally, with more than 2 billion people being overweight and accounting for approximately 30% of the world population (2). Gastroesophageal reflux disease (GERD), a known obesity-related complication, is a condition that occurs when reflux of stomach contents causes troublesome symptoms such as heart burn, regurgitation and chest pain (3). According to a meta-analysis, the global pooled prevalence of weekly gastroesophageal reflux symptoms is roughly 13% (4). Interestingly, the incidence of GERD in morbidly obese patient is up to 73% (5).

Bariatric surgery is considered the most effective therapy for morbid obesity at present and sleeve gastrectomy (SG) is now the most widely performed bariatric procedure (6). A large number of studies have reported good overall results with regards to surgical safety, resolution of obesity-related morbidities, and medium-term results for SG (7–9). However, SG is associated with a high incidence of GERD in long-term follow-up (10). For this reason, SG is not recommended for morbid obesity with GERD. Roux-en-Y gastric bypass is the best option for patients with obesity and GERD, but the long-term follow up to gastric Y-bypass outcomes showed that the treatment efficacy of gastric bypass on reflux symptoms might have been overestimated (11). Recently, the invention of a new surgical approach that reduces the incidence of postoperative GERD has gained good overall short-term results (12, 13). This study aimed to assess the effectiveness, safety, and results of laparoscopic SG (LSG) and LSG combined with fundoplication (LSGFD) on patients who were morbidly obese with or without GERD over an average of 34 months follow-up.

Abbreviations: EWL, excess weight loss; GERD, gastroesophageal reflux disease; GERD-Q, gastroesophageal reflux disease questionnaire; LSG, laparoscopic sleeve gastrectomy; LSGFD, laparoscopic sleeve gastrectomy combined with fundoplication; SG, sleeve gastrectomy; TWL, total weight loss.

Materials and methods

Ethics statement

This study involved human participants and was reviewed and approved by the Independent Ethics Committee of People's Hospital of Xinjiang Uygur Autonomous Region December 2017(NO.2017-94-XJS). We have received patients consent for participation in this study (operation consent, new technology consent etc.).

Data sources

This retrospective study analyzed data from Fifty-six patients who either underwent LSG or the modified anti-reflux fundoplication procedure (LSGFD) from January 2018 to

January 2020. All the patients were classified as morbidly obese and were suitable candidates for surgery following the recommendations of the China Society for Bariatric and Metabolic Surgery. All the procedures were performed at the same hospital by a single surgeon who has extensive experience in laparoscopic bariatric and GERD surgery. The minimum follow-up time was 22 months and there were 11 cases (5 cases of LSG and 6 cases of LSGFD)lost during the follow-up period. Of the 45 bariatric surgical procedures performed on patients, 23 were LSG procedures for patients who did not have GERD (defined as a DeMeester score of <14.7 or GERD questionnaire [GERD-Q] score of < 8) and 22 were LSGFD (Figure 1) for patients who experienced GERD. All patients were examined preoperative for the severity GERD by means of the GERD-Q, esophageal 24-hour multichannel intraluminal impedance, a pH monitoring study, and an upper gastrointestinal scope to detect reflux disease signs, esophagitis (classified according to the Los Angeles classification), and

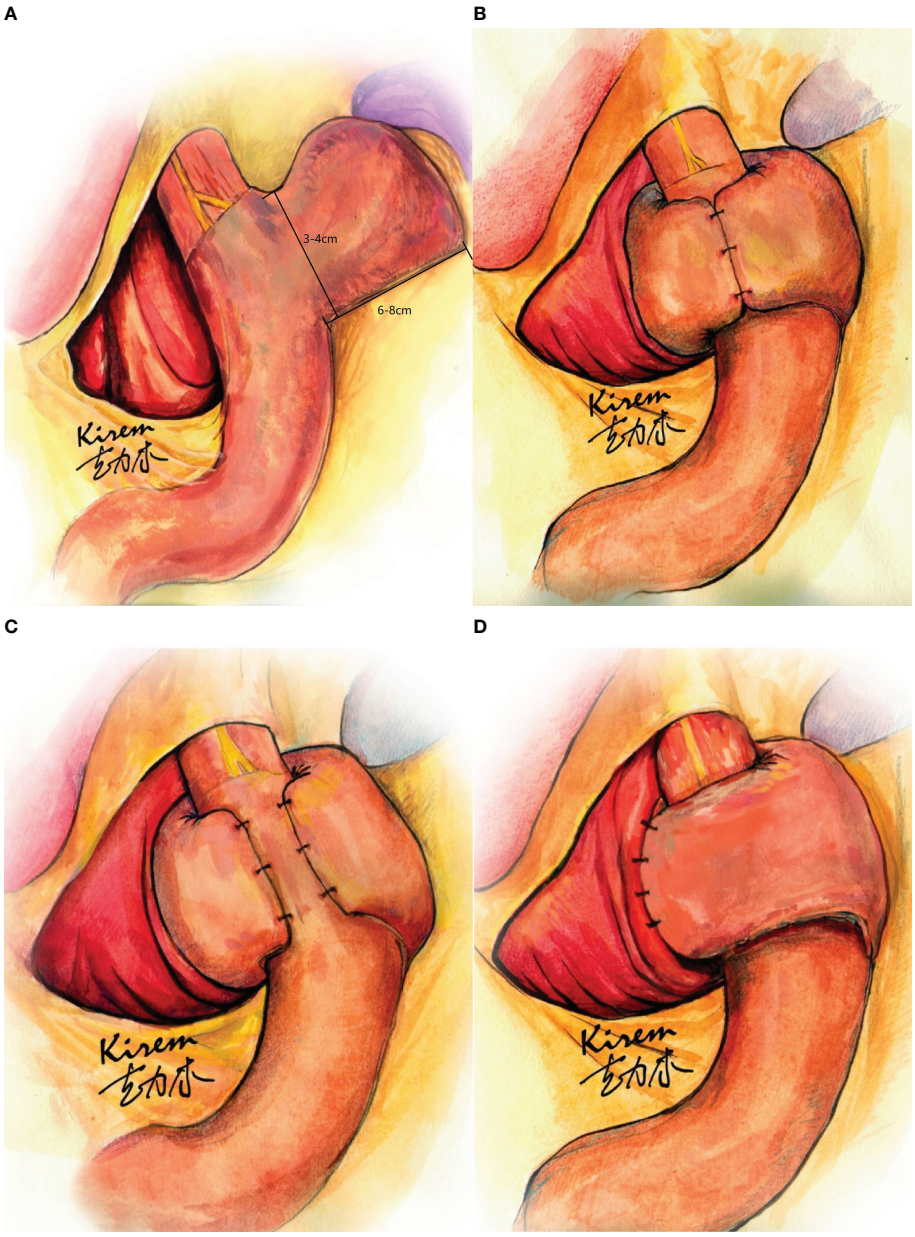

FIGURE 1
Laparoscopic sleeve gastrectomy with fundoplication (LSGFD). **(A)** Sleeve gastrectomy with preserved fin shaped fundus; **(B)** Sleeve gastrectomy with Nissen fundoplication; **(C)** sleeve gastrectomy with Toupet fundoplication; **(D)** Sleeve gastrectomy with Dor fundoplication.

Barrett's esophagus. The preoperative characteristics of the study population are summarized in Table 1. All patients underwent a multidisciplinary evaluation preoperative by a psychologist, dietician, and anesthesiologist; instrumental evaluation included polysomnography, abdominal ultrasound, and upper endoscopy. Informed consent for surgery was obtained from each patient preoperatively. The primary outcome of the study was the weight loss parameters (% excess weight loss [EWL] and % total weight loss [TWL]) at a mean of 34 (22–48) months after surgery. The secondary outcomes include changes in the GERD-Q, the incidence of *de novo* GERD (defined as a GERD-Q score of ≥ 8 at 6 months postoperatively), and the incidence of the resolution of GERD (defined as a GERD-Q score of < 8 at 6 months postoperatively). The percentage of EWL and TWL were calculated as follows:

$$\%EWL = 100\% \times (\text{initial BMI} - \text{follow up BMI})/(\text{initial BMI} - 23)$$

$$\%TWL = 100\% \times (\text{initial BMI} - \text{follow up BMI})/(\text{initial BMI} - 0)$$

Surgical technique

Laparoscopic techniques were used for both of the procedures included in this study.

The procedure for LSG was as follows: After effective general anesthesia was obtained, routine disinfection of the surgical field was performed, and four trocars were introduced. The surgeon stood at the patient's right side. A 10-mm trocar was inserted 3 cm above the umbilicus (this trocar was used for the insertion of a 30° angled optic that guaranteed complete intraperitoneal exploration); a second 5 or 10-mm trocar was inserted 4 cm below the costal margin in the left midclavicular line; a third trocar of 5-mm was inserted 2 cm below the costal margin in the right anterior axillary line; and a fourth trocar of 12 mm was inserted at the umbilical level in the right midclavicular line. A 2 mm skin incision was made under the xiphoid and a self-made "S"-shaped thick iron wire liver lobe retractor was inserted (this retractor was used to expose the lesser curvature of the stomach around the esophageal cardia). The first surgical step was the dissociation of the greater curvature, fundus, and posterior wall of the stomach with the ultrasonic scalpel, starting 3 cm from the pylorus and ending with the dissociation of the fundus. The esophagus was intubated with a 36-F bougie which was advanced to the side of the lesser curvature of the stomach. If a hiatal hernia was present, it was repaired. The next surgical step was sleeve gastrectomy which started 3 cm from the pylorus and ended with the resection of most of the greater gastric curvature and the fundus. After it was confirmed that there was no air leakage at the gastric incision margin, the anastomotic margin of the residual stomach was continuously sutured with a surgical barbed suture to prevent bleeding and leakage.

The procedure for LSGFD was as follows: The difference between this surgery and LSG was that a small, fin-shaped part of the fundus was preserved during gastric resection (Figure 1A). To ensure the reliability of the weight loss effect, the retained gastric fundus should not be made too large; approximately 3–4 cm in width and 6–8 cm in length, or enough for appropriate folding (due to individual differences in esophageal thickness), and the appearance is similar to that of a fin. The residual gastric cavity was checked for margin leakage *via* gastric gas injection, and the residual gastric suture was continuously stitched to strengthen the absorbable suture and prevent postoperative bleeding and fistula formation. A Nissen or Toupet or Dor fundoplication was performed, depending upon the length of fundus preserved after the SG (Figures 1B–D).

Statistical analysis

Continuous variables with a normal distribution are expressed as the mean ± standard deviation. Categorical variables are expressed with the use of frequencies. To compare the preoperative and postoperative parameters for each surgery, we used the X^2 test for categorical variables and Student's paired t test for continuous data. The independent samples test was used to compare the parameters between LSG and LSGFD. A P value of 0.05 was considered statistically significant. Statistical analyses were performed using SPSS version 26.0 (IBM Corp., Armonk, N.Y., USA).

TABLE 1 Patient's demographics and preoperative evaluations.

Parameters	LSG (n=23)	LSGFD (n=22)	P
Sex, % of females	73.9	77.3	0.524
Age (yrs), mean ± SD (range)	36.3± 10.7 (20-57)	37.9 ± 9.1 (21-56)	0.592
Hypertension, n (%)	7 (30.4%)	6 (27.3%)	0.815
Sleep apnea syndrome, n (%)	16 (69.6%)	12 (54.5%)	0.299
Diabetes Mellitus Type II, n (%)	7 (30.4%)	6 (27.3%)	0.815
Weight (Kg), mean ± SD (range)	111.6 ± 11.8 (92-135)	104.3 ± 17.0 (79.5-143)	0.098
BMI (Kg/m^2), mean ± SD (range)	39.6 ± 4.5 (33.4-50.8)	38.4 ± 5.7 (31.1-50.2)	0.442

SD, standard deviation; LSG, Laparoscopic sleeve gastrectomy; LSGFD, Laparoscopic sleeve gastrectomy with fundoplication; BMI, body mass index; EWL, excess weight loss; TWL, total weight loss.

10.3389/fendo.2022.1041889

Results

A total of 45 patients completed the preoperative evaluation, of whom 23 patients underwent LSG while 22 patients underwent LSGFD. A questionnaire-based evaluation (GERD-Q) was completed by trained resident physician. The patient's basic demographic characteristics and improvement of weight-related parameters are shown in Table 1. There were no significant differences in these parameters between the groups.

Table 2 highlights the preoperative and postoperative data. Only four trocars were used for all the procedures, and additional trocars were not necessary. No intraoperative complications were reported. The perioperative and postoperative mortality rate was 0%. The mean length of hospital stay was 7.3 ± 2.1 (range 4–11) days for LSG and 6.5 ± 1.7 (range 3–11) days for LSGFD, there was no significant difference between the groups. There were no reported medium or long- term complications following LSG and LSGFD. Major complications (1(4.3%) LSG vs 2(9.0%) LSGFD): There was one (4.5%) case of leak after LSGFD. Bleeding was diagnosed in one (4.3%) patient in LSG group versus one (4.5%) patient in LSGFD. Minor complications (5(21.7%) LSG vs 5(22.7%) LSGFD: Nausea & vomiting diagnosed in 3 (13.0%) patients in LSG and 4 (18.2%) in LSGFD. Wound infections diagnosed in 2 (8.7%)patients in LSG and 1 (4.5%) in LSGFD.

Table 3 shows the changes in weight related evaluation after LSG and LSGFD, reflected as a significant decrease in weight from 111.6 ± 11.8 Kg to 79.8 ± 12.2 Kg after LSG, and from 104.3 ± 17.0 Kg to 73.7 ± 13.1 Kg after LSGFD.

Table 4 shows the changes in GERD symptoms based on GERD-Q scores. Interestingly, the GERD-Q scores decreased after LSGFD (from 8.86 ± 1.3 to 6.45 ± 0.8), while there was an increase after LSG(from 6.70 ± 0.5 to 7.26 ± 1.7). The scores indicated a statistical significance in both groups when compared with the preoperative and postoperative status.

Table 5 demonstrates the follow-up results. The EWL percent (EWL%) at 6, 12, and the mean of 34 (22–48) months was 55.2 ± 21.3%, 76.6 ± 21.6%, and 70.2 ± 21.8%, respectively, after LSG and 53.4 ± 27.8%, 83.3 ± 28.5%, and 77.9 ± 31.3%, respectively, after LSGFD. The TWL percent (TWL%) at 6, 12, and the mean of 34 (22–48) months was 22.1 ± 7.6%, 31.0 ± 8.2%, and 28.5 ± 8.1%, respectively, after LSG and 20.0 ± 9.3%, 31.2 ± 8.0%, and 29.0 ± 9.2%, respectively, after LSGFD. The two groups did not have any significant difference in these parameters, $P > 0.05$. The incidence of de novo GERD (defined as a GERD-Q score ≥ 8) after LSG was 12(52.2%) at

TABLE 2 Perioperative and postoperative data.

Surgical procedure	LSG (n=23)	LSGFD (n=22)	P
Perioperative course			
Trocars, n, mean ± SD (range)	4 ± 0 (4)	4 ± 0 (4)	
Conversion, n (%)	0 (0)	0 (0)	
Postoperative course			
Length of hospital stay, d, mean ± SD (range)	7.3 ± 2.1 (4-11)	6.5 ± 1.7 (3-11)	0.150
Major complications (%)	1 (4.3%)	2 (9.0%)	0.483
Bleeding (%)	1 (4.3%)	1 (4.5%)	0.744
Leak (X-rays,endoscopy), n (%)	0 (0)	1 (4.5%)	0.489
Minor complications (%)	5 (21.7%)	5 (22.7%)	0.609
Nausea &vomit(%)	3 (13.0%)	4 (18.2%)	0.474
Wound infections (%)	2 (8.7%)	1 (4.5%)	0.517
Reoperation, n (%)	0 (0)	0 (0)	
30-d readmission, n (%)	0 (0)	0 (0)	
Deaths, n (%)	0 (0)	0 (0)	

SD, standard deviation; LSG, Laparoscopic sleeve gastrectomy; LSGFD, Laparoscopic sleeve gastrectomy with fundoplication.

TABLE 3 Comparison of preoperative and postoperative weight related evaluation after LSG and LSGFD.

	LSG (n=23)			LSGFD (n=22)		
	Preoperative	Postoperative	*P* value	Preoperative	Postoperative	*P* value
Weight (Kg), mean ± SD	111.6 ± 11.8	79.8 ± 12.2	0.000*	104.3 ± 17.0	73.7 ± 13.1	0.000*
BMI(Kg/m2), mean ± SD	39.6 ± 4.5	28.3 ± 4.2	0.000*	38.4 ± 5.7	27.3 ± 5.2	0.000*

LSG, Laparoscopic sleeve gastrectomy; LSGFD, Laparoscopic sleeve gastrectomy with fundoplication; BMI, body mass index. *Statistically significant.

10.3389/fendo.2022.1041889

TABLE 4 (A) Changes in questionnaire scores after LSG and LSGFD.

Questionnaire	LSG (n=23)			LSGFD (n=22)		
	Preoperative	Postoperative	*P* value	Preoperative	Postoperative	*P* value
GERD-Q	6.70 ± 0.5	7.26 ± 1.7	0.016*	8.86 ± 1.3	6.45 ± 0.8	0.0004*

LSG, Laparoscopic sleeve gastrectomy; LSGFD, Laparoscopic sleeve gastrectomy with fundoplication; GERD-Q, gastroesophageal reflux disease questionnaire; *Statistically significant.

TABLE 4 (B) Comparison of preoperative and postoperative gastroesophageal reflux disease questionnaire (GERD-Q) scores after LSG and LSGFD.

GERD-Q	LSG (n=23)	LSGFD (n=22)	*P* value
Preoperative	6.70 ± 0.5	8.86 ± 1.3	0.000*
Postoperative	7.26 ± 1.7	6.45 ± 0.8	0.045*

LSG, Laparoscopic sleeve gastrectomy; LSGFD, Laparoscopic sleeve gastrectomy with fundoplication; *Statistically significant.

the 12 month and 7 (30.4%) at the mean 34 (22–48) month follow-up. Remission of reflux symptoms (defined as a GERD-Q score < 8) was seen in 19 (86.4%) of 22 patients at 12 months and 20 (90.9%) of 22 patients at mean 34 (22–48) months after LSGFD.

Discussion

The incidence of GERD in patients who are obese is higher than that of the general population. The prevalence of GERD in patients who are obese and are considered for bariatric surgery ranges from 50% to 73% (5, 14–16). The most commonly performed bariatric procedure in the world is LSG and several studies have already published the medium and long-term results which demonstrate positive effects with regard to weight loss and comorbidity resolution (17, 18). However, LSG plays an adverse role on the outcomes of GERD (19). In a meta-analysis, Oor et al. (20) reviewed 33 studies, of which 30 studies reported the effect of LSG on the prevalence of GERD symptoms, 12 reported a decrease in the postoperative prevalence of GERD symptoms, and a total of 24 studies reported the incidence of new-onset GERD symptoms, The incidence of *de novo* GERD following LSG can be up to 35% and new-onset esophagitis ranged from 6.3% to 63.3%.These series have raised significant concern and debate around the effect of LSG on GERD. The contributive factors to GERD include a decrease in low esophageal sphincter(LES) pressure (21), esophageal motility dysfunction, injury to the anti-reflux barrier (disruption of the angle of His and division of sling fibers) (22), increased number of transient LES relaxations, reduction in the compliance of the gastric (5), and increased gastric pressure (23). There are still concerns regarding the real effects of LSG on GERD, while Roux-en-Y gastric bypass has demonstrated a postoperative reduction of GERD. Therefore, to treatment and prevention the occurrence or aggravation of GERD after surgery, our research team made an innovative design LSGFD in 2014, which was confirmed by the animal experiments and achieved significant weight-loss and anti-reflux effects.

We chose to perform a LSGFD procedure and aimed to combine the weight loss effect of bariatric surgery with the anti-reflux effect of fundoplication to relieve GERD, or prevent the occurrence of *de novo* GERD, after LSG. Our study examined the results of 45 patients who underwent LSG or LSGFD and

TABLE 5 Results of follow-up.

Items	6 months			12 months			24+ months		
	LSG	LSGFD	p	LSG	LSGFD	p	LSG	LSGFD	p
Weight (Kg), mean ± SD	87.0 ± 12.9	83.0 ± 13.5	0.319	76.9 ± 11.5	71.4 ± 12.1	0.127	79.8 ± 12.2	73.7 ± 13.1	0.113
BMI (Kg/m2), mean ± SD	30.9 ± 5.1	30.8 ± 5.9	0.931	27.3 ± 4.4	23.6 ± 4.2	0.447	28.3 ± 4.2	27.3 ± 5.2	0.470
EWL (%), mean ± SD	55.2 ± 21.3	53.4 ± 27.8	0.815	76.6 ± 21.6	83.3 ± 28.5	0.371	70.2 ± 21.8	77.9 ± 31.3	0.342
TWL (%), mean ± SD	22.1 ± 7.6	20.0 ± 9.3	0.401	31.0 ± 8.2	31.2 ± 8.0	0.925	28.5 ± 8.1	29.0 ± 9.2	0.847
Other comorbidities									
Sleep apnea, n (%)	7 (30.4%)	6 (27.3%)	0.815	2 (8.7%)	3 (13.6%)	0.635	2 (8.7%)	3 (13.6%)	0.560
Hypertension, n (%)	3 (13.0%)	4 (18.2%)	0.634	2 (8.7%)	2 (9.1%)	0.936	2 (8.7%)	2 (9.1%)	0.936
Diabetes, n (%)	1 (4.3%)	2 (9.1%)	0.524	0 (0%)	1(4.5%)	0.301	0 (0%)	0 (0%)	–

LSG, Laparoscopic sleeve gastrectomy; LSGFD, Laparoscopic sleeve gastrectomy with fundoplication; GERD, gastroesophageal reflux disease.

monitored the patients for an average of 34 months postoperatively to determine their GERD symptoms and body weight. This study demonstrated that both procedures resulted in a decrease in body weight and there was no statistically significant difference between the two procedures. In addition, this data showed that a significant resolution of GERD after LSGFD and that there was a higher incidence of *de novo* GERD after LSG, based on the GERD-Q score. Several studies have examined the short-term effects of SG combined with fundoplication (sleeve-F) surgery (22). Olmi et al. (12) reported data for 40 patients affected by morbid obesity and GERD who concurrently underwent LSG - Rossetti fundoplication (R-sleeve) and showed good results after follow-up of 12 months. However, one patient experienced food bolus. The BMI and %EWL were 31.2Kg/m^2 and 61.7%, respectively, and 95% of the patients were without GERD symptoms. In 2020, 220 patients with obesity underwent LSG and a modified Rossetti anti-reflux fundoplication procedure with good postoperative weight loss results and improvement in GERD (13). Our study the retained gastric fundus should not be made too large, which may ensure a good weight loss effect by removing more gastric tissue and we believe that the folded part may has little or no contact with food and has little effect on the secretion of ghrelin hormone. LSGFD with good short-term and medium-term results in weight loss and GERD resolution, while the longer term follow-up result needs a further observation in GERD and weight loss outcomes.

Anatomic changes associated with the LSG procedure may exacerbate GERD symptoms or induce GERD in previously asymptomatic patients. The LSGFD procedure preserves the angle of His and fundoplicatian raises the pressure of the LES to reduce postoperative GERD, thereby treating and/or reducing GERD in patients with a preoperative diagnosis. Our results show that LSG and LSGFD are feasible and safe and no intraoperative complications were reported however, we had one case of leak following LSGFD who recovered after 2 weeks of conservative treatment, other minor complications were cured after symptomatic treatment before discharge. There are several innovations in our procedure: 1) We used a self-made "S"-shaped thick iron wire liver lobe retractor to aid in complete exploration of the lesser curvature of the stomach, especially around the esophageal cardia; 2) we performed a fundoplication depending on the length of the preserved fundus after SG, which may ensure a good weight loss effect by removing more gastric tissue and avoid resection of gastric fold tissue than R-sleeve procedure. In our study, postoperative weight loss was satisfactory with a higher EWL% following LSGFD than LSG. There is no statistically significant difference in weight loss effect between these two procedures. The best weight loss effect was observed at the 12-month follow-up in both procedures. A resolution of GERD symptoms was reported in 86.4% and 90.9% of patients, respectively, at 12 months and the mean 34 (22–48) months after LSGFD. The incidence of *de novo* GERD after LSG was 52.2% at the 12 month and 30.4% at the mean 34 (22–48) months follow up.

Our study had some limitations. The retrospective single center study design had a small population of only 45 patients may be led to selective bias. The postoperative GERD-related results were only based on the GERD-Q score and there was a lack of stronger evidence. Future studies may utilize an objective data assessment with a 24-hour pH-impedance study. It is considered short term for bariatric surgery, while the longer term follow-up result needs a further observation in GERD and weight loss outcomes.

In conclusion, LSG is the most commonly performed bariatric surgical procedure and has a good impact on postoperative weight loss and obesity related morbidities. The effect of LSG on GERD is controversial and LSG is associated with higher rate of postoperative GERD. Despite several limitations, this study highlights that the LSGFD is a feasible and safe procedure in patients who are morbidly obese with GERD, as it has good postoperative results. The incidence of *de novo* GERD after LSG is high and surgeons should evaluate the GERD cautiously before the surgery. LFDSG has a good clinical effect in the treatment of obesity combined with GERD, and LFDSG prevent the occurrence and development of GERD. Future studies should utilize objective assessments to create stronger evidence and make use of a prospective design.

Data availability statement

The original contributions presented in the study are included in the article/supplementary material. Further inquiries can be directed to the corresponding author.

Ethics statement

This study involved human participants and was reviewed and approved by the Independent Ethics Committee of People's Hospital of Xinjiang Uygur Autonomous Region December 2017 (NO.2017-94-XJS). We have received patients consent for participation in this study (operation consent, new technology consent etc.).

Author contributions

AA and MM drafted the manuscript and revised the final version. PM, YT, XL and JC contributed to the investigation

and interpretation of the literature. KA revised the final draft. All authors contributed to the article and approved the submitted version.

Funding

This study was funded by the Research Center of the National Health Commission of Medical and Health Science and Technology Development of China (No. WA2020RW25).

Acknowledgments

We would like to thank editage (https://www.editage.cn) for language editing.

Conflict of interest

The authors declare that the research was conducted in the absence of any commercial or financial relationships that could be construed as a potential conflict of interest.

Publisher's note

References

1. Mayoral LP, Andrade GM, Mayoral EP, Huerta TH, Canseco SP, Rodal Canales FJ, et al. Obesity subtypes, related biomarkers & heterogeneity. *Indian J Med Res* (2020) 151(1):11–21. doi: 10.4103/ijmr.IJMR_1768_17

2. Caballero B. Humans against obesity: Who will win? *Adv Nutr (Bethesda Md)* (2019) 10(suppl_1):S4–9. doi: 10.1093/advances/nmy055

3. Vakil N, van Zanten SV, Kahrilas P, Dent J, Jones RGlobal Consensus Group. The Montreal definition and classification of gastroesophageal reflux disease: a global evidence-based consensus. *Am J Gastroenterol* (2006) 101(8):1900–43. doi: 10.1111/j.1572-0241.2006.00630.x

4. Eusebi LH, Ratnakumaran R, Yuan Y, Solaymani-Dodaran M, Bazzoli F, Ford AC. Global prevalence of, and risk factors for, gastro-oesophageal reflux symptoms: A meta-analysis. *Gut* (2018) 67(3):430–40. doi: 10.1136/gutjnl-2016-313589

5. Bou Daher H, Sharara AI. Gastroesophageal reflux disease, obesity and laparoscopic sleeve gastrectomy: The burning questions. *World J Gastroenterol* (2019) 25(33):4805–13. doi: 10.3748/wjg.v25.i33.4805

6. Welbourn R, Hollyman M, Kinsman R, Dixon J, Liem R, Ottosson J, et al. Bariatric surgery worldwide: Baseline demographic description and one-year outcomes from the fourth IFSO global registry report 2018. *Obes Surg* (2019) 29 (3):782–95. doi: 10.1007/s11695-018-3593-1

7. Sakran N, Raziel A, Goitein O, Szold A, Goitein D. Laparoscopic sleeve gastrectomy for morbid obesity in 3003 patients: Results at a high-volume bariatric center. *Obes Surg* (2016) 26(9):2045–50. doi: 10.1007/s11695-016-2063-x

8. Wang X, Chang X, Gao L, Zheng CZ, Zhao X, Yin K, et al. Effectiveness of laparoscopic sleeve gastrectomy for weight loss and obesity-associated co-morbidities: a 3-year outcome from mainland Chinese patients. *Surg Obes Related Dis* (2016) 12(7):1305–11. doi: 10.1016/j.soard.2016.03.004

9. García-Díaz J, Ferrer-Márquez M, Moreno-Serrano A, Barreto-Rios R, Alarcón-Rodríguez R, Ferrer-Ayza M. Outcomes, controversies and gastric volume after laparoscopic sleeve gastrectomy in the treatment of obesity. *Cirugia y cirujanos* (2016) 84(5):369–75. doi: 10.1016/j.circir.2015.10.013

10. Felsenreich DM, Ladinig LM, Beckerhinn P, Sperker C, Langer FB. Update: 10 years of sleeve gastrectomy–the first 103 patients. *Obes Surg* (2018) 28(11):3586–94. doi: 10.1007/s11695-018-3399-1

11. Holmberg D, Santoni G, Xie S, Lagergren J. Gastric bypass surgery in the treatment of gastro-oesophageal reflux symptoms. *Aliment Pharmacol Ther* (2019) 50:159–66. doi: 10.1111/apt.15274

12. Olmi S, Caruso F, Uccelli M, Cioffi S, Cesana G. Laparoscopic sleeve gastrectomy combined with Rossetti fundoplication (R-sleeve) for treatment of morbid obesity and gastroesophageal reflux. *Surg Obes Related Dis* (2017) 13 (12):1945–50. doi: 10.1016/j.soard.2017.08.017

13. Olmi S, Uccelli M, Cesana GC, Ciccarese F, Bonaldi M. Modified laparoscopic sleeve gastrectomy with Rossetti anti-reflux fundoplication. results after 220 procedures with 24 months follow-up. *Surg Obes Related Dis* (2020) 16 (9):1202–11. doi: 10.1016/j.soard.2020.03.029

14. Dupree CE, Blair K, Steele SR, Martin MJ. Laparoscopic sleeve gastrectomy in patients with preexisting gastroesophageal reflux disease. *JAMA Surg* (2014) 149 (4):328. doi: 10.1001/jamasurg.2013.4323

15. Sharara AI, Rustom L, Daher HB, Rimmani HH, Safadi B. Prevalence of gastroesophageal reflux and risk factors for erosive esophagitis in obese patients considered for bariatric surgery. *Digestive Liver Dis* (2019) 51(10):1375–9. doi: 10.1016/j.dld.2019.04.010

16. Merrouche M, Sabaté J, Jouet P, Harnois F, Scaringi S, Coffin B, et al. Gastro-esophageal reflux and esophageal motility disorders in morbidly obese patients before and after bariatric surgery. *Obes Surg* (2007) 17(7):894–900. doi: 10.1007/s11695-007-9166-3

17. Zhao H, Jiao L. Comparative analysis for the effect of roux-en-Y gastric bypass vs sleeve gastrectomy in patients with morbid obesity: Evidence from 11 randomized clinical trials (Meta-analysis). *Int J Surg (London England)* (2019) 72 (12):216–223. doi: 10.1016/j.ijsu.2019.11.013

18. Peterli R, Wölnerhanssen BK, Peters T, Vetter D, Kröll D, Borbély Y, et al. Effect of laparoscopic sleeve gastrectomy vs laparoscopic roux-en-Y gastric bypass on weight loss in patients with morbid obesity: The SM-BOSS randomized clinical trial. *JAMA* (2018) 319(3):255–65. doi: 10.1001/jama.2017.20897

19. Gu L, Chen B, Du N, Fu R, Huang X, Mao F, et al. Relationship between bariatric surgery and gastroesophageal reflux disease: A systematic review and meta-analysis. *Obes Surg* (2019) 29(12):4105–13. doi: 10.1007/s11695-019-04218-3

20. Oor JE, Roks DJ, Ünlü Ç, Hazebroek EJ. Laparoscopic sleeve gastrectomy and gastroesophageal reflux disease: A systematic review and meta-analysis. *Am J Surg* (2016) 211(1):250–67. doi: 10.1016/j.amjsurg.2015.05.031

21. Gorodner V, Buxhoeveden R, Clemente G, Solé L, Caro L, Grigaites A. Does laparoscopic sleeve gastrectomy have any influence on gastroesophageal reflux disease? preliminary results. *Surg Endoscopy* (2015) 29(7):1760–8. doi: 10.1007/s00464-014-3902-2

22. Felinska E, Billeter A, Nickel F, Contin P, Berlth F, Chand B, et al. Do we understand the pathophysiology of GERD after sleeve gastrectomy? *Ann New York Acad Sci* (2020) 1482(1):26–35. doi: 10.1111/nyas.14467

23. Aiolfi A, Micheletto G, Marin J, Rausa E, Bona D. Laparoscopic sleeve-fundoplication for morbidly obese patients with gastroesophageal reflux: Systematic review and meta-analysis. *Obes Surg* (2021) 31(4):1714–21. doi: 10.1007/s11695-020-05189-6

frontiers | Frontiers in Endocrinology

TYPE Original Research
PUBLISHED 09 December 2022
DOI 10.3389/fendo.2022.954127

OPEN ACCESS

EDITED BY
Jeff M. P. Holly,
University of Bristol, United Kingdom

REVIEWED BY
Dengrong Jiang,
Johns Hopkins University,
United States
Luca Busetto,
Università degli Studi di Padova, Italy
Caishun Zhang,
Qingdao University, China

*CORRESPONDENCE
Binu P. Thomas
binu.thomas@utsouthwestern.edu

SPECIALTY SECTION
This article was submitted to Obesity, a section of the journal Frontiers in Endocrinology

RECEIVED 27 May 2022
ACCEPTED 25 November 2022
PUBLISHED 09 December 2022

CITATION
Anwar N, Tucker WJ, Puzziferri N, Samuel TJ, Zaha VG, Lingvay I, Almandoz J, Wang J, Gonzales EA, Brothers RM, Nelson MD and Thomas BP (2022) Cognition and brain oxygen metabolism improves after bariatric surgery-induced weight loss: A pilot study.
Front. Endocrinol. 13:954127.
doi: 10.3389/fendo.2022.954127

Cognition and brain oxygen metabolism improves after bariatric surgery-induced weight loss: A pilot study

Nareen Anwar[1,2], Wesley J. Tucker[3], Nancy Puzziferri[4,5], T. Jake Samuel[3], Vlad G. Zaha[2,5], Ildiko Lingvay[5,6], Jaime Almandoz[5], Jing Wang[3], Edward A. Gonzales[3], Robert Matthew Brothers[3], Michael D. Nelson[3] and Binu P. Thomas[2,7,8]*

[1]Department of Biomedical Engineering, University of Texas at Dallas, Richardson, TX, United States, [2]Advanced Imaging Research Center, University of Texas Southwestern Medical Center, Dallas TX, United States, [3]Department of Kinesiology, University of Texas at Arlington, Arlington, TX, United States, [4]Department of Surgery, Oregon Health and Science University, Portland, OR, United States, [5]Department of Internal Medicine, University of Texas Southwestern Medical Center, Dallas, TX, United States, [6]Department of Population and Data Sciences, University of Texas Southwestern Medical Center, Dallas, TX, United States, [7]Department of Radiology, University of Texas Southwestern Medical Center, Dallas, TX, United States, [8]Department of Bioengineering, University of Texas at Arlington, Arlington, TX, United States

Objective: The primary objectives of this pilot study were to assess cognition and cerebral metabolic rate of oxygen ($CMRO_2$) consumption in people with severe obesity before (baseline), and again, 2- and 14-weeks after sleeve gastrectomy bariatric surgery.

Methods: Six people with severe/class 3 obesity (52 ± 10 years, five females, body mass index (BMI) = 41.9 ± 3.9 kg/m^2), and 10 normal weight sex- and age-matched healthy controls (HC) (48 ± 6 years, eight females, 22.8 ± 1.9 kg/m^2). Global $CMRO_2$ was measured non-invasively using MRI and cognition using the Integneuro testing battery.

Results: Following a sleeve gastrectomy induced weight loss of 6.4 ± 2.5 kg (% total-body-weight-lost = 5.4) over two-weeks, cognition total scores improved by 0.8 ± 0.5 T-scores (p=0.03, 15.8% improvement from baseline). Weight loss over 14-weeks post-surgery was 15.4 ± 3.6 kg (% total-body-weight-lost = 13.0%) and cognition improved by 1.1 ± 0.4 (p=0.003, 20.6% improvement from baseline). At 14-weeks, cognition was 6.4 ± 0.7, comparable to 6.0 ± 0.6 observed in the HC group. Baseline $CMRO_2$ was significantly higher compared to the HC (230.4 ± 32.9 vs. 177.9 ± 33.9 μmol O_2/100 g/min, p=0.02). Compared to baseline, $CMRO_2$ was 234.3 ± 16.2 μmol O_2/100 g/min at 2-weeks after surgery (p=0.8, 1.7% higher) and 217.3 ± 50.4 at 14-weeks (p=0.5, 5.7% lower) after surgery. 14-weeks following surgery, $CMRO_2$ was similar to HC (p=0.17).

Conclusion: Sleeve gastrectomy induced weight loss was associated with an increase in cognition and a decrease in $CMRO_2$ observed 14-weeks after surgery. The association between weight loss, improved cognition and $CMRO_2$ decrease should be evaluated in larger future studies.

KEYWORDS

obesity, cognition, cerebral metabolic rate of oxygen, bariatric surgery, sleeve gastrectomy, cerebral blood flow, oxygen extraction fraction, venous oxygenation

Introduction

Obesity is a global epidemic and more than one-third of the world's population is over-weight, with excess body weight linked to a variety of health concerns (1). In the U.S. in 2020,42.4% of adults had obesity and 9.2% had severe obesity (body mass index [BMI] > 40 kg/m^2) (2), with annual direct healthcare costs attributed to excess body weight exceeding $480 billion (3, 4). Obesity is associated with cardiometabolic diseases such as type 2 diabetes mellitus, hypertension, hypercholesterolemia, cerebral small vessel disease, and Alzheimer's disease, all of which lead to accelerated aging of the body and brain (5–8). Obesity has also been linked to decreased cognitive function, especially memory, executive function, processing speed, attention and decision making (9, 10). However, less is known regarding the underpinning mechanisms of the relationship between obesity and cognition.

Brain health can be assessed by measurements of brain vascular dilation, neural energy consumption, and cognitive function. To evaluate the effects of obesity on brain health we previously assessed brain vascular dilation as indexed by cerebral vascular reactivity (CVR), i.e. the vasodilatory responsiveness of the cerebral vasculature during a hypercapnic challenge induced by CO_2 inhalation, and assessed cognitive function using validated neurocognitive testing (11). We observed blunting of CVR in the middle cerebral artery (MCA) and cognitive function in participants with obesity compared to those of age-matched healthy weight controls (11). This indicates that cerebral vascular dilatory responsiveness is decreased with obesity, which may have partly contributed to the diminished cognitive function (9–11).

Measurement of the cerebral metabolic rate of oxygen ($CMRO_2$) provides information about the brain's neural energy consumption (12, 13). $CMRO_2$ assessment has provided insight into brain health in mild cognitive impairment (14), multiple sclerosis (15), neonates (16), addiction (17), Alzheimer's disease (18) and to assess the effect of hyperoxia gas inhalation on the brain (19). However, little is known regarding cerebral oxygen metabolism in people with obesity.

Bariatric surgery is an effective long-term treatment for obesity that leads to improvements in various conditions including hypertension (20), diabetes (21), and neurocognitive function (22). However, other mechanisms with which bariatric surgery improves neurocognitive function remain to be elucidated. Emerging evidence suggests that bariatric surgery modulates a number of molecular targets that may improve vascular function, such as attenuation of oxidative stress and inflammation (23, 24), and improvements in vascular endothelial function (23); each of which could improve cerebral oxygen metabolism.

Based on this background, the present pilot study tested the hypothesis that $CMRO_2$ is higher in people with obesity, and improves with sleeve gastrectomy bariatric surgery. We further hypothesized that $CMRO_2$ would be associated with cognitive function. To accomplish this goal, we studied participants with severe/class 3 obesity before and after sleeve gastrectomy and compared their $CMRO_2$ and cognitive function to that from healthy weight controls with similar age and sex. $CMRO_2$ and cognitive function were assessed in people with obesity at 2-weeks and 14-weeks post sleeve gastrectomy to assess the early and medium term changes after surgery induced weight loss.

Materials and methods

Study objectives

This was a non-randomized observational pilot study. The primary objective was to assess the changes in $CMRO_2$ and cognition in bariatric surgery candidates (BSC) with severe/class 3 obesity pre- and post-surgery at 2- and 14-weeks. All $CMRO_2$ and cognitive function measures were compared to healthy normal weight controls of similar age and sex as the BSC group (HC). Measurements on HC were performed at one time. Another group of young (18-39 years) healthy normal weight reference controls (RC) were evaluated cross-sectionally to assess the effect of age (independent of BMI) on $CMRO_2$. All participants refrained from alcohol and caffeine for a minimum

of 12 h prior to all data collection visits. The study was reviewed and approved by the University of Texas Southwestern Medical Center Institutional Review Board and all participants provided written informed consent prior to participation.

Participants

BSC with severe/class 3 obesity were recruited from the weight management clinics at the UT Southwestern Health System (Dallas, TX). Healthy control participants (HC and RC) were recruited from the community during the same dates.

Inclusion criteria

We recruited three separate groups of adults (age>18 years): (1) BSC with BMI 35-40 kg/m^2 with co-morbidities or BMI >40 kg/m^2, who planned to undergo bariatric surgery for weight management, (2) HC with BMI 18.5-24.9 kg/m^2, with similar age and sex as the BSC group, and free of underlying co-morbidities, and (3) RC with BMI 18.5-24.9 kg/m^2 (18-39 years).

Exclusion criteria

Bariatric surgery candidates were excluded if they had significant anemia (hemoglobin< 10 mg/dl), abnormal renal function (serum creatinine above normal limit for age and sex), chronic respiratory conditions (chronic obstructive pulmonary disease or asthma), pregnancy, waist circumference > 65 in (1.651 meters), incretin mimetic or dipeptidyl peptidase IV inhibitor use during the prior 3 months.

Control participants (both HC and RC), were excluded for history of cardiovascular (e.g. hypertension, type 2 diabetes) or cerebrovascular diseases (e.g. history of stroke, transient ischemic attack), major psychiatric or neurological disorders. All participants were also excluded if they reported any contraindications to MRI.

Bariatric surgery

All BSC included in this study underwent sleeve gastrectomy surgery at the UT Southwestern Health System (Dallas, TX).

Anthropometric assessment

Height and weight were measured for all participants with a standard stadiometer and scale (Health-O-Meter, Sun Beam Inc., Boca Raton, FL, USA) for calculation of BMI in kg/m^2. Waist circumference measurements were taken at the midpoint between lowest rib & top of hip using a standard Gullick tape measure. All anthropometric measurements were performed in duplicate and averaged with participants wearing only a hospital gown.

Cognitive function assessment

Cognitive function was assessed in BSC pre- and post-surgery and in HC using Integneuro computerized testing battery (Brain Resources Ltd., Australia). Cognitive function in multiple domains was tested and a composite score was generated from all domains. The assessed domains included response speed, impulsivity, attention, information processing, memory, executive function, and emotion identification. The same cognitive tests were repeated in BSC at 2-weeks and 14-weeks after surgery. In a prior study, carry-over effects from repeated cognitive function testing were not observed when tests were performed more than a week apart (25).

MRI experiments

Experiments were performed on a 3 Tesla MRI scanner using an 8-channel head coil (Philips Healthcare, Best, The Netherlands) for signal reception. A body coil was used for radio-frequency transmission. Foam padding was placed around the head to minimize motion during MRI scan acquisition. Global $CMRO_2$ and the associated oxygen extraction fraction (OEF) and global cerebral blood flow are functional MRI biomarkers that were measured in the brain for all study participants.

Global $CMRO_2$

We used a validated technique to measure the brain's global oxygen metabolism using magnetic resonance imaging (MRI) (26–28). The technique does not require any exogenous tracer, is acquired on a standard 3 Tesla MRI scanner and has a test retest coefficient of variability of less than 4% (29). This method provides quantitative global brain metabolism results expressed as μmol O_2/100 g/min brain tissue. $CMRO_2$ is calculated using the Fick principle based on the brain's arterio-venous difference in oxygen content:

$$CMRO_2 = CBF \times OEF \times Ca = CBF \times (Ya - Yv) \times Ca \quad (1)$$

where CBF is the cerebral blood flow, measured with MRI and represents the amount of blood supply to the brain. Ya is the arterial blood oxygen saturation fraction (in %), measured with a pulse oximeter (*In vivo*, Philips Healthcare, Best, The Netherlands), placed on the index finger. Yv is the venous oxygen saturation fraction (in %), measured with MRI, and OEF = (Ya - Yv) is the OEF. Ca is a constant representing the oxygen carrying capacity of unit volume of blood and is 8.97

μmol O_2/mL blood (30). Ca is adjusted for hematocrit, and a hematocrit value of 0.42 was chosen for males and 0.4 was chosen for females (14). The scan duration of a complete set of $CMRO_2$ measurement is 4 min.

CBF is quantified using the phase contrast (PC) MRI technique. The PC MRI technique is routinely used to quantify CBF and extensively described previously (14, 31). Imaging parameters for the PC scan are as follows: single-slice acquisition, voxel size 0.45 × 0.45 × 5 mm^3, field-of-view (FOV) = 230 × 230 × 5 mm^3, maximum velocity encoding = 80 cm/s, and scan duration = 30 s. The flux in the four major feeding arteries, left and right internal carotid arteries and the left and right vertebral arteries is measured using an in-house MATLAB (Math-works, Natick, MA, USA) script using methods extensively described previously (14, 31). Briefly, the combined flux from the above mentioned four major feeding arteries is calculated to determine the total flow as mL/min. To determine CBF in mL/100g/min, total brain volume, which is the sum of gray matter and white matter, is obtained from the high-resolution T_1-weighted magnetization-prepared-rapid-acquisition-of-gradient-echo image (voxel size = 1 × 1 × 1mm^3, scan duration = 4 min) using functions from the Functional magnetic resonance imaging of the brain Software Library (FSL, Oxford University, Oxford, UK) and normalized to the CBF.

Yv (oxygenation in venous vessels) was measured using T_2-Relaxation-Under-Spin-Tagging (TRUST) MRI (14, 26). Briefly, TRUST is based on T2 relaxation time rather than the MRI signal strength itself. The TRUST sequence used the following imaging parameters: single-shot echo-planar imaging acquisition in the axial plane, voxel size = 3.44 × 3.44 × 5 mm^3, FOV = 220 × 220 × 5 mm^3, repetition time (TR) = 3000 ms, echo time (TE) = 3.6 ms, inversion time (TI) = 1022 ms, labeling slab thickness = 80 mm, gap between the imaging slice and labeling slab = 20 mm, and four different T_2 weightings, with effective TE = 0 ms, 40 ms, 80 ms, and 160 ms, corresponding to 0, 4, 8, and 16 refocusing pulses during the T_2 preparation in the pulse sequence, and scan duration = 1 min 12s.

Statistical analysis

Data are presented as mean ± SD. Repeated measures ANOVA was used to assess cognitive function, and $CMRO_2$ in BSC before, 2- and 14-weeks after surgery. Unpaired t-tests were used to assess the differences in $CMRO_2$ between the group of BSC (three time points) and the HC group. The Pearson correlation coefficient was used to measure the relationship between BMI and cognitive function total score, as well as the relationships between both BMI and waist circumference and $CMRO_2$ and CBF. The significance level alpha was 0.05; no corrections for multiple comparisons was performed.

Results

Participants

Six BSC with severe/class 3 obesity (52 ± 10 years, five females, 41.9 ± 3.9 kg/m^2), 10 HC of similar age (48 ± 6 years, 8 females, 22.8 ± 1.9 kg/m^2), and seven RC (24 ± 5 years, 2 females, 23.1 ± 1.9 kg/m^2) participated in this study. All participants had at minimum a high school education. Participant characteristics at baseline have previously been published, (11) with pertinent information included in Table 1. Prior to surgery, $CMRO_2$ was significantly higher in BSC than HC (230.4 ± 32.9 μmol O_2/100 g/min vs. 177.9 ± 33.9 μmol O_2/100 g/min, p=0.02), while there was no significant difference in cognitive function (5.3 ± 0.7 vs. 6.0 ± 0.6, p=0.07). Cognitive function was only assessed in five BSC as the neurocognitive software was not available for our first participant. $CMRO_2$ data was not acquired for two of 10 participants from the HC group due to technical difficulties.

Effect of sleeve gastrectomy bariatric surgery

Sleeve gastrectomy bariatric surgery induced a weight loss of 6.4 ± 2.5 kg (% total-body-weight-lost = 5.4) over 2-weeks and 15.4 ± 3.6 kg (% total-body-weight-lost = 13.0%) over 14-weeks. Pre-surgery, mean BMI of the BSC group was 41.9 ± 3.6 kg/m^2, which significantly decreased to 39.7 ± 3.4 kg/m^2, 2-weeks post-surgery and to 36.4 ± 4.5 kg/m^2, 14-weeks post-surgery compared to pre-surgery (Figure 1A).

Cognitive function improved in the BSC group 2-weeks (6.2 ± 0.6, p=0.03) and 14-weeks post-surgery (6.4 ± 0.7, p=0.003) compared to their cognition pre-surgery (Figure 1B). Cognitive function scores improved by 0.8 ± 0.5 T-scores (p=0.03, 15.8% improvement from baseline over 2-weeks) and 1.1 ± 0.4 (p=0.003, 20.6% improvement from baseline over 14-weeks).

Pearson correlation for the change from pre-surgery to 14-weeks post-surgery in cognitive function and BMI was R^2 = 0.9 (p=0.015) (Figure 1C).

Baseline $CMRO_2$ was significantly higher in the BSC group (230.4 ± 32.9 vs. 177.9 ± 33.9 μmol O_2/100 g/min, p=0.02) compared to the HC group (Table 2). Compared to baseline, $CMRO_2$ was 234.3 ± 16.2 μmol O_2/100 g/min at 2-weeks after surgery (p=0.8, 1.7% higher) and 217.3 ± 50.4 at 14-weeks (p=0.5, 5.7% lower) after surgery (Table 2). 2-weeks after surgery $CMRO_2$ was significantly higher in the BSC group compared to the HC group (p=0.004) (Table 2). 14-weeks following surgery, $CMRO_2$ was similar to HC (p=0.17). (Figure 2). CBF and OEF were not significantly different between the HC and BSC pre-surgery. CBF and OEF were also not significantly different post versus pre surgery in the BSC

TABLE 1 Baseline participants' characteristics by group.

	Young healthy reference control (RC) group	Healthy normal weight control (HC) group	Bariatric surgery candidates (BSC) group	p-value: BSC versus HC
N	7	10	6	–
Sex (M, F)	(5, 2)	(2, 8)	(1, 5)	–
Age (years)	24 ± 5	48 ± 6	52 ± 10	0.36
Ethnicity				
Non-Hispanic	6 (86%)	9 (90%)	6 (100%)	–
Hispanic	1 (14%)	1 (10%)	–	–
Race				
White	6 (86%)	9 (90%)	4 (67%)	–
Black	–	–	1 (17%)	–
Asian	1 (14%)	1 (10%)	–	–
American Indian	–	–	1 (17%)	–
Weight (kg)	70.3 ± 8.6	66.3 ± 7.3	118.1 ± 18.0	<0.001
Body mass index (kg/m^2)	23.1 ± 1.9	22.8 ± 1.9	41.9 ± 3.9	<0.0001
$CMRO_2$ (μmol/100g/min)	174.0 ± 22.2	177.9 ± 33.9	230.4 ± 32.9	0.02
Cognitive function total (T-score)	–	6.0 ± 0.6	5.3 ± 0.7	0.07
Comorbidities				
Hypertension	–	2 (20%)	5 (83%)	–
Hypercholesterolemia	–	–	4 (67%)	–
Diabetes	–	–	2 (33%)	–
Hypothyroidism	–	2 (20%)	3 (50%)	–
Anxiety/depression	–	2 (20%)	4 (67%)	–
Medications				
ACE inhibitor	–	–	4 (67%)	–
Beta-blocker	–	–	2 (33%)	–
Statin	–	–	1 (17%)	–
Biguanide	–	–	2 (33%)	–
Levothyroxine	–	2 (20%)	3 (50%)	–
SSRIs	–	2 (20%)	3 (50%)	–

Values are mean ± standard deviation; "-": test not done or data not available.

group. Please refer to Table 2 for global $CMRO_2$ and the associated global CBF and OEF in HC and BSC groups.

Relationship of $CMRO_2$ and CBF with obesity

$CMRO_2$ (p=0.004) and CBF (p=0.02) were significantly correlated with BMI when combining all participants (RC, HC, BSC at the pre-surgery stage) (Figures 3A, C). We also observed a significant positive correlation between waist circumference and $CMRO_2$ (p=0.002) and CBF (p=0.03) (Figures 3B, D).

Discussion

This exploratory pilot study evaluated the impact of weight loss following sleeve gastrectomy bariatric surgery on cognitive function and $CMRO_2$ in BSC with severe/class 3 obesity. Reduction in BMI following bariatric surgery was associated with an increase in cognitive function, aligning with a previous report that found that bariatric surgery was associated with improved neurocognitive function for up to 3 years post-surgery (22, 32).

$CMRO_2$ was higher in BSC pre-surgery, compared to HC of a similar age. 2-weeks post-surgery, $CMRO_2$ was still higher compared to the HC suggesting that changes do not occur early in the post-operative course, independent of weight loss, probably due to incomplete recovery from surgery requiring more systemic resources. 14-weeks post-surgery, $CMRO_2$ in the BSC group was not significantly different compared to the HC group, suggesting that weight loss due to bariatric surgery may be associated with normalization of $CMRO_2$ in BSC.

The exact mechanism leading to improved cognitive function post-surgery is not yet understood, but previous research suggests that reduced inflammation, improved glycemic control, reduction in serum leptin level and increase in serum ghrelin level post

10.3389/fendo.2022.954127

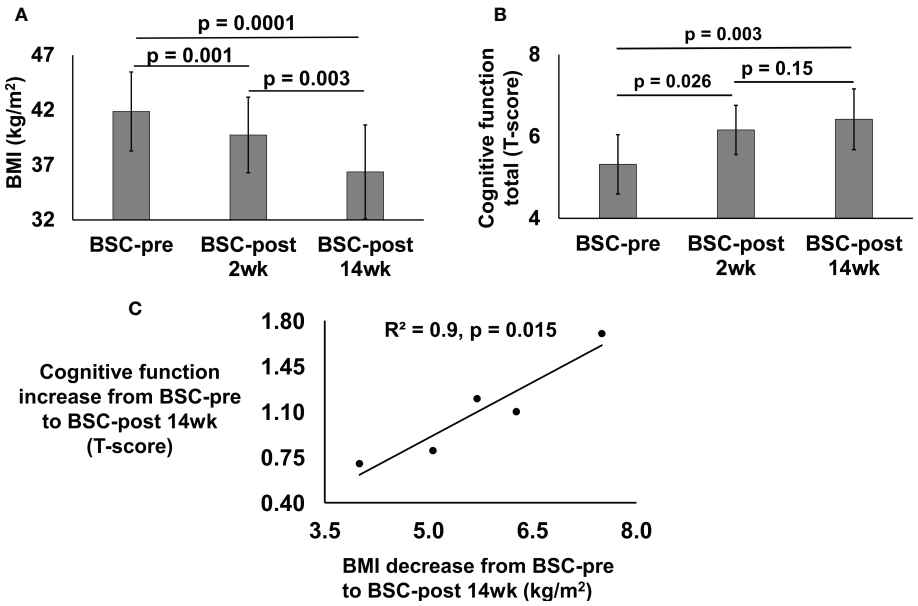

FIGURE 1
BMI (kg/m2) **(A)** and cognitive function total (T-score) **(B)** of the bariatric surgery candidates (BSC) group with severe/class 3 obesity before (BSC-pre), two weeks after (BSC-post 2wk), and fourteen weeks after (BSC-post 14wk) surgery. BMI data was assessed for 6 participants; cognitive function was assessed for 5 participants. Cross correlation between the BMI decrease from BSC-pre to BSC-post 14wk and cognitive function increase from BSC-pre to BSC-post 14 wk **(C)**, p = 0.015.

bariatric surgery may be associated with better cognitive function (33).

Post-surgery diet may also have some effect on $CMRO_2$, which cannot be controlled for in these data. The improvement in $CMRO_2$ may be associated with the typical lower calorie, low-carbohydrate, liquid diet consumed post-surgery. Post-surgery gastric volume is also smaller, leading to early satiation and a subdued response in the brain to food cues once satiated (34), limiting excess food intake (35) that may lead to less energy supply and demand in the brain and thus potentially to a decrease in $CMRO_2$.

We interpret the higher $CMRO_2$ in the BSC at baseline to reflect inefficient brain oxygen metabolism. Indeed, research from our group suggests that $CMRO_2$ increases with age at about 2.6 μmol O_2/100 g/min per decade, showing a relationship between increased $CMRO_2$ and increasing age, which suggests that increased age and $CMRO_2$ are linked to decreased brain function and efficiency (31). We observed a comparable per decade increase with age in $CMRO_2$ between the RC and HC group, in line with results from the previous report (31). $CMRO_2$ in our RC group is similar to values previously reported (31). Cognitive function decreases with age, while $CMRO_2$ increases, possibly due to imbalances in oxygen delivery, consumption, and demand (36). Higher $CMRO_2$ in the BSC group supports this hypothesis. This may suggest that obesity accelerates brain ageing. Collectively, our results may suggest that normalization in $CMRO_2$ following bariatric surgery may be associated with improvement in overall cognitive function.

The effect of co-morbidities or medication use in the group with obesity cannot be ruled out from this pilot exploratory study. Future studies must focus on the role of diabetes or other metabolic co-morbidities on $CMRO_2$ and cognitive function.

TABLE 2 Global $CMRO_2$ and the associated global CBF and OEF in HC and BSC groups.

	Healthy normal weight control (HC) group	Bariatric surgery candidates (BSC) group pre-surgery	Bariatric surgery candidates (BSC) group 2-weeks post-surgery	Bariatric surgery candidates (BSC) group 14-weeks post-surgery
$CMRO_2$ (μmol/100g/min)	177.9 ± 33.8	230.4 ± 32.9 (p=0.02)	234.3 ± 16.2 (p=0.004)	217.3 ± 50.4
CBF (ml/100g/min)	66.7 ± 13.4	80.1 ± 10.6	77.9 ± 9.5	68.6 ± 11.5
OEF (%)	31.8 ± 5.8	35.2 ± 4.3	37.0 ± 4.3	38.4 ± 5.2

Values are mean ± standard deviation (p-value comparison with HC).
non-significant p-values are not listed in the table.

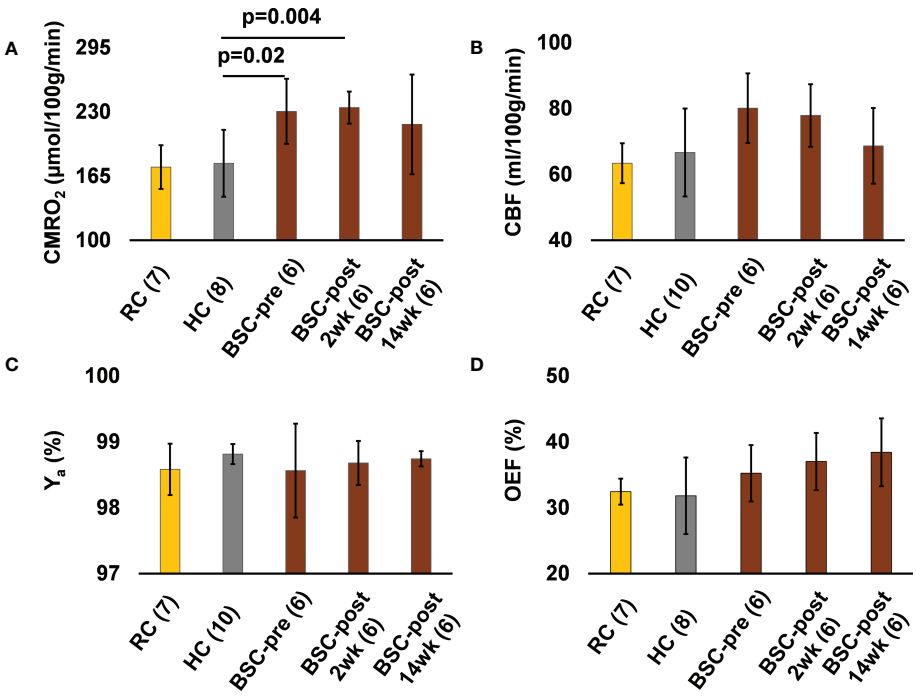

FIGURE 2
The CMRO2 **(A)**, CBF **(B)**, Ya **(C)**, and OEF **(D)** values of the young healthy weight reference controls (RC) group, healthy normal weight controls (HC) of similar age and sex as the BSC group, and the bariatric surgery candidates group before (BSC-pre), two weeks after (BSC-post 2wk), and fourteen weeks after (BSC-post 14wk) surgery. Numbers in brackets next to each group label indicates the number of participants in the group.

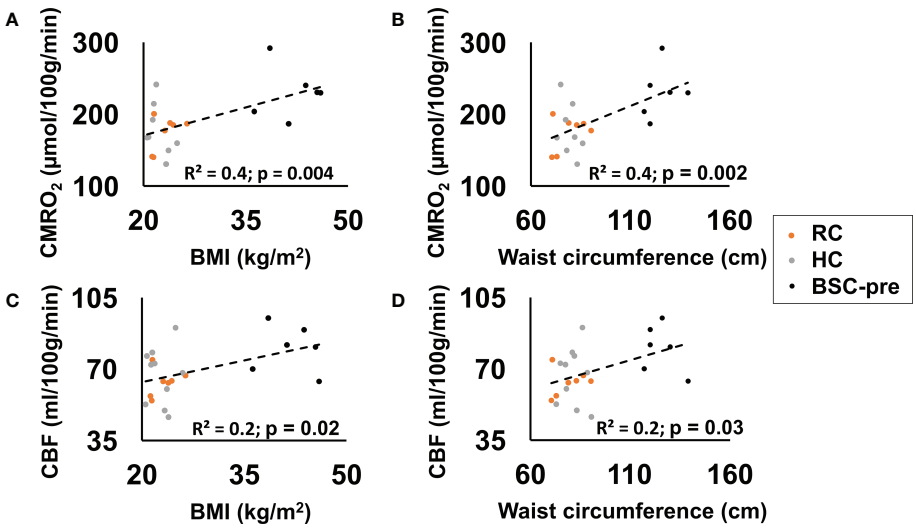

FIGURE 3
CMRO2 (p=0.004) **(A)** and CBF (p=0.02) **(C)** correlated significantly with BMI (reference control - RC, healthy normal weight controls - HC, bariatric surgery candidates at the pre-surgery stage - BSC-pre). CMRO2 (p=0.002) **(B)** and CBF (p=0.03) **(D)** correlated significantly with waist 7circumference.

Studies must also aim to differentiate the effects on these outcomes in participants with obesity and metabolic co-morbidities compared to participants with obesity, without metabolic co-morbidities, to better understand the impact of obesity on health. The impact of different surgical techniques, non-surgical lifestyle/dietary weight loss, anti-obesity medications, and exercise should also be explored in future studies.

Limitations and future studies

The findings from this exploratory pilot study should be considered with respect to the study limitation that the sample size is small. The results are therefore hypothesis generating. Practice effects cannot be fully ruled out from repeated assessments at baseline and 2-weeks after surgery in participants with obesity. Also, cognitive assessments in the HC group were performed only one time, at baseline, and not repeated the same number of times as in the BSC group.

Conclusion

In this exploratory pilot study, we evaluated the changes in cognitive function and $CMRO_2$ in people with severe obesity who underwent bariatric surgery. The results are hypothesis generating, suggesting that obesity may be associated with metabolic inefficiency and sleeve gastrectomy induced weight loss may improve metabolic efficiency, contributing to improvements in cognitive function.

Data availability statement

The original contributions presented in the study are included in the article/Supplementary Material. Further inquiries can be directed to the corresponding author.

Ethics statement

The studies involving human participants were reviewed and approved by Institutional Review Board. The patients/participants provided their written informed consent to participate in this study.

Author contributions

NA and BT contributed to the data analysis and interpretation of the results, and to the drafting of the manuscript. WT, TS, EG, MN, and BT performed the MRI experiments. WT, TS, EG, and MN performed the cognitive function testing. NP VZ, IL, JA, RB, MN, and BT contributed to the concept and design of the study. JA help with recruiting participants for the study. NP performed the bariatric surgery procedures. JW contributed to the statistical analysis. MN obtained funding for the study. MN and BT supervised the study. All authors edited and approved the final version of the manuscript.

Funding

This research was funded by a University of Texas Southwestern Medical Center's Center for Translation Medicine (CTM) Pilot Program Grant (UL1 TR001105).

Conflict of interest

The authors declare that the research was conducted in the absence of any commercial or financial relationships that could be construed as a potential conflict of interest.

Publisher's note

All claims expressed in this article are solely those of the authors and do not necessarily represent those of their affiliated organizations, or those of the publisher, the editors and the reviewers. Any product that may be evaluated in this article, or claim that may be made by its manufacturer, is not guaranteed or endorsed by the publisher.

References

1. Hruby A, Hu FB. The epidemiology of obesity: A big picture. *Pharmacoeconomics* (2015) 33(7):673–89. doi: 10.1007/s40273-014-0243-x

2. Hales CM, Carroll MD, Fryar CD, Ogden CL. Prevalence of obesity and severe obesity among adults: United states 2017-2018. *NCHS Data Brief* (2020) 360):1–8.

3. Waters H, Graf M. *America's obesity crisis: the health and economic costs of excess weight*. (Santa Monica, California: Milken Institute) (2018). p. 30. Available at: https://milkeninstitute.org/.

4. Virani SS, Alonso A, Aparicio HJ, Benjamin EJ, Bittencourt MS, Callaway CW, et al. Heart disease and stroke statistics-2021 update: A report from the American heart association. *Circulation* (2021) 143(8):e254–743. doi: 10.1161/CIR.0000000000000950

5. Tershakovec AM, Jawad AF, Stouffer NO, Elkasabany A, Srinivasan SR, Berenson GS. Persistent hypercholesterolemia is associated with the development of obesity among girls: the bogalusa heart study. *Am J Clin Nutr* (2002) 76(4):730–5. doi: 10.1093/ajcn/76.4.730

6. Gustafson D, Rothenberg E, Blennow K, Steen B, Skoog I. An 18-year follow-up of overweight and risk of Alzheimer disease. *Arch Intern Med* (2003) 163 (13):1524–8. doi: 10.1001/archinte.163.13.1524

7. Re RN. Obesity-related hypertension. *Ochsner J* (2009) 9(3):133–6.

8. Hakim AM. Small vessel disease. *Front Neurol* (2019) 10:1020. doi: 10.3389/fneur.2019.01020

9. Prickett C, Brennan L, Stolwyk R. Examining the relationship between obesity and cognitive function: a systematic literature review. *Obes Res Clin Pract* (2015) 9(2):93–113. doi: 10.1016/j.orcp.2014.05.001

10. Deckers K, Van Boxtel MPJ, Verhey FRJ, Kohler S. Obesity and cognitive decline in adults: Effect of methodological choices and confounding by age in a longitudinal study. *J Nutr Health Aging* (2017) 21(5):546–53. doi: 10.1007/s12603-016-0757-3

11. Tucker WJ, Thomas BP, Puzziferri N, Samuel TJ, Zaha VG, Lingvay I, et al. Impact of bariatric surgery on cerebral vascular reactivity and cognitive function: a non-randomized pilot study. *Pilot Feasibility Stud* (2020) 6:21. doi: 10.1186/s40814-020-00569-2

12. Fox PT, Raichle ME. Focal physiological uncoupling of cerebral blood flow and oxidative metabolism during somatosensory stimulation in human subjects. *Proc Natl Acad Sci U.S.A.* (1986) 83(4):1140–4. doi: 10.1073/pnas.83.4.1140

13. Attwell D, Laughlin SB. An energy budget for signaling in the grey matter of the brain. *J Cereb Blood Flow Metab* (2001) 21(10):1133–45. doi: 10.1097/00004647-200110000-00001

14. Thomas BP, Sheng M, Tseng BY, Tarumi T, Martin-Cook K, Womack KB, et al. Reduced global brain metabolism but maintained vascular function in amnestic mild cognitive impairment. *J Cereb Blood Flow Metab* (2017) 37 (4):1508–16. doi: 10.1177/0271678X16658662

15. Ge Y, Zhang Z, Lu H, Tang L, Jaggi H, Herbert J, et al. Characterizing brain oxygen metabolism in patients with multiple sclerosis with T2-relaxation-under-spin-tagging MRI. *J Cereb Blood Flow Metab* (2012) 32(3):403–12. doi: 10.1038/jcbfm.2011.191

16. Liu P, Huang H, Rollins N, Chalak LF, Jeon T, Halovanic C, et al. Quantitative assessment of global cerebral metabolic rate of oxygen (CMRO2) in neonates using MRI. *NMR BioMed* (2014) 27(3):332–40. doi: 10.1002/nbm.3067

17. Liu P, Lu H, Filbey FM, Tamminga CA, Cao Y, Adinoff B. MRI Assessment of cerebral oxygen metabolism in cocaine-addicted individuals: hypoactivity and dose dependence. *NMR BioMed* (2014) 27(6):726–32. doi: 10.1002/nbm.3114

18. Silvestrini M, Pasqualetti P, Baruffaldi R, Bartolini M, Handouk Y, Matteis M, et al. Cerebrovascular reactivity and cognitive decline in patients with Alzheimer disease. *Stroke* (2006) 37(4):1010–5. doi: 10.1161/01.Str.0000206439.62025.97

19. Xu F, Ge Y, Lu H. Noninvasive quantification of whole-brain cerebral metabolic rate of oxygen (CMRO2) by MRI. *Magn Reson Med* (2009) 62(1):141–8. doi: 10.1002/mrm.21994

20. Schiavon CA, Bersch-Ferreira AC, Santucci EV, Oliveira JD, Torreglosa CR, Bueno PT, et al. Effects of bariatric surgery in obese patients with hypertension: The GATEWAY randomized trial (Gastric bypass to treat obese patients with steady hypertension). *Circulation* (2018) 137(11):1132–42. doi: 10.1161/CIRCULATIONAHA.117.032130

21. Schauer PR, Bhatt DL, Kirwan JP, Wolski K, Aminian A, Brethauer SA, et al. Bariatric surgery versus intensive medical therapy for diabetes - 5-year outcomes. *N Engl J Med* (2017) 376(7):641–51. doi: 10.1056/NEJMoa1600869

22. Alosco ML, Galioto R, Spitznagel MB, Strain G, Devlin M, Cohen R, et al. Cognitive function after bariatric surgery: evidence for improvement 3 years after surgery. *Am J Surg* (2014) 207(6):870–6. doi: 10.1016/j.amjsurg.2013.05.018

23. Vazquez LA, Pazos F, Berrazueta JR, Fernandez-Escalante C, Garcia-Unzueta MT, Freijanes J, et al. Effects of changes in body weight and insulin resistance on inflammation and endothelial function in morbid obesity after bariatric surgery. *J Clin Endocrinol Metab* (2005) 90(1):316–22. doi: 10.1210/jc.2003-032059

24. Hawkins MA, Alosco ML, Spitznagel MB, Strain G, Devlin M, Cohen R, et al. The association between reduced inflammation and cognitive gains after bariatric surgery. *Psychosom Med* (2015) 77(6):688–96. doi: 10.1097/PSY.0000000000000125

25. Falleti MG, Maruff P, Collie A, Darby DG. Practice effects associated with the repeated assessment of cognitive function using the CogState battery at 10-minute, one week and one month test-retest intervals. *J Clin Exp Neuropsychol* (2006) 28(7):1095–112. doi: 10.1080/13803390500205718

26. Lu H, Ge Y. Quantitative evaluation of oxygenation in venous vessels using T2-Relaxation-Under-Spin-Tagging MRI. *Magn Reson Med* (2008) 60(2):357–63. doi: 10.1002/mrm.21627

27. Lu H, Xu F, Grgac K, Liu P, Qin Q, van Zijl P. Calibration and validation of TRUST MRI for the estimation of cerebral blood oxygenation. *Magn Reson Med* (2012) 67(1):42–9. doi: 10.1002/mrm.22970

28. Jiang D, Deng S, Franklin CG, O'Boyle M, Zhang W, Heyl BL, et al. Validation of T2 -based oxygen extraction fraction measurement with (15) O positron emission tomography. *Magn Reson Med* (2021) 85(1):290–7. doi: 10.1002/mrm.28410

29. Liu P, Xu F, Lu H. Test-retest reproducibility of a rapid method to measure brain oxygen metabolism. *Magn Reson Med* (2013) 69(3):675–81. doi: 10.1002/mrm.24295

30. Guyton AC, Hall JE. *Respiration*. Philadelphia: Saunders: Elsevier (2005).

31. Lu H, Xu F, Rodrigue KM, Kennedy KM, Cheng Y, Flicker B, et al. Alterations in cerebral metabolic rate and blood supply across the adult lifespan. *Cereb Cortex* (2011) 21(6):1426–34. doi: 10.1093/cercor/bhq224

32. Alosco ML, Spitznagel MB, Strain G, Devlin M, Cohen R, Crosby RD, et al. Pre-operative history of depression and cognitive changes in bariatric surgery patients. *Psychol Health Med* (2015) 20(7):802–13. doi: 10.1080/13548506.2014.959531

33. Alosco ML, Spitznagel MB, Strain G, Devlin M, Cohen R, Crosby RD, et al. Improved serum leptin and ghrelin following bariatric surgery predict better postoperative cognitive function. *J Clin Neurol* (2015) 11(1):48–56. doi: 10.3988/jcn.2015.11.1.48

34. Baboumian S, Pantazatos SP, Kothari S, McGinty J, Holst J, Geliebter A. Functional magnetic resonance imaging (fMRI) of neural responses to visual and auditory food stimuli pre and post roux-en-Y gastric bypass (RYGB) and sleeve gastrectomy (SG). *Neuroscience* (2019) 409:290–8. doi: 10.1016/j.neuroscience.2019.01.061

35. Puzziferri N, Zigman JM, Thomas BP, Mihalakos P, Gallagher R, Lutter M, et al. Brain imaging demonstrates a reduced neural impact of eating in obesity. *Obes (Silver Spring)* (2016) 24(4):829–36. doi: 10.1002/oby.21424

36. Catchlove SJ, Macpherson H, Hughes ME, Chen Y, Parrish TB, Pipingas A. An investigation of cerebral oxygen utilization, blood flow and cognition in healthy aging. *PloS One* (2018) 13(5):e0197055. doi: 10.1371/journal.pone.0197055

frontiers | Frontiers in Endocrinology

TYPE Original Research
PUBLISHED 21 December 2022
DOI 10.3389/fendo.2022.1072513

OPEN ACCESS

EDITED BY
Shaozhuang Liu,
Qilu Hospital, Shandong University, China

REVIEWED BY
Li Ding,
Tianjin Medical University General Hospital, China
Yanmin Wang,
California Medical Innovations Institute, United States
Jiangfan Zhu,
Tongji University, China

*CORRESPONDENCE
Jie Meng
mengjie@csu.edu.cn
Liyong Zhu
zly8128@126.com

†These authors have contributed equally to this work and share first authorship

SPECIALTY SECTION
This article was submitted to Obesity, a section of the journal Frontiers in Endocrinology

RECEIVED 17 October 2022
ACCEPTED 08 December 2022
PUBLISHED 21 December 2022

CITATION
Cheng X, Fu Z, Xie W, Zhu L and Meng J (2022) Preoperative circulating peroxiredoxin 1 levels as a predictor of non-alcoholic fatty liver disease remission after laparoscopic bariatric surgery.
Front. Endocrinol. 13:1072513.
doi: 10.3389/fendo.2022.1072513

Preoperative circulating peroxiredoxin 1 levels as a predictor of non-alcoholic fatty liver disease remission after laparoscopic bariatric surgery

Xiaoyun Cheng[1,2,3†], Zhibing Fu[4†], Wei Xie[5], Liyong Zhu[4*] and Jie Meng[1,3*]

[1]Department of Pulmonary and Critical Care Medicine, The Third Xiangya Hospital of Central South University, Changsha, Hunan, China, [2]Department of Pulmonary and Critical Care Medicine, Xiangya Hospital of Central South University, Changsha, Hunan, China, [3]Hunan Key Laboratory of Organ Fibrosis, Central South University, Changsha, Hunan, China, [4]Department of General Surgery, The Third Xiangya Hospital, Central South University, Changsha, China, [5]Department of Cardiology, Xiangya Hospital, Central South University, Changsha, China

Background: Non-alcoholic fatty liver disease (NAFLD) is associated with obesity and insulin resistance and can be improved after bariatric surgery. Circulating Peroxiredoxin 1 (Prdx1) protein was reported to regulate energy metabolism and inflammation. This study aimed to investigate the roles of serum prdx1 in NAFLD patients with obesity undergoing LSG and to develop a prognostic model to predict the remission of severe NAFLD.

Methods: The data of 93 participants from a tertiary hospital were assessed. Before laparoscopic sleeve gastrectomy (LSG) and three months after LSG, anthropometric parameters, laboratory biochemical data, and abdominal B-ultrasound results were collected, and their hepatic steatosis index (HSI) and triglyceride-glucose index (TyG) were calculated. A NAFLD improvement (NAFLD-I) nomogram prediction model was constructed using the least absolute shrinkage and selection operator (LASSO) regression and multiple regression, and its predictive ability was verified in a validation cohort.

Results: The baseline Prdx1 (OR: 0.887, 95% CI: 0.816-0.963, p=0.004), preoperative TyG (OR: 8.207, 95% CI: 1.903-35.394, p=0.005) and HSI (OR: 0.861, 95% CI: 0.765-0.969, p=0.013) levels were independently associated with NAFLD-I at three months after LSG in NAFLD patients with obesity. In the primary and validation cohorts, the area under the receiver operating characteristic (AUC) of the developed nomogram model was 0.891 and 0.878, respectively. The preoperative circulating Prdx1 levels of NAFLD patients with obesity were significantly reduced after LSG (25.32 [18.99-30.88] *vs.* 23.34 [15.86-26.42], p=0.001). Prdx1 was related to obesity and hepatic steatosis based on correlation analysis.

Conclusion: The nomogram based on preoperative serum prdx1, HSI and TyG could be an effective tool for predicting remission of severe NAFLD after LSG.

KEYWORDS

non-alcoholic fatty liver disease, insulin resistance, obesity, peroxiredoxin 1, laparoscopy sleeve gastrectomy, nomogram

1 Introduction

In recent years, the prevalence of non-alcoholic fatty liver disease (NAFLD) has increased significantly (1). More worryingly, a data framework predicted that a growing number of NAFLD patients would develop non-alcoholic steatohepatitis (NASH)-related end-stage or malignant liver diseases (2), who have become the main population for liver transplantation. The aggravating incidence of NAFLD and the severe consequences of disease progression makes it necessary to develop effective methods to predict NAFLD response to LSG treatment. In this regard, serological biomarkers and models have attracted significant clinical attention due to their non-invasive, low cost, simple maneuverability and strong repeatability advantages.

Hepatic steatosis, inflammation and fibrosis in NAFLD are closely related to obesity and insulin resistance (IR) (3, 4). Accumulating evidence suggests that the Peroxiredoxin (PRDX) family is a key antioxidant enzyme regulating the balance between glucose and lipid metabolism (5). PRDX members, including Prdx1 (6), Prdx2 (7), Prdx3 (8), Prdx4 (9) and Prdx6 (10, 11), were reported to be overexpressed in obesity, type 2 diabetes mellitus (T2DM) and atherosclerosis (12). Prdx1 and Prdx4 are the secretory members of the PRDX family. Elevated circulating Prdx4 was found to be associated with certain components (e.g., hypertension and triglycerides [TG]) and mature inflammatory markers (e.g., high-sensitivity C-reactive protein [hs-CRP] and procalcitonin) of the metabolic syndrome (13) and has been incorporative in a T2DM DESIR model in men (14).

vPrdx1 is the main PRDX family member in the pancreas (15) (16), liver insulin resistance, inflammation and steatosis (17). An increase in Prdx1 is released through exosomes in response to various environmental stressors (18), such as inflammatory cytokines (19), oxidative stress (20) and streptozotocin (STZ) administration (21). At present, two studies have reported an increase in Prdx1 in T2DM was positively correlated with the homeostasis model assessment of insulin resistance (HOMA-IR) ($r = 0.276$, $p< 0.01$) (18, 22). However, the level and change of circulating Prdx1 in the evolution of NAFLD have not yet been reported.

Metabolic surgery is the most effective treatment to achieve substantial and lasting weight loss in individuals with obesity (23). Among patients with severe obesity undergoing metabolic surgery, the prevalence of NAFLD was found to exceed 90%, the prevalence of NASH was reported to approximate 37% (24 to 98%), with up to 5% of the patients at high risk for unanticipated liver cirrhosis (24). After bariatric surgery, visceral fat and insulin resistance are reduced within a few days (25), liver fatty acid uptake is reversed (26), and liver inflammation is improved (27, 28). LSG has replaced the Roux-en-Y gastric bypass surgery (RYGB) as the most common bariatric operation (29). In particular, NAFLD individuals benefit more from LSG than RYGB (30), with a reported -2.5 (95% CI: -3.5 to -1.5) median NAFLD activity score (NAS) improvement at 192 days after LSG (31).

Since circulating Prdx1 is closely related to chronic metabolism diseases (i.e., arteriosclerosis, diabetes, etc.) and inflammation, we hypothesized that increased circulating Prdx1 might be a biomarker of obesity, insulin resistance and NAFLD and therefore played an important role in the clinical response after LSG.

2 Methods

2.1 Study design and patients

The study design was a prospective observational study conducted at a single center, as shown in Figure 1. All subjects gave their informed consent for inclusion before participating in the study. The study was conducted in conformity with the Declaration of Helsinki, and the protocol was approved by the Ethics Committee of the Third Xiangya Hospital (Project identification code: R20047). According to the indications and contraindications of LSG guidelines (32), from April 2019 to October 2019, NAFLD patients who underwent LGS in the Department of General Surgery, the Third Xiangya Hospital, were consecutively enrolled. Subjects met all the following inclusion criteria: (1) with the hepatic steatosis index (HSI)>36 and preoperative diagnosis of severe/moderate NAFLD by B-ultrasound; (2) individuals with obesity that combined with other comorbidities of metabolic syndrome; (3) aged 18 to 65 years old. The exclusion criteria were: (1) with the contraindications of LSG; (2) severe infection or organic diseases, such as myocardial infarction, renal failure, and

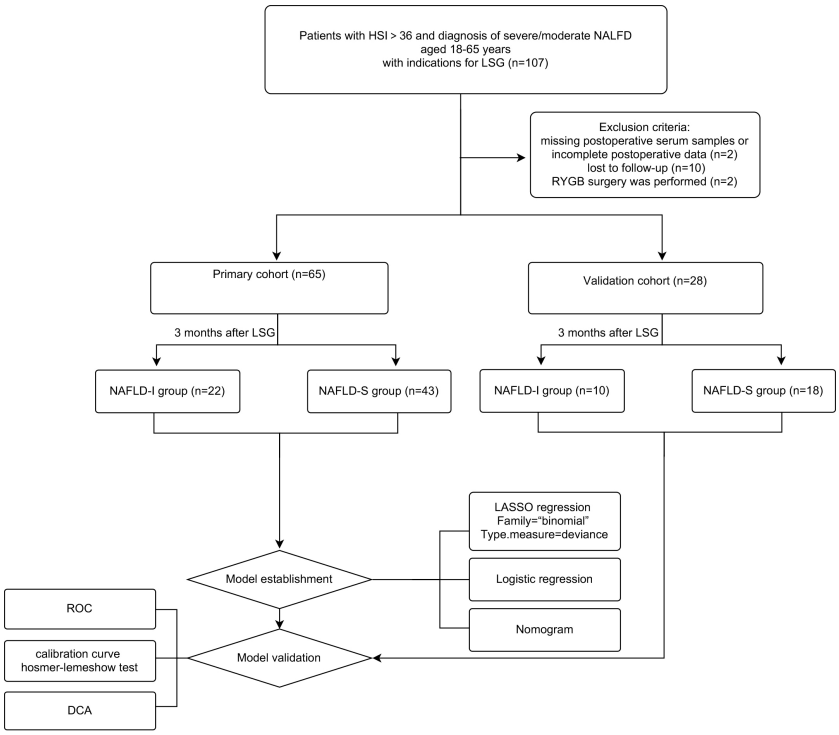

FIGURE 1
Flow diagram of study design. NAFLD, non-alcoholic fatty liver disease; NAFLD-I, NAFLD improvement (postoperative HSI<36 and without diagnostic fatty liver by ultrasound); NAFLD-S, NAFLD sustain; LSG, laparoscopic sleeve gastrectomy; RYGB, Roux-en-Y gastric bypass surgery; LASSO, least absolute shrinkage, and selection operator; ROC, receiver operating characteristic curve; DCA, decision curve analysis.

stroke; (3) long-term use of liver injury-inducing drugs, alcoholism, or drug addiction; (4) previous metabolic surgery; (5) missing serum samples, incomplete data, or loss to follow-up. In accordance with previous reports, the LSG was performed by the same medical team (33). Finally, a total of 93 patients were enrolled and randomly divided into primary cohort (n=65) and validation cohort (n=28) at 7:3. During the same period, fifty-seven healthy adult controls were recruited at the health examination center of the same Hospital. The inclusion criteria were adults with a BMI of 18.5 to 24.0 kg/m2. Exclusion criteria were acute or chronic systemic disease, pharmacological treatment, alcohol abuse, history of abdominal surgery, and absence of informed consent.

2.2 The data, calculated index and definition

Anthropometric parameters, laboratory biochemical data, and abdominal B-ultrasound results were collected before LSG and three months after LSG. Circulating PRDX1 levels were measured using a commercially available enzyme-linked immunosorbent assay (ELISA) kit (KA0536, Abnova, Taiwan, China) in the serum of isolated blood samples collected from the patients. Preoperative fasting serum was assessed to measure PRDX1 concentration.

The anthropometric parameters included height, weight, waist circumference, and hip circumference. Laboratory results included white blood cell (WBC) count, neutrophil to lymphocyte ratio (NLR), platelet count, fasting blood glucose (FBS), fasting insulin (FINS), C-peptide level, triglyceride (TG), total cholesterol (TC), low-density lipoprotein (LDL), high-density lipoprotein (HDL); alanine aminotransferase (ALT), aspartate aminotransferase (AST), albumin (ALB), globulin (GLB), blood urea nitrogen (BUN), creatinine and uric acid (UA). For the imaging examination, abdominal B-ultrasound was performed by two experienced radiologists using the Diagnostic Ultrasound System and Transducers (Philips EPIQ7C, N.V., Amsterdam, the Netherlands). Body mass index (BMI), HSI, non-alcoholic fatty liver disease fibrosis score (NFS), fibrosis 4 score (F4), HOMA-IR, quantitative insulin sensitivity check index (QUICKI), triglyceride-glucose index (TyG), the percentage of total body weight loss (%TBWL), and percentage of excess weight loss (%EWL) were calculated. The formula of each index and their threshold in the Chinese population are shown in Table 1.

TABLE 1 The formula and threshold of calculated index.

Index	Formula	Threshold	References
NAFLD			
HSI	$HSI = 8 \times (ALT/AST) + BMI$ (+2, *if female*; +2 *if diabetes*)	>36	(34)
NFS	$NFS = 1.675 + (0.037 \times age) + (0.094 \times BMI) + (1.13 \times diabetes\ [YES = 1, NO = 0]) + (0.99 \times \frac{AST}{ALT}) - (0.013 \times PLT) \times (0.66 \times albumin)$	<-1.455:F0-F2: -1.455 to 0.675: Uncertain >0.675: F3-F4	(34)
F4	$F4 = (age \times AST)/(PLT \times \sqrt{ALT})$	<1.3: F0-F2: <2.67: F3-F4	(35)
IR			
HOMA-IR	$HOMA\text{-}IR = FPG \times FINS/22.5$	<2.69	(36)
QUICKI	$QUICKI = 1/(Log\ FPG + Log\ FINS)$	≤0.339	(37)
TyG	$TyG = Ln\ [TG \times FINS/2]$	Male>8.81,Female> 8.73	(38)
Weight loss			
BMI	$BMI = weight/height\hat{}2$	≥ 28 kg/m^2: obesity	(39)
%TBWL	$\%TBWL = [(initial\ weight) - (postop\ weight)]/[(initial\ weight)] \times 100$	-	(40)
%EWL	%EWL = (initial weight – postoperative weight)/(initial weight – ideal weight for BMI of 25 × 100	-	(29)

HSI, hepatic steatosis index; NFS, non-alcoholic fatty liver disease fibrosis score; F4, fibrosis 4 score, HOMA-IR, the homeostasis model assessment of insulin resistance; QUICKI, quantitative insulin sensitivity check index; TyG, triglyceride-glucose index; BMI, body mass index; %TBWL, percentage total body weight loss; %EWL, percentage excess weight loss. Age: year; PLT: ×10^9; albumin: g/dL; AST and ALT: U/L; FPG: mmol/L; FINS: μU/mL; TG: mg/dL; FINS: mg/dl; weight: kg; height: m.

HSI has been validated by ultrasonography and magnetic resonance imaging (MRI) and is widely used in clinical studies of metabolic diseases (3, 41). A specificity of 92% was reported for diagnosing NAFLD in patients with HSI >36 (42), and the same cut-off value was thereby adopted in our study. NAFLD improvement (NAFLD-I) was referred to as HSI<36 at three months after LSG, with no fatty liver diagnosed by postoperative ultrasound; otherwise, NAFLD sustain (NAFLD-S) was considered.

2.3 Statistical analysis

SPSS v19 (IBM, Armonk, NY) and GraphPad Prism (GraphPad, San Diego, California) were used for statistical analyses and to draw indicated plots. Enumeration data are shown as n (%) and were compared with the chi-square tests. All measurement data are expressed in median (25th–75th percentiles [Q1–Q3]) and were analyzed using nonparametric tests. The Wilcoxon paired rank test was used for preoperative and postoperative group comparisons. A p-value< 0.05 was considered statistically significant.

The data were further processed with R studio (version 4.2.0; R studio, Boston, Massachusetts). Briefly, we installed the "glmnet" package to perform LASSO regression in the primary cohort to select the preoperative variables with the strongest influence on NAFLD-I. Factors with p< 0.05 in multivariate logistics regression were considered independent influencing factors of NAFLD-I and were used to develop our predictive nomogram model using the "rms" package.

In addition, the discrimination (receiver operator characteristic curve [ROC] by "pROC" package), calibration (calibration curve and Hosmer–Lemeshow test by "rms" and "ResourceSelection" package) and clinical utility (decision curve analysis [DCA] by "ggDCA" package) of our constructed nomogram were verified both in the primary cohort and the validation cohort. Lastly, the Spearman correlation coefficient was used to analyze the associations between preoperative parameters.

3 Results

3.1 Characteristics of the NAFLD at baseline and surgical outcomes

A total of 93 NAFLD patients were enrolled (median age: 30 years [inter-quartile range: 24-34]), comprising 29 (31.18%) males and 64 (68.82) females. The median body weight was 100.30 (90.65-118.15) kg, and the median BMI was 37.16 (34.17-42.70) kg/m^2. Regarding comorbidities, 33.33% of the patients were diagnosed with T2DM before surgery. Three months after

LSG, obesity, low-grade inflammation, insulin resistance, hepatic steatosis, hyperlipidemia and hyperuricemia were found to be significantly alleviated compared with before LSG (Table 2). Postoperative abdominal B-ultrasonography showed no, mild, moderate and severe NAFLD in 36 (38.71%), 22 (23.66%), 27 (29.03%) and 8 (8.60%) cases, respectively. The patients' BMI, body weight and hip circumference were significantly reduced (p<0.001). TBWL% and EWL% were 18.33 (13.57-23.62) and 25.28 (18.76-32.23), respectively. We also observed a decrease in WBC count, NE% and NLR (p<0.001). Postoperative HOMA-IR, TyG and HSI were significantly lower than before the operation (p<0.001). Statistically significant differences were observed between post- and pre-surgical levels of ALT, AST, TG, UA (p<0.001), TC (p=0.015) and HDL (p=0.046).

Further analysis showed no significant differences in the baseline age, gender, degree of obesity, insulin resistance, hepatic steatosis and circulating Prdx1 levels between the primary cohort and the validation cohort (p > 0.05) (Table 3), suggesting that both cohorts were homogeneous.

3.2 Preoperative and postoperative circulating Prdx1 Levels in NAFLD patients with obesity

The median age of the normal control group was 32 (23.5-41.5) years and comprised 22 (38.60%) males and 35 (61.40%) females. The participants in the Control cohort's median BMI was 21.49 (20.19-23.32) kg/m^2 and had no history of T2DM or NAFLD. Their weight, HOMA-IR, QUICKI, TyG and HSI are shown in Table 3. The Control group was comparable with the NAFLD group in terms of age (Z=-1.556, p=0.120) and sex (χ2 =

TABLE 2 The analysis of preoperative and postoperative indicators by the Wilcoxon paired rank test tests.

	Pre-operation (n=93)	Post-operation (n=93)	Z value	p value
HSI	51.23(46.56-58.49)	39.89 (35.21-46.09)	-8.228	0.000**
BMI	37.16 (34.17-42.70)	29.71(26.03-34.82)	-7.604	0.000**
Weight	100.30 (90.65-118.15)	80.00 (69.90-97.20)	-7.494	0.000**
Waistline	114.00 (104.00-128.00)	105.50 (88.00-141.00)	-1.444	0.149
Hip circumference	119.00 (112.00-127.00)	104.00 (94.00-113.00)	-7.747	0.000**
WBC	7.73 (6.42-8.99)	6.64 (5.62-7.95)	-5.304	0.000**
NE%	60.25 (56.10-66.43)	56.70 (50.90-61.80)	-4.062	0.000**
LY%	29.75 (25.00-35.23)	34.60 (29.60-39.40)	-4.728	0.000**
NLR	2.01 (1.62-2.65)	1.63 (1.27-2.08)	-4.507	0.000**
Platelet	285.00 (242.50-325.50)	268.00 (237.75-319.00)	-2.060	0.039*
HOMA-IR	6.71 (4.86-12.80)	2.98 (1.93-4.27)	-8.236	0.000**
QUICKI	0.46 (0.41-0.49)	1.47 (1.31-1.69)	-8.339	0.000**
TyG	8.93 (8.64-9.58)	8.58 (8.28-8.88)	-5.977	0.000**
ALT	40.00 (26.00-68.00)	16.00 (12.00-26.50)	-8.073	0.000**
AST	28.00 (21.00-40.00)	18.00 (15.00-24.50)	-7.153	0.000**
TG	1.67 (1.30-2.47)	1.35 (0.99-1.71)	-5.363	0.000**
TC	5.00 (4.40-5.64)	4.43 (4.04-5.38)	-2.445	0.015*
LDL	2.96 (2.29-3.49)	2.99 (2.55-3.62)	-1.496	0.135
HDL	1.07 (0.97-1.17)	1.03 (2.55-3.62)	-1.993	0.046*
UA	445.00 (368.00-506.00)	379.00 (322.00-444.00)	-4.832	0.000**
NFS	-1.73 (-2.47-0.00)	-1.89 (-2.76- -0.62)	-1.316	0.188
F4	0.48 (0.35-0.63)	0.51 (0.35-0.67)	-5.121	0.609

*p<0.05, **p<0.001.
HSI, hepatic steatosis index; BMI, body mass index; WBC, white blood cell; NE%, neutrophil percentage; LY%, lymphocytes percentage; NLR, lymphocyte ratio; HOMA-IR, the homeostasis model assessment of insulin resistance; QUICKI, quantitative insulin sensitivity check index; TyG, triglyceride-glucose index; ALT, alanine transaminase; AST, aspartate transaminase; TG, triglyceride; TC, total cholesterol; LDL, low-density lipoprotein; HDL, high-density lipoprotein; UA, uric acid; NFS, non-alcoholic fatty liver disease fibrosis score; F4, fibrosis 4 score.

TABLE 3 Preoperative variables between the primary cohort, the validation cohort, and the control cohort.

	Primary cohort (n=65)	Validation cohort (n=28)	*p* value	Control cohort (n=57)
Age (year)	28 (24-33.5)	32 (24-37.75)	0.261	32 (23.5-41.5)
Male (%)	20 (30.77)	9 (32.14)	0.896	22 (38.60)
T2DM (%)	21(32.31)	10(35.71)	0.749	0
NAFLD-I (%)	22(33.8)	10 (35.71)	0.862	–
BMI	36.88(34.27-42.99)	37.75(33.20-41.52)	0.821	21.49(20.19-23.32)
Weight	100.30(90.30-122.20)	100.30(92.23-112.10)	0.666	57.80 (53.40-62.50)
HOMA-IR	7.22(5.20-12.80)	6.12(3.76-13.68)	0.197	2.39(2.19-2.77)
QUICKI	0.45(0.41-0.48)	0.47(0.40-0.52)	0.197	0.33(0.32-0.34)
TyG	8.93(8.55-9.57)	8.91(8.76-9.64)	0.431	7.92(7.64-8.14)
HSI	51.23(41.56-58.94)	51.34(46.17-56.53)	0.776	29.08(27.48-31.60)
Prdx1	25.32(17.75-34.01)	26.60(18.89-32.02)	0.688	12.38 (8.370-15.71)

T2DM, diabetes mellitus type 2; NAFLD-I, hepatic steatosis index improvement; BMI, body mass index; HOMA-IR, the homeostasis model assessment of insulin resistance; QUICKI, quantitative insulin sensitivity check index; TyG, triglyceride-glucose index.

0.866, p=0.352). Preoperative Prdx1 (ng/mL) was significantly higher in NAFLD patients with obesity than in normal controls (25.51 [18.51-32.83] *vs.* 12.38 [8.370-15.71], p<0.001). Postsurgical serum collection was conducted one month after surgery in 33 patients. The Wilcoxon paired rank tests showed that patients after LSG had a lower concentration of Prdx1 than those before surgery (25.32 [18.99-30.88] *vs.* 23.34 [15.86-26.42], p=0.001) (Figure 2).

3.3 Identifying independent influencing factors

The Lasso analysis identified three predictors with non-zero regression coefficients (Figures 3A, B). In multivariate logistic regression analysis, we found that preoperative TyG (OR = 8.207, 95% CI = 1.903-35.394, *p*=0.005), HSI (OR = 0.861, 95% CI = 0.765-0.969, *p*=0.013) and circulating Prdx1 (OR = 0.887, 95% CI = 0.816-0.963, *p*=0.004) were independently associated with NAFLD remission at three months after LSG (Table 4).

3.4 Predictive model construction, validation and evaluation

We developed a Lasso-Logistic nomogram model to assess the independent factors associated with NAFLD remission three months after LSG (Figures 4A, B). Then, ROC curves were used to determine the discrimination of this prediction model. Based on the results, our nomogram demonstrated high predictive values (area under the receiver operating characteristic [AUC] for the primary cohort: 0.891, 95% CI: 0.816-0.966; AUC for validation cohort: 0.878, 95% CI: 0.716-1.000) (Figures 5A, B). Additionally, findings from the calibration graph (Figures 6A, B) and Hosmer-Lemeshow test showed that our constructed nomogram was highly consistent with the actual observation (Hosmer-Lemeshow test in primary cohort: *p*=0.495; validation cohort: *p*=0.138), and the clinical utility of the nomogram model was assessed *via* DCA in both the primary and validation cohorts (Figures 7A, B), which showed that the application of the nomogram model had higher net benefit than "treat all NAFLD patients with LSG" and "treat none of NAFLD patients with LSG" when the risk threshold was between 0.5% and 99.8% in the primary cohort and between 5.4% and 83.3% in the validation cohort.

3.5 Correlation analysis

Correlation analysis showed that HSI was positively correlated with HOMA-IR (r=0.530, *p*<0.001), Prdx1 (r=0.383, *p*=0.002) and body weight (r=0.799, *p*<0.001) (Figure 8). Additionally, Prdx1 was positively correlated with hepatic steatosis, obesity, ALT and AST.

4 Discussion

The most common bariatric procedures are sleeve gastrectomy (SG) and Roux-en-Y gastric bypass (RYGB), which are both effective in alleviating hepatic steatosis, while SG was reported to be associated with fewer complications (43). A published study (44) investigating liver fat fraction at one-year

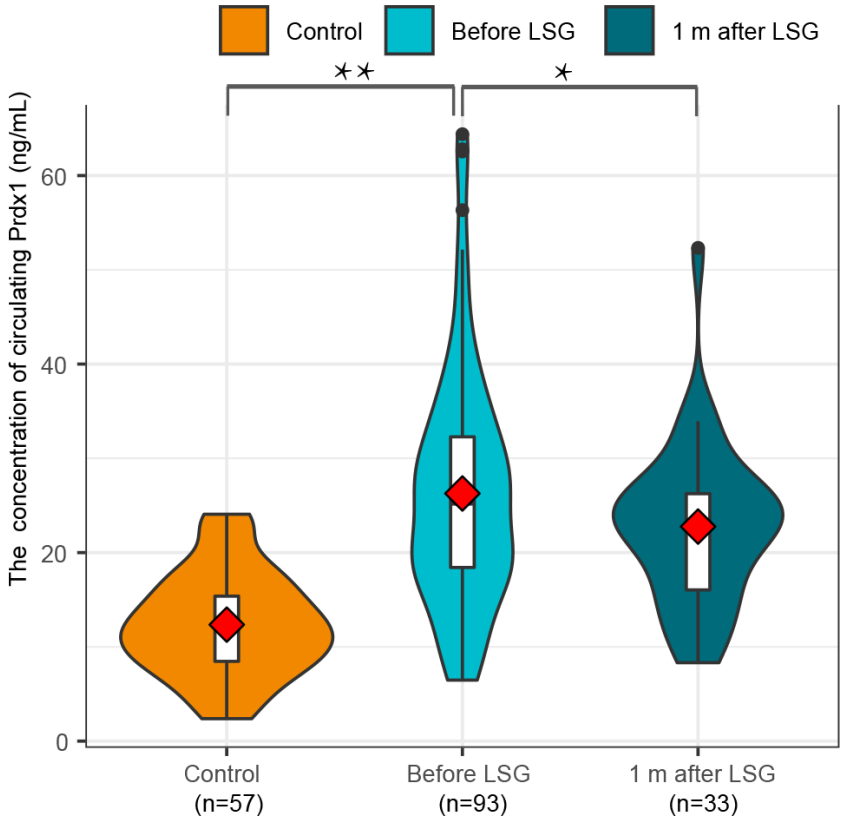

FIGURE 2
A comparison of circulating Prdx1 levels in NAFLD patients with obesity before and after surgery.

follow-up after LSG found a reduction of -19.7% (95% CI: -22.5% to -16.9%). Most studies about NAFLD have focused on the efficacy of LSG after one year or longer. In this present study, we assessed the remission of NAFLD at three months after LSG because it was at that time period that we observed improvements in relevant pathological status (i.e., insulin resistance, obesity) and liver biopsy after surgery. Studies have shown that within three months after bariatric surgery, insulin resistance usually returns to a normal level (45), with significant weight loss achieved in patients with obesity (46). A reduction in hepatic fat content and improvement in hepatic insulin resistance are considered the earliest beneficial effects of bariatric surgery (47). In this study, liver biopsies were performed to confirm that hepatic steatosis, fibrosis and

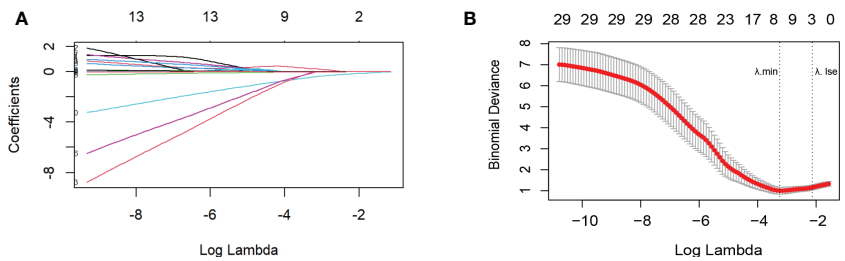

FIGURE 3
Variable selection by the LASSO binary logistic regression model. **(A)** The plot of the coefficient profile against log(lambda). As lambda reduced, the compression parameter decreased, and the absolute value of both coefficients increased. **(B)** Three factors with regression coefficients greater than 0 were selected (lambda value between lambda.min and lambda.1se). The optimized lambda value was between lambda.min and lambda.1se, indicating that three factors with regression coefficients greater than zero were selected.

TABLE 4 Multivariate logistic regression of NAFLD-I (n=65).

Variables	B	S.E.	Wals	*p*	Exp(B)	95%CI for Exp(B)	
						(2.5%)	(97.5%)
TyG	2.105	0.746	7.969	0.005	8.207	1.903	35.394
Circulating Prdx1	-0.120	0.042	8.075	0.004	0.887	0.816	0.963
HSI	-0.150	0.061	6.125	0.013	0.861	0.765	0.969

NAFLD-I, non-alcoholic fatty liver disease improvement; TyG, triglyceride-glucose index; Prdx1, Peroxiredoxin 1.

NAFLD activity scores decreased three months after surgery (48). In addition, we also found an early remission of NAFLD after LSG could be accurately predicted using the proposed nomogram based on the patients' preoperative TyG, HSI and Prdx1 concentration.

A previous study reported that preoperative steatosis (p = 0.006) and insulin resistance index (p = 0.010) were independent predictors of postsurgical persistent severe steatosis one year after surgery *via* liver biopsy (49). However, the wide application of serial liver biopsy is limited due to its invasiveness, variability

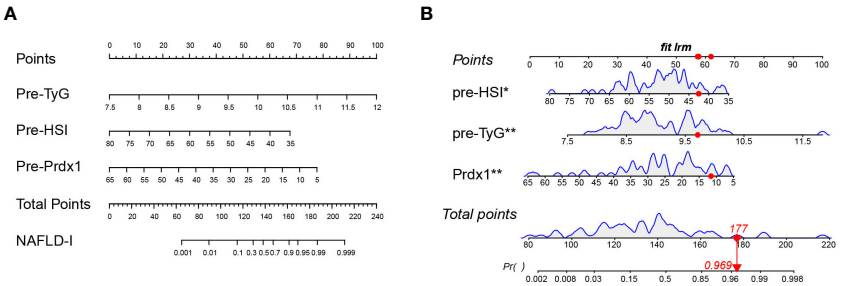

FIGURE 4
Nomogram prediction model. **(A)** TyG, HSI, and Prdx1 as risk factors of the model. **(B)** Example of a dynamic nomogram. For the patient with preoperative HSI of 42.53, TyG of 9.71, and prdx1 concentration of 11.55 ng/mL, his/her total score in this nomogram model was 177 points, and the corresponding probability of NAFLD remission at three months after LSG was predicted to be 96.9%. NAFLD-I, non-alcoholic fatty liver disease improvement; TyG, triglyceride-glucose index; Prdx1, Peroxiredoxin 1.

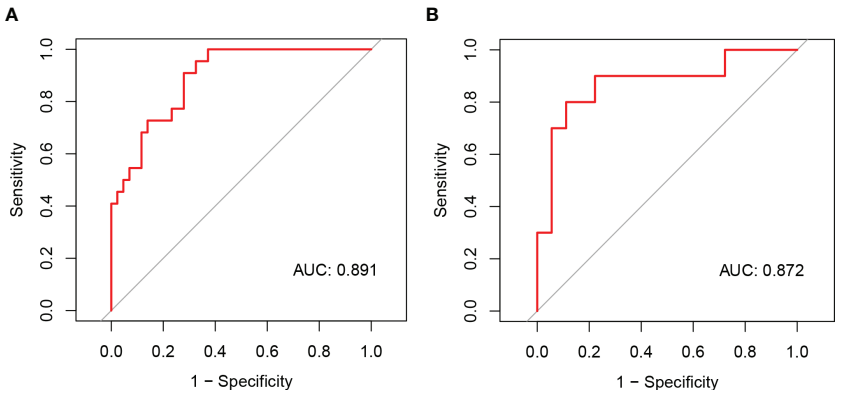

FIGURE 5
The ROC curves of the nomogram model of NAFLD remission at three months after LSG in the primary **(A)** and validation cohorts **(B)**.

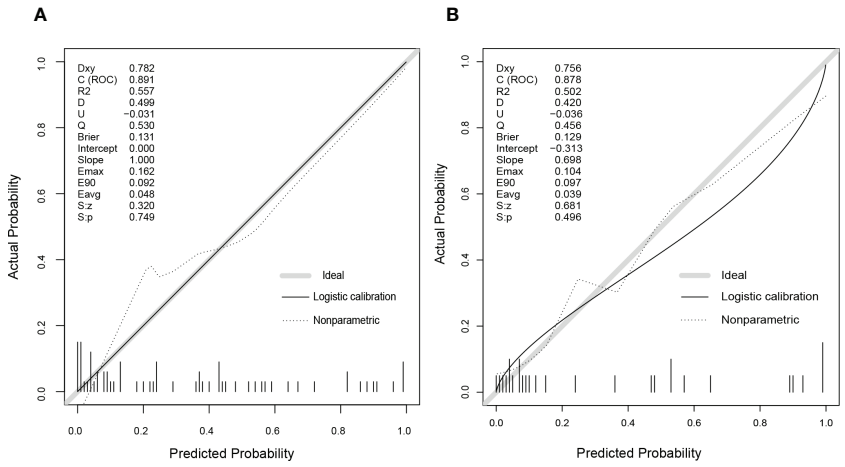

FIGURE 6
The calibration curves of the nomogram model in the primary **(A)** and validation cohorts **(B)**. As shown on graphs, the X-axis represented the predicting probability of postoperative NAFLD remission, and the Y-axis illustrated the actual outcomes in follow-up. The diagonal grey line was the perfect prediction made by the ideal model, the solid black line was the performance by nomogram, and the dashed line was the corrected model performance. As the model performance approached the diagonal grey line, the nomogram's prediction accuracy increased.

in sample collection, and inconsistent evaluation. In terms of imaging exams, MRI is not routinely performed in NAFLD as it is time-consuming and expensive. A meta-analysis indicated that B-ultrasound and transient elastography failed to identify and stage NAFLD in individuals with high BMI (50). Comparatively, a serological model could demonstrate high accuracy in diagnosing hepatic steatosis. HSI is composed of BMI, DM and ALT/AST ratio. Encouragingly, a previous study showed that its AUC for diagnosing NAFLD was 0.81 in the training cohort and 0.82 in the validation cohort (51). More importantly, our study suggested that HSI not only had a good performance in diagnosing NAFLD but was also an important independent predictor of early NAFLD remission after LSG (OR: 0.861, 95% CI: 0.765-0.969, p=0.013). Our correlation analysis of preoperative indicators showed that preoperative TyG was significantly associated with insulin resistance and obesity, consistent with a previous report (52). Interestingly, we also found that HSI was positively correlated with circulating Prdx1 (r=0.383, p =0.002). Several studies have observed increased inflammatory proteins, such as C-reactive protein, which declined after bariatric surgery in T2DM patients with obesity (53).

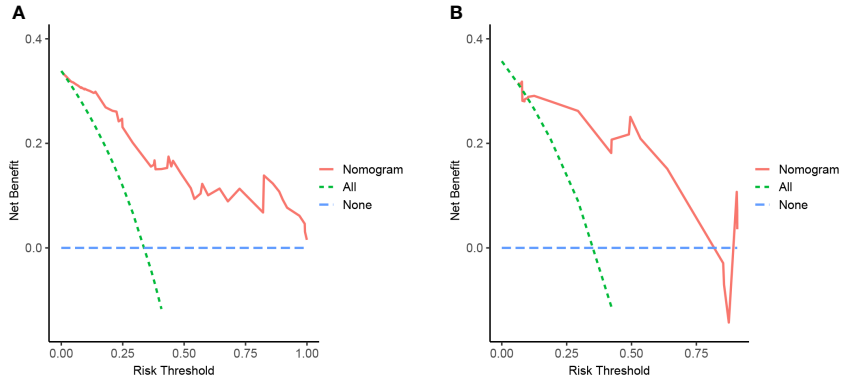

FIGURE 7
Nomogram of NAFLD remission at 3 months after LSG with decision curve analysis (DCA). The Y-axis showed net benefit. The blue line represented the assumption that none of NAFLD patients have been performed with LSG, while the green line represented the assumption that all patients have been performed with LSG, and the red line represented using this nomogram to predict NAFLD-I in patients. Clinical application value increased with increasing distance between red solid line and blue line. **(A)** from the training set, **(B)** from the validation set.

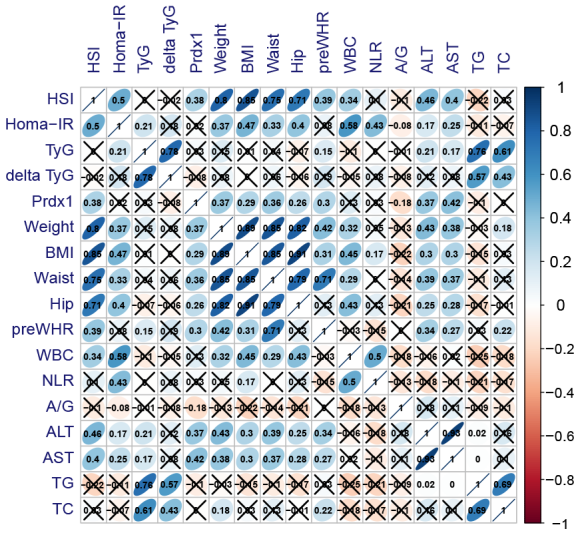

FIGURE 8
Association between baseline indications and postoperative Prdx1. Blue presented highly positive correlation coefficients, whereas red presented highly negative correlation coefficients. HSI, hepatic steatosis index; TyG, triglyceride-glucose index; delta TyG, the change of TyG was quantified by subtracting preoperative values from postoperative values; Prdx1, Peroxiredoxin 1; BMI, body mass index; WHR, waist-to-hip ratio; WBC, white blood cells; NLR, neutrophil to lymphocyte ratio; A/G, albumin/globulin; ALT, alanine transaminase; AST, aspartate transaminase; TG, triglyceride; TC, total cholesterol.

Circulating PRDX1 was recently identified as a damage-associated molecular pattern (DAMP) that acted as a proinflammatory factor by activating the Toll-like receptor 4-mediated signaling (54). In chronic inflammation, more than a quarter of Prdx1 was secreted actively to the outside of cells as exosomes (55, 56) or through a mechanism of redox-dependent secretion (57). Cross-sectional studies showed that Prdx1 increased in chronic metabolic diseases (i.e., atherosclerosis, diabetes, etc.). However, there is limited research on Prdx1 in the evolution of NAFLD. Our study showed for the first time a high circulating Prdx1 concentration in NAFLD patients with obesity and that its level decreased one month after LSG. Moreover, high baseline Prdx1 levels were associated with poor remission of NAFLD three months after LSG (OR: 0.887, 95% CI: 0.816-0.963, p=0.004). We also observed that Prdx1 plasma concentration positively correlated with BMI, HSI, AST and ALT. Given these observations, combined with recent evidence which showed that the overexpression of Prdx1 induced by oxidative stress enhanced insulin resistance and the accumulation of lipid droplets in mouse's HepG2 cells (6), we speculated that Prdx1 might be involved in inflammation, oxidative stress and liver fat deposition in NAFLD patients with obesity. However, this hypothesis could not be confirmed in this present study, and additional studies are needed for further clarification.

Of the complex factors in NAFLD (obesity, lipid metabolism disorders, genes, etc.), insulin resistance is the one that has changed most dramatically within one week after LSG. After one week following SG, HOMA-IR reduced significantly from 6.7 ± 11 to 3.0 ± 1.6 (p = 0.019) (3). In addition, a study that reported improved NAFLD with a low-calorie ketogenic diet (VLCKD) found that baseline insulin resistance was a positive independent predictor (r=0.414, p=0.009) of HSI reduction (58). Comparatively, a study of 4784 Chinese adults reported that TyG was a better predictor for NAFLD when compared with HOMA-IR (AUC=0.761) (59). Furthermore, we found that higher TyG was more likely to lead to NAFLD remission, suggesting that excessive insulin resistance might be strongly recommended as an indication of LSG intervention in NAFLD. The most likely reason was that insulin resistance was more significantly reversed in patients with higher baseline TyG, based on our correlation analysis, in which pre-surgical TyG showed a strong positive correlation with delta TyG (r=0.78, p< 0.001). Similarly, two five-year prospective studies found that patients with refractory insulin resistance had persistent obesity and steatosis after surgery (60, 61).

According to our findings, baseline TyG was an independent predictor of HSI remission at three months after LSG in NAFLD patients with obesity, and it is the first time that circulating Prdx1 is proposed as a promising biomarker to assess postoperative improvement of obesity and NAFLD. Significant insulin resistance remissions are more likely to occur in patients with higher TyG.

Despite the interesting and novel findings reported, our study had some limitations. First, the sample size was limited, even though we internally validated the predictive ability of the nomogram *via* bootstrapping (Supplementary Figure 1), and compared it with another prediction model which was built (Supplementary Figures 2, 3A) and validated (Supplementary Figures 3B–D) in all samples (n=93). Second, we used

B-ultrasound results and surrogate parameters as a standard instead of histology in this study; thus, our prediction results might not perfectly match NAFLD remission assessed by pathological criteria. In addition, NASH is a severe complication of NAFLD, which might also be associated with fibrosis, cirrhosis and hepatocellular carcinoma. We could not assess the different pathological prognoses of NAFLD (non-alcoholic fatty liver and NASH) due to a lack of liver histology data in this study, even though HSI and ultrasonography were externally validated against liver biopsy or magnetic resonance spectroscopy (62).

In summary, TyG and Prdx1 were identified as important predictors of NAFLD remission, which could be used as an early non-invasive marker or as adjuncts to liver biopsy to confirm NAFLD remission. A future clinical follow-up study would provide further evidence for assessing the changes in TyG and Prdx1 over time in patients with NAFLD.

Data availability statement

The raw data supporting the conclusions of this article will be made available by the authors, without undue reservation.

Ethics statement

The studies involving human participants were reviewed and approved by the Ethics Committee of the Third Xiangya Hospital (Project identification code: R20047). The patients/participants provided their written informed consent to participate in this study.

Author contributions

All authors contributed to the conception and design of the study. XC, JM and ZF organized the database. XC, ZF, WX and LZ performed the statistical analysis. All authors wrote the first draft of the manuscript. All authors wrote sections of the manuscript. All authors contributed to the article and approved the submitted version.

Funding

This study was supported by the National Natural Science Foundation of China (No. 81873585, No. 82090020, No. 82090024, No. 82073918 and No. 82070070) and Natural Science Foundation of Hunan Province (No.2020SK2088, 2018JJ3835).

Acknowledgments

Thanks to all the peer reviewers and editors for their opinions and suggestions.

Conflict of interest

The authors declare that the research was conducted in the absence of any commercial or financial relationships that could be construed as a potential conflict of interest.

Publisher's note

Supplementary material

The Supplementary Material for this article can be found online at: https://www.frontiersin.org/articles/10.3389/fendo.2022.1072513/full#supplementary-material

References

1. Targher G, Tilg H, Byrne CD. Non-alcoholic fatty liver disease: A multisystem disease requiring a multidisciplinary and holistic approach. *Lancet Gastroenterol Hepatol* (2021) 6(7):578–88. doi: 10.1016/s2468-1253(21)00020-0

2. Cheung A, Figueredo C, Rinella ME. Nonalcoholic fatty liver disease: Identification and management of high-risk patients. *Am J Gastroenterol* (2019) 114(4):579–90. doi: 10.14309/ajg.0000000000000058

3. Hajifathalian K, Mehta A, Ang B, Skaf D, Shah SL, Saumoy M, et al. Improvement in insulin resistance and estimated hepatic steatosis and fibrosis after endoscopic sleeve gastroplasty. *Gastroint endosc* (2021) 93(5):1110–8. doi: 10.1016/j.gie.2020.08.023

4. Pareek M, Schauer PR, Kaplan LM, Leiter LA, Rubino F, Bhatt DL. Metabolic surgery: Weight loss, diabetes, and beyond. *J Am Coll Cardiol* (2018) 71(6):670–87. doi: 10.1016/j.jacc.2017.12.014

5. Ray PD, Huang BW, Tsuji Y. Reactive oxygen species (Ros) homeostasis and redox regulation in cellular signaling. *Cell signalling* (2012) 24(5):981–90. doi: 10.1016/j.cellsig.2012.01.008

6. Tang Z, Xia N, Yuan X, Zhu X, Xu G, Cui S, et al. Prdx1 is involved in palmitate induced insulin resistance *Via* regulating the activity of P38mapk in Hepg2 cells. *Biochem Biophys Res Commun* (2015) 465(4):670–7. doi: 10.1016/j.bbrc.2015.08.008

7. Murri M, Insenser M, Bernal-Lopez MR, Perez-Martinez P, Escobar-Morreale HF, Tinahones FJ. Proteomic analysis of visceral adipose tissue in pre-obese patients with type 2 diabetes. *Mol Cell Endocrinol* (2013) 376(1-2):99–106. doi: 10.1016/j.mce.2013.06.010

8. Wolf G, Aumann N, Michalska M, Bast A, Sonnemann J, Beck JF, et al. Peroxiredoxin iii protects pancreatic ß cells from apoptosis. *J Endocrinol* (2010) 207 (2):163–75. doi: 10.1677/joe-09-0455

9. Ding Y, Yamada S, Wang KY, Shimajiri S, Guo X, Tanimoto A, et al. Overexpression of peroxiredoxin 4 protects against high-dose streptozotocin-induced diabetes by suppressing oxidative stress and cytokines in transgenic mice. *Antioxidants Redox Signaling* (2010) 13(10):1477–90. doi: 10.1089/ars.2010.3137

10. Arriga R, Pacifici F, Capuani B, Coppola A, Orlandi A, Scioli MG, et al. Peroxiredoxin 6 is a key antioxidant enzyme in modulating the link between glycemic and lipogenic metabolism. *Oxid Med Cell Longevity* (2019) 2019:9685607. doi: 10.1155/2019/9685607

11. Pacifici F, Arriga R, Sorice GP, Capuani B, Scioli MG, Pastore D, et al. Peroxiredoxin 6, a novel player in the pathogenesis of diabetes. *Diabetes* (2014) 63 (10):3210–20. doi: 10.2337/db14-0144

12. Barceló-Batllori S, Corominola H, Claret M, Canals I, Guinovart J, Gomis R. Target identification of the novel antiobesity agent tungstate in adipose tissue from obese rats. *Proteomics* (2005) 5(18):4927–35. doi: 10.1002/pmic.200500050

13. Abbasi A, Corpeleijn E, Postmus D, Gansevoort RT, de Jong PE, Gans RO, et al. Peroxiredoxin 4, a novel circulating biomarker for oxidative stress and the risk of incident cardiovascular disease and all-cause mortality. *J Am Heart Assoc* (2012) 1(5):e002956. doi: 10.1161/jaha.112.002956

14. Abbasi A, Corpeleijn E, Gansevoort RT, Gans RO, Struck J, Schulte J, et al. Circulating peroxiredoxin 4 and type 2 diabetes risk: The prevention of renal and vascular endstage disease (Prevend) study. *Diabetologia* (2014) 57(9):1842–9. doi: 10.1007/s00125-014-3278-9

15. Stancill JS, Corbett JA. The role of Thioredoxin/Peroxiredoxin in the β-cell defense against oxidative damage. *Front Endocrinol* (2021) 12:718235. doi: 10.3389/fendo.2021.718235

16. Stancill JS, Broniowska KA, Oleson BJ, Naatz A, Corbett JA. Pancreatic β-cells detoxify H(2)O(2) through the Peroxiredoxin/Thioredoxin antioxidant system. *J Biol Chem* (2019) 294(13):4843–53. doi: 10.1074/jbc.RA118.006219

17. Zhang Z, Ji Z, He J, Lu Y, Tian W, Zheng C, et al. Guanine nucleotide-binding protein G(I) subunit alpha 2 exacerbates Nash progression by regulating peroxiredoxin 1-related inflammation and lipophagy. *Hepatol (Baltimore Md)* (2021) 74(6):3110–26. doi: 10.1002/hep.32078

18. El Eter E, Al Masri A, Habib S, Al Zamil H, Al Hersi A, Al Hussein F, et al. Novel links among peroxiredoxins, endothelial dysfunction, and severity of atherosclerosis in type 2 diabetic patients with peripheral atherosclerotic disease. *Cell Stress chaperones* (2014) 19(2):173–81. doi: 10.1007/s12192-013-0442-y

19. Min Y, Kim MJ, Lee S, Chun E, Lee KY. Inhibition of Traf6 ubiquitin-ligase activity by Prdx1 leads to inhibition of nfkb activation and autophagy activation. *Autophagy* (2018) 14(8):1347–58. doi: 10.1080/15548627.2018.1474995

20. Stancill JS, Happ JT, Broniowska KA, Hogg N, Corbett JA. Peroxiredoxin 1 plays a primary role in protecting pancreatic β-cells from hydrogen peroxide and peroxynitrite. *Am J Physiol Regulatory Integr Comp Physiol* (2020) 318(5):R1004–r13. doi: 10.1152/ajpregu.00011.2020

21. Yasmin S, Cerchia C, Badavath VN, Laghezza A, Dal Piaz F, Mondal SK, et al. A series of ferulic acid amides reveals unexpected peroxiredoxin 1 inhibitory activity with in vivo antidiabetic and hypolipidemic effects. *ChemMedChem* (2021) 16(3):484–98. doi: 10.1002/cmdc.202000564

22. Subba R, Ahmad MH, Ghosh B, Mondal AC . Targeting Nrf2 in type 2 diabetes mellitus and depression: Efficacy of natural and synthetic compounds. *European journal of pharmacology* (2022) 925:174993. doi: 10.1016/j.ejphar.2022.174993

23. Jakobsen GS, Småstuen MC, Sandbu R, Nordstrand N, Hofsø D, Lindberg M, et al. Association of bariatric surgery vs medical obesity treatment with long-term medical complications and obesity-related comorbidities. *Jama* (2018) 319 (3):291–301. doi: 10.1001/jama.2017.21055

24. Chalasani N, Younossi Z, Lavine JE, Diehl AM, Brunt EM, Cusi K, et al. The diagnosis and management of non-alcoholic fatty liver disease: Practice guideline by the American association for the study of liver diseases, American college of gastroenterology, and the American gastroenterological association. *Am J Gastroenterol* (2012) 107(6):811–26. doi: 10.1038/ajg.2012.128

25. Rizzello M, Abbatini F, Casella G, Alessandri G, Fantini A, Leonetti F, et al. Early postoperative insulin-resistance changes after sleeve gastrectomy. *Obes Surg* (2010) 20(1):50–5. doi: 10.1007/s11695-009-0017-2

26. Immonen H, Hannukainen JC, Kudomi N, Pihlajamäki J, Saunavaara V, Laine J, et al. Increased liver fatty acid uptake is partly reversed and liver fat content normalized after bariatric surgery. *Diabetes Care* (2018) 41(2):368–71. doi: 10.2337/dc17-0738

27. Brunner KT, Henneberg CJ, Wilechansky RM, Long MT. Nonalcoholic fatty liver disease and obesity treatment. *Curr Obes Rep* (2019) 8(3):220–8. doi: 10.1007/s13679-019-00345-1

28. Chalasani N, Younossi Z, Lavine JE, Charlton M, Cusi K, Rinella M, et al. The diagnosis and management of nonalcoholic fatty liver disease: Practice guidance from the American association for the study of liver diseases. *Hepatol (Baltimore Md)* (2018) 67(1):328–57. doi: 10.1002/hep.29367

29. Grönroos S, Helmiö M, Juuti A, Tiusanen R, Hurme S, Löyttyniemi E, et al. Effect of laparoscopic sleeve gastrectomy vs roux-En-Y gastric bypass on weight loss and quality of life at 7 years in patients with morbid obesity: The sleevepass randomized clinical trial. *JAMA Surg* (2021) 156(2):137–46. doi: 10.1001/jamasurg.2020.5666

30. Kalinowski P, Paluszkiewicz R, Ziarkiewicz-Wróblewska B, Wróblewski T, Remiszewski P, Grodzicki M, et al. Liver function in patients with nonalcoholic fatty liver disease randomized to roux-En-Y gastric bypass versus sleeve gastrectomy: A secondary analysis of a randomized clinical trial. *Ann Surg* (2017) 266(5):738–45. doi: 10.1097/sla.0000000000002397

31. Billeter AT, Senft J, Gotthardt D, Knefeli P, Nickel F, Schulte T, et al. Combined non-alcoholic fatty liver disease and type 2 diabetes mellitus: Sleeve gastrectomy or gastric bypass?-a controlled matched pair study of 34 patients. *Obes Surg* (2016) 26(8):1867–74. doi: 10.1007/s11695-015-2006-y

32. Bhandari M, Fobi MAL, Buchwald JN. Standardization of bariatric metabolic procedures: World consensus meeting statement. *Obes Surg* (2019) 29 (Suppl 4):309–45. doi: 10.1007/s11695-019-04032-x

33. Yu Z, Li W, Sun X, Tang H, Li P, Ji G, et al. Predictors of type 2 diabetes mellitus remission after metabolic surgery in Asian patients with a bmi< 32.5 Kg/M (2). *Obes Surg* (2021) 31(9):4125–33. doi: 10.1007/s11695-021-05544-1

34. Kwo PY, Cohen SM, Lim JK. Acg clinical guideline: Evaluation of abnormal liver chemistries. *Am J Gastroenterol* (2017) 112(1):18–35. doi: 10.1038/ajg.2016.517

35. Shah AG, Lydecker A, Murray K, Tetri BN, Contos MJ, Sanyal AJ. Comparison of noninvasive markers of fibrosis in patients with nonalcoholic fatty liver disease. *Clin Gastroenterol hepatol: Off Clin Pract J Am Gastroenterol Assoc* (2009) 7(10):1104–12. doi: 10.1016/j.cgh.2009.05.033

36. Zhou M, Zhu L, Cui X, Feng L, Zhao X, He S, et al. The triglyceride to high-density lipoprotein cholesterol (Tg/Hdl-c) ratio as a predictor of insulin resistance but not of β cell function in a Chinese population with different glucose tolerance status. *Lipids Health Dis* (2016) 15:104. doi: 10.1186/s12944-016-0270-z

37. Jang JY, Moon S, Cho S, Cho KH, Oh CM. Visit-to-Visit Hba1c and glucose variability and the risks of macrovascular and microvascular events in the general population. *Sci Rep* (2019) 9(1):1374. doi: 10.1038/s41598-018-37834-7

38. Yu X, Wang L, Zhang W, Ming J, Jia A, Xu S, et al. Fasting triglycerides and glucose index is more suitable for the identification of metabolically unhealthy individuals in the Chinese adult population: A nationwide study. *J Diabetes Invest* (2019) 10(4):1050–8. doi: 10.1111/jdi.12975

39. Wu Y. Overweight and obesity in China. *BMJ* (2006) 333(7564):362–3. doi: 10.1136/bmj.333.7564.362

40. Hedjoudje A, Abu Dayyeh BK, Cheskin LJ, Adam A, Neto MG, Badurdeen D, et al. Efficacy and safety of endoscopic sleeve gastroplasty: A systematic review and meta-analysis. *Clin Gastroenterol hepatol: Off Clin Pract J Am Gastroenterol Assoc* (2020) 18(5):1043–53.e4. doi: 10.1016/j.cgh.2019.08.022

41. Guo JY, Chen HH, Lee WJ, Chen SC, Lee SD, Chen CY. Fibroblast growth factor 19 and fibroblast growth factor 21 regulation in obese diabetics, and non-alcoholic fatty liver disease after gastric bypass. *Nutrients* (2022) 14(3):645. doi: 10.3390/nu14030645

42. Sviklāne L, Olmane E, Dzērve Z, Kupčs K, Pīrāgs V, Sokolovska J. Fatty liver index and hepatic steatosis index for prediction of non-alcoholic fatty liver disease in type 1 diabetes. *J Gastroenterol Hepatol* (2018) 33(1):270–6. doi: 10.1111/jgh.13814

43. Wölnerhanssen BK, Peterli R, Hurme S, Bueter M, Helmiö M, Juuti A, et al. Laparoscopic roux-En-Y gastric bypass versus laparoscopic sleeve gastrectomy: 5-year outcomes of merged data from two randomized clinical trials (Sleevepass and Sm-boss). *Br J Surg* (2021) 108(1):49–57. doi: 10.1093/bjs/znaa011

44. Seeberg KA, Borgeraas H, Hofsø D, Småstuen MC, Kvan NP, Grimnes JO, et al. Gastric bypass versus sleeve gastrectomy in type 2 diabetes: Effects on hepatic steatosis and fibrosis: A randomized controlled trial. *Ann Internal Med* (2022) 175 (1):74–83. doi: 10.7326/m21-1962

45. Kwon Y, Jang M, Lee Y, Ha J, Park S. Metabolomic analysis of the improvements in insulin secretion and resistance after sleeve gastrectomy: Implications of the novel biomarkers. *Obes Surg* (2021) 31(1):43–52. doi: 10.1007/s11695-020-04925-2

46. Yip S, Plank LD, Murphy R. Gastric bypass and sleeve gastrectomy for type 2 diabetes: A systematic review and meta-analysis of outcomes. *Obes Surg* (2013) 23 (12):1994–2003. doi: 10.1007/s11695-013-1030-z

47. Lefere S, Onghena L, Vanlander A, van Nieuwenhove Y, Devisscher L, Geerts A. Bariatric surgery and the liver-mechanisms, benefits, and risks. *Obes reviews: an Off J Int Assoc Study Obes* (2021) 22(9):e13294. doi: 10.1111/obr.13294

48. Aldoheyan T, Hassanain M, Al-Mulhim A, Al-Sabhan A, Al-Amro S, Bamehriz F, et al. The effects of bariatric surgeries on nonalcoholic fatty liver disease. *Surg endosc* (2017) 31(3):1142–7. doi: 10.1007/s00464-016-5082-8

49. Mathurin P, Gonzalez F, Kerdraon O, Leteurtre E, Arnalsteen L, Hollebecque A, et al. The evolution of severe steatosis after bariatric surgery is related to insulin resistance. *Gastroenterology* (2006) 130(6):1617–24. doi: 10.1053/j.gastro.2006.02.024

50. Musso G, Gambino R, Cassader M, Pagano G. Meta-analysis: Natural history of non-alcoholic fatty liver disease (Nafld) and diagnostic accuracy of non-invasive tests for liver disease severity. *Ann Med* (2011) 43(8):617–49. doi: 10.3109/07853890.2010.518623

51. Kotronen A, Peltonen M, Hakkarainen A, Sevastianova K, Bergholm R, Johansson LM, et al. Prediction of non-alcoholic fatty liver disease and liver fat using metabolic and genetic factors. *Gastroenterology* (2009) 137(3):865–72. doi: 10.1053/j.gastro.2009.06.005

52. Martínez-Urbistondo D, San Cristóbal R, Villares P, Martínez-González M, Babio N, Corella D, et al. Role of nafld on the health related qol response to lifestyle in patients with metabolic syndrome: The predimed plus cohort. *Front Endocrinol* (2022) 13:868795. doi: 10.3389/fendo.2022.868795

53. Zhao J, Jiang Y, Qian J, Qian Z, Yang H, Shi W, et al. A nomogram model based on the combination of the systemic immune-inflammation index and prognostic nutritional index predicts weight regain after laparoscopic sleeve gastrectomy. *Surg Obes related diseases: Off J Am Soc Bariatric Surg* (2022). doi: 10.1016/j.soard.2022.07.014

54. He Y, Li S, Tang D, Peng Y, Meng J, Peng S, et al. Circulating peroxiredoxin-1 is a novel damage-associated molecular pattern and aggravates acute liver injury *Via* promoting inflammation. *Free Radical Biol Med* (2019) 137:24–36. doi: 10.1016/j.freeradbiomed.2019.04.012

55. Checconi P, Salzano S, Bowler L, Mullen L, Mengozzi M, Hanschmann EM, et al. Redox proteomics of the inflammatory secretome identifies a common set of redoxins and other glutathionylated proteins released in inflammation, influenza virus infection and oxidative stress. *PloS One* (2015) 10(5):e0127086. doi: 10.1371/journal.pone.0127086

56. Dorey A, Cwiklinski K, Rooney J, De Marco Verissimo C, López Corrales J, Jewhurst H, et al. Autonomous non antioxidant roles for fasciola hepatica secreted thioredoxin-1 and peroxiredoxin-1. *Front Cell infect Microbiol* (2021) 11:667272. doi: 10.3389/fcimb.2021.667272

57. Mullen L, Hanschmann EM, Lillig CH, Herzenberg LA, Ghezzi P. Cysteine oxidation targets peroxiredoxins 1 and 2 for exosomal release through a novel mechanism of redox-dependent secretion. *Mol Med* (2015) 21(1):98–108. doi: 10.2119/molmed.2015.00033

58. Watanabe M, Risi R, Camajani E, Contini S, Persichetti A, Tuccinardi D, et al. Baseline homa ir and circulating Fgf21 levels predict nafld improvement in patients undergoing a low carbohydrate dietary intervention for weight loss: A prospective observational pilot study. *Nutrients* (2020) 12(7):2141. doi: 10.3390/nu12072141

59. Guo W, Lu J, Qin P, Li X, Zhu W, Wu J, et al. The triglyceride-glucose index is associated with the severity of hepatic steatosis and the presence of liver fibrosis in non-alcoholic fatty liver disease: A cross-sectional study in Chinese adults. *Lipids Health Dis* (2020) 19(1):218. doi: 10.1186/s12944-020-01393-6

60. Russo MF, Lembo E, Mari A, Angelini G, Verrastro O, Nanni G, et al. Insulin resistance is central to long-term reversal of histologic nonalcoholic steatohepatitis after metabolic surgery. *J Clin Endocrinol Metab* (2021) 106 (3):750–61. doi: 10.1210/clinem/dgaa892

61. Mathurin P, Hollebecque A, Arnalsteen L, Buob D, Leteurtre E, Caiazzo R, et al. Prospective study of the long-term effects of bariatric surgery on liver injury in patients without advanced disease. *Gastroenterology* (2009) 137(2):532–40. doi: 10.1053/j.gastro.2009.04.052

62. Stern C, Castera L. Non-invasive diagnosis of hepatic steatosis. *Hepatol Int* (2017) 11(1):70–8. doi: 10.1007/s12072-016-9772-z

frontiers | Frontiers in Endocrinology

TYPE Original Research
PUBLISHED 27 December 2022
DOI 10.3389/fendo.2022.1041027

OPEN ACCESS

EDITED BY
Peng Zhang,
Affiliated Beijing Friendship Hospital, Capital Medical University, China

REVIEWED BY
Yanmin Wang,
California Medical Innovations Institute, United States
Jin Lu,
Second Military Medical University, China

*CORRESPONDENCE
Mingwei Zhong
zmwgz@126.com

SPECIALTY SECTION
This article was submitted to Obesity, a section of the journal Frontiers in Endocrinology

RECEIVED 10 September 2022
ACCEPTED 30 November 2022
PUBLISHED 27 December 2022

CITATION
Zhang W, Shi B, Li S, Liu Z, Li S, Dong S, Cheng Y, Zhu J, Zhang G and Zhong M (2022) Sleeve gastrectomy improves lipid dysmetabolism by downregulating the USP20-HSPA2 axis in diet-induced obese mice. *Front. Endocrinol.* 13:1041027. doi: 10.3389/fendo.2022.1041027

Sleeve gastrectomy improves lipid dysmetabolism by downregulating the USP20-HSPA2 axis in diet-induced obese mice

Wenjie Zhang[1,2], Bowen Shi[1,2], Shirui Li[1,2], Zenglin Liu[1,2], Songhan Li[1,2], Shuohui Dong[1,2], Yugang Cheng[3], Jiankang Zhu[3], Guangyong Zhang[3] and Mingwei Zhong[1,3]*

[1]Department of General Surgery, Shandong Provincial Qianfoshan Hospital, Shandong University, Jinan, China, [2]Cheeloo College of Medicine, Shandong University, Jinan, China, [3]Department of General Surgery, The First Affiliated Hospital of Shandong First Medical University, Jinan, China

Introduction: Obesity is a metabolic disease accompanied by abnormalities in lipid metabolism that can cause hyperlipidemia, non-alcoholic fatty liver disease, and artery atherosclerosis. Sleeve gastrectomy (SG) is a type of bariatric surgery that can effectively treat obesity and improve lipid metabolism. However, its specific underlying mechanism remains elusive.

Methods: We performed SG, and sham surgery on two groups of diet-induced obese mice. Histology and lipid analysis were used to evaluate operation effect. Immunohistochemistry, immunoblotting, real-time quantitative PCR, immunoprecipitation, immunofluorescence and mass spectrometry were used to reveal the potential mechanisms of SG.

Results: Compared to the sham group, the SG group displayed a downregulation of deubiquitinase ubiquitin-specific peptidase 20 (USP20). Moreover, USP20 could promote lipid accumulation *in vitro*. Co-immunoprecipitation and mass spectrometry analyses showed that heat-shock protein family A member 2 (HSPA2) potentially acts as a substrate of USP20. HSPA2 was also downregulated in the SG group and could promote lipid accumulation *in vitro*. Further research showed that USP20 targeted and stabilized HSPA2 via the ubiquitin-proteasome pathway.

Conclusion: The downregulation of the USP20-HSPA2 axis in diet-induced obese mice following SG improved lipid dysmetabolism, indicating that USP20-HSPA2 axis was a noninvasive therapeutic target to be investigated in the future.

KEYWORDS

sleeve gastrectomy, lipid dysmetabolism, USP20, HSPA2, diet-induced obese

Introduction

Obesity has become a global public health concern, placing a high disease burden on society (1). Obesity causes abnormal lipid metabolism, which results in hyperlipidemia, non-alcoholic fatty liver disease, and artery atherosclerosis (2). Bariatric surgery can effectively reduce body weight and obesity-related complication risks in patients with morbid obesity (3). There are several types of bariatric surgeries, however, the sleeve gastrectomy (SG) ranks among the most frequently performed procedures (4). Several studies have observed that SG contributed to weight loss and improved lipid metabolism in human and animal models (5–8). However, the mechanism by which SG improves lipid metabolism remains elusive.

In eukaryotic cells, ubiquitination plays an important role in post-translational modification (9). Deubiquitination is the opposite of ubiquitination, and both processes are always in a dynamic equilibrium (10). When proteins are marked by ubiquitin chains, the proteasome targets and degrades the ubiquitinated proteins (11). Deubiquitinases (DUB) in the deubiquitination process remove ubiquitin chains to preserve the labeled substrate proteins (12). Ubiquitin-specific peptidase 20 (USP20) is a pivotal member of the DUB family and regulates the stability of multiple proteins *via* the ubiquitin-proteasome pathway (13, 14). USP20 is also associated with multiple biological processes (15–19). Emerging studies and trials have revealed the important role of USP20 in improving lipid metabolism and the treatment of metabolic diseases, including obesity, hyperlipidemia, hepatic steatosis, and diabetes (20). Whether USP20 plays a role in lipid metabolism homeostasis mediated by SG is unknown.

Heat-shock protein family A member 2 (HSPA2) is a member of the evolutionarily conserved heat-shock protein chaperone family (21). HSPA2 participates in spermatogenesis and was originally recognized as a testis-specific chaperone protein (22). Subsequent research has shown that HSPA2 gene polymorphisms are highly correlated with obesity, where individuals with the homozygous genotype are susceptible to obesity, suggesting that HSPA2 may play a pivotal role in the initiation and progression of obesity and related metabolic disorders (23).

This study aimed to investigate the underlying mechanisms of SG as a treatment for obesity in improving lipid metabolism on diet-induced obese (DIO) mice.

Materials and methods

Animals

Eight-week-old C57BL/6J male mice were purchased from Weitong Lihua Experimental Animal Technology. They were kept under 12-hour light and dark cycles at 22°C, with *ad libitum* access to normal food and water. After a week of adaptive feeding, the mice were fed an *ad libitum* high-fat diet (HFD) for 16 weeks to induce obesity (n = 25). Mice with body weights in the range of 42–48 g were considered as successful DIO models (n = 17). Thereafter, the obese mice were divided into two groups. One group underwent SG (SG group = 10), and the other group underwent sham surgery (sham group = 7). After surgery, the mice were fed the same HFD as during pre-operation for 10 weeks. Four SG mice died from complications of surgery and one sham mouse was excluded because of vision loss. Finally, six SG and six sham mice were included in the analyses (Figure 1A). All protocols for animal experiments were approved by the Medical Ethics Committee of Shandong Provincial Qianfoshan Hospital, Shandong University, and all animal studies complied with relevant ethical regulations for animal testing and research.

Surgical procedures

Before surgery, C57BL/6J mice were fed Ensure (Abbott, USA) for 2 d and were subsequently fasted overnight. SG and sham surgery were performed under anesthesia with 2% isoflurane. The lateral 80% of the stomach was excised to reform a tubular stomach. The cardia and pylorus were retained. The procedure of sham included analogous isolation of the stomach and manual pressure along a vertical line between the esophageal sphincter and the pylorus with blunt forceps (24). After surgery, mice were single-housed and their diet was gradually advanced to an HFD, which was consistent with the preoperative diet. Body weight changes were recorded weekly, and the animals were euthanized 10 weeks after surgery.

Histology, immunohistochemistry, and lipid analysis

Frozen or paraffin sections were used for histology and immunohistochemistry. Fresh frozen sections were used for Oil Red O staining to evaluate lipid content. Moreover, formalin-fixed paraffin-embedded sections were prepared for hematoxylin and eosin (H&E) staining and immunohistochemistry analysis. For immunohistochemistry, antigen retrieval was performed using heated citrate buffer (Solarbio, China) before blocking endogenous peroxidase activity. After blocking with 10% goat serum, the sections were incubated with primary antibodies against USP20 (ProteinTech, 1:200) or HSPA2 (ProteinTech, 1:200) overnight at 4°C. Thereafter, the sections were incubated with HRP-conjugated anti-rabbit/mouse IgG for 0.5 h at 37°C. The color was developed using 3,3′-diaminobenzidine (Beyotime, China), and the nuclei were stained with hematoxylin (Beyotime). Three images from each section were captured using a light microscope (Olympus, Japan). Additionally, total cholesterol (TC) and triglyceride (TG) levels in the serum and liver were measured using an enzymatic assay kit (Nanjing Jiancheng, China), according to the manufacturer's protocol.

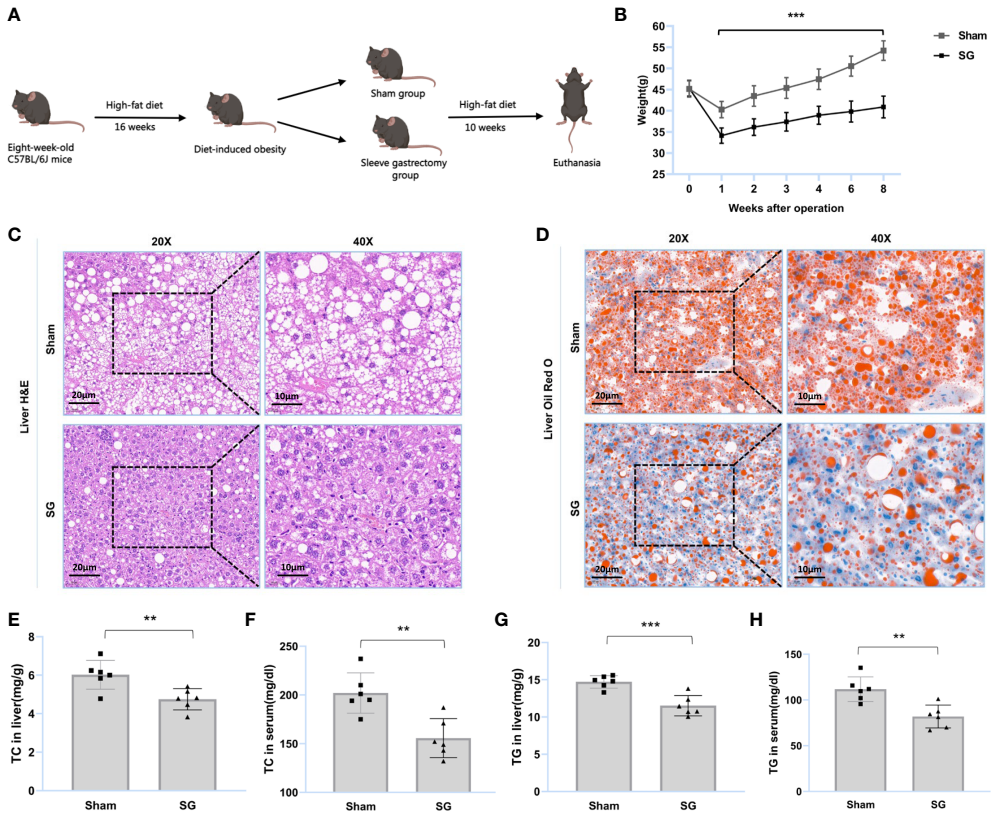

FIGURE 1
SG improves lipid dysmetabolism of DIO mice. **(A)** Flow diagram of SG model establishment in DIO mice. **(B)** Body weight after surgery (n = 6). **(C, D)** H&E and Oil Red O staining of liver tissue from sham and SG group. Scale bars were shown in the figure. **(E, F)** Liver and serum TC levels of sham and SG group (n = 6). **(G, H)** Liver and serum TG levels of sham and SG group (n = 6). The data are expressed as mean ± SEM, Student's t-test was used for intergroup comparisons. **p < 0.01, ***p < 0.001.

Cell cultures and treatments

HepG2 human hepatocellular carcinoma cells and human embryonic kidney 293T (HEK-293T) cells were purchased from the Chinese Academy of Sciences Cell Bank (Shanghai, China). Short tandem repeat profiling was used to validate the identities of all cell lines. HepG2 and HEK-293T cells were cultured in DMEM/HIGH GLUCOSE medium (Gibco, USA) containing 10% fetal bovine serum (FBS; Gibco, USA). The incubator conditions were set at 37°C, 5% CO_2. Palmitic acid (Sigma-Aldrich, Germany) was added to the culture medium to establish a lipid-loaded cell model *in vitro*, which was used to mimic an *in vivo* high-fat environment.

Oil red O staining and lipid quantification

HepG2 human hepatocellular carcinomas cells were washed three times with phosphate-buffered saline (PBS), and subsequently fixed with 4% paraformaldehyde for 0.5 h. Fixed cells were washed with 60% isopropanol and stained for 0.5 h in Oil Red O solution. Before nuclear counterstaining with hematoxylin, cells were washed again with 60% isopropanol. Finally, three images of each sample were captured using a light microscope (Olympus). To quantify the lipid content, 100% isopropanol was used to extract the Oil Red O stained lipid droplets, and the absorbance was measured at 495 nm.

Antibody, immunoblotting, immunoprecipitation, and immunofluorescence

The primary antibody information is summarized in Supplementary Table S1. Immunoblotting, IP, and IF were performed as previously described (25, 26). Briefly, a RIPA buffer containing a protease inhibitor mixture (Beyotime) and phosphatase inhibitor cocktail (Beyotime) was used to harvest and extract total proteins. A BCA kit was used to determine the protein concentration. Total proteins were separated using 8%,

10%, and 15% SDS-polyacrylamide gel electrophoresis (PAGE), and subsequently transferred onto a polyvinylidene difluoride membrane (Millipore, Germany). Proteins were incubated overnight with the indicated antibodies. After incubation, the signal was detected using electrochemiluminescence reagents (Thermo Scientific). For IP, total proteins were incubated with the indicated antibodies for 4–6 h to form protein-antibody complexes. Thereafter, the protein-antibody complexes were incubated with protein A/G magnetic beads (Santa Cruz Biotechnology, USA) for 16–20 h at 4°C. The mixture was subsequently centrifuged at 1000 rpm for 5 min to collect immunoprecipitants. The immunoprecipitants were washed five times with lysis buffer before solubilization in sample buffer and analysis using SDS-PAGE. For IF, cells were fixed with 4% paraformaldehyde and blocked with goat serum. Thereafter, cells were incubated with the primary antibody overnight and subsequently washed three times with PBS. Fluorescent secondary antibody incubation was performed before nuclear staining with 4', 6-diamidino-2-phenylindole (Beyotime). The samples were analyzed using a fluorescence microscope (Olympus).

Real-time quantitative PCR

Total RNA was extracted from cells and tissues using RNA extraction kits (Feijie, China) according to the PrimeScript RT Master Mix (Takara, Japan) with the manufacturer's cDNA. Real-time quantitative PCR was conducted using FastStart Essential DNA Green Master (Roche, Switzerland) on a Roche LightCycler 480 (Roche). The expression values for the indicated genes were normalized to those of β-actin. The primers were synthesized by the Shenzhen Huada Gene Company and are presented in Supplementary Table S2.

Mass spectrometry based non-targeted proteomics

According to the manufacturer's protocol, gel pieces were digested overnight using trypsin at 37°C. The mass spectrometer type was Thermo Scientific™ Q Exactive Plus. The tryptic peptides flowed at a constant rate of 400 nL/min on an EASY-nLC 1000 UPLC system, and the Orbitrap detected intact peptides and fragments at a resolution of 70,000 and 17,500, respectively. It was a data-dependent procedure that alternated between one MS scan followed by 20 MS/MS scans with a 15.0 s dynamic exclusion. Automatic gain control was set at 5E4. Proteome discoverer 1.3 was used to process the resulting data, and tandem MS spectra were performed against the SwissProt human database (20387 sequences). Trypsin was specified as a cleavage enzyme that allowed up to two missing cleavages. Mass error was set to 10 ppm for precursor ions and 0.02 Da for fragment ions. Carbamidomethyl on Cys was specified as fixed modification and oxidation on Met was specified as variable modification. The peptide confidence was high, and the peptide ion score was >20.

DNA constructs and transfection

Flag-USP20 and Myc-HSPA2 cDNA, USP20 and HSPA2 short hairpin RNA (shRNA) lentiviral constructs, and corresponding controls were purchased from ViGene Biosciences (Shandong, China). DNA sequencing was performed to verify the above plasmids using Invitrogen Biotechnologies (Shanghai, China). Supplementary Table S3 provides detailed information on DNA constructs. Transfection was performed using Lipofectamine™ 2000 (Invitrogen, USA) according to the manufacturer's instructions.

Cycloheximade analyses and *in vivo* ubiquitination

For CHX determination, cells were treated with 100 μg/mL CHX before collection for immunoblotting at the indicated time. For *in vivo* ubiquitination, expression plasmids encoding Myc-HSPA2, HA-ubiquitin, and Flag-USP20 were used to transfect the cells alone or in combination. Twenty-four hours after transfection, cells were treated with MG-132 and lysed for immunoblotting and IP analysis.

Statistical analysis

Immunoblotting statistics were performed using ImageJ 1.53e. The standard error of the mean (SEM) was defined as the present form for all data. An unpaired two-tailed Student's *t*-test was used for intergroup comparisons using GraphPad Prism 9. Statistical significance was set at $p < 0.05$.

Results

SG improves lipid dysmetabolism of DIO mice

SG was found to improve lipid dysmetabolism in DIO mice. The main process of the trial is summarized in Figure 1A. The results showed that the body weights of the SG group were significantly lower than those of the sham group (Figure 1B and Supplementary figure S1). H&E staining showed that SG reduced the number of ballooning hepatocytes and attenuated hepatic steatosis (Figure 1C). Oil Red O staining showed that SG attenuated DIO hepatic lipid accumulation (Figure 1D).

Furthermore, the TC and TG levels in the liver and serum of SG group individuals were significantly reduced (Figures 1E-H and Supplementary Figures S2, S3). These results suggested that SG can improve lipid metabolism in DIO mice.

USP20 promotes lipid accumulation *in vitro*

To explore whether USP20 was involved in the improvement of lipid metabolism after surgery, we first investigated its expression in the mouse liver. Compared to those of the sham group, both the mRNA and protein levels of USP20 in the SG group were downregulated (Figures 2A–C), implying that USP20 might be involved in the regulation of lipid metabolism. To verify whether USP20 promotes lipid accumulation, Oil Red O staining of lipid-loaded HepG2 cells was performed, which showed that USP20 overexpression could promote lipid accumulation (Figure 2D) while USP20 knockdown attenuates it (Figure 2E). Moreover, USP20 overexpression resulted in significantly higher levels of TC and TG (Figure 2F), whose accumulations were significantly reduced under USP20 knockdown (Figure 2G). Our research demonstrated that SG downregulates the expression level of USP20, which attenuates lipid accumulation *in vitro*.

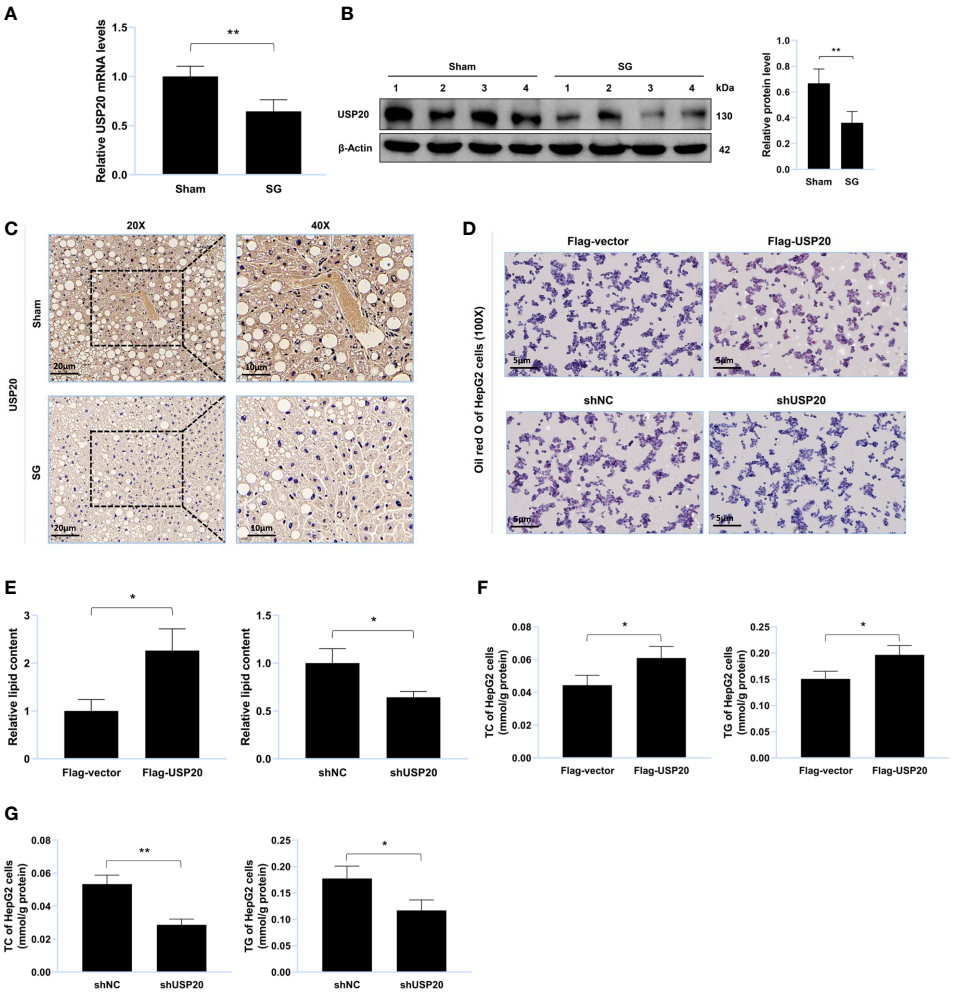

FIGURE 2
USP20 promotes lipid accumulation *in vitro*. **(A)** Relative mRNA level of USP20 in liver from sham group and SG group (n = 4). **(B)** Western blot detection of USP20 in liver from sham group and SG group (n = 4). **(C)** Immunohistochemistry detection of USP20 in liver from sham group and SG group. Scale bars were shown in the figure. **(D)** HepG2 cells were transfected with Flag-USP20, Flag-vector, shUSP20 and shNC. Lipid accumulation of HepG2 cells was assessed by Oil Red O staining. Scale bars were shown in the figure. **(E)** Relative lipid content of HepG2 cells (n = 3). **(F, G)** TC and TG content of HepG2 cells (n = 3). The data are expressed as mean ± SEM, Student's t-test was used for intergroup comparisons. *p < 0.05, **p < 0.01.

HSPA2 promotes lipid accumulation *in vitro*

MS was used to identify USP20 substrates (Supplementary Table S4) and HSPA2 was identified as a potential substrate. Thereafter, we researched the expression level of HSPA2 in the mouse liver. Compared to the sham group, the protein level of HSPA2 and not mRNA, was downregulated in the SG group (Figures 3A–C), implying that HSPA2 may regulate lipid metabolism. Oil Red O staining of the lipid-loaded cell model showed that HSPA2 overexpression promoted lipid accumulation (Figure 3D), while HSPA2 knockdown attenuated lipid accumulation (Figure 3E). Similarly, HSPA2 overexpression resulted in significantly higher levels of TC and TG (Figure 3F), while HSPA2 knockdown significantly reduced the accumulation of TC and TG (Figure 3G). The above results showed that SG downregulates the expression level of HSPA2, and that HSPA2 also promotes lipid accumulation *in vitro*.

USP20 targets and stabilizes HSPA2 at the protein level

To verify whether USP20 targeted HSPA2, HepG2 cells were transfected with Flag-USP20 cDNA and USP20 short hairpin RNA. The results indicated that overexpression and knockdown

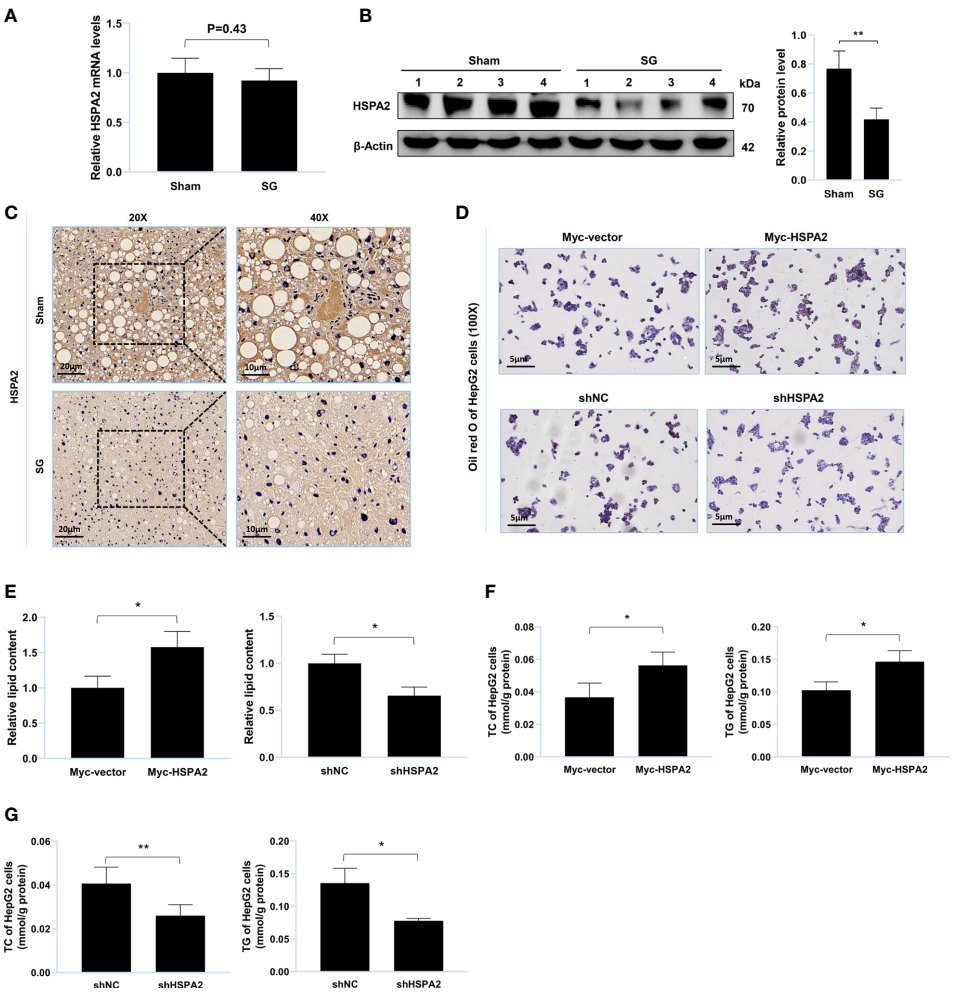

FIGURE 3
HSPA2 promotes lipid accumulation *in vitro*. **(A)** Relative mRNA level of HSPA2 in liver from sham group and SG group (n = 4). **(B)** Western blot detection of HSPA2 in liver from sham group and SG group (n = 4). **(C)** Immunohistochemistry detection of HSPA2 in liver from sham group and SG group. Scale bars were shown in the figure. **(D)** HepG2 cells were transfected with Myc-HSPA2, Myc-vector, shHSPA2 and shNC. Lipid accumulation of HepG2 cells was assessed by Oil Red O staining. Scale bars were shown in the figure. **(E)** Relative lipid content of HepG2 cells (n = 3). **(F, G)** TC and TG content of HepG2 cells (n = 3). The data are expressed as mean ± SEM, Student's t-test was used for intergroup comparisons. *p < 0.05, **p < 0.01.

10.3389/fendo.2022.1041027

of USP20 caused respective upregulation and downregulation of HSPA2 at the protein level (Figure 4A). However, no significant change in USP20 was observed upon cell transfection with Myc-HSPA2 cDNA and HSPA2 short hairpin RNA (Figure 4B). Cells were subsequently treated with CHX, and we found that overexpression of USP20 significantly delayed the degradation of HSPA2 (Figures 4C, D). Real-time quantitative PCR showed that there was no reciprocal regulation between USP20 and HSPA2 at the mRNA level (Figures 4E, F). These results suggested that USP20 targets and stabilizes HSPA2 at the protein level.

USP20 stabilizes HSPA2 *via* deubiquitination

To gain insight into the USP20-HSPA2 axis mechanism, we first examined whether there was an interaction between USP20 and HSPA2. Immunoblotting suggested that co-immunoprecipitation occurred when Flag-USP20 and Myc-HSPA2 were co-expressed in HEK-293T cells (Figure 5A). The endogenous IP showed similar results (Figures 5B, C). Moreover, IF analysis showed that USP20 co-localized with HSPA2 in the cytoplasm of HEK-293T cells (Figure 5D). These results indicated

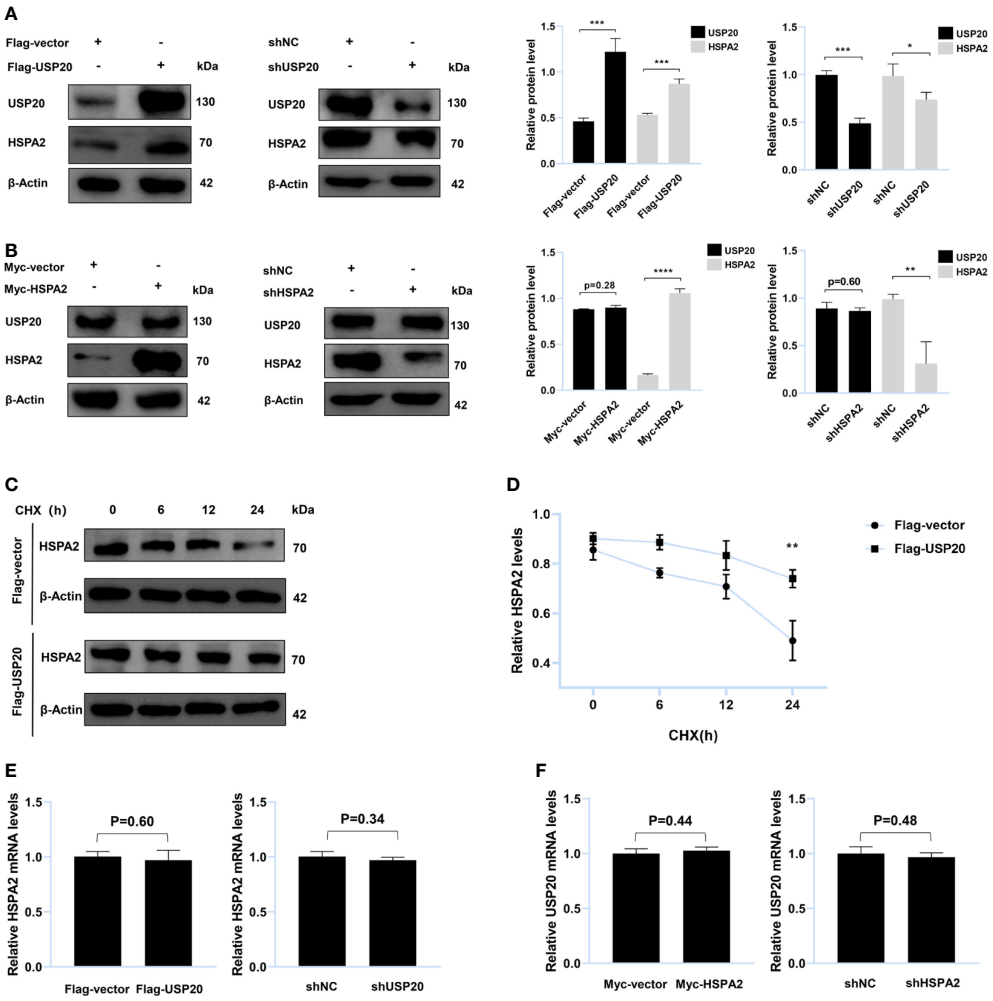

FIGURE 4
USP20 targets and stabilizes HSPA2 at protein level. **(A)** Immunoblotting analysis of HepG2 cells stably expressing Flag-USP20, Flag-vector, shUSP20 and shNC with the indicated antibodies (n = 3). **(B)** Immunoblotting analysis of HepG2 cells stably expressing Myc-HSPA2, Myc-vector, shHSPA2 and shNC with the indicated antibodies (n = 3). **(C)** Transfection with the indicated expression vectors was performed in HepG2 cells. After 24h, 100μg/ml of CHX was used to treat HepG2 cells for the indicated times and then analyzed by immunoblotting with the indicated antibodies (n = 3). **(D)** Quantitative results of HSPA2 protein levels (HSPA2/β-actin, n = 3). **(E)** PCR analysis of HepG2 cells stably expressing Flag-USP20, Flag-vector, shUSP20 and shNC with the indicated primers (n = 3). **(F)** PCR analysis of HepG2 cells stably expressing Myc-HSPA2, Myc-vector, shHSPA2 and shNC with the indicated primers (n = 3). The data are expressed as mean ± SEM, Student's t-test was used for intergroup comparisons. *p < 0.05, **p < 0.01, ***p < 0.001 and ****p < 0.0001.

an interaction between USP20 and HSPA2, and owing to the deubiquitinating enzyme function of USP20, we tested whether USP20 induced the deubiquitination of HSPA2. As shown in Figure 5E, Myc-HSPA2 was ubiquitinated in the presence of HA-ubiquitin, and the co-expression of Flag-USP20 reduced the ubiquitination of Myc-HSPA2. Our results therefore demonstrated that the mechanism of the USP20-HSPA2 axis involves the stabilization of HSPA2 by USP20 *via* deubiquitination.

Our results demonstrated that in DIO mice, USP20 is a DUB that targets HSPA2 and stabilizes HSPA2 *via* deubiquitination. It also showed that SG improves lipid metabolism by downregulating the USP20-HSPA2 axis to some degree (Figure 6).

Discussion

Obesity is a serious health concern that causes a great deal of personal and societal issues (1, 2). Although SG results in a considerable decrease in body mass index and an improvement in lipid dysmetabolism, limitations such as operative trauma and surgical risk lead to unpredictable surgical treatment results in obese patients (3, 4). SG improves lipid metabolism in a weight-loss-independent manner, which has been demonstrated by some studies (27, 28). Therefore, it is vital to elucidate the mechanism by which SG improves lipid metabolism to develop a noninvasive therapy. We propose a possible mechanism demonstrated in DIO mice, involving the downregulation of the USP20-HSPA2 axis. It has also been found that USP20 is a DUB that removes ubiquitin linked to HSPA2 and protects mice from lipid dysmetabolism.

We conducted SG on an individual in a DIO mouse model, which is a model that has been recognized worldwide because it simulates the metabolic characteristics and natural history of obesity (29). After the SG, we observed obvious weight reduction and metabolism improvement, thereby demonstrating the success of model establishment. Within the mechanism of lipid metabolism after SG, bile acids and bile acid receptors have attracted great attention (8, 30, 31). Some studies have shown that the improvement in metabolism of SG is associated with the

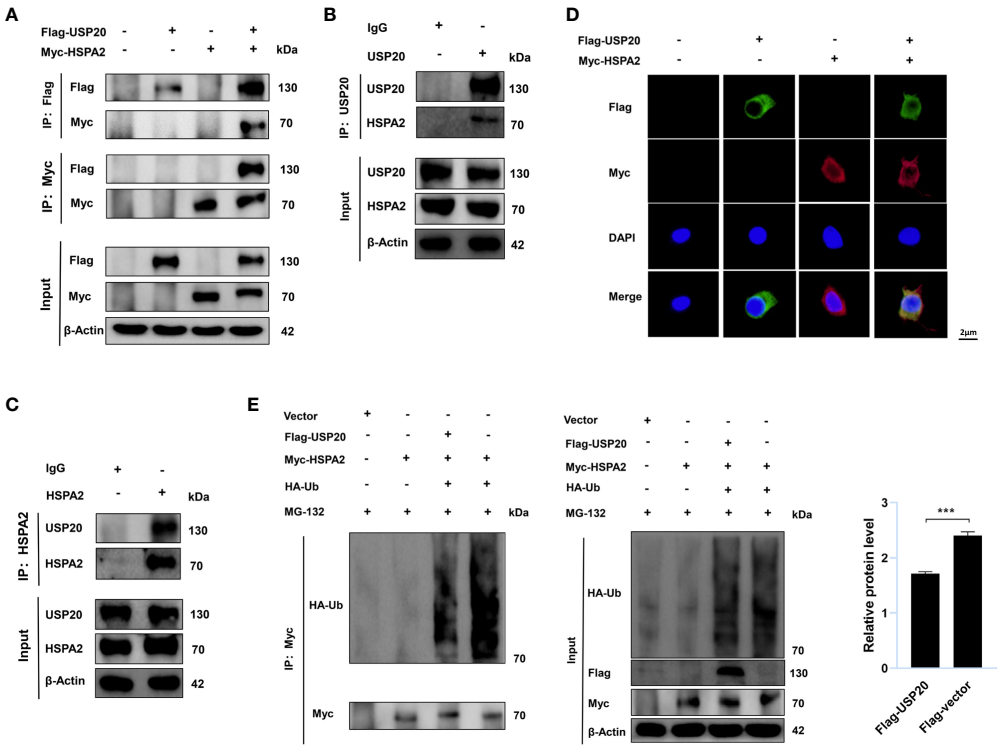

FIGURE 5
USP20 stabilizes HSPA2 via deubiquitination. **(A)** After 48h transfection of HEK293T cells with the indicated expression vectors, cellular lysates were analyzed by IP and immunoblotting with the indicated antibodies. **(B, C)** The lysates of HEK293T cells were analyzed by IP and immunoblotting with the indicated antibodies. **(D)** Transfection with the indicated expression vectors was performed in HEK293T cells. And 48h after transfection, indirect IF staining was performed with the indicated antibodies. Nuclear staining was performed with 4′, 6-diamidino-2-phenylindole. Scale bars were shown in the figure. **(E)** Transfection with the indicated expression vectors was performed in HEK293T cells. After 48h, cells were treated with MG-132 (10μM) for 6h and then analyzed by IP and immunoblotting with the indicated antibodies. Three times experiments were performed for above results. The data are expressed as mean ± SEM, Student's t-test was used for intergroup comparisons. ***$p < 0.001$.

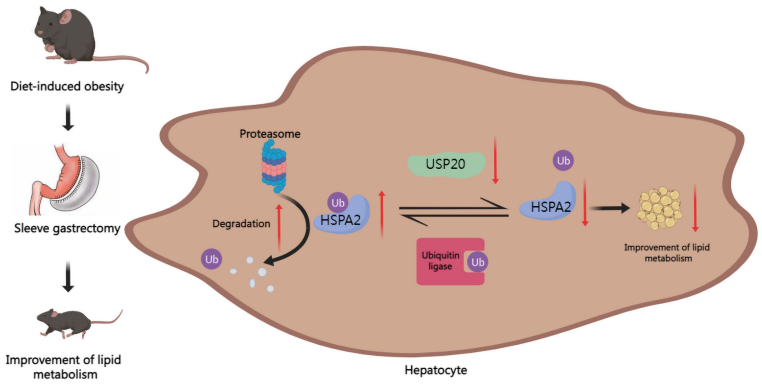

FIGURE 6
Graph of the potential mechanism of the regulatory network. SG improves lipid dysmetabolism *via* downregulating USP20-HSPA2 axis in DIO mice.

elevation of serum bile acid (27, 32). Several nuclear receptors are activated by bile acids to regulate physiological functions. Farnesoid X receptor (FXR) and Takeda G protein-coupled receptor 5 (TGR5) are two of the most important receptors. According to some studies, cholic acid, a natural FXR ligand, protects the liver from steatosis and treats hyperlipidemia in mice (33). Steroidal FXR agonists have been found to play a beneficial role in nonalcoholic fatty liver disease (34–36). Ding et al. suggested an essential role of TGR5 in reducing liver lipid accumulation after SG (37). However, the downstream mechanisms of bile acid receptors are not completely clear. In eukaryotic cells, the ubiquitin–proteasome system (UPS) is the most noteworthy post-transcriptional modification, which is widely involved in multiple physiological and pathological regulation (38). Some studies have found that bile acid signaling pathways perform several diverse biological functions *via* UPS (39–41). DUBs are proteases that function in the reverse direction of ubiquitination, and mediate deubiquitination (12). More than 90 members of the DUB family are further divided into seven subfamilies, and USP20 belongs to the USP subfamily (14). According to the latest research, USP20 knockout mice present a series of characteristics associated with the improvement of lipid dysmetabolism, which suggests that bile acid likely achieves its function *via* USP20 in SG (20). We observed USP20 downregulation in the SG group and an *in vitro* study confirmed that the expression changes of USP20 regulated lipid metabolism. Further investigation into the relevant pathways and molecular mechanisms is needed.

According to molecular weight, the heat shock protein family is generally divided into six groups: 27-kDa, 40-kDa, 60-kDa, 70-kDa, 90-kDa, and large heat shock proteins (42). The primary functions of heat shock proteins include protein folding, protein complex assembly, protein transportation, and protein degradation (42–44). The 70-kDa heat shock proteins are ubiquitously expressed and are considered to regulate lipid metabolism because of their chaperone properties (44–46). HSPA2 is a 70-kDa heat shock protein (HSP70) that has been identified as a potential substrate of USP20 by MS analysis. Unlike USP20, HSPA2 presents downregulation in the SG group only at the protein level. We also observed HSPA2 promoted lipid accumulation *in vitro*. Further studies found that USP20 positively regulates HSPA2 only at the protein level, which confirms that USP20 plays a vital role in lipid metabolism improvement by targeting HSPA2 after SG. Ding et al. found that the ubiquitin ligase RNF144A suppresses the growth and metastasis of breast cancer by regulating the stability of HSPA2 (47). Furthermore, the circBoule RNA of mouse sperm interacts with HSPA2, and circBoule RNA targets and regulates the stability of HSPA2 *via* ubiquitination (48). These results suggest that the ubiquitin-proteasome pathway is involved in HSPA2 related biological functions. These results were consistent with our findings that USP20 interacted with HSPA2 and stabilized HSPA2 *via* deubiquitination.

Our study identified a new pathway involved in SG where the downregulation of USP20-HSPA2 axis improved lipid metabolism. Zhang et al. showed that the overexpression of HSP70 enhances TG accumulation with the upregulation of fatty acid biosynthesis enzymes, including fatty acid synthase, stearoyl-CoA desaturase and acetyl-CoA carboxylase (49). HSP70 promotes TC accumulation by reducing the expression levels of the ATP-binding cassette transporter A1 and ATP binding cassette transporter G1 (50). Therefore, fatty acid biosynthesis and cholesterol transport are the possible pathways by which the USP20-HSPA2 axis achieves biological functions. Some limitations of this study include the necessity of *in vivo* experiments to verify the effect of the USP20-HSPA2 axis on lipid metabolism. In addition, the intermediate links connecting SG and USP20 still need to be identified. The downstream pathway of the USP20-HSPA2 axis needs further studies for validation. We hope to address these limitations in our future studies.

In conclusion, our study provides evidence that the USP20-HSPA2 axis is downregulated in the SG group. USP20 stabilizes HSPA2 *via* deubiquitination to promote lipid accumulation, which may be a noninvasive therapeutic target for replacing surgery.

Data availability statement

The data presented in the study are deposited in the PRIDE repository, accession number PXD037693.

Ethics statement

The animal study was reviewed and approved by the Medical Ethics Committee of Shandong Provincial Qianfoshan Hospital, Shandong University.

Author contributions

Conceptualization, WZ and MZ. Methodology, WZ, YC, JZ, GZ. Validation, WZ, BS, SRL, ZL, SHL, SD. Data analysis, WZ. Writing original draft preparation, WZ. All authors contributed to the article and approved the submitted version.

Funding

This work was supported by National Natural Science Foundation of China (81900705).

Acknowledgments

The authors express appreciation to Dr. Yu Tianming for his performance of SG procedure on mice, which was crucial in the establishment of SG murine model described in this study.

Conflict of interest

The authors declare that the research was conducted in the absence of any commercial or financial relationships that could be construed as a potential conflict of interest.

Publisher's note

All claims expressed in this article are solely those of the authors and do not necessarily represent those of their affiliated organizations, or those of the publisher, the editors and the reviewers. Any product that may be evaluated in this article, or claim that may be made by its manufacturer, is not guaranteed or endorsed by the publisher.

Supplementary material

The Supplementary Material for this article can be found online at: https://www.frontiersin.org/articles/10.3389/fendo.2022.1041027/full#supplementary-material

References

1. Piché M-E, Tchernof A, Després J-P. Obesity phenotypes, diabetes, and cardiovascular diseases. *Circ Res* (2020) 126(11):1477–500. doi: 10.1161/CIRCRESAHA.120.316101

2. Deprince A, Haas JT, Staels B. Dysregulated lipid metabolism links nafld to cardiovascular disease. *Mol Metab* (2020) 42:101092. doi: 10.1016/j.molmet.2020.101092

3. Arterburn DE, Telem DA, Kushner RF, Courcoulas AP. Benefits and risks of bariatric surgery in adults: A review. *JAMA* (2020) 324(9):879–87. doi: 10.1001/jama.2020.12567

4. Alalwan AA, Friedman J, Park H, Segal R, Brumback BA, Hartzema AG. Us national trends in bariatric surgery: A decade of study. *Surgery* (2021) 170(1):13–7. doi: 10.1016/j.surg.2021.02.002

5. Ding L, Zhang E, Yang Q, Jin L, Sousa KM, Dong B, et al. Vertical sleeve gastrectomy confers metabolic improvements by reducing intestinal bile acids and lipid absorption in mice. *Proc Natl Acad Sci U.S.A.* (2021) 118(6):e2019388118. doi: 10.1073/pnas.2019388118

6. Hutch CR, Trakimas DR, Roelofs K, Pressler J, Sorrell J, Cota D, et al. Oea signaling pathways and the metabolic benefits of vertical sleeve gastrectomy. *Ann Surg* (2020) 271(3):509–18. doi: 10.1097/SLA.0000000000003093

7. Oberbach A, Schlichting N, Heinrich M, Kullnick Y, Retschlag U, Lehmann S, et al. Gastric mucosal devitalization reduces adiposity and improves lipid and glucose metabolism in obese rats. *Gastrointest Endosc* (2018) 87(1):288–299.e6. doi: 10.1016/j.gie.2017.04.038

8. Albaugh VL, Banan B, Ajouz H, Abumrad NN, Flynn CR. Bile acids and bariatric surgery. *Mol Aspects Med* (2017) 56:75–89. doi: 10.1016/j.mam.2017.04.001

9. Popovic D, Vucic D, Dikic I. Ubiquitination in disease pathogenesis and treatment. *Nat Med* (2014) 20(11):1242–53. doi: 10.1038/nm.3739

10. Mevissen TET, Komander D. Mechanisms of deubiquitinase specificity and regulation. *Annu Rev Biochem* (2017) 86:159–92. doi: 10.1146/annurev-biochem-061516-044916

11. Rape M. Ubiquitylation at the crossroads of development and disease. *Nat Rev Mol Cell Biol* (2018) 19(1):59–70. doi: 10.1038/nrm.2017.83

12. Lange SM, Armstrong LA, Kulathu Y. Deubiquitinases: From mechanisms to their inhibition by small molecules. *Mol Cell* (2022) 82(1):15–29. doi: 10.1016/j.molcel.2021.10.027

13. Oh E, Akopian D, Rape M. Principles of ubiquitin-dependent signaling. *Annu Rev Cell Dev Biol* (2018) 34:137–62. doi: 10.1146/annurev-cellbio-100617-062802

14. Li Q, Ye C, Tian T, Jiang Q, Zhao P, Wang X, et al. The emerging role of ubiquitin-specific protease 20 in tumorigenesis and cancer therapeutics. *Cell Death Dis* (2022) 13(5):434. doi: 10.1038/s41419-022-04853-2

15. Li W, Shen M, Jiang Y-Z, Zhang R, Zheng H, Wei Y, et al. Deubiquitinase Usp20 promotes breast cancer metastasis by stabilizing Snai2. *Genes Dev* (2020) 34(19-20):1310–5. doi: 10.1101/gad.339804.120

16. Wu C, Luo K, Zhao F, Yin P, Song Y, Deng M, et al. Usp20 positively regulates tumorigenesis and chemoresistance through B-catenin stabilization. *Cell Death Differ* (2018) 25(10):1855–69. doi: 10.1038/s41418-018-0138-z

17. Zhang M, Zhang M-X, Zhang Q, Zhu G-F, Yuan L, Zhang D-E, et al. Usp18 recruits Usp20 to promote innate antiviral response through deubiquitinating Sting/Mita. *Cell Res* (2016) 26(12):1302–19. doi: 10.1038/cr.2016.125

18. Jean-Charles P-Y, Wu J-H, Zhang L, Kaur S, Nepliouev I, Stiber JA, et al. Usp20 (Ubiquitin-specific protease 20) inhibits tnf (Tumor necrosis factor)-triggered smooth muscle cell inflammation and attenuates atherosclerosis. *Arterioscler Thromb Vasc Biol* (2018) 38(10):2295–305. doi: 10.1161/ATVBAHA.118.311071

19. Yuan J, Luo K, Deng M, Li Y, Yin P, Gao B, et al. Herc2-Usp20 axis regulates DNA damage checkpoint through claspin. *Nucleic Acids Res* (2014) 42(21):13110–21. doi: 10.1093/nar/gku1034

20. Lu X-Y, Shi X-J, Hu A, Wang J-Q, Ding Y, Jiang W, et al. Feeding induces cholesterol biosynthesis *Via* the Mtorc1-Usp20-Hmgcr axis. *Nature* (2020) 588 (7838):479–84. doi: 10.1038/s41586-020-2928-y

21. Scieglinska D, Krawczyk Z. Expression, function, and regulation of the testis-enriched heat shock Hspa2 gene in rodents and humans. *Cell Stress Chaperones* (2015) 20(2):221–35. doi: 10.1007/s12192-014-0548-x

22. Yin Y, Cao S, Fu H, Fan X, Xiong J, Huang Q, et al. A noncanonical role of nod-like receptor Nlrp14 in pgclc differentiation and spermatogenesis. *Proc Natl Acad Sci U.S.A.* (2020) 117(36):22237–48. doi: 10.1073/pnas.2005533117

23. Zouari Bouassida K, Chouchane L, Jellouli K, Chérif S, Haddad S, Gabbouj S, et al. Polymorphism of stress protein Hsp70-2 gene in tunisians: Susceptibility implications in type 2 diabetes and obesity. *Diabetes Metab* (2004) 30(2):175–80. doi: 10.1016/S1262-3636(07)70104-0

24. Ryan KK, Tremaroli V, Clemmensen C, Kovatcheva-Datchary P, Myronovych A, Karns R, et al. Fxr is a molecular target for the effects of vertical sleeve gastrectomy. *Nature* (2014) 509(7499):183–8. doi: 10.1038/nature13135

25. Dong S, Liang S, Cheng Z, Zhang X, Luo L, Li L, et al. Ros/Pi3k/Akt and Wnt/B-catenin signalings activate hif-1α-Induced metabolic reprogramming to impart 5-fluorouracil resistance in colorectal cancer. *J Exp Clin Cancer Res* (2022) 41(1):15. doi: 10.1186/s13046-021-02229-6

26. Li S, Dong S, Shi B, Xu Q, Li L, Wang S, et al. Attenuation of Ros/Chloride efflux-mediated Nlrp3 inflammasome activation contributes to alleviation of diabetic cardiomyopathy in rats after sleeve gastrectomy. *Oxid Med Cell Longev* (2022) 2022:4608914. doi: 10.1155/2022/4608914

27. Myronovych A, Kirby M, Ryan KK, Zhang W, Jha P, Setchell KD, et al. Vertical sleeve gastrectomy reduces hepatic steatosis while increasing serum bile acids in a weight-Loss-Independent manner. *Obes (Silver Spring)* (2014) 22(2):390–400. doi: 10.1002/oby.20548

28. Frikke-Schmidt H, Zamarron BF, O'Rourke RW, Sandoval DA, Lumeng CN, Seeley RJ. Weight loss independent changes in adipose tissue macrophage and T cell populations after sleeve gastrectomy in mice. *Mol Metab* (2017) 6(4):317–26. doi: 10.1016/j.molmet.2017.02.004

29. Garibay D, Cummings BP. A murine model of vertical sleeve gastrectomy. *J Vis Exp* (2017) 130):56534. doi: 10.3791/56534

30. Fiorucci S, Distrutti E, Carino A, Zampella A, Biagioli M. Bile acids and their receptors in metabolic disorders. *Prog Lipid Res* (2021) 82:101094. doi: 10.1016/j.plipres.2021.101094

31. Sinclair P, Brennan DJ, le Roux CW. Gut adaptation after metabolic surgery and its influences on the brain, liver and cancer. *Nat Rev Gastroenterol Hepatol* (2018) 15(10):606–24. doi: 10.1038/s41575-018-0057-y

32. Steenackers N, Vanuytsel T, Augustijns P, Tack J, Mertens A, Lannoo M, et al. Adaptations in gastrointestinal physiology after sleeve gastrectomy and roux-En-Y gastric bypass. *Lancet Gastroenterol Hepatol* (2021) 6(3):225–37. doi: 10.1016/S2468-1253(20)30302-2

33. Watanabe M, Houten SM, Wang L, Moschetta A, Mangelsdorf DJ, Heyman RA, et al. Bile acids lower triglyceride levels *Via* a pathway involving fxr, shp, and srebp-1c. *J Clin Invest* (2004) 113(10):1408–18. doi: 10.1172/JCI21025

34. Neuschwander-Tetri BA, Loomba R, Sanyal AJ, Lavine JE, Van Natta ML, Abdelmalek MF, et al. Farnesoid X nuclear receptor ligand obeticholic acid for non-cirrhotic, non-alcoholic steatohepatitis (Flint): A multicentre, randomised, placebo-controlled trial. *Lancet* (2015) 385(9972):956–65. doi: 10.1016/S0140-6736(14)61933-4

35. Younossi ZM, Ratziu V, Loomba R, Rinella M, Anstee QM, Goodman Z, et al. Obeticholic acid for the treatment of non-alcoholic steatohepatitis: Interim analysis from a multicentre, randomised, placebo-controlled phase 3 trial. *Lancet* (2019) 394(10215):2184–96. doi: 10.1016/S0140-6736(19)33041-7

36. Mudaliar S, Henry RR, Sanyal AJ, Morrow L, Marschall H-U, Kipnes M, et al. Efficacy and safety of the farnesoid X receptor agonist obeticholic acid in patients with type 2 diabetes and nonalcoholic fatty liver disease. *Gastroenterology* (2013) 145(3):574–82.e1. doi: 10.1053/j.gastro.2013.05.042

37. Ding L, Sousa KM, Jin L, Dong B, Kim B-W, Ramirez R, et al. Vertical sleeve gastrectomy activates gpbar-1/Tgr5 to sustain weight loss, improve fatty liver, and remit insulin resistance in mice. *Hepatology* (2016) 64(3):760–73. doi: 10.1002/hep.28689

38. Pohl C, Dikic I. Cellular quality control by the ubiquitin-proteasome system and autophagy. *Science* (2019) 366(6467):818–22. doi: 10.1126/science.aax3769

39. Miao J, Xiao Z, Kanamaluru D, Min G, Yau PM, Veenstra TD, et al. Bile acid signaling pathways increase stability of small heterodimer partner (Shp) by inhibiting ubiquitin-proteasomal degradation. *Genes Dev* (2009) 23(8):986–96. doi: 10.1101/gad.1773909

40. Huang X, Wang B, Chen R, Zhong S, Gao F, Zhang Y, et al. The nuclear farnesoid X receptor reduces P53 ubiquitination and inhibits cervical cancer cell proliferation. *Front Cell Dev Biol* (2021) 9:583146. doi: 10.3389/fcell.2021.583146

41. Guo C, Xie S, Chi Z, Zhang J, Liu Y, Zhang L, et al. Bile acids control inflammation and metabolic disorder through inhibition of Nlrp3 inflammasome. *Immunity* (2016) 45(4):802–16. doi: 10.1016/j.immuni.2016.09.008

42. Wu J, Liu T, Rios Z, Mei Q, Lin X, Cao S. Heat shock proteins and cancer. *Trends Pharmacol Sci* (2017) 38(3):226–56. doi: 10.1016/j.tips.2016.11.009

43. Saibil H. Chaperone machines for protein folding, unfolding and disaggregation. *Nat Rev Mol Cell Biol* (2013) 14(10):630–42. doi: 10.1038/nrm3658

44. Morán Luengo T, Mayer MP, Rüdiger SGD. The Hsp70-Hsp90 chaperone cascade in protein folding. *Trends Cell Biol* (2019) 29(2):164–77. doi: 10.1016/j.tcb.2018.10.004

45. Rosenzweig R, Nillegoda NB, Mayer MP, Bukau B. The Hsp70 chaperone network. *Nat Rev Mol Cell Biol* (2019) 20(11):665–80. doi: 10.1038/s41580-019-0133-3

46. Kampinga HH, Craig EA. The Hsp70 chaperone machinery: J proteins as drivers of functional specificity. *Nat Rev Mol Cell Biol* (2010) 11(8):579–92. doi: 10.1038/nrm2941

47. Yang Y-L, Zhang Y, Li D-D, Zhang F-L, Liu H-Y, Liao X-H, et al. Rnf144a functions as a tumor suppressor in breast cancer through ubiquitin ligase activity-dependent regulation of stability and oncogenic functions of Hspa2. *Cell Death Differ* (2020) 27(3):1105–18. doi: 10.1038/s41418-019-0400-z

48. Gao L, Chang S, Xia W, Wang X, Zhang C, Cheng L, et al. Circular rnas from play conserved roles in protection against stress-induced fertility decline. *Sci Adv* (2020) 6(46):eabb7426. doi: 10.1126/sciadv.abb7426

49. Zhang J, Fan N, Peng Y. Heat shock protein 70 promotes lipogenesis in Hepg2 cells. *Lipids Health Dis* (2018) 17(1):73. doi: 10.1186/s12944-018-0722-8

50. Zhao Z-W, Zhang M, Chen L-Y, Gong D, Xia X-D, Yu X-H, et al. Heat shock protein 70 accelerates atherosclerosis by downregulating the expression of Abca1 and Abcg1 through the Jnk/Elk-1 pathway. *Biochim Biophys Acta Mol Cell Biol Lipids* (2018) 1863(8):806–22. doi: 10.1016/j.bbalip.2018.04.011

frontiers | Frontiers in Endocrinology

TYPE Original Research
PUBLISHED 04 January 2023
DOI 10.3389/fendo.2022.1024769

OPEN ACCESS

EDITED BY
Shaozhuang Liu,
Qilu Hospital, Shandong University, China

REVIEWED BY
Maude Le Gall,
Institut National de la Santé et de la Recherche Médicale (INSERM), France
Manu Landecho,
University Clinic of Navarra, Spain
Cunchuan Wang,
First Affiliated Hospital of Jinan University, China

*CORRESPONDENCE
Zefeng Xia
xiazefeng@sina.com
Kaixiong Tao
kaixiongtao@hust.edu.cn

†These authors share first authorship

SPECIALTY SECTION
This article was submitted to Obesity, a section of the journal Frontiers in Endocrinology

RECEIVED 22 August 2022
ACCEPTED 01 December 2022
PUBLISHED 04 January 2023

CITATION
Wang G, Wang Y, Bai J, Li G, Liu Y, Deng S, Zhou R, Tao K and Xia Z (2023) Increased plasma genistein after bariatric surgery could promote remission of NAFLD in patients with obesity.
Front. Endocrinol. 13:1024769.
doi: 10.3389/fendo.2022.1024769

Increased plasma genistein after bariatric surgery could promote remission of NAFLD in patients with obesity

Geng Wang[1†], Yu Wang[1,2†], Jie Bai[1], Gang Li[1], Yang Liu[1], Shichang Deng[1], Rui Zhou[3], Kaixiong Tao[1*] and Zefeng Xia[1*]

[1]Department of Gastrointestinal Surgery, Union Hospital, Tongji Medical College, Huazhong University of Science and Technology, Wuhan, China, [2]Department of Gastrointestinal Surgery, Second Affiliated Hospital, Zhejiang University School of Medicine, Hangzhou, Zhejiang, China, [3]Cancer Center, Union Hospital, Tongji Medical College, Huazhong University of Science and Technology, Wuhan, China

Background: Bariatric surgery is associated with a positive effect on the progress of non-alcoholic associated fatty liver disease (NAFLD). Although weight loss is the obvious mechanism, there are also weight-independent mechanisms.

Methods: We collected blood samples from 5 patients with obesity before and 3 months after surgery and performed an LC-MS-based untargeted metabolomics test to detect potential systemic changes. We also constructed sleeve gastrectomy (SG) mice models. The plasma, liver and intestine samples were collected and analyzed by qPCR, ELISA and HPLC. Cohousing experiments and feces transplantation experiments were performed on mice to study the effect of gut microbiota. Genistein administration experiments were used to study the in vivo function of the metabolites.

Results: Plasma genistein (GE) was identified to be elevated after surgery. Both clinical data and rodent models suggested that plasma GE is negatively related to the degree of NAFLD. We fed diet-induced obese (DIO) mice with GE, and we found that there was significant remission of NAFLD. Both in vivo and in vitro experiments showed that GE could restrict the inflammation state in the liver and thus relieve NAFLD. Finally, we used co-housing experiments to alter the gut microbiota in mice, and it was identified that sleeve gastrectomy (SG) mice had a special gut microbiota phenotype, which could result in higher plasma GE levels. By feces transplantation experiment (FMT), we found that only feces from the SG mice (and not from other lean mice) could induce higher plasma GE levels.

Conclusion: Our studies showed that SG but not calorie restriction could induce higher plasma GE levels by altering the gut microbiota. This change

could promote NAFLD remission. Our study provides new insights into the systemic effects of bariatric surgery. Bariatric surgery could affect remote organs via altered metabolites from the gut microbiota. Our study also identified that additional supplement of GE after surgery could be a therapy for NAFLD.

KEYWORDS

bariatric surgery, genistein, gut microbiota, non-alcoholic fatty liver disease, obese, sleeve gastrectomy

Introduction

The prevalence of non-alcoholic fatty liver disease (NAFLD), an obese-related disease, is rising fast and is a growing economic burden all over the world[spice] (1). Previous studies confirmed that NAFLD is typically accompanied by central obesity and metabolic syndrome (MetS) (2). During the progress of NAFLD and non-alcoholic steatohepatitis (NASH), the liver's capacity to handle the primary metabolic energy substrates is overwhelmed and toxic lipid species accumulate in the liver. Thus, in order to treat NAFLD, we need to control the fatty acid supply and restore the disposal function in the liver. By now, there are many ongoing clinical trials of pharmacotherapies for the treatment of NASH, including CCR2/5 inhibitor, PPARα/δ ligand, FXR ligand/agonist, and ASK-1 inhibitor (1). In addition to drugs, bariatric surgery has been proven to be another powerful therapeutic method for NAFLD and NASH (3–5).

Although many guidelines stated that it is premature to consider bariatric surgery as an option to specially treat NASH (6), clinical data confirmed that surgery is the most effective treatment for weight loss and thus resolved NAFLD and NASH in up to 80% of the patients (7). Notably, some studies suggested that there are weight-independent factors involved. Gut microbiota and bile acid composition may be very important during this process (7). Obesity could decrease microbial diversity and cause a reduction of certain bacterium types (8). Our previous study and other studies showed that this could lead to changes in metabolites (9, 10). The metabolites may enter the circulation system and reach the liver *via* the portal vein. Our study on animal models confirmed that metabolites from the gut microbiota played important roles in NAFLD restriction after sleeve gastrectomy (11). However, the effects and mechanism of the metabolites on NAFLD in patients with obesity remain largely unknown.

In the current study, we collected plasma samples from patients with obesity before and after bariatric surgery. Metabolite sequencing was performed to analyze the differences. We identified genistein (GE) as a special metabolite, as it is increased after bariatric surgery. Since previous studies suggested that genistein is a member of phytoestrogen and could improve insulin resistance, we tried to investigate whether increased genistein after sleeve gastrectomy (SG) plays a role in NAFLD remission.

Methods

Human blood specimen and clinical data collection

From June to December 2020, five patients with obesity were included in the study. All the patients had normal levels of fasting blood glucose (FBG) and HbAlc. They all received SG and were safely discharged without any complications. They were followed up for 3 months. Their clinical characters are listed in Table 1. Informed consent was obtained from all the patients in accordance with the Declaration of Helsinki and its subsequent amendments. Peripheral blood was collected from patients before surgery and 3 months after SG surgery and centrifuged at 3,000g for 10 min, and the supernatant was collected and stored in a -80°C refrigerator for later use. Laboratory examination was conducted to study the plasma ALT, AST, UA, HDL, and LDL by the Department of Laboratory Medicine. The CT protocol used abdominal CT scan performed using GE (GE 750HD (64), GE Health, Waukesha, Wisconsin, USA). Quality control and image analysis were performed by the same radiologist. A CT diagnosis of hepatic steatosis was made by measuring liver attenuation (LA) in Hounsfield units (HU). Lower LA was related to higher lipid accumulation (12), and CT values ≤40 HU were considered as NAFLD (13, 14).

Untargeted metabolomics

Untargeted metabolomic analysis was performed using LC-MS/MS technology, and high-resolution mass spectrometer Q Exactive (Thermo Fisher Scientific, USA) was used to collect data in both positive and negative ion modes to improve

10.3389/fendo.2022.1024769

TABLE 1 Clinical baselines and characteristics before and 3 months after SG.

Patient number	1	2	3	4	5
Age	32	23	31	35	27
Gender	Female	Female	Female	Female	Female
Baseline BMI	40.6	43.7	36.4	38.1	44.1
Postsurgical BMI	31.7	31.2	26.5	29.1	36.4
Type 2 DM	No	No	No	No	No
Hypertension	No	No	No	Yes	No
NAFLD	Yes	Yes	Yes	Yes	Yes
Baseline ALT (U/L)	189	153	167	59	172
Postsurgical ALT (U/L)	87	69	64	53	102
Baseline AST (U/L)	78	45	63	45	83
Postsurgical AST (U/L)	36	36	35	32	70
Baseline UA (μmol/L)	530	438	462	403	515
Postsurgical UA (μmol/L)	512	422	477	371	428
Baseline LDL (mmol/L)	2.97	3.53	5.53	2.79	4.26
Postsurgical LDL (mmol/L)	2.72	3.26	3.97	2.53	3.45
Baseline HDL (mmol/L)	0.71	0.84	0.75	1.04	0.67
Postsurgical HDL (mmol/L)	0.89	1.13	1.01	1.27	0.94

metabolite coverage. Compound Discoverer 3.0 (Thermo Fisher Scientific, USA) software was used for LC-MS/MS data processing, mainly for peak extraction, peak alignment, and compound identification. The self-developed metabolomics R software package metaX and the metabolome information analysis process were used for data preprocessing, statistical analysis, and metabolite classification annotation and functional annotation. Dimensionality reduction of multivariate raw data was done through PCA (principal component analysis), in order to analyze the grouping, trend (similarity and difference between sample groups and between groups), and outliers of the observed variables in the data set value (whether there are abnormal samples). PLS-DA (partial least squares method-discriminant analysis) was performed to modulate the VIP value of the first two principal components, combined with the fold change obtained by univariate analysis and T test (Student t test) to screen differential metabolites.

Metabolic assays

Mouse liver metabolic assays were performed as previously reported (15, 16). Briefly, blood was collected from mice through the inner canthus after mice had fasted for 6 h. The serum was separated and stored at -80°C before use. Aspartate aminotransferase (AST) triglyceride (TG) in the liver was measured using commercial kits (Abcam, USA) on a fully automatic biochemical analyzer (Hitachi 917, Japan). The concentrations of GE were tested by the high-performance liquid chromatography (HPLC) system (Thermo Fisher, USA). After centrifugation at 17,000×*g* for 15 min at 4°C, the protein was then precipitated by adding 100 mM HCl and centrifuging at 17,000×*g* for another 15 min at 4°C. The remaining supernatant was injected onto a 250 mm ACE C-18 column (Hichrom, UK), and genistein was quantified using 210 nm UV detection. A mobile phase containing 2.5% acetonitrile and 0.1% phosphoric acid (ultra-pure electrochemical HPLC grade) was used for HPLC separation at a flow rate of 1.0 ml/min. Genistein was quantified by comparison with a standard range of pure Genistein (0.50 to 500 mM). All procedures were performed according to the manufacturer's instructions.

Animals and diet

The IACUC number for animal ethics approval is 2468. All animal studies were approved by the Institutional Animal Care and Use Committee of Tongji Medicine College. All applicable institutional guidelines for the care and use of animals were followed. Six-week-old female C57BL/6J mice were purchased from Beijing HFK Bioscience Co., Ltd., and raised in specific pathogen-free (SPF) conditions in the Tongji Medicine School

Animal Center. The mice were housed at 22 ± 2°C on a 12-h light cycle. For the diet-induced obesity (DIO) model, the mice were fed a high-fat diet (HFD) (H10060, 60% fat, 20% protein, 20% carbohydrate, Beijing HFK Bioscience Co., Ltd.) for 10 weeks to induce obesity before SG surgery (17).

SG and postoperative care

SG and postoperational care were performed as previously described (18). Briefly, all the operations were carried out in SPF conditions, and the mice were fasted overnight before surgery. Surgeries were carried out under 1% pentobarbital sodium (80 mg/kg). For SG, the abdominal cavity is opened at the position 2–3 mm below the gastroesophageal junction, ophthalmic scissors are used to start from the left side of the stomach (greater curvature), 80% of the stomach tissue along the great curvature of the stomach is removed, and the fundus is completely removed. Then, the remaining approximately 20% of the stomach is sutured and put back into the abdominal cavity.

For a 4-day perioperative period, mice were provided a liquid diet Osmolite (Abbott Laboratories, Columbus, OH). Osmolite contains approximately 29% of calories from lipid and 54% of calories from hydrolyzable carbohydrate (mostly sugars). After 4 days, all mice returned to a normal diet.

For the DIO-sham group, we also opened the abdominal cavity and, after isolating the gastric tissue and esophagus, we kept the exposure time the same as that of the SG group. Then, we closed the abdominal wall. For the pair-weight group, we frequently recorded the weight of the mice and, by restricting food intake, we kept these mice at similar weight levels compared with the SG mice. Normal-diet mice received a normal diet all the time and served as a control group.

Analysis of the abundance of GE in serum and other organs

To analyze whether SG could affect the abundance of GE in different parts of the body, we set four groups. There are five mice in each group: the DIO-SG group, the DIO-sham group, the pair-weight group, and the normal diet group. They are age matched. Their body weight and blood samples were collected every week. 6 weeks after surgery, the mice were sacrificed and the intestine, liver, and serum were collected for investigation by qPCR, ELISA, and HPLC.

Cohousing experiments and feces transplantation experiments

For cohousing experiments, we set two groups. In each group, there are six mice. All the mice were female to avoid fighting in one cage. In the SG group, six DIO mice received SG and they were raised for 6 weeks after surgery. In the SG cohousing group, another six DIO mice also received SG but they were divided into two cages and in each cage the three SG mice were cohoused with three DIO mice. They were also cohoused for 6 weeks.

For the fecal microbiota transplantation (FMT) experiment, we followed the procedures reported previously (19). Briefly, about 0.1 g fresh feces from the donor mice was collected in the 1 ml EP tube. Phosphate-buffered saline (PBS) was added to dilute the stool to 1 ml. The mix was homogenized and filtered. The liquid was then centrifuged at 500g for 5 min at 4°C to remove the large particles. Then, the suspended particles were used for oral gavage immediately. We used 200 µl for the gavage once a day for 2 weeks. Notably, before oral gavage, the recipient mice received antibiotics administration (2000 U/l penicillin + 2 mg/ml streptomycin diluted in drinking water) for 7 days (20).

There are three groups of recipient mice. All the mice were 6-week-old mice fed with a normal diet. In the SG-FMT group, the mice received feces from SG mice (1 month after SG surgery). In the DIO-FMT group, the mice received feces from DIO mice. Moreover, in the pair-weight FMT group, the mice received feces from pair-weight control mice. The serum was collected every week, and the intestine and liver were collected after the mice were sacrificed. The feces from different groups were collected and sent for 16S rRNA gene sequencing using the MO BIO PowerSoil Kit (MO BIO). Principal component analysis (PCA) was performed to confirm the changes of the gut microbiota after cohousing or FMT treatment. Details are shown in Supplementary Figure 1.

GE administration experiments

For GE administration experiments, there are three groups and in each group there are five mice. In the DIO group, the mice received HFD as previously mentioned. In the control group, there are age-matched mice which received a normal diet and had a normal body weight. In the GE group, there were DIO mice fed with HFD containing GE (HFD plus 0.2% GE diet) for 8 weeks[spice]16]. GE was provided by LC Laboratories, USA. Purity was >99%.

For SG+GE experiments, we aimed to study the effects of supplement of GE after SG. There are five mice in each group. The SG group is the DIO mice which underwent SG and fed with HDF. The SG+GE group received the same procedure but was fed with HFD+0.2%GE. After 6 weeks, they were sacrificed and analyzed.

Mouse sample collection

The mice were sacrificed 6 weeks after the SG operation by CO_2 anesthesia as previously reported (21). The blood was

10.3389/fendo.2022.1024769

collected and centrifuged at 4,000g for 15 min to obtain serum. The liver was quickly resected, rinsed with ice-cold PBS, and quickly put in liquid nitrogen. Cecal contents were gently squeezed out of the excised cecum into cold cryotubes and frozen rapidly. Serum, liver, and cecal content samples were stored at -80°C until further analysis.

HE staining

The liver samples were collected and were fixed in buffered formalin (4%) overnight and embedded in paraffin. Five-micrometer-thick serial sections were prepared from paraffin-embedded tissues and stained with hematoxylin and eosin (H&E) to observe the distribution of lipid accumulation.

Immunohistochemistry

The tissue sections were deparaffinized and hydrated in water. Sections were incubated for 5–10 min at 37°C to retrieve mycobacterium antigens. Then, they were rinsed thoroughly in Tris-buffered saline and proceeded with the immunostaining procedure. The slides were washed two times for 5 min in TBS plus 0.025% Triton X-100 (Sigma-Aldrich) and then blocked with 1.00% BSA (Sigma-Aldrich) in TBS for 2 h at room temperature. Then, the Rat mAb F4/80 (Abcam, ab15694) was diluted to the manufacturer's recommendations (1/200) and the sections were incubated overnight at 4°C. After washing two times for 5 min TBS plus 0.025% Triton X-100, the slides were incubated in 0.30% H_2O_2 (Sigma-Aldrich) in TBS for 15 min. After two times washing in TBS buffer, secondary antibody goat anti-rat (HRP; Abcam) was diluted in TBS with 1.00% BSA (1/200), applied to slides, and incubated for 1 h at room temperature. The samples were rinsed with buffer TBS plus 0.025% Triton X-100, three times for 10 min, and then 3,3-diamino-benzidine (DAB; Sigma-Aldrich) chromogen was used for 10 min at room temperature. DAB produced a brown precipitate (where the secondary HRP antibody binds to the primary) that was insoluble in alcohol, xylene, and other organic solvents most commonly used in the laboratories. The slides were rinsed in running tap water for 10 min and stained with nuclear counterstained Mayer's hematoxylin (Sigma-Aldrich) for better visualization of the tissue morphology. Dehydration, clearance, and mounting using a compatible mounting medium were carried out.

ELISA

The concentrations of TNF-α, IL-1β, and MCP-1 in the serum, liver, and cecum of human were examined by ELISA kits (IL-1β: MLB00C, R&D; TNFα: MTA00B, R&D; MCP-1: MJE00B, R&D). All procedures were performed according to the manufacturer's instructions.

RNA extraction and RT-qPCR

Total RNA extraction was performed using the miRNeasy Micro Kit according to the manufacturer's instructions. Briefly, 500 µl of Qiazol solution (a buffer containing guanidinium thiocyanate, GITC) was used to lyse the tissue. 100 µl of chloroform was added. The mixture was vortexed and centrifuged at 12,000 rpm for 15 min at 4°C. The supernatant was obtained, and 1.5 volume of 100% ethanol was added. The mixture was centrifuged through an extraction column (Qiagen S.A.). The column was washed with RWT buffer and REP buffer, respectively. RNA was eluted in 20 µl of RNase-free water and quantified using NanoDrop. RNA samples were stored at –80°C prior to RT-PCR. Complementary DNA (cDNA) was synthesized from total RNA using PrimeScript™ RT Master Mix Kit (Takara). For RT reactions, 100–500 ng of RNA extract was used. The cDNA specimens were stored at –20°C until PCR. Quantitative real-time PCR was performed using SYBR Green with an ABI StepOnePlus system (Life Technologies, Carlsbad, CA, USA). The primers used are listed in Table 2. All the gene expression levels were normalized to the GAPDH levels. The relative quantification of mRNA was calculated by a comparative Ct method ($2^{-\Delta ct}$).

Cell culture and treatment

Cells of murine macrophage RAW264.7 were seeded into 12-well plates at a density of 4×10^5 cells/ml and cultured at 37°C with 5% CO_2. The culture medium was DMEM containing 10% FBS with 1% penicillin/streptomycin. Cells were pretreated with different concentrations of genistein for 4 h, and then, 300 mM palmitate was added. After 18 h, 10 ng/ml LPS was added to the medium. The cells were then incubated for an additional 6 h. Bone marrow-derived macrophages (BMDMs) were isolated

TABLE 2 Sequences of the primers.

Gene name	Primers
Tnfa-F	CTGGATGTCAATCAACAATGGGA
Tnfa-R	ACTAGGGTGTGAGTGTTTTCTGT
IL-1β-F	GAAATGCCACCTTTTGACAGTG
IL-1β-R	TGGATGCTCTCATCAGGACAG
Mcp-1-F	TTAAAAACCTGGATCGGAACCAA
Mcp-1-R	GCATTAGCTTCAGATTTACGGGT
Gapdh-F	AGGTCGGTGTGAACGGATTTG
Gapdh-R	TGTAGACCATGTAGTTGAGGTCA

from the femur of wild-type C57/BL6 mice. The isolated progenitor cells were resuspended in RPMI-1640 medium supplemented with 10 ng/ml macrophage colony-stimulating factor (M-CSF) (Invitrogen), seeded in polystyrene dishes, and incubated for 3 days at 37°C and 5% CO_2 in a humidified incubator. The culture medium was replenished on day 3, and the cells were incubated for an additional 4 days. At the end of the 7-day culture period, >95% of the cells were positive for macrophage markers F4/80 and CD11b.

Macrophage migration assay

BMDM migration was investigated in Transwell cell culture chambers with polycarbonate membranes (8-mm pore size, Corning Costar, Corning, NY, USA). Cells were added to the upper chamber, and either vehicle or different concentrations of genistein were added to both the upper and lower chambers. After 4 h, 20 ng/ml MCP-1 (Invitrogen) was added to the bottom chamber. After 24 h, cells remaining on the upper side of the membrane were scraped off with a cotton swab. The migrated cells in the bottom chamber were fixed with methanol for 15 min, stained with 0.1% crystal violet for 30 min, and counted under a microscope. Three replicate wells were analyzed in each experiment, with cells counted in 15 randomly chosen fields of view per well.

Statistical analysis

Data were analyzed with SPSS 21.0 (IBM Corp., USA). Continuous variables were reported as means ± standard deviation. Mann–Whitney U test or Wilcoxon test was used to compare between-group differences. Differences among three or more groups were compared by analysis of the ANOVA test. Spearman correlation analysis was used to analyze the relationship between CT values and serum GE levels. Bar plots were generated with GraphPad Prism 8.0 (GraphPad Software, San Diego, USA). p values <0.05 indicated statistical significance. $^{*}p < 0.05$, $^{**}p < 0.01$, $^{***}p < 0.001$.

Results

NAFLD is relieved after SG in patients with obesity

Clinical baselines and characteristics of the five patients included in the study are listed in Table 1. 3 months after SG, the patients with obesity had significantly decreased BMI (Figure 1A). Liver function was also improved in terms of the levels of aspartate aminotransferase (AST) and triglyceride (TG) (Figures 1B, C). There was also significant remission of NAFLD evaluated by the CT value (Figures 1D, E).

Plasma and local levels of genistein are increased after SG in patients with obesity

The blood samples from patients with obesity before surgery and 3 months after surgery were collected and sent for untargeted metabolomic analysis (Figures 2A–C). We found that genistein (GE), a member of soy isoflavones, was significantly increased after SG (Figure 2D). In patients with obesity, the plasma levels of GE tended to be negatively related to the NAFLD degree (evaluated by CT values), but there was no significant difference due to the limited samples ($p = 0.0833$) (Figure 2E).

Abundance of genistein is decreased in mice with obesity and could be restored by SG

We further tested this finding in rodent models. We found that in the cecum, liver, and serum, GE is decreased in diet-induced obese (DIO) mice. Moreover, after SG, the GE levels were recovered (Figures 3A–C). However, although there is similar weight loss in the pair-weight control group (Figure 3D), this group did not have significantly increased plasma GE levels compared with the SG group (Figure 3E).

GE could relieve NAFLD in mice with obese and better relief NAFLD after SG

By feeding DIO mice with GE, we found that NAFLD was relieved by decreased infiltration of macrophages and fewer lipid accumulation (shown by HE staining, Figures 4A, B). Interestingly, by adding GE to the diet after SG, the mice had better NAFLD relief compared with those without GE supplement (Figure 4C). Additional GE after surgery also contributed to better liver function in terms of serum AST and TG (Figures 4D, E).

GE could decrease inflammation in the liver in mice with NAFLD

In mice with obesity, there is increased inflammation in the liver and administration of GE could restrict inflammation (Figures 5A–C for mRNA levels and Figures 5D–F for protein levels). Since *in vivo* experiments suggested that GE could restrict inflammation in the liver, we used *in vitro* experiments

10.3389/fendo.2022.1024769

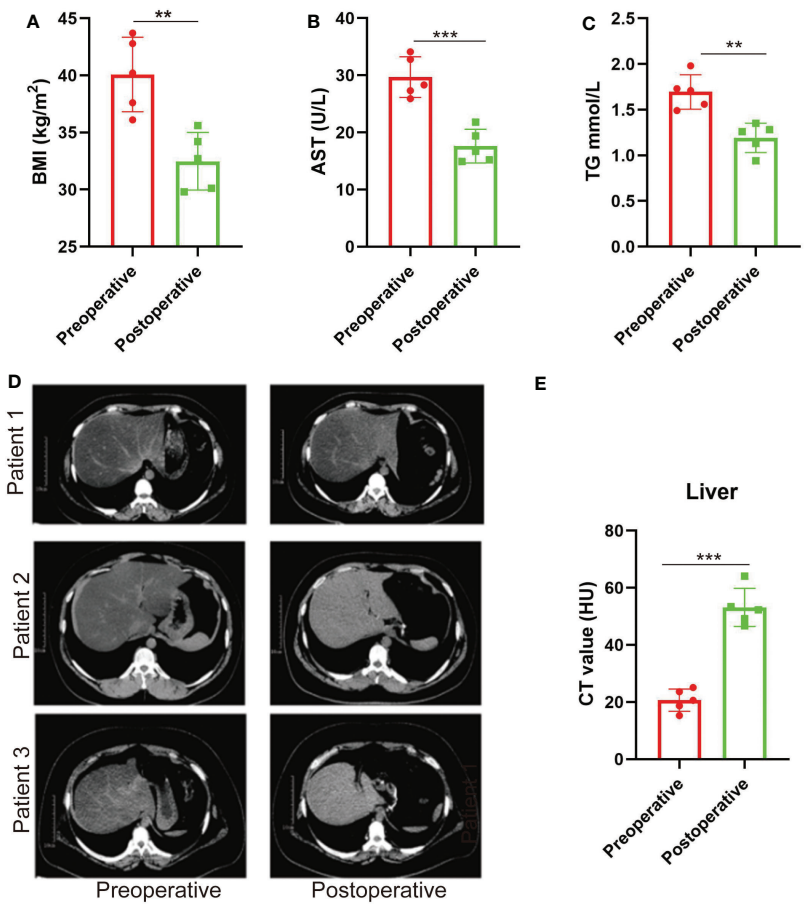

FIGURE 1
NAFLD is relieved after SG in patients with obesity. **(A–C)** BMI values, plasma AST, and TG before and 3 months after SG on patients with obesity. n = 5. **(D)** CT scan images of the liver in patients with obesity before and 3 months after SG surgery (three out of the five patients). **(E)** CT values of the liver before and 3 months after SG surgery on patients with obesity. n = 5. Wilcoxon test was used to compare the data before and after surgery. Data are presented as mean ± SEM, $^{**}p < 0.01$, $^{***}p < 0.001$.

to study the effect of GE stimulation on *in vitro* cultured macrophages. The results suggested that GE could inhibit TNF-α, IL-1β, and MCP-1 secretion (Figures 5G–I). It could also restrict macrophage migration (Figure 5J).

Transplantation of feces from SG mice could induce GE abundance in recipient mice

Since there is coprophage in mice, cohousing experiments were used to change the gut microbiota (22). The mice that underwent SG were cohoused with DIO mice. We found that the cohoused mice had decreased levels of GE (Figures 6A–C). We then used oral gavage to repeat the experiments. We directed 6-week-old normal mice with feces from SG mice, obese mice, and pair-weight control mice. Only feces from the SG mice could increase GE levels in the recipient mice (Figures 6D–F).

Discussion

In this study, we found that in patients with obesity, the degree of NAFLD is negatively related to plasma GE abundance. In rodent models, diet-induced obese (DIO) mice also had decreased levels of genistein in the gut, liver, and serum. Moreover, the GE levels were restored after SG. Both *in vivo* and *in vitro* experiments showed that higher levels of GE could improve NAFLD in mice. Together, our finding suggested that GE has a therapeutic effect on NAFLD.

NAFLD is a progressive disease. The excessive accumulation of lipids constitutes the first stage (2). The more complex stage is NASH, characterized by the presence of hepatic steatosis and

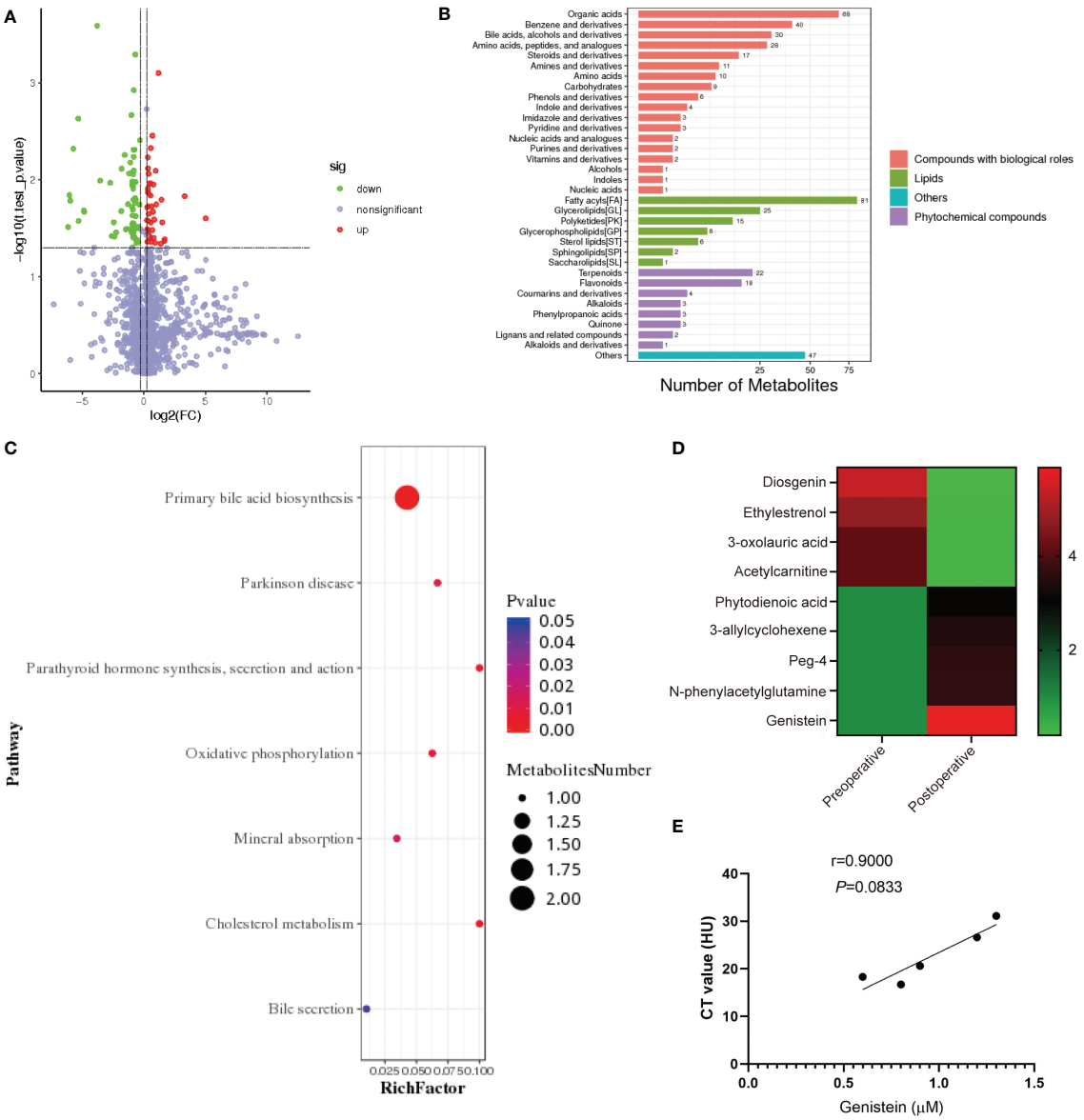

FIGURE 2
Plasma and local levels of genistein are increased after SG in patients with obesity. **(A)** Metabolite volcano map before and after SG in patients with obesity. **(B)** KEGG shows the affection of SG on metabolism in patients with obesity. **(C)** Analysis of the effect of SG on metabolism in patients with obesity. **(D)** Heatmap of relevant differential metabolites before and after SG. **(E)** Correlation analysis of the NAFLD degree and genistein abundance in patients with obesity. Spearman correlation was performed to study the relationship. Data are presented as mean ± SEM, **p < 0.01, ***p< 0.001.

hepatocellular damage. The third stage is cirrhosis, HCC, and liver failure (23). Inflammatory processes are the key factors during the progression (1). A vast network of immune cells is mobilized during NAFLD/NASH, and numerous studies investigated the detailed mechanisms (1, 23). Previous studies reported that gut microbiota could cause inflammation in the liver (24). Interestingly, gavage with the "beneficial microbiota" could protect the mice against inflammation (25). It seems that certain gut microbiota had an anti-inflammation effect. Some studies showed that the gut microbiota could affect the function of intestinal epithelial cells (26). However, this could not explain the changes on the liver since the bacterium did not directly contact with the liver cells. On the other hand, gut microbiota has great potential to produce bioactive compounds such as metabolites (27). Our previous study showed that after SG, the metabolites may enter the liver *via* the intestinal vessels and then induce metabolic processes in the liver (10, 11). Thus, we further investigated the effects of metabolites on liver after SG.

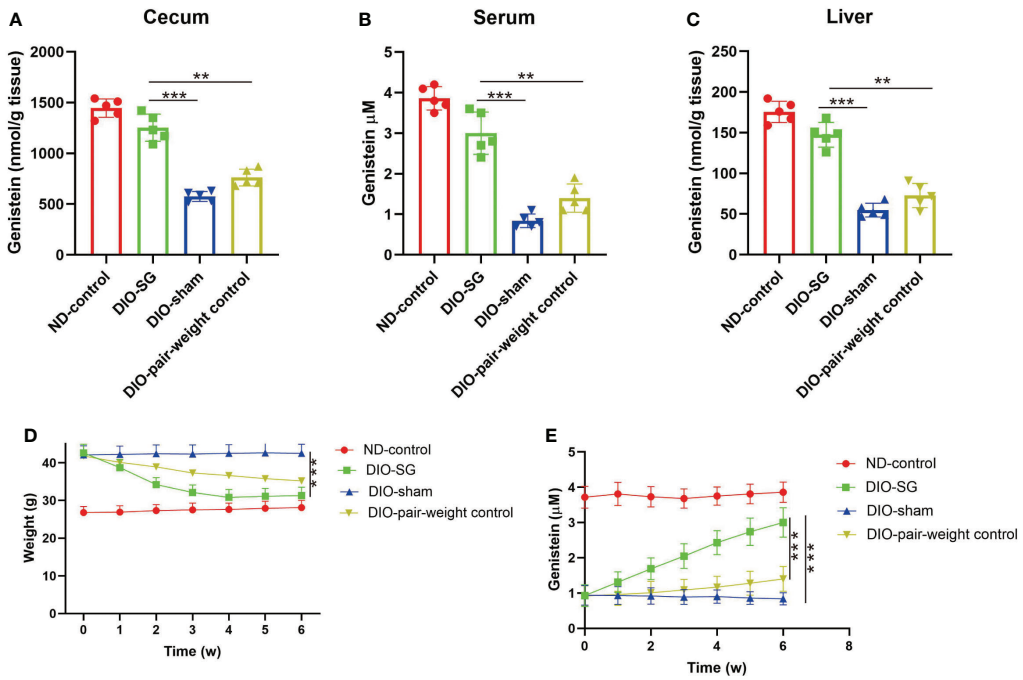

FIGURE 3
Abundance of genistein is decreased in mice with obesity and could be restored by SG. **(A–C)** The concentration of genistein in the cecum, serum, and liver in different groups. n = 5 in each group. **(D)** The changes of body weight in each group. **(E)** The changes of plasma levels of GE in each group. The details of the group were introduced in the "Methods" part. ANOVA test was used to compare the differences among the groups. Data are presented as mean ± SEM, $*p < 0.05$.

We first screened the potential candidates. Blood samples from patients who received SG before and 3 months after SG were collected and analyzed by metabolite sequencing. Numerous metabolites were increased after surgery. Among these metabolites, we noticed a special candidate, genistein (GE). GE is abundant in leguminous plant food such as soybean and chickpeas (28). In the liver, GE is a potent phytoestrogen and could remit NASH through anti-lipid accumulation, antioxidation, and anti-apoptosis properties (29, 30). Thus, we speculated that increased postsurgical levels of GE could relieve NAFLD in patients with obesity.

A previous study showed that GE could protect the incubated human hepatocytes against NAFLD-like medium *via* the ER and GPER pathways (29). However, the role for GE after SG is unknown. To verify the effect of GE on the liver, we fed mice with water containing GE and took the liver for pathological examination. By HE staining, we found that after SG, there are fewer inflammatory cells infiltrated in the liver. This is further confirmed by an immunohistochemical study. There were a decreased number of macrophages (F4/80 +) in the liver after surgery. The tissue-resident phagocytes and the recruited macrophages could secrete cytokines and chemokines and contribute to NASH (31). Among the inflammatory molecules upregulated in NAFLD, monocyte chemoattractant protein-1 (MCP-1) is a special chemokine. It could promote migration of inflammatory cells by chemotaxis and integrin activation (32). It is positively correlated with obesity and NAFLD (33). In our study, we found that there are higher levels of MCP-1 in DIO mice. Supplement of GE could decrease MCP-1 levels. We also cultured macrophages *in vitro* and stimulated the cells with GE. Decreased levels of MCP-1 were also observed. Together, these findings identified that GE could contribute the restriction of cell infiltration.

IL-1β and TNF-α are important pro-inflammatory cytokines. They were markedly increased in NASH patients (34). A previous study suggested that chronic IL-1β and TNF-α exposure may activate specific populations of inflammatory cells in the liver (35). This further leads to NF-kB activation. Continuous NF-kB activation further results in downstream effects such as fibrosis, autophagy, and release of the reactive oxide species (ROS) (36). These are all important factors related to the progress of NAFDL to NASH. In our study, we found that GE could decrease the levels of IL-1β and TNF-α both *in vivo* and *in vitro*. By adding higher concentrations of GE to the cell culture system, there is less BMDM migration. These

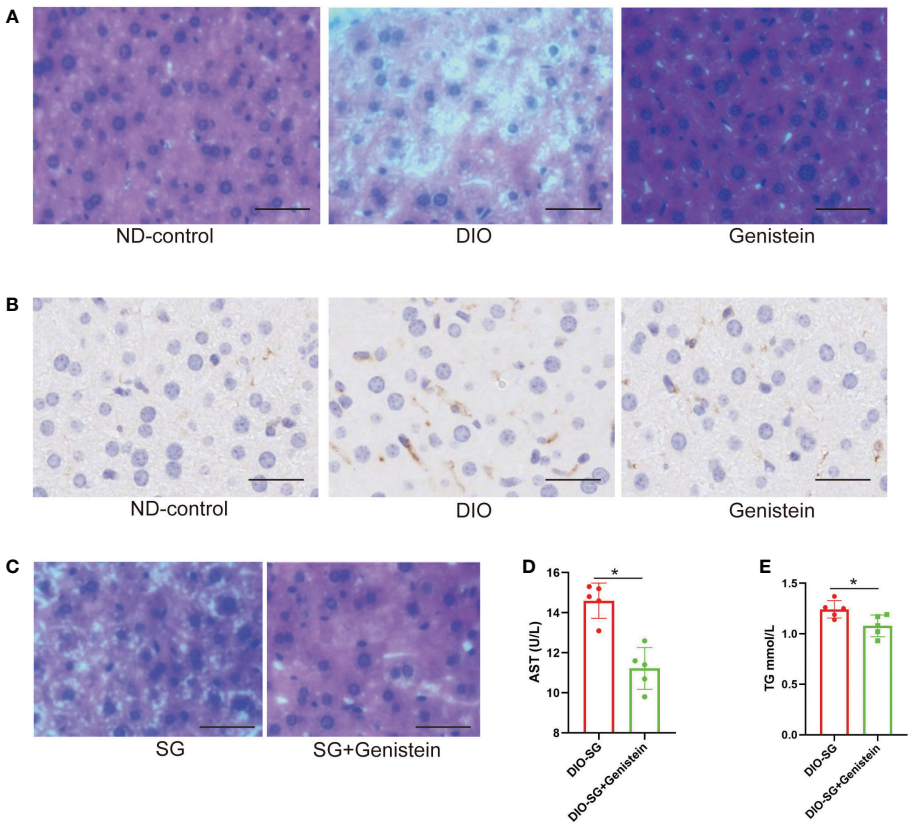

FIGURE 4
Genistein could relieve NAFLD and decrease the inflammation status in the liver. **(A, B)** The infiltration of macrophages (marked by F4/80) and lipid accumulation were detected by immunohistochemistry in the liver tissue of mice from different age-matched groups. ND-control: normal mice fed with a normal diet. DIO: diet-induced obese mice. DIO+GE: DIO mice fed with HFD containing 2% GE for 8 weeks. Scale bar = 50 μm. **(C)**. HE staining of livers from SG and SG+ GE mice. Scale bar = 50 μm **(D, E)**. Serum AST and TG concentrations in SG and SG + GE mice. The DIO mice received and were fed with HFD (the SG group) or HFD+0.2% GE (the SG+GE group) for 8 weeks. n = 5 in each group. Mann–Whitney U test was used to analyze the differences between the two groups. Data are presented as mean ± SEM, $*p < 0.05$. The P value in the image used in Figures 4E is equal to 0.0833, less than 0.05.

experiments suggested that GE may restrict cell migration by inhibiting IL-1β and TNF-α expression levels.

Furthermore, we investigated the mechanism of how SG induced the abundance of GE. Our study showed that in healthy mice there were higher levels of GE and in obese mice they were decreased. Moreover, the GE level was increased after SG in patients and in rodent models. Since we did not offer higher consumption of soybean-related food to patients after surgery, we wondered whether this change was caused by alteration of the gut microbiota. Coprophagy of mice inspired researchers to use cohoused mice to homogenize the gut microbiota (37). Since GE is a metabolite from the gut microbiota, it could be caused by changes of the gut microbiota after surgery. Then, what if mice underwent SG but their gut microbiota remained unchanged? It is very hard to fulfill this. However, by cohousing with obese mice, the SG mice could keep their gut microbiota nearly unchanged after surgery (Supplementary Figure 1A). We found that these mice did not have increased GE levels. This study showed that the gut microbiota is the key for the GE changes after SG.

It has already been fully verified that SG could significantly improve the metabolic state *via* weight-loss-dependent and independent mechanisms (38). On the one hand, rapid weight loss could largely remit the metabolic disorder. On the other hand, there are other reports showing that SG improved glycemia independent of weight loss by restoring hepatic insulin sensitivity and remodeling adipose tissue (39, 40). In our study, we tried to figure out whether the increase of plasma GE is caused by weight loss or surgery. The pair-weight control group was studied. In this group, mice received limited food to keep their weight at the same level to the SG group. Out study suggested that SG but not energy-restriction methods increased plasma GE. This finding suggested that SG increase GE *via* a weight-independent mechanism.

Finally, we tried to study whether additional supply of GE could enhance the NAFLD improvement after SG. Mice in the

10.3389/fendo.2022.1024769

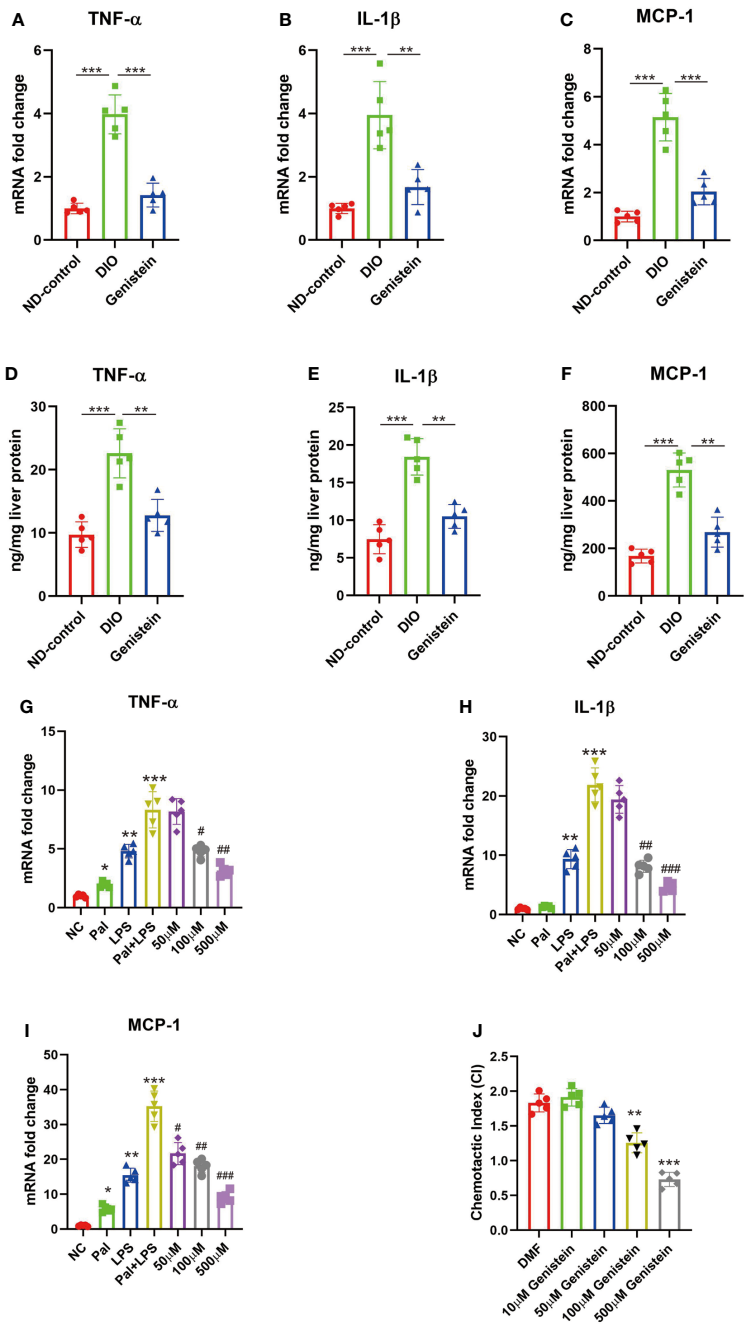

FIGURE 5
Genistein could reduce pro-inflammatory cytokine production and chemotactic migration in macrophages in the liver. **(A–C)** The mRNA levels of TNF-α, IL-1β, and MCP-1 in the liver from different groups, tested by qPCR. **(D–F)** The protein levels of levels of TNF-α, IL-1β, and MCP-1 in the liver from different groups, tested by ELISA. The age-matched female mice received 6 weeks of normal diet (Control), HFD diet (HFD), and GE diet (HFD+0.2%GE). n = 5 in each group. **(G–I)** RAW 264.7 cells were stimulated with palmitic acid (Pal) followed by LPS, with or without addition of varying doses of genistein. The negative control (NC) group was only treated with the vehicle, dimethylformamide (DMF). Changes in the expression of TNF-a, IL-1β, and MCP-1 were determined using qPCR. **(J)** Genistein inhibits BMDM migration toward MCP-1. BMDMs were incubated with MCP-1 in a Transwell with vehicle (DMF) or different doses of genistein. The chemotactic index (CI) for a treatment condition was calculated as the ratio of average number of migrated cells in the treatment group relative to the control group (incubated in medium only). ANOVA test was used to compare the differences among the groups. Data are presented as mean ± SEM, * stands for $p < 0.05$, ** stands for $p < 0.01$ and *** stands for $p < 0.001$, compared with the negative control (NC) group. For G-I, # stands for the GE stimulation group compared with the Pal+LPS stimulation group, #$p < 0.05$, ##$p < 0.01$, ###$p < 0.001$.

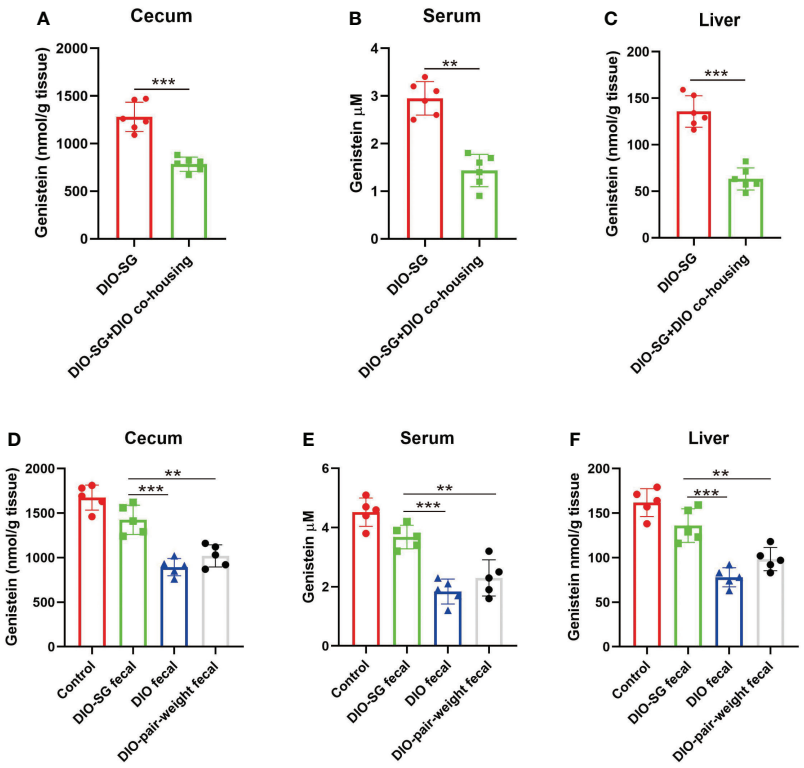

FIGURE 6
Transplantation of feces from SG mice could induce GE abundance in recipient mice. **(A–C)** Genistein concentrations in cecum, serum, and liver in different groups. n = 6. DIO-SG group: DIO mice underwent SG and fed alone in one cage. DIO-SG+DIO cohousing group: DIO mice underwent SG and cohoused with DIO mice (3 + 3 in one cage) for 6 weeks. **(D–F)** Genistein concentrations in cecum, serum, and liver in different groups. n = 5. There are four groups, in each group the normal-diet-fed mice are recipient mice and received oral gavage of feces from SG mice (DIO-SG fecal group), DIO mice (DIO fecal group), and pair-weight mice (DIO-pair-weight fecal group). The control group contains five mice which were fed with a normal diet and did not receive oral gavage. ANOVA test was used to compare the differences among the groups. Mann–Whitney U test was used to analyze the differences between the two groups. Data are presented as mean ± SEM, ** stands for $p < 0.01$, and *** stands for $p < 0.001$.

SG group was fed with water containing GE for 4 weeks, and we found a better remission of NAFLD. This finding showed that dietary supplement after bariatric surgery is very important. There are cases in which patients did not achieve satisfying weight loss and metabolic improvement. In addition to the surgical technique, nutrition management is also very important.

Together, our study identified genistein as a beneficial metabolite induced by SG. Genistein supplementation after SG could better alleviate liver inflammation and relieve NAFLD. Our study stressed the importance of dietary management after surgery. Surgery plus nutrient therapy could be a better treatment for patients with metabolic syndrome.

Data availability statement

The datasets presented in this study can be found in online repositories. The names of the repository/repositories and accession number(s) can be found in the article/Supplementary Material.

Ethics statement

The studies involving human participants were reviewed and approved by Ethics Committee of Wuhan Union Hospital. The patients/participants provided their written informed consent to participate in this study. The animal study was reviewed and approved by Animal Care Committee of Wuhan Union Hospital.

Author contributions

Study design: GW and ZX. Animal experiments and mechanism study: YW and RZ. Clinical sample: JB, GL and YL. Formal analysis: SD and KT. Writing, reviewing, and editing:

YW and GW. Performing surgery and supervising: ZX. Funding acquisition: GW. All authors contributed to the article and approved the submission.

Funding

This study is supported by the National Natural Science Foundation of China (81700488).

Acknowledgments

We are grateful to the surgeons and nurses for their assistance in collecting the clinical samples. We also thank technicians of the animal center for their caring of the animals. We also thank Dr. Yuanjue Wu for help analyzing the data.

Conflict of interest

The authors declare that the research was conducted in the absence of any commercial or financial relationships that could be construed as a potential conflict of interest.

Publisher's note

Supplementary material

The Supplementary Material for this article can be found online at: https://www.frontiersin.org/articles/10.3389/fendo.2022.1024769/full#supplementary-material

SUPPLEMENTARY FIGURE 1
Quality control of the FMT experiments. **(A)** Principal component analysis (PCA) of gut microbiota before and after co-housing experiments. PCoA plots show significant differences in community from different groups in the gut. DIO-SG: The mice which had underwent SG. DIO: The diet induce obese mice. DIO-SG+DIO cohousing: SG mice cohoused with obese mice. n=5 in each group. The mice were female and age matched. **(B)** PCA of gut microbiota before and after oral gavage of feces experiments. PCoA plots show significant differences in community from different groups in the gut. **(C)** Serum GE levels in mice fed with HFD and HFD+GE. n=5.

References

1. Friedman SL, Neuschwander-Tetri BA, Rinella M, Sanyal AJ. Mechanisms of NAFLD development and therapeutic strategies. *Nat Med* (2018) 24(7):908–22. doi: 10.1038/s41591-018-0104-9

2. Younossi Z, Anstee QM, Marietti M, Hardy T, Henry L, Eslam M, et al. Global burden of NAFLD and NASH: Trends, predictions, risk factors and prevention. *Nat Rev Gastroenterol Hepatol* (2018) 15(1):11–20. doi: 10.1038/nrgastro.2017.109

3. Chauhan M, Singh K, Thuluvath PJ. Bariatric surgery in NAFLD. *Dig Dis Sci* (2022) 67(2):408–22. doi: 10.1007/s10620-021-07317-3

4. Lassailly G, Caiazzo R, Buob D, Pigeyre M, Verkindt H, Labreuche J, et al. Bariatric surgery reduces features of nonalcoholic steatohepatitis in morbidly obese patients. *Gastroenterology* (2015) 149(2):379–88; quiz e15-6. doi: 10.1053/j.gastro.2015.04.014

5. Seymour KA, Abdelmalek MF. The role of bariatric surgery in the management of nonalcoholic steatohepatitis. *Curr Opin Gastroenterol* (2021) 37 (3):208–15. doi: 10.1097/MOG.0000000000000721

6. Chavez-Tapia NC, Tellez-Avila FI, Barrientos-Gutierrez T, Mendez-Sanchez N, Lizardi-Cervera J, Uribe M. Bariatric surgery for non-alcoholic steatohepatitis in obese patients. *Cochrane Database Syst Rev* (2010) 1):CD007340. doi: 10.1002/14651858.CD007340.pub2

7. Talavera-Urquijo E, Beisani M, Balibrea JM, Alverdy JC. Is bariatric surgery resolving NAFLD via microbiota-mediated bile acid ratio reversal? A comprehensive review. *Surg Obes Relat Dis* (2020) 16(9):1361–9. doi: 10.1016/j.soard.2020.03.013

8. Hills RDJr., Pontefract BA, Mishcon HR, Black CA, Sutton SC, Theberge CR. Gut microbiome: Profound implications for diet and disease. *Nutrients* (2019) 11 (7):1613–52. doi: 10.3390/nu11071613

9. Hoozemans J, de Brauw M, Nieuwdorp M, Gerdes V. Gut microbiome and metabolites in patients with NAFLD and after bariatric surgery: A comprehensive review. *Metabolites* (2021) 11(6):353–76. doi: 10.3390/metabo11060353

10. Wang G, Wang Q, Bai J, Li G, Tao K, Wang G, et al. RYGB increases postprandial gastric nesfatin-1 and rapid relieves NAFLD via gastric nerve detachment. *PloS One* (2020) 15(12):e0243640. doi: 10.1371/journal.pone.0243640

11. Wang G, Wang Q, Bai J, Zhao N, Wang Y, Zhou R, et al. Upregulation of intestinal NLRP6 inflammasomes after roux-en-Y gastric bypass promotes gut immune homeostasis. *Obes Surg* (2020) 30(1):327–35. doi: 10.1007/s11695-019-04152-4

12. Kato H, Isaji S, Azumi Y, Kishiwada M, Hamada T, Mizuno S, et al. Development of nonalcoholic fatty liver disease (NAFLD) and nonalcoholic steatohepatitis (NASH) after pancreaticoduodenectomy: Proposal of a postoperative NAFLD scoring system. *J hepato-biliary-pancreatic Sci* (2010) 17 (3):296–304. doi: 10.1007/s00534-009-0187-2

13. Ajmera VH, Gunderson EP, VanWagner LB, Lewis CE, Carr JJ, Terrault NA. Gestational diabetes mellitus is strongly associated with non-alcoholic fatty liver disease. *Am J Gastroenterol* (2016) 111(5):658–64. doi: 10.1038/ajg.2016.57

14. Zeb I, Li D, Nasir K, Katz R, Larijani VN, Budoff MJ. Computed tomography scans in the evaluation of fatty liver disease in a population based study: The multi-ethnic study of atherosclerosis. *Acad Radiol* (2012) 19(7):811–8. doi: 10.1016/j.acra.2012.02.022

15. Wu Y, Zhang L, Na R, Xu J, Xiong Z, Zhang N, et al. Plasma genistein and risk of prostate cancer in Chinese population. *Int Urol Nephrol* (2015) 47(6):965–70. doi: 10.1007/s11255-015-0981-5

16. Jeon S, Park YJ, Kwon YH. Genistein alleviates the development of nonalcoholic steatohepatitis in ApoE(-/-) mice fed a high-fat diet. *Mol Nutr Food Res* (2014) 58(4):830–41. doi: 10.1002/mnfr.201300112

17. Ryan KK, Tremaroli V, Clemmensen C, Kovatcheva-Datchary P, Myronovych A, Karns R, et al. FXR is a molecular target for the effects of vertical sleeve gastrectomy. *Nature* (2014) 509(7499):183–8. doi: 10.1038/nature13135

18. Du J, Hu C, Bai J, Peng M, Wang Q, Zhao N, et al. Intestinal glucose absorption was reduced by vertical sleeve gastrectomy via decreased gastric

leptin secretion. *Obes Surg* (2018) 28(12):3851–61. doi: 10.1007/s11695-018-3351-4

19. Bokoliya SC, Dorsett Y, Panier H, Zhou Y. Procedures for fecal microbiota transplantation in murine microbiome studies. *Front Cell Infect Microbiol* (2021) 11:711055. doi: 10.3389/fcimb.2021.711055

20. Zhou D, Pan Q, Shen F, Cao HX, Ding WJ, Chen YW, et al. Total fecal microbiota transplantation alleviates high-fat diet-induced steatohepatitis in mice via beneficial regulation of gut microbiota. *Sci Rep* (2017) 7(1):1529. doi: 10.1038/s41598-017-01751-y

21. Underwood W, Anthony R. AVMA guidelines for the euthanasia of animals: 2020 edition. *Retrieved March* (2020) 2013(30):2020–1.

22. Robertson SJ, Lemire P, Maughan H, Goethel A, Turpin W, Bedrani L, et al. Comparison of Co-housing and littermate methods for microbiota standardization in mouse models. *Cell Rep* (2019) 27(6):1910–1919.e2. doi: 10.1016/j.celrep.2019.04.023

23. Byrne CD, Targher G. *NAFLD: A multisystem disease. J Hepatol* (2015) 62(1 Suppl):S47–64. doi: 10.1016/j.jhep.2014.12.012

24. Aron-Wisnewsky J, Vigliotti C, Witjes J, Le P, Holleboom AG, Verheij J, et al. Gut microbiota and human NAFLD: disentangling microbial signatures from metabolic disorders. *Nat Rev Gastroenterol Hepatol* (2020) 17(5):279–97. doi: 10.1038/s41575-020-0269-9

25. Wang J, Chen WD, Wang YD. The relationship between gut microbiota and inflammatory diseases: The role of macrophages. *Front Microbiol* (2020) 11:1065. doi: 10.3389/fmicb.2020.01065

26. Mathewson ND, Jenq R, Mathew AV, Koenigsknecht M, Hanash A, Toubai T, et al. Gut microbiome-derived metabolites modulate intestinal epithelial cell damage and mitigate graft-versus-host disease. *Nat Immunol* (2016) 17(5):505–13. doi: 10.1038/ni.3400

27. De Vos WM, Tilg H, Van Hul M, Cani PD. Gut microbiome and health: Mechanistic insights. *Gut* (2022) 71(5):1020–32. doi: 10.1136/gutjnl-2021-326789

28. Dixon RA, Ferreira D. Genistein. *Phytochemistry* (2002) 60(3):205–11. doi: 10.1016/S0031-9422(02)00116-4

29. Farruggio S, Cocomazzi G, Marotta P, Romito R, Surico D, Calamita G, et al. Genistein and 17beta-estradiol protect hepatocytes from fatty degeneration by mechanisms involving mitochondria, inflammasome and kinases activation. *Cell Physiol Biochem* (2020) 54(3):401–16. doi: 10.33594/000000227

30. Amanat S, et al. Genistein supplementation improves insulin resistance and inflammatory state in non-alcoholic fatty liver patients: A randomized, controlled trial. *Clin Nutr* (2018) 37(4):1210–5. doi: 10.1016/j.clnu.2017.05.028

31. Kazankov K, Jørgensen SMD, Thomsen KL, Møller HJ, Vilstrup H, George J, et al. The role of macrophages in nonalcoholic fatty liver disease and nonalcoholic steatohepatitis. *Nat Rev Gastroenterol Hepatol* (2019) 16(3):145–59. doi: 10.1038/s41575-018-0082-x

32. Singh S, Anshita D, Ravichandiran V. MCP-1: Function, regulation, and involvement in disease. *Int Immunopharmacol* (2021) 101(Pt B):107598. doi: 10.1016/j.intimp.2021.107598

33. Zhong L, Huang L, Xue Q, Liu C, Xu K, Shen W, et al. Cell-specific elevation of Runx2 promotes hepatic infiltration of macrophages by upregulating MCP-1 in high-fat diet-induced mice NAFLD. *J Cell Biochem* (2019). doi: 10.1002/jcb.28456

34. Hirsova P, Ibrahim SH, Krishnan A, Verma VK, Bronk SF, Werneburg NW, et al. Lipid-induced signaling causes release of inflammatory extracellular vesicles from hepatocytes. *Gastroenterology* (2016) 150(4):956–67. doi: 10.1053/j.gastro.2015.12.037

35. Park HS, Song JW, Park JH, Lim BK, Moon OS, Son HY, et al. TXNIP/VDUP1 attenuates steatohepatitis via autophagy and fatty acid oxidation. *Autophagy* (2021) 17(9):2549–64. doi: 10.1080/15548627.2020.1834711

36. Wang Q, Ou Y, Hu G, Wen C, Yue S, Chen C, et al. Naringenin attenuates non-alcoholic fatty liver disease by down-regulating the NLRP3/NF-OєB pathway in mice. *Br J Pharmacol* (2020) 177(8):1806–21. doi: 10.1111/bph.14938

37. Turner PV. The role of the gut microbiota on animal model reproducibility. *Anim Model Exp Med* (2018) 1(2):109–15. doi: 10.1002/ame2.12022

38. Hutch CR, Trakimas DR, Roelofs K, Pressler J, Sorrell J, Cota D, et al. Oea signaling pathways and the metabolic benefits of vertical sleeve gastrectomy. *Ann Surg* (2020) 271(3):509–18. doi: 10.1097/SLA.0000000000003093

39. Abu-Gazala S, Horwitz E, Ben-Haroush Schyr R, Bardugo A, Israeli H, Hija A, et al. Sleeve gastrectomy improves glycemia independent of weight loss by restoring hepatic insulin sensitivity. *Diabetes* (2018) 67(6):1079–85. doi: 10.2337/db17-1028

40. Harris DA, Mina A, Cabarkapa D, Heshmati K, Subramaniam R, Banks AS, et al. Sleeve gastrectomy enhances glucose utilization and remodels adipose tissue independent of weight loss. *Am J Physiol Endocrinol Metab* (2020) 318(5):E678–88. doi: 10.1152/ajpendo.00441.2019

frontiers | Frontiers in Endocrinology

TYPE Original Research
PUBLISHED 24 January 2023
DOI 10.3389/fendo.2022.1036243

OPEN ACCESS

EDITED BY
Katherine Samaras,
St Vincent's Hospital Sydney, Australia

REVIEWED BY
Taryel Omarov,
Azerbaijan Medical University, Azerbaijan
Halit Eren Taskin,
Istanbul University Cerrahpasa, Türkiye
Chun Hai Tan,
Surgicare Bariatric and General Surgery Clinic, Singapore

*CORRESPONDENCE
Wah Yang
yangwah@qq.com
Cunchuan Wang
twcc@jnu.edu.cn

†These authors have contributed equally to this work and share first authorship

SPECIALTY SECTION
This article was submitted to Obesity, a section of the journal Frontiers in Endocrinology

RECEIVED 04 September 2022
ACCEPTED 28 December 2022
PUBLISHED 24 January 2023

CITATION
Chen G, Sun L, Jiang S, Chen X, Zhu J, Zhao X, Yu S, Dong Z, Chen Y, Zhang W, Yang W and Wang C (2023) Effects of bariatric surgery on testosterone level and sexual function in men with obesity: A retrospective study.
Front. Endocrinol. 13:1036243.
doi: 10.3389/fendo.2022.1036243

Effects of bariatric surgery on testosterone level and sexual function in men with obesity: A retrospective study

Guoji Chen[1,2,3,4†], Luping Sun[5†], Shuwen Jiang[1,2,3], Xiaomei Chen[1,2], Jie Zhu[1,2,3], Xin Zhao[1,2,3], Shuqing Yu[1,2], Zhiyong Dong[1,2,3], Yuan Chen[1,2,3], Wen Zhang[6], Wah Yang[1,2,3*] and Cunchuan Wang[1,2,3*]

[1]Department of Metabolic and Bariatric Surgery, The First Affiliated Hospital of Jinan University, Guangzhou, China, [2]Jinan University Institute of Obesity and Metabolic Disorders, Guangzhou, China, [3]Joint Institute of Metabolic Medicine between State Key Laboratory of Pharmaceutical Biotechnology, The University of Hong Kong and Jinan University, Guangzhou, China, [4]Department of Gastrointestinal Surgery, The First People's Hospital of Zhaoqing, Zhaoqing, China, [5]Department of urinary Surgery, First Affiliated Hospital of Jinan University, Guangzhou, China, [6]School of Nursing, Jinan University, Guangzhou, Guangdong, China

Introduction: Bariatric surgeries induce well-documented weight loss and resolve obesity comorbidities. Sexual function is one of the aspects of life quality and may benefit from surgery. Few studies have revealed the impact of bariatric surgeries on sexual function in Chinese men with obesity.

Methods: This is a retrospective cohort study of patients undergoing bariatric surgery [laparoscopic sleeve gastrectomy (LSG) or laparoscopic Roux-en-Y gastric bypass (LRYGB)]. Data were collected between September 2017 and February 2022. The International Index of Erectile Function (IIEF) questionnaire was used to evaluate erectile function, intercourse satisfaction, orgasmic function, sexual desire, and overall satisfaction. Sex hormones and other blood tests were evaluated before and at least 1 year after the surgery.

Results: Fifty-nine Chinese male patients completed the IIEF questionnaire. The multivariate logistic regression analysis revealed that body mass index (BMI) was the single independent risk factor of the severity of erectile dysfunction (ED). Preoperative testosterone levels had negative correlations with BMI and waist circumference. Thirty-seven patients completed the postoperative questionnaire with a mean follow-up of 23.2 months.

Conclusion: BMI and waist circumference were negatively correlated with testosterone levels. BMI was an independent risk factor for the severity of ED. LSG and LRYGB led to positive and sustained improvement in sexual function of men with obesity. The two procedures had a comparable effect, more subjects being needed. Sex hormone levels also could be reversible. However, more weight

loss did not predict a positive change in sexual function. A greater BMI loss might predict a greater increase in testosterone.

KEYWORDS

sleeve gastrectomy (SG), gastric bypass, bariatric surgery, sexual function (male), obesity

1 Introduction

The available data show a notably increasing trend in the prevalence of obesity in urban and rural China, where the estimated number rose from 37 million in 2004 to 85 million in 2018 (1). The population with obesity will likely keep increasing as Chinese economic society progresses. Both observational and high-quality randomized trials have shown that bariatric surgeries result in sustained weight loss and remission and improvement in type 2 diabetes mellitus (T2DM) and other obesity-related comorbidities, reducing the risks of microvascular and macrovascular complications (2–4). In an observational study, men with obesity were more likely to report erectile dysfunction (ED), reflecting hypogonadotropic hypogonadism (HH) (5). A multicenter cohort study has reported that nearly 74% of men with obesity were dissatisfied with their sex life (6). Sexual function is a private and sensitive topic not frequently discussed, correlating with patients' well-being postoperatively. In addition to established outcome reporting standards for weight loss and comorbidities, there are validated instruments or questionnaires evaluating quality-of-life outcomes, including sex life, after bariatric surgeries (7). However, these standard instruments or questionnaires are not specifically focused on sexual function.

Recent studies demonstrated considerable improvement in sexual function after bariatric surgeries (8, 9). Considering cultural preferences, many people are reluctant to answer questions about sexual function in eastern countries (10). The impacts of bariatric surgery on sexual function in Chinese men with obesity were seldom studied. We conducted this retrospective study to explain the influence of obesity on sexual function and sex hormones, as well as the change in these perspectives after bariatric surgery.

2 Materials and methods

2.1 Ethics

Data of the study were extracted from the Chinese Obesity and Metabolic Surgery Database (COMES Database), which is endorsed by the Chinese Society for Metabolic and Bariatric Surgery (CSMBS). It is managed by the Chinese Obesity and Metabolic Surgery Collaborative (COMES Collaborative), which consists of bariatric surgeons, bariatric nurses, researchers, and healthcare professionals from 138 hospitals in China that increased gradually in the past 3 years. The study was approved by the Institutional Ethics Committee (KY-2022-131).

2.2 Study design

This is a retrospective cohort study. The cohort of patients at a single medical institution underwent laparoscopic sleeve gastrectomy (LSG) or laparoscopic Roux-en-Y gastric bypass (LRYGB) between September 2017 and February 2022. Follow-up time was defined as the time between the operation and the date of the last completion of the validated questionnaire for sexual function [International Index of Erectile Function (IIEF)]. All operations were performed by the same surgical team in our hospital. Standardized laparoscopic procedures were performed for all patients, which were described previously (11). Before the operation and on the follow-up day, patients were invited to finish the IIEF questionnaire on paper or online. Patients willing to participate in the study and completed the preoperative questionnaire were recruited for a follow-up visit at least 1 year postoperatively, including blood tests, anthropometric measurements, and re-collecting of their IIEF questionnaires. If a patient did not return to the hospital for our study, his most recent follow-up results were used for analysis and his blood test results from another hospital would be recorded in the COMES Database. The indication of surgeries and techniques were described previously (12, 13).

Inclusion criteria were as follows: men with obesity with ages ranging from 18 to 60 years; of Chinese nationality; patients who had regular sex lives. Patients finishing follow-up at least 1 year will be enrolled in the postoperative analysis. Exclusion criteria were as follows: patients with a history of psychiatric disease (severe depression and bipolar disorder), pituitary gland disease or hyperthyroidism, a habit of taking phosphodiesterase (PDE) inhibitors, e.g., sildenafil, and occurrence of mortality or major complications within 30 days after the operation (7). Once the patient chose "did not attempt intercourse" in the IIEF questionnaire, he would be excluded from the study. The study flowchart is shown in Figure 1.

Our primary outcomes were subjective feelings measured by the IIEF questionnaire and objective sex hormone test. Secondary outcomes were the weight loss effect and change in other blood test results.

Patients were asked to choose the answer to every item of the IIEF questionnaire at their direct feelings. Before bariatric surgeries, we did not give vitamin or microelement supplementation to the patients. After the operation, our team offered a multidisciplinary medically supervised weight loss program *via* Internet or telephone, which were composed of diet and behavioral and exercise advice, and pharmacotherapy advice would be available when necessary. Calcium tablet and multivitamin supplementations were

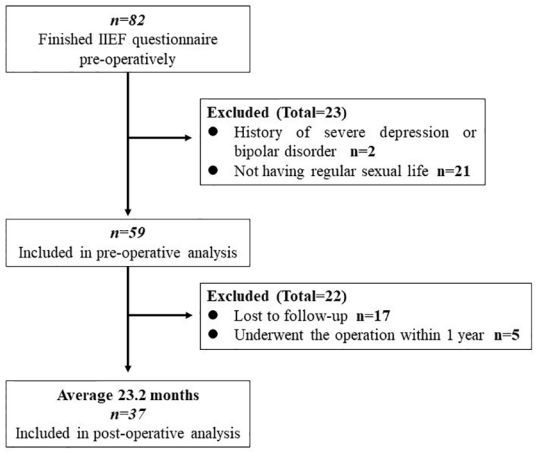

FIGURE 1
Study flow.

recommended to the patients, which were described previously (14). All patients enrolled in the study were informed of the right to exit the study at any time. All of the data were stored and available in a prospective managed database (the COMES Database).

2.3 Anthropometric measurements and blood tests

Anthropometric measurements were collected before and after the operation as follows: neck circumference, breast circumference, waist circumference, hip circumference, weight, height, and body mass index (BMI). Blood tests were always collected at fasting state, including glycosylated hemoglobin (HbA_{1c}), fasting plasma glucose (FPG), hemoglobin, C-reactive protein (CRP), vitamins, zinc (Zn), copper (Cu), iron (Fe), ferritin, hydroxyvitamin D [1, 25-(OH2) D3], total testosterone (TT), estradiol (E2), follicle-stimulating hormone (FSH), luteinizing hormone (LH), progesterone (PRO), prolactin (PRL), total cholesterol (TC), triglyceride (TG), high-density lipoprotein cholesterol (HDL-c), and low-density lipoprotein cholesterol (LDL-c), which were tested before surgery and at least 1 year after the operation. The percentage of excess weight loss (% EWL), percentage of total weight loss (%TWL), and percentage of excess BMI loss (%EBMIL) were calculated according to the standardized outcome reporting system (7).

2.4 Measures of sexual function

The IIEF is a widely used questionnaire with high sensitivity and specificity assessing men's sexual function or erectile function (EF) concerned with medical treatment (15). Based on the syndrome of male sexual dysfunction, the IIEF questionnaire has been attested for its high quality and credibility in evaluating the efficacy of sexual ED therapies including sildenafil and other oral treatments (16–18). The usage of IIEF can be extended to diagnosing and assessing effectiveness in clinical monitoring (18, 19). As a result, total scores of IIEF and domain of EF scores are important. The 15-item questionnaire is composed of five domains: EF (items 1–5 and 15), intercourse satisfaction (IS; items 6–8), orgasmic function (OF; items 9 and 10), sexual desire (SD; items 11 and 12), and overall satisfaction (OS; items 13 and 14). The overall score of IIEF is 5–75, including 0–30 scores of EF, 0–15 scores of IS, 0–10 scores of OF, 2–10 scores of SD, and 2–10 scores of OS, respectively. Abnormal EF, also known as ED, is defined as scores of EF ≤25 (20). According to Sexual Health Inventory for Men (SHIM), scores of EF ranging from 22 to 25 are classified as mild ED, 17–21 as mild to moderate ED, 11–16 as moderate ED, ≤10 as severe ED (21).

2.5 Statistical analysis

Paired t-test was used to compare the preoperative and postoperative outcomes. We hypothesized that male patients' IIEF scores improved by 10 beyond 1 year after the operation; the ratio of loss to follow-up was 30%, and the standard deviation was 10; 23 patients were needed to ensure a power of 95.0%, with a 2-sided alpha error of 0.05.

The normal distribution was attested *via* the Shapiro–Wilk normality test ($P > 0.05$). Two-sided P values <0.05 were considered statistically significant. Mean ± standard deviation was used for the description of continuous data, while median and percentile (25th and 75th) were used for non-normal distribution data. In order to identify potential risk factors correlated with scores of IIEF and EF domain, bivariate regression was applied. Univariate analysis was used for the recognition of potential predictors. Multivariate analysis including multiple linear regression or logistic regression was then used for further analysis. Paired t-test and two independent-samples t-tests were used if our data were distributed normally, and a nonparametric test was applied if the data were not normal. Chi-square test was used for categorical variables, and Fisher's exact test would be applied for analysis when needed. The calculation of sample size was analyzed by PASS version 15.0 (NCSS Statistical Software, USA). Data were analyzed by Statistical Package for Social Sciences (SPSS), version 24.0 (SPSS Inc., USA). Heatmaps were constructed *via* GraphPad Prism version 8 (GraphPad Software, USA).

3 Results

3.1 Demographic data

Fifty-nine male patients with obesity were enrolled in our study, with a mean BMI of 40.37 ± 7.57 kg/m^2 (ranging from 28.09 to 59.99 kg/m^2) and mean age of 32.1 ± 6.7 years (ranging from 22 to 51 years). Seventeen of these patients were lost to follow-up visits. Five of them had undergone bariatric surgery in less than 1 year, not meeting our follow-up criteria. Consequently, 37 patients were involved in the postoperative analysis. No severe complication or mortality occurred in the first 30 days postoperatively.

In the studied patients, 50 (84.7%, 50/59) of them had scores that conformed to the ED definition. Thirty-one patients completed the IIEF questionnaire at least 1 year after the operation. Twenty-eight patients underwent LSG, while the other 31 patients underwent LRYGB. The mean follow-up was 23.2 months, ranging from 12 to 45 months. Demographic data were shown in Table 1.

10.3389/fendo.2022.1036243

TABLE 1 Demographic data of patients (n = 59).

	Mean ± SD	Min	Max
BMI (kg/m^2)	40.31 ± 7.57	28.09	59.99
Age (years)	32.1 ± 6.7	22.0	51.0
Height (cm)	173.98 ± 6.53	159.30	188.00
Weight (kg)	122.12 ± 24.04	80.00	183.20
Neck circumference (cm)	45.9 ±4.4	32.0	56.0
Chest circumference (cm)	126.3 ± 11.3	99.5	154.0
Waist circumference (cm)	123.7 ± 11.2	83.5	170.0
Hip circumference (cm)	127.5 ± 15.4	93.5	162.0
Marital status (n, %)		**Type of surgery (n, %)**	
Married	36, 61.0%	LSG	28, 47.5%
Unmarried/divorced/widower	23, 39.0%	LRYGB	31, 52.5%
Educational level (n, %)		**Severity of ED score (n, %)**	
master's degree or above	2, 3.6%	non-ED	9, 15.3%
bachelor's degree	32, 54.2%	mild	24, 40.7%
college or below	25, 42.4%	mild to moderate	17, 28.8%
Smoking (n, %)	32, 54.2%	moderate	9, 15.3%
Drinking (n, %)	21, 35.6%	severe	0
Comorbidities (n, %)			
T2DM	25, 42.4%		
Hypertension	13, 22.0%		
Dyslipidemia	38, 64.4%		
OSA	25, 42.3%		

BMI, body mass index; T2DM, type 2 diabetes mellitus; OSA, obstructive sleep apnea; LSG, laparoscopic sleeve gastrectomy; LRYGB, laparoscopic Roux-en-Y gastric bypass; ED, erectile dysfunction.

3.2 Logistic regression analysis of preoperative International Index of Erectile Function (IIEF) and erectile function (EF) scores

Pearson's correlation was used to identify potential predictors between preoperative IIEF scores and clinical and anthropometric variables. Only vitamin E was a positive factor related to preoperative IIEF scores (r = 0.283, P = 0.035).

Univariate analysis showed that BMI, level of serum Zn, C-peptide, and HOMA-IR were predictive factors of preoperative ED grade. No significant difference was found in some important parameters, such as T2DM, hypertension, smoking, drinking, educational level, and marital status. The multivariate logistic regression analysis revealed that BMI was the single independent risk factor (OR = 1.14, 95% CI 1.05–1.23, P < 0.001). We adjusted for testosterone level, and BMI was still the independent risk factor. Details are presented in Table 2 and Figure 2.

3.3 Multiple linear regression for the preoperative level of testosterone

Pearson's correlation showed that the preoperative testosterone level had significant relations with BMI, weight, neck circumference, breast circumference, waist circumference, hip circumference, vitamin A, vitamin E, albumin, HDL-c, and HOMA-IR. Blood test results of testosterone reflected the TT in the body. Considering that part of testosterone is combined with albumin and sex hormone-binding globulin (SHBG) in the blood and TT can be calculated from these parameters (22), non-negligible variance inflation factors (VIFs) existed between TT and albumin. Meanwhile, non-negligible VIFs also existed between BMI and weight and neck/chest/waist/hip circumference; hence, we constructed two multiple linear regression models. Preoperative testosterone levels had negative correlations with BMI (β = -0.047, P = 0.004) and waist circumference (β = -0.020, P = 0.005). Details are shown in Table 3.

10.3389/fendo.2022.1036243

TABLE 2 Univariate and multivariate analyses of risk factors related to preoperative ED grade.

Univariate analysis			Multivariable logistic regression analysis			
			Model 1		Model 2	
Variable	F/ ^{2}	P value	OR (95%CI)	P value	Adjusted OR	P value
T2DM	2.645	0.477*				
Hypertension	5.375	0.131*				
Marital status	1.908	0.604*				
Education level	9.649	0.078*				
BMI	4.277	0.017	1.14 (1.05, 1.23)	0.001	1.18 (1.08, 1.30)	<0.001
HbA1c	0.504	0.681				
Basal insulin	2.098	0.111				
Testosterone	1.320	0.295			1.77 (0.97, 3.25)	0.064
FSH	0.248	0.862				
LH	0.283	0.838				
Progesterone	0.550	0.651				
Prolactin	0.883	0.457				
Estradiol	1.383	0.259				
Zn	6.687	0.002	0.93 (0.80, 1.04)	0.373	0.92 (0.79, 1.08)	0.321
C-peptide	4.845	0.008	0.89 (0.55, 1.42)	0.612	0.99 (0.85, 1.16)	0.145
HOMA-IR	4.387	0.013	1.04 (0.86, 1.26)	0.660	0.99 (0.81, 1.21)	0.922

T2DM, type 2 diabetes mellitus; BMI, body mass index; HbA1c, glycosylated hemoglobin; Zn, zinc; HOMA-IR, homeostasis model assessment of insulin resistance
Only significant or other important parameters are shown in the table. *Fisher's exact test.
Model 2 was adjusted for testosterone level.
Test proportional odds assumption: ^{2} = 8.499, P = 0.386 (Model 1), ^{2} =9.840, P = 0.454 (Model 2).
Both the logistic regression models could get past the proportional odds assumption test (P > 0.05).
LH, luteinizing hormone; FSH, follicle-stimulating hormone.

3.4 Changes in IIEF scores and levels of sex hormones

Preoperation vs. postoperation

Eleven patients (29.7%, 11/37) had EF scores less than 25 at the last follow-up, but only two patients had slightly decreased scores of IIEF and EF domain, while the others showed increased scores. Overall, there were significant improvements in scores of IIEF (preoperation 52.22 ± 10.79 vs. postoperation 61.46 ± 7.93, P < 0.001) and its domains in the patients, meaning that they were more satisfied with their EF and sex life postoperatively. Changes in IIEF scores were shown *via* heatmaps (Figures 3, 4). In the postoperative sex hormonal profile measurement, patients' testosterone levels also significantly rose from 2.87 ± 1.00 ng/ml to 5.45 ± 0.84 ng/ml (P < 0.001). Serum FSH and LH increased significantly. The decrease in prolactin and estradiol reached statistical significance. Data from the questionnaire were presented in Table 4. With excellent weight loss, HbA1c, FPG, basal insulin, HOMA-IR, and triglyceride significantly decreased. Ferritin significantly decreased, but none reached the standard of deficiency. Several patients who lacked vitamin B2 and B12 were advised regular supplements. In Table 5, alterations of sex hormones and other important clinical and anthropometric parameters are shown in detail.

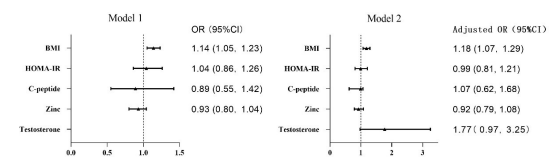

FIGURE 2
Forest plots of logistic regression analysis of preoperative IIEF and EF scores. BMI was the independent risk factor. BMI, body mass index; HOMA-IR, homeostasis model assessment of insulin resistance.

3.5 LSG vs. LRYGB

We tried to compare the effect of LSG and LRYGB on sexual function. There was no significant difference in baseline and weight loss between the LSG and LRYGB groups. A significant difference in IIEF and its domains was not found in the two independent-sample t-tests. A difference in the levels of testosterone was not found either. LSG and LRYGB exerted similar and positive effects on sexual function. Details are shown in Table 6.

Finally, we aimed to determine predictive factors of sexual function improvement and testosterone improvement (ΔIIEF, ΔEF, and

TABLE 3 Correlation between preoperative testosterone level and anthropometric and clinical variables (n = 59).

Variable	Testosterone level		Multiple linear regression			
			Model 1		Model 2	
	r	P*	β	P	β	P
BMI	-0.451	< 0.001	-0.047	0.004		
Weight	-0.470	< 0.001				
Neck circumference	-0.457	0.001				
Chest circumference	-0.482	< 0.001				
Waist circumference	-0.548	< 0.001			-0.020	0.005
Hip circumference	-0.437	0.001			-0.093	0.684
Vitamin A	0.350	0.008	0.210	0.151	0.228	0.110
Vitamin E	0.282	0.033	0.144	0.322	0.142	0.336
Albumin	0.305	0.026				
HDL-c	0.315	0.015	0.143	0.277	0.137	0.299
Basal insulin	-0.232	0.076	0.083	0.613	-0.144	0.304
Constant			4.701		5.311	

P*, Pearson's correlation; r: correlation coefficient.
HDL-c, high-density lipoprotein cholesterol.

Δtestosterone). Potential relationships were explored between postoperative scores of IIEF or postoperative level of testosterone and all parameters above, including ΔBMI, %EWL, %TWL, and %EBMIL. Still, none of the calculations reached statistical significance. However, there was a tendency that with greater BMI loss, testosterone level increased more (r = -0.307, P = 0.065). Univariate analysis is shown in Table 7.

4 Discussion

The main results of our study demonstrated the worsening and dominating impacts of obesity on sexual dysfunction, emphasizing the impressive postsurgical effects on sexual function in the studied group of the Chinese population. Sexual function was evaluated by IIEF scores, and a comparison of the two main surgical procedures (LSG and LRYGB) was presented. In the background of the conservative and traditional culture in China, it is rare and even a taboo to discuss sex life. Many patients did not have regular sex lives and were not willing to participate in our study. These reasons limited our sample size. Since most other related studies recruited a similar sample size and reported the outcome of a half year or 1 year postoperatively, our study showed that bariatric surgeries had sustained and favorable impacts on sexual function, testosterone level, and comorbidities with a longer follow-up.

4.1 Correlations of sexual dysfunction

Arolfo et al. (23) found a negative Spearman's correlation between preoperative serum Zn and quality-of-life scores. Microelements in men with obesity may have relationships with sexual function. Interestingly, our univariate analysis of ED grade also displayed statistical significance between Zn and ED grade. Apart from Zn, we found that vitamin E had a positive correlation with preoperative IIEF scores. Vitamin A and vitamin

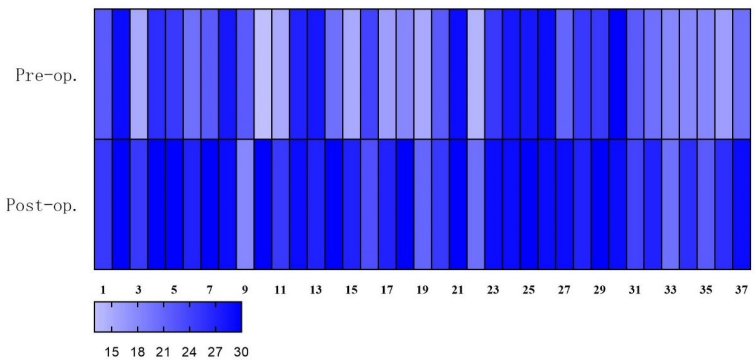

FIGURE 3
Heatmap: total scores of sexual function (IIEF scores) improved significantly postoperatively. Deeper color means higher scores.

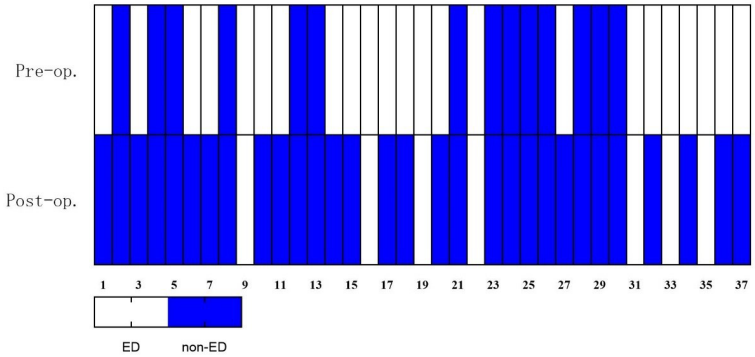

FIGURE 4
Heatmap: changes in EF domain based on erectile dysfunction classification. ED is diagnosed if EF scores ≤25. Patients with ED decreased from 27 (73.0%) to 11 (29.7%). EF, erectile function; ED, erectile dysfunction.

E had positive relations with the preoperative level of testosterone. Obesity results in oxidative stress, while vitamins A and E are antioxidants in the body, and antioxidant treatment, including vitamins in men, can increase serum sex hormone levels (24). Zn participated in the synthesis of testosterone. But which microelement can best reflect sexual function is unclear. Multifactorial mechanisms may be involved.

Sarhan et al. (8) found that weight was the factor predicting scores of preoperative IIEF, and both age and BMI predicted preoperative testosterone levels. It had been estimated that one-third of men with obesity, T2DM, or metabolic syndrome have subnormal free testosterone concentrations and HH (25, 26). But in our study, only vitamin A level correlated significantly with preoperative IIEF scores. Higher BMI and higher waist circumference were correlated with a lower testosterone level. Mechanisms may include that excess body fat plays a fundamental role in inflammation status, leading to a decreased level of gonadotropin and testosterone (25, 27).

Few other studies tried to find out the relationships between ED grade and parameters. Analyses of our data were focused on ED grade, showing that BMI was the independent risk factor and that a higher BMI led to more apparent syndromes of ED. Secondary T2DM and hypertension may not contribute very adversely on erectile or sexual function. But with younger age than most samples of articles focused on bariatrics and sexual function, short durations of comorbidities (many of these comorbidities were diagnosed for the first time before the operation) might not take the lead.

4.2 Impact of bariatrics on sexual function

With the mean %EWL over 80% after bariatric surgeries, IIEF scores and its five domains significantly increased. Total scores of IIEF rose to 61.46 ± 7.93, which were similar to those of the normal control group of Rosen et al. (15) in their establishing procedure of IIEF and to other articles concentrated on sexual function influenced by bariatrics (28). Our result is similar to those of prior articles that all domains increased (8, 23), while some articles did not show a significant increase in every domain (29, 30). Although there were still 11 patients with EF domain scores ≤25, nine of them improved compared with preoperative scores. A study reported significant improvements in EF measured by the simplified version of IIEF (IIEF-5) in 39 men with obesity and ED 1 year following RYGB (31). IIEF-5 is a questionnaire assessing EF, and IIEF can evaluate sexual function from multidimensional scales. At the same time, there was an increasing marginal significance in testosterone level (P = 0.052) (31). Taskin et al. (32) revealed that patients with T2DM (mean age = 51.5 ± 9.3 years, mean BMI = 34.9 ± 3.8 kg/m^2) experienced a mean increase of testosterone level of 1.4 ± 1.2 ng/ml 6 months after sleeve gastrectomy with transit bipartition (SG-TB). Our results showed significant and sustained improvements in sex hormones, reversing the HH trend. Testosterone level rose from 2.87 ± 1.00 ng/ml to 5.45 ± 0.84 ng/ml. The advances in sexual function were accompanied by favorable changes in metabolic conditions. Recent studies applying the IIEF questionnaire revealed that bariatric surgeries positively impacted

TABLE 4 Changes of IIEF score and its five domains.

	Preoperation (n=59)		Postoperation (n=37)		P value*
	Mean ± SD	Median (IQR)	Mean ± SD	Median (IQR)	
IIEF	52.22 ± 10.79	50 (43.5, 62)	61.46 ± 7.93	61 (56, 67.5)	<0.001
Erectile function	21.84 ± 5.08	22 (18, 26.5)	26.86 ± 3.35	27 (25, 30)	<0.001
Orgasmic function	7.76 ± 1.85	8 (6.5, 9.5)	9.00 ± 1.27	9 (8.5, 10)	<0.001
Sexual desire	6.51 ± 1.90	7 (5, 8)	7.43 ± 1.41	7 (6.5, 8)	0.008
Intercourse satisfaction	9.03 ± 2.80	9 (6, 11)	10.51 ± 2.52	11 (8, 12.5)	0.001
Overall satisfaction	6.92 ± 1.98	7 (6, 8)	7.68 ± 1.81	8 (6.5, 8.5)	0.034

IIEF, International Index of Erectile Function.
P value*: paired t-test.

10.3389/fendo.2022.1036243

TABLE 5 Changes in anthropometric and clinical variables before and after bariatric surgery.

Variable	Preoperation (n=59)			Postoperation (n=37)			P value*
	Mean	SD	Range	Mean	SD	Range	
Anthropometric measurements							
BMI (kg/m^2)	41.31	7.57	28.09-59.99	27.78	4.24	19.79-36.11	<0.001
Weight (kg)	122.12	24.04	80.00-183.20	84.33	15.48	58.00-120.00	<0.001
%EWL				85.0	37.6	8.6-199.7	
%TWL				30.3	14.1	1.6-59.6	
%EBMIL				88.0	36.3	23.7-198.7	
Waist circumference (cm)	123.7	18.2	83.5-170.0	101.9	15.3	75.5-130.0	<0.001
Hip circumference (cm)	127.5	15.4	93.5-162.0	106.6	11.9	92.5-135.5	<0.001
Sex hormones							
Testosterone (ng/ml)	2.87	1.00	1.22-5.93	5.45	0.84	3.97-7.2	<0.001
Estradiol (pg/ml)	42.62	27.22	10.50-155.48	32.58	11.90	12.00-55.35	0.036
Prolactin (ng/ml)	11.59	5.95	4.51-40.95	8.33	4.45	0.20-21.41	<0.001
Progesterone (ng/ml)	0.49	0.51	0.05-3.58	4.45	8.34	0.20-4.28	0.310
LH (mIU/ml)	4.54	2.08	1.64-12.11	5.66	1.36	2.89-8.67	0.005
FSH (mIU/ml)	5.21	2.82	1.29-13.58	6.73	2.97	2.25-16.73	<0.001
Blood glucose metabolism, hemoglobin, and CRP							
HbA1c (%)	6.78	1.76	4.80-11.60	4.23	0.17	4.3-6.3	<0.001
Basal insulin (mIU/L)	22.33	13.09	4.58-73.71	7.03	5.56	1.37-29.32	<0.001
FPG (mmol/L)	7.17	2.77	4.10-14.84	5.13	0.79	4.04-27.20	<0.001
HOMA-IR	5.52	10.29	5.25-50.59	0.82	1.05	0.10-4.70	0.010
Hemoglobin (g/L)	154.99	11.75	127.70-179.00	150.40	12.00	122.00-173.00	0.082
CRP (mg/L)	8.85	11.49	0.70-71.82	2.52	4.38	0.24-21.23	0.008
Vitamins and microelements							
Vitamin A (nmol/L)	1.33	0.53	0.40-2.25	1.36	0.47	0.42-2.31	0.204
Vitamin B1 (nmol/L)	70.43	19.02	45.25-129.09	70.08	17.01	45.98-111.62	0.478
Vitamin B2 (ng/L)	331.50	58.58	196.96-498.32	292.73	56.96	197.00-422.67	0.004
Vitamin B6 (nmol/L)	31.02	15.70	11.25-61.91	30.25	11.14	12.42-53.92	0.793
Vitamin C (nmol/L)	51.58	13.95	31.07-85.58	56.65	17.15	30.51-96.62	0.187
Vitamin E (ng/ml)	13.12	1.88	9.54-16.84	12.85	1.85	9.33-16.16	0.727
1, 25-(OH_2) D_3 (ng/ml)	16.14	6.46	4.69-35.90	35.20	65.41	6.74-360.05	0.116
Vitamin B12 (pg/ml)	414.08	213.65	211.48-1244.86	282.78	187.87	2.72-736.08	0.002
Ferritin (ng/ml)	283.72	178.40	13.75-1082.88	171.23	101.67	26.42-389.04	<0.001
Fe (μmol/L)	17.71	6.23	7.70-36.20	20.68	6.58	11.50-37.10	0.051
Zn (μmol/L)	9.57	3.33	4.90-23.00	9.23	3.87	4.47-27.20	0.790
Cu (μmol/L)	15.96	3.70	10.10-26.60	15.10	4.42	2.10-25.50	0.172
Lipid metabolism							
Total cholesterol (mmol/L)	5.07	1.24	1.12-8.95	4.65	0.80	2.03-7.37	0.168
Triglyceride (mmol/L)	2.58	1.88	0.58-8.84	1.45	0.96	0.50-4.61	0.001

(Continued)

TABLE 5 Continued

Variable	Preoperation (n=59)			Postoperation (n=37)			P value*
	Mean	SD	Range	Mean	SD	Range	
HDL-c (mmol/L)	1.09	0.50	0.64-3.09	1.16	0.62	0.59-1.73	0.788
LDL-c (mmol/L)	3.02	0.79	0.96-5.22	2.63	0.59	1.49-4.46	0.053

HOMA-IR, homeostasis model assessment of insulin resistance; 1, 25-(OH2) D3, 1, 25 - dihydroxy - vitamin D; Fe, iron; Zn, zinc; Cu, Copper
*:paired t-test.
%EWL, percentage of excess weight loss; %TWL, percentage of total weight loss; %EBMIL, percentage of excess BMI loss; FPG, fasting plasma glucose; LH, luteinizing hormone; FSH, follicle-stimulating hormone; CRP, C-reactive protein; HDL-c, high-density lipoprotein cholesterol; LDL-c, low-density lipoprotein cholesterol.

sexual function in men with obesity 1 year postoperatively in different countries (8, 21, 23, 29, 30).

Mora et al. (33) found that ΔBMI had positive correlations with ΔIIEF and ΔEF, concluding that weight loss is the major contributor to improved sexual function. Taskin et al. (31) found that ΔBMI predicted the change in testosterone level. We have tried to establish a statistical model to find out predictors of improving the degree of sexual function (ΔIIEF scores), EF (ΔEF scores), and testosterone level (Δtestosterone). ΔTestosterone level seemed to have a correlation with BMI loss. This result might be limited by the sample size. However, no statistical significance was found between these parameters and the weight loss effect (ΔBMI, %EWL, %TWL, and %EBMIL). This may be due to effects of other factors after surgery. Playing a dominant role in the impairment of sexual function and testosterone level, a higher BMI led to decreased testosterone, chronic inflammation and oxidative stress, insulin resistance and T2DM, hypertension, drug usage, excess fat covering genitalia, and psychological factors. In combination, these factors impair sexual function (27, 34, 35). With good weight loss after surgery, these negative influences gradually disappeared and metabolic abnormality improved. Then, the sexual function and sex hormone levels ameliorated.

A previous article reported a negative impact on sexual function. With a mean follow-up of 31.8 months, laparoscopic adjustable gastric banding did not maintain sufficient weight loss (mean BMI loss was 7.51 kg/m^2, while in our study, it was 13.35 kg/m^2), and a worsening trend of scores in IIEF and EF appeared (36). This outcome demonstrated that unfulfilled weight loss might cause worse EF. The two objects of our study having decreased EF scores had %EWL >50%, showing better testosterone levels and other indexes. As Table 7 illustrated, patients did not suffer from evident deficiency of vitamins or microelements.

Apart from the factors discussed above, sexual function is affected by relationships with the lover. As Gokalp et al. (28) pointed out, along with improvements in male patients' IIEF scores, their partners became more pleased with their sex lives. Couples were able to benefit from LSG from another perspective. In addition, IIEF cannot assess fertility and premature ejaculation. Fertility outcome was not included in our study. However, Fariello et al. (37) revealed that testicular oxidative stress

TABLE 6 Outcomes of bariatric surgery and IIEF scores of the two groups after bariatric surgery.

	LSG	LRYGB	P value
Subjects (n)	18	19	
Preoperative BMI	41.98 ± 7.89	40.32 ± 8.02	0.530
Preoperative age	30.8 ± 7.3	32.8 ± 6.9	0.407
Preoperative T2DM	8	8	0.887
Preoperative hypertension	2	5	0.231*
%TWL	28.57% ± 10.79%	31.84% ± 16.83%	0.484
%EWL	85.79% ± 30.76%	84.21% ± 43.94%	0.901
%EBMIL	89.52% ± 27.87%	86.36% ± 44.59%	0.813
Postoperative IIEF	62.67 ± 8.89	60.32 ± 6.95	0.375
Erectile function	27.28 ± 3.20	26.47 ± 3.53	0.473
Orgasmic function	8.94 ± 1.35	9.05 ± 1.22	0.800
Sexual desire	7.61 ± 1.54	7.26 ± 1.28	0.459
Intercourse satisfaction	11.22 ± 2.71	9.84 ± 2.19	0.097
Overall satisfaction	7.67 ± 2.33	7.68 ± 1.20	0.977
Postoperative testosterone	4.99 ± 0.79	5.26 ± 0.90	0.552

*:Fisher's exact test; the others were two independent-samples t-test. Scores of IIEF questionnaire: mean ± standard deviation.
LSG, laparoscopic sleeve gastrectomy; LRYGB, laparoscopic Roux-en-Y gastric bypass; %TWL, percentage of total weight loss; %EWL, percentage of excess weight loss; %EBMIL, percentage of excess BMI loss; IIEF, International Index of Erectile Function.

TABLE 7 Univariate analysis of the change in IIEF scores, EF scores, and testosterone level.

	ΔIIEF		ΔEF		ΔTestosterone	
	r	P	r	P	r	P
ΔBMI	-0.123	0.470	-0.123	0.470	-0.304	0.065
EWL	-0.037	0.826	-0.140	0.410	0.073	0.668
TWL	0.182	0.282	0.100	0.555	0.055	0.748
EBMIL	0.189	0.262	0.135	0.425	0.055	0.745

BMI, body mass index; %TWL, percentage of total weight loss; %EWL, percentage of excess weight loss; %EBMIL, percentage of excess BMI loss; IIEF, International Index of Erectile Function; EF: erectile function.
The change in IIEF scores, EF scores, and testosterone level were defined as: (postoperative data minus preoperative data). We did not find predictors among weight loss effect and other indexes, but it showed a tendency that with more BMI loss, testosterone level increased more.

decreased after weight loss 6 months postoperatively, and both seminal quality and sex hormone profile improved.

4.3 Effects of LSG and LRYGB

LSG and LRYGB, the most widely used bariatric procedures worldwide and in China (38, 39), nearly reached the ratio of 1:1 in our study. A single operative procedure was incorporated within almost all articles previously published. El-Tholoth et al. (21) compared the proportion of men with ED after LSG and LRYGB, with more mild-to-moderate ED being found in the LRYGB group (LSG n = 0 vs. LRYGB n = 2). Mild ED and non-ED were not different in proportion. Our center found that the two procedures exerted a positive and comparable influence on sexual function evaluated by the IIEF questionnaire. The two groups did not significantly differ in EF and satisfaction with their sex lives. Still, the deficiencies of vitamins, microelements, and hemoglobin in the 19 patients undergoing LRYGB were not found during their follow-ups. It should also be noted that more samples are needed to prove this non-inferior effect. The lack of subjects made the result only hypothetical.

4.4 Strengths and limitations

The limitation of this retrospective study lies in the data size, keeping us from considering more socioeconomic factors. Two reasons limited the sample size. Firstly, many patients with obesity were not in a romantic relationship or not married, not having a regular sex life, which explains why our study and similar studies include only tens of subjects. Secondly, the number of men with obesity undergoing bariatric surgeries is several times smaller than that of women as a matter of experience in our center. We could not obtain a consecutive data series because it is inconvenient for patients to regularly travel long journeys back to our hospital from different cities. This can be resolved by future multicenter studies in which patients can be regularly evaluated nearby. With a mean follow-up period longer than that of many other studies, significant improvements in sex life and sex hormones were observed in this study. To the best of our knowledge, this is the first report on the sexual function of men with obesity before and after bariatric surgery in China. Also, limited data were found in Asia. Consequently, our data can bring about some new evidence. Our retrospective study might be the start of a multicenter study from which we can get a more comprehensive view of the sex lives of men with obesity undergoing bariatric surgery. In addition to the results above, fertility and correlations between sexual ability and other indices are expected.

5 Conclusions

BMI and waist circumference were negatively correlated with the level of testosterone. BMI was an independent risk factor for the severity of ED. LSG and LRYGB led to positive and sustained improvement in sexual function of men with obesity. The two surgical procedures had a comparable effect; more subjects are needed. Impaired sex hormone levels also could be reversible. The mechanism might be concerned with many factors, as the degree of weight loss effect and other indexes could not predict the improving degree of scores of sexual function. A greater BMI loss might predict a greater increase in testosterone.

Data availability statement

The original contributions presented in the study are included in the article/supplementary material. Further inquiries can be directed to the corresponding authors.

Ethics statement

The studies involving human participants were reviewed and approved by IRB of the First Affiliated Hospital of Jinan University (KY-2022-131). The patients/participants provided their written informed consent to participate in this study. Written informed consent was obtained from the individual(s) for the publication of any potentially identifiable images or data included in this article.

Author contributions

All authors listed have made a substantial, direct, and intellectual contribution to the work and approved it for publication.

Conflict of interest

The authors declare that the research was conducted in the absence of any commercial or financial relationships that could be construed as a potential conflict of interest.

Publisher's note

References

1. Wang L, Zhou B, Zhao Z, Yang L, Zhang M, Jiang Y, et al. Body-mass index and obesity in urban and rural China: Findings from consecutive nationally representative surveys during 2004-18. *Lancet* (2021) 398(10294):53–63. doi: 10.1016/S0140-6736(21)00798-4

2. Mingrone G, Panunzi S, De Gaetano A, Guidone C, Iaconelli A, Capristo E, et al. Metabolic surgery versus conventional medical therapy in patients with type 2 diabetes: 10-year follow-up of an open-label, single-centre, randomised controlled trial. *Lancet* (2021) 397(10271):293–304. doi: 10.1016/S0140-6736(20)32649-0

3. Courcoulas AP, King WC, Belle SH, Berk P, Flum DR, Garcia L, et al. Seven-year weight trajectories and health outcomes in the longitudinal assessment of bariatric surgery (LABS) study. *JAMA Surg* (2018) 153(5):427–34. doi: 10.1001/jamasurg.2017.5025

4. Chen Y, Corsino L, Shantavasinkul PC, Grant J, Portenier D, Ding L, et al. Gastric bypass surgery leads to long-term remission or improvement of type 2 diabetes and significant decrease of microvascular and macrovascular complications. *Ann Surg* (2016) 263(6):1138–42. doi: 10.1097/SLA.0000000000001509

5. Bajos N, Wellings K, Laborde C, Moreau C, Group CSF. Sexuality and obesity, a gender perspective: results from French national random probability survey of sexual behaviours. *BMJ* (2010) 340:c2573. doi: 10.1136/bmj.c2573

6. Steffen KJ, King WC, White GE, Subak LL, Mitchell JE, Courcoulas AP, et al. Changes in sexual functioning in women and men in the 5 years after bariatric surgery. *JAMA Surg* (2019) 154(6):487–98. doi: 10.1001/jamasurg.2018.1162

7. Brethauer SA, Kim J, El Chaar M, Papasavas P, Eisenberg D, Rogers A, et al. Standardized outcomes reporting in metabolic and bariatric surgery. *Obes Surg* (2015) 25(4):587–606. doi: 10.1007/s11695-015-1645-3

8. Sarhan MD, Khattab M, Sarhan MD, Maurice KK, Hassan H. Impact of bariatric surgery on Male sexual health: a prospective study. *Obes Surg* (2021) 31(9):4064–9. doi: 10.1007/s11695-021-05522-7

9. de Almeida Menezes M, Herbella FAM, de Godoy Dos Santos G, Valezi AC. Influence of gastric bypass on obese women sexual function-a prospective study. *Obes Surg* (2021) 31(8):3793–8. doi: 10.1007/s11695-021-05509-4

10. Aldeghaither S, Alnaami M, Aldohayan A, Bamehriz F, Alhaizan S, Aldeghaither M, et al. Reliability and validity study of the translated Arabic version of moorehead-ardelt quality of life questionnaire II. *Saudi Med J* (2022) 43(3):301–6. doi: 10.15537/smj.2022.43.3.20210689

11. Hu S, Huang B, Loi K, Chen X, Ding Q, Luo L, et al. Patients with prader-willi syndrome (PWS) underwent bariatric surgery benefit more from high-intensity home care. *Obes Surg* (2022) 32(5):1631–40. doi: 10.1007/s11695-022-05999-w

12. Yang J, Wang C, Cao G, Yang W, Yu S, Zhai H, et al. Long-term effects of laparoscopic sleeve gastrectomy versus roux-en-Y gastric bypass for the treatment of Chinese type 2 diabetes mellitus patients with body mass index 28-35 kg/m(2). *BMC Surg* (2015) 15:88. doi: 10.1186/s12893-015-0074-5

13. Yang W, Wang C, Chinese O, Metabolic Surgery C. Metabolic surgery needs stronger endorsement in Asian T2DM patients with low BMI. *Obes Surg* (2022) 32(1):212–3. doi: 10.1007/s11695-021-05636-y

14. Guan B, Yang J, Chen Y, Yang W, Wang C. Nutritional deficiencies in Chinese patients undergoing gastric bypass and sleeve gastrectomy: Prevalence and predictors. *Obes Surg* (2018) 28(9):2727–36. doi: 10.1007/s11695-018-3225-9

15. Rosen RC, Riley A, Wagner G, Osterloh IH, Kirkpatrick J, Mishra A. The international index of erectile function (IIEF): a multidimensional scale for assessment of erectile dysfunction. *Urology* (1997) 49(6):822–30. doi: 10.1016/S0090-4295(97)00238-0

16. Padma-Nathan H, McMurray JG, Pullman WE, Whitaker JS, Saoud JB, Ferguson KM, et al. On-demand IC351 (Cialis) enhances erectile function in patients with erectile dysfunction. *Int J Impot Res* (2001) 13(1):2–9. doi: 10.1038/sj.ijir.3900631

17. Porst H, Rosen R, Padma-Nathan H, Goldstein I, Giuliano F, Ulbrich E, et al. The efficacy and tolerability of vardenafil, a new, oral, selective phosphodiesterase type 5 inhibitor, in patients with erectile dysfunction: the first at-home clinical trial. *Int J Impot Res* (2001) 13(4):192–9. doi: 10.1038/sj.ijir.3900713

18. Porst H, Gacci M, Buttner H, Henneges C, Boess F. Tadalafil once daily in men with erectile dysfunction: an integrated analysis of data obtained from 1913 patients from six randomized, double-blind, placebo-controlled, clinical studies. *Eur Urol.* (2014) 65(2):455–64. doi: 10.1016/j.eururo.2013.09.037

19. Burnett AL. Commentary RE: The international index of erectile function (IIEF): A multidimensional scale for assessment of erectile dysfunction. *Urology* (2020) 145:308–9. doi: 10.1016/j.urology.2020.04.071

20. Cappelleri JC, Rosen RC, Smith MD, Mishra A, Osterloh IH. Diagnostic evaluation of the erectile function domain of the international index of erectile function. *Urology* (1999) 54(2):346–51. doi: 10.1016/S0090-4295(99)00099-0

21. El-Tholoth HS, Bedaiwi AK, Binjawhar A, Almulhem AA, Bedaiwi KK, Alshurafa H, et al. Male Sexual function after weight-loss surgeries in a group of Saudi population. *Urol Ann* (2021) 13(2):125–9. doi: 10.4103/UA.UA_144_19

22. Ksiazek A, Medras M, Zagrodna A, Slowinska-Lisowska M, Lwow F. Correlative studies on vitamin d and total, free bioavailable testosterone levels in young, healthy men. *Sci Rep* (2021) 11(1):20198.

23. Arolfo S, Scozzari G, Di Benedetto G, Vergine V, Morino M. Surgically induced weight loss effects on sexual quality of life of obese men: a prospective evaluation. *Surg Endosc.* (2020) 34(12):5558–65. doi: 10.1007/s00464-019-07356-y

24. Saylam B, Cayan S. Do antioxidants improve serum sex hormones and total motile sperm count in idiopathic infertile men? *Turk J Urol* (2020) 46(6):442–8. doi: 10.5152/tud.2020.20296

25. Dhindsa S, Ghanim H, Batra M, Dandona P. Hypogonadotropic hypogonadism in men with diabesity. *Diabetes Care* (2018) 41(7):1516–25. doi: 10.2337/dc17-2510

26. Dhindsa S, Miller MG, McWhirter CL, Mager DE, Ghanim H, Chaudhuri A, et al. Testosterone concentrations in diabetic and nondiabetic obese men. *Diabetes Care* (2010) 33(6):1186–92. doi: 10.2337/dc09-1649

27. Mintziori G, Nigdelis MP, Mathew H, Mousiolis A, Goulis DG, Mantzoros CS. The effect of excess body fat on female and male reproduction. *Metabolism* (2020) 107:154193. doi: 10.1016/j.metabol.2020.154193

28. Gokalp F, Koras O, Ugur M, Yildirak E, Sigva H, Porgali SB, et al. Bariatric surgery has positive effects on patients' and their partners' sexual function: A prospective study. *Andrology* (2021) 9(4):1119–25. doi: 10.1111/andr.13000

29. Machado FP, Rhoden EL, Pioner SR, Halmenschlager G, de Souza LVB, Lisot BC, et al. Weight loss through bariatric surgery in men presents beneficial effects on sexual function, symptoms of testosterone deficiency, and hormonal profile. *Sex Med* (2021) 9(4):100400. doi: 10.1016/j.esxm.2021.100400

30. Fahmy A, Abdeldaiem H, Abdelsattar M, Aboyoussif T, Assem A, Zahran A, et al. Impact of bariatric surgery on sexual dysfunction in obese men. *Sex Med* (2021) 9(2):100322. doi: 10.1016/j.esxm.2021.100322

31. Kun L, Pin Z, Jianzhong D, Xiaodong H, Haoyong Y, Yuqian B, et al. Significant improvement of erectile function after roux-en-Y gastric bypass surgery in obese Chinese men with erectile dysfunction. *Obes Surg* (2015) 25(5):838–44. doi: 10.1007/s11695-014-1465-x

32. Taskin HE, Al M. Testosterone changes in men with obesity and type 2 diabetes 6 months after sleeve gastrectomy with transit bipartition. *Surg Laparosc Endosc Percutan Tech.* (2022) 32(2):188–96. doi: 10.1097/SLE.0000000000001039

33. Mora M, Aranda GB, de Hollanda A, Flores L, Puig-Domingo M, Vidal J. Weight loss is a major contributor to improved sexual function after bariatric surgery. *Surg Endosc.* (2013) 27(9):3197–204. doi: 10.1007/s00464-013-2890-y

34. Sarwer DB, Lavery M, Spitzer JC. A review of the relationships between extreme obesity, quality of life, and sexual function. *Obes Surg* (2012) 22(4):668–76. doi: 10.1007/s11695-012-0588-1

35. Nimbi FM, Virginia C, Cinzia DM, Michela DT, Gianfranco S, Emanuela P. The relation between sexuality and obesity: the role of psychological factors in a sample of obese men undergoing bariatric surgery. *Int J Impot Res* (2022) 34(2):203–14. doi: 10.1038/s41443-020-00388-2

36. Ranasinghe WK, Wright T, Attia J, McElduff P, Doyle T, Bartholomew M, et al. Effects of bariatric surgery on urinary and sexual function. *BJU Int* (2011) 107(1):88–94. doi: 10.1111/j.1464-410X.2010.09509.x

37. Fariello RM, de Carvalho RC, Spaine DM, Andretta RR, Caetano EMJr., Sa GPD, et al. Analysis of the functional aspects of sperm and testicular oxidative stress in individuals undergoing metabolic surgery. *Obes Surg* (2021) 31(7):2887–95. doi: 10.1007/s11695-021-05350-9

38. Welbourn R, Hollyman M, Kinsman R, Dixon J, Liem R, Ottosson J, et al. Bariatric surgery worldwide: Baseline demographic description and one-year outcomes from the fourth IFSO global registry report 2018. *Obes Surg* (2019) 29(3):782–95. doi: 10.1007/s11695-018-3593-1

39. Yang W, Zhu S, Cheng Z, Zhang N, Wu L, Chen Y, et al. Laparoscopic roux-en-Y gastric bypass for excess weight and diabetes: a multicenter retrospective cohort study in China. *Mini-invasive Surgery.* (2021) 5:11. doi: 10.20517/2574-1225.2021.06

frontiers | Frontiers in Endocrinology

TYPE Review
PUBLISHED 15 February 2023
DOI 10.3389/fendo.2023.1031610

OPEN ACCESS

EDITED BY
Peng Zhang,
Affiliated Beijing Friendship Hospital, Capital Medical University, China

REVIEWED BY
Marlena Holter,
Cornell University, United States
Juan Salazar,
Universidad del Zulia, Venezuela
Ansarullah,
Jackson Laboratory, United States

*CORRESPONDENCE
Qiang Xu
xuqiang@pumch.cn

†These authors have contributed equally to this work

SPECIALTY SECTION
This article was submitted to Obesity, a section of the journal Frontiers in Endocrinology

RECEIVED 30 August 2022
ACCEPTED 19 January 2023
PUBLISHED 15 February 2023

CITATION
Liu T, Zou X, Ruze R and Xu Q (2023) Bariatric Surgery: Targeting pancreatic β cells to treat type II diabetes. *Front. Endocrinol.* 14:1031610. doi: 10.3389/fendo.2023.1031610

Bariatric Surgery: Targeting pancreatic β cells to treat type II diabetes

Tiantong Liu[1,2†], Xi Zou[1,3†], Rexiati Ruze[1,3†] and Qiang Xu[1*]

[1]Department of General Surgery, Peking Union Medical College Hospital, Beijing, China, [2]School of Medicine, Tsinghua University, Beijing, China, [3]Chinese Academy of Medical Sciences and Peking Union Medical College, Beijing, China

Pancreatic β-cell function impairment and insulin resistance are central to the development of obesity-related type 2 diabetes mellitus (T2DM). Bariatric surgery (BS) is a practical treatment approach to treat morbid obesity and achieve lasting T2DM remission. Traditionally, sustained postoperative glycemic control was considered a direct result of decreased nutrient intake and weight loss. However, mounting evidence in recent years implicated a weight-independent mechanism that involves pancreatic islet reconstruction and improved β-cell function. In this article, we summarize the role of β-cell in the pathogenesis of T2DM, review recent research progress focusing on the impact of Roux-en-Y gastric bypass (RYGB) and vertical sleeve gastrectomy (VSG) on pancreatic β-cell pathophysiology, and finally discuss therapeutics that have the potential to assist in the treatment effect of surgery and prevent T2D relapse.

KEYWORDS

bariatric surgery, type II diabetes mellitus, β-cell, islet regeneration, vertical sleeve gastrectomy, Roux-en-Y gastric bypass

Introduction

Entering the 21st century, the prevalence of obesity is increasing and posting a significant public health threat to most countries worldwide (1). Traditional treatment options for obesity include diet control, physical exercise, and pharmacological interventions (2). However, severe obesity is difficult to treat. It is widely recognized that pharmacotherapy and lifestyle intervention alone will barely lead to weight loss in most cases, while bariatric surgery (BS) is the most effective and sustainable strategy to achieve short- and long-term weight loss in such a setting (3).

Over the past few decades, the number of bariatric surgeries performed has increased exponentially worldwide for good reasons (4, 5). Studies have demonstrated that the BS contributes to sustained weight loss and facilitates the management of obesity-associated comorbidities, including cardiovascular, respiratory, musculoskeletal, reproductive, and renal diseases, and also experiences significant improvement (6–10). The general mental health status and patient-reported life quality also significantly increased after the surgery (3,

11–14). For another, the popularity of minimally invasive surgery and the increased number of qualified surgeons and surgical centers that perform BS has revolutionized the procedure by vastly increasing its safety profile. Moreover, from a public health perspective, the prevalence of BS can efficiently reduce the healthcare burden upon individuals and cut the overall healthcare cost (15).

The clinical benefits of BS are multi-faceted. At a population level, the average body weight loss expectation for patients receiving a bariatric procedure is expected to be over 60%, while approximately 80% of patients complicated by T2DM go into remission (9, 16). Two years following BS, about four-fifths of all diabetic patients still have sustained diabetes resolution (8, 9). The improvement in glucose tolerance can be sustained up to 5 years after surgery compared to simple lifestyle intervention or medications (17). Roux-en-Y gastric bypass (RYGB) and vertical sleeve gastrectomy (VSG) are the two most commonly performed bariatric procedures but exploit distinct surgical strategies (Figure 1; Table 1). The two approaches have slightly different, almost comparable clinical outcomes (Figure 2). While VSG is a cheaper, more straightforward, and less reconstructive approach, it has worse outcomes regarding body weight loss and T2DM remission rate (18, 19). Still, both procedures have higher expected weight loss than traditional vertical banded gastroplasty (VBG) and adjustable gastric banding (AGB) (20). Although BS has been proven safe and effective, the overall complication rate following BS was 10–18% (21). Short-term surgical complications, such as anastomotic gastric leaks (22), fistula tract formation (22), and small-bowel obstruction (SBO) (23), neurological disorders and muscle weakness, and nutritional deficiencies (24), can be dreaded in some patients. Long-term complications include gallstone disease (25) and bone loss (26). On the other hand, BS is not a 'magic bullet' to T2DM for all obese patients. At least 40% of patients seeking do not have adequate, long-lasting T2DM remission (27, 28). Even for patients with diabetes under control at the beginning, the remission does not seem to stay efficacious forever. About 20-30% of obese patients with an initial response experience relapse early or late within ten years (27, 28). The Swedish Obese Subjects (SOS) study demonstrated a 10-year relapse rate as high as 50% (29).

Despite the undisputable effect of BS on treating T2DM, there is only a limited understanding of the complicated mechanism behind the process, while even less is known about the mechanism that underlies the relapse of T2DM after surgery. The remission of T2DM was once considered a combined result of decreased food intake, nutrient absorption, and weight loss (30). However, this hypothesis was contradictory to the fact that glucose tolerance can be improved within days after the surgery, long before substantial weight change, indicating a glycemic control mechanism that is potentially independent of weight control (31–33).

In this review, we review the recent progress in the impact of BS on pancreatic β-cell and discuss novel therapeutics that have the potential to improve β-cell function and sustain the efficacy of surgery in the treatment of T2DM.

Current recommendations for bariatric surgery

The recommendations for the patient population suitable for BS have remained almost unchanged over the last three decades (34). As recommended by most guidelines, BS should be considered for patients with a body mass index (BMI)≥40 kg/m^2, BMI≥35kg/m^2 with associated comorbidities that are expected to improve with weight loss, or BMI≥30–35 kg/m2 complicated with T2DM or arterial hypertension with poor control despite optimal medical therapy (35, 36). RYGB and VSG provide almost comparable effects regarding weight loss and T2DM treatment; thus, the choice of

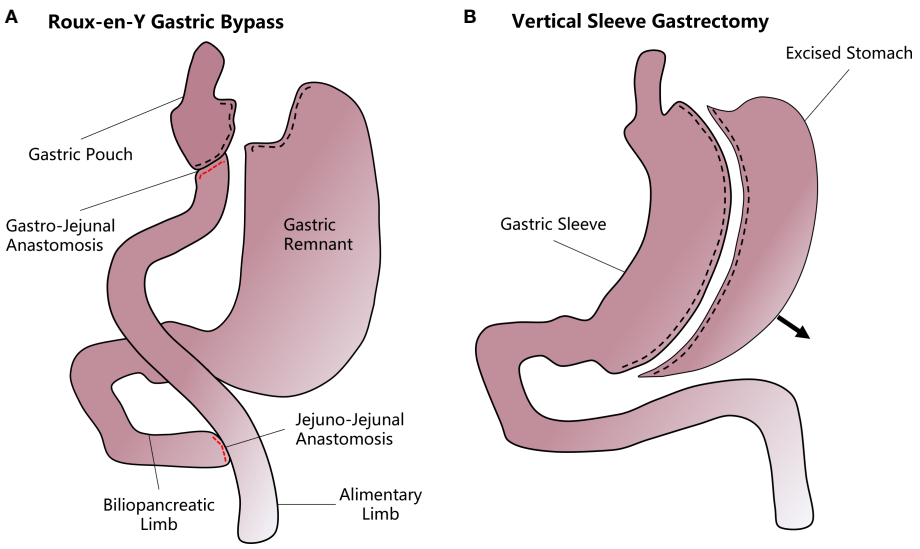

FIGURE 1
A diagram of how vertical sleeve gastrectomy (VSG) and Roux-en-Y gastric bypass (RYGB) are performed. **(A)** In the RYGB procedure, the upper gastrointestinal tract is transected from near the gastric fundus and the jejunum to form a small gastric pouch. The stomach remnant and the duodenum and proximal jejunum are bypassed and attached to the mid-jejunum through a jejunal-jejunal anastomosis. Another gastro-jejunal anastomosis allows the connection of the gastric pouch and distal jejunum. **(B)** In VSG, most of the stomach is resected along the greater curvature while the remnant stomach forms a sleeve structure that greatly decreases the accommodative capacity and increases the chyme's diversion rate.

TABLE 1 Possible β-cell centered strategies that can supplement T2DM treatment for disease relapse after bariatric surgeries.

Strategy	Advantages	Disadvantages
Stem cell differentiation	• Standardized and unlimited supply of donor materials • No rejection issue	• Tumor risk • Incomplete understanding of induced differentiation *in vitro*
Stimulating β-cell proliferation	• Simple and controllable • No rejection issue	• Lack of agents with sufficient treatment effect
Reprogramming of non-β-cells	• Achievable through both *in vivo* and *in vitro* approaches • No rejection issue	• Failure of stable induced reprogramming of human cells
Xenogeneic pancreas transplantation	• Unlimited supply of donor organ • Promising β-cell function	• Strong rejection of donor cells
Allogeneic pancreas transplantation	• The full potential of β-cell function	• Shortage of donor organ • Rejection of donor cells

procedures should comprehensively consider institution experience, patient preference, and physician evaluation (6).

The role of β-cell in the onset of obesity-related type 2 diabetes mellitus

In adults, pancreatic β-cell is a group of highly differentiated insulin-secreting cells (37). As an endogenous preventive mechanism, the β-cell responds to hyperglycemia with a compensatory increase in insulin secretion and cell mass expansion (38, 39). β-cell mass is not homogenous. The asynchronization of intra-islet cell differentiation, metabolic stress, and aging collectively lead to the overall heterogeneity of β-cell morphology and function (40). These cells are susceptible to autoimmune attack and distorted metabolic environments, characterized by progressive cell apoptosis under pathological conditions (41, 42). It is well established that excessive caloric or fat intake leads to insulin resistance and β-cell function impairment, as the central mechanism that underlies T2DM (43). In this model, a persistent hyperglycemic state poses so-called 'glucotoxicity' to pancreatic islets, which induces β-cell apoptosis and gradually results in the dysfunction of β-cell, secondary to the progressive loss of the β-cell population (44). Chronic insulin resistance has been shown to accelerate this process (40, 45, 46). Although constant cell renewing compensates for the reduction in β-cell mass before age 30 (47), the cell turnover rate gradually slows down, and finally, cell loss cannot be counterbalanced by new cell replacement anymore beyond this age (48).

Systemic low-grade tissue inflammation is a hallmark of obesity (49). Widespread tissue immune cell infiltration and release of proinflammatory factors collectively promote insulitis and β-cell loss (50). Obesity also induces the proliferation of islet-resident M1 macrophages, which account for local inflammation and impairs β-cell function (51, 52). Similarly, enhanced TNF-α and CCL2 expression were correlated with hampered glucose-stimulated insulin secretion (GSIS) (53).

Whether the overall islet degeneration is because of β-cell death or loss of function once remained debated (54). Talchai et al. proved that, during the pathogenesis of T2DM, matured β-cells lost their identity and reverted to progenitor-like cells expressing naïve markers, including L-Myc, Nanog, and Oct4 (55). By morphometric quantification, an average of 30% of β-cells underwent dedifferentiation in donor islets from the T2DM group, while less than 10% in nondiabetic controls (56). The dedifferentiation was reversible. Evidence showed that a fraction of dedifferentiated cells could again transdifferentiate into glucagon-secreting cells that resemble α-cells (55). Insulin therapy can induce the dedifferentiated cell to re-differentiate to mature neurogenin3-negative, insulin-positive β-cells (45), possibly the primary mechanism for that intensive insulin therapy improved β-cell function and resulted in prolonged glycemic remissions (57).

Procedure	RYGB	VSG
Basic Mechanism for Weight Loss	Satiety and Nutrient Malabsorption	Satiety
Cost	High	Low
Surgery Duration	Long	Short
Hospital Stay	Long	Short
Expected Weight Loss	High	Low
Complication Rate	High	Low
Supplement Requirement	Yes	No
T2DM Resolution Rate	60-80%	About 50%

FIGURE 2
A comparison between two most commonly performed bariatric procedures.

Bariatric surgery promotes T2DM remission in a weight-independent manner

The role of BS in the remission of T2DM remains partially understood. Many plausible mechanisms, which are not necessarily exclusive to each other, have been proposed in recent years (58). Traditional views held that food intake restriction, nutrient malabsorption, and subsequent weight loss caused by altered gastrointestinal (GI) anatomy is the central mechanism for T2DM resolution shared by various bariatric procedures (59). However, several lines of evidence indicated that the improved glycemic control is independent of weight loss and calorie intake, at least partially. First, it was observed that the remission rate of T2DM in leaner individuals is similar to that in severely obese patients (60), indicating that the correlation between glucose tolerance control and weight change was disproportional. Second, the improvement of glucose homeostasis, insulin secretion, and insulin sensitivity usually occurs days after the surgery, long before significant weight loss, and regardless of specific bariatric procedures (19, 61). Third, such rapid changes only exist in RYGB or VSG that require digestive tract reconstruction but not in restrictive surgical techniques such as vertical banded gastroplasty (VBG) and laparoscopic adjustable gastric banding (LAGB), which promote weight loss solely by decreasing nutrient intake (62). All this evidence provided evidence of the necessity to divide the glucose-lowering effect of BS into the early effect and the late effect. While the late effect, or weight loss, plays a vital role in the durable remission of T2DM. Researchers realized that the early effect was potentially a combined result of restriction of gastric volume, lowered nutrient absorption, increased gastric emptying rate, postprandial synthesis of secretin, altered GI hormone secretion release pattern, and sensitized hepatic insulin response regardless of specific procedures (31, 63–65). These tend to be immediate effects of GI reconstruction, after which insulin sensitivity and glucose tolerance are improved prior to significant weight change (66, 67). As the primary causative factor of T2DM in the case of obesity, the impaired β-cell function is largely alleviated after BS, and the alteration has been gradually considered central to the remission of T2DM (68). In the following sections, we will focus on the functional and physiological change of pancreatic β-cells and the driving factors that may govern that change after RYGB and VSG.

Bariatric surgery promotes T2DM remission by modulating β-cell function

The role of β-cell in RYGB

The RYGB procedure involves creating a small stomach pouch connecting to the rerouted small intestine (Roux limb) (69). Since the upper intestine senses nutrient passage and activates a gut-brain-liver axis to maintain glycemia under physiological conditions (70), the exclusion of duodenum from the main gastrointestinal tract (GI tract) breaks the balance by leading to the delivery of a large amount of insufficiently digested food to the lower digestive tract. It induces the secretion of strong gut hypoglycemic hormones, mainly glucagon-like peptide (GLP-1) and peptide YY (PYY) (71) (Figure 3).

For a long time, it was observed that diabetes remission was affected by the time of diabetes duration, poor preoperative glycemic control, and preoperative insulin dosage. People inferred that perhaps less deterioration in β-cell mass or function before surgery might maximize the effect of the surgery-induced pattern change of gut peptides that glucose balance. As verified in the male Zucker Diabetic Fatty (ZDF) rat model, the RYGB procedure efficiently restored pancreatic islet function and improved glucose tolerance in males (72). Increased insulin sensitivity and enhanced insulin secretion improved glucose metabolism (72). Histopathologically, pancreas hyperplasia (73) and β-cell regeneration (74) were observed shortly after RYGB. Compared to the sham surgery group, there was a 60% increase in β-cell mass in the RYGB rat islets three months post-surgery, possibly resulting from islet neogenesis (73). Preservation of β-cell mass was also observed in Goto-Kakizaki (GK) rats (75). Tracking of mature β-cell markers indicated a decreased ratio of dedifferentiated cells (76) and apoptotic β-cell (77). However, considering the pronounced differences in gastrointestinal tract structure, nutrient composition, and endocrine pattern, results in rodent models may not be easily translated into a human.

In porcine models, more significant pancreatic islet number, mass size, and improved β-cell function were observed receiving RYGB surgery compared to the diet control group (78). However, other evidence exists to support that β-cell mass remains unchanged after BS (32, 79, 80). Some groups argue that the elevated expression of cell markers such as insulin, Pdx-1, Maf A, Pcsk1, and Glut2 are outcomes of improved glycemia rather than drivers (31). As proof of the argument, the ex vivo β-cell function was not improved (32).

In real-world T2DM patient cohorts, altered insulin secretion and sensitivity can independently or jointly improve glucose homeostasis after RYGB, as measured by various available techniques (81–84). As mentioned previously, the glucose-lowering effect can be divided into early- and late-stage. In a prospective study, the oral glucose tolerance test (OGTT) was measured immediately and one year after RYGB in 119 morbidly obese participants, indicating sustained late-stage islet function improvement (82). The calculated disposition index (DI) and proinsulin-to-insulin (PI/I) ratio of the surgery group were significantly higher than the lifestyle intervention group (82). However, the early-stage data was lacking. To present a longitudinal comparison of early-stage and late-stage β-cell function, Nannipieri et al. measured glycosylated hemoglobin and OGTT after 45 days and one year after surgery and mathematically correlated blood glucose, insulin, and C-peptide concentrations (83). They observed sustained insulin sensitivity improvement regardless of the existence of T2DM, while the background β-cell function before the surgery was a significant determinant of T2DM remission (83). The enhanced insulin response was durable as measured during a two-year observation (81, 84).

The exact mechanism underlies the alteration of β-cell physiology and improved glucose homeostasis after gastric bypass is mainly elusive. The rapid amelioration of islet function has multiple potential explanations. In Nannipieri's experimental design, the designated nutrient uptake after RYGB was roughly 800 kcal (83), while the effect of calorie restriction or fasting on plasma glucose equilibrium and insulin sensitivity has been well documented (66). It is of equal

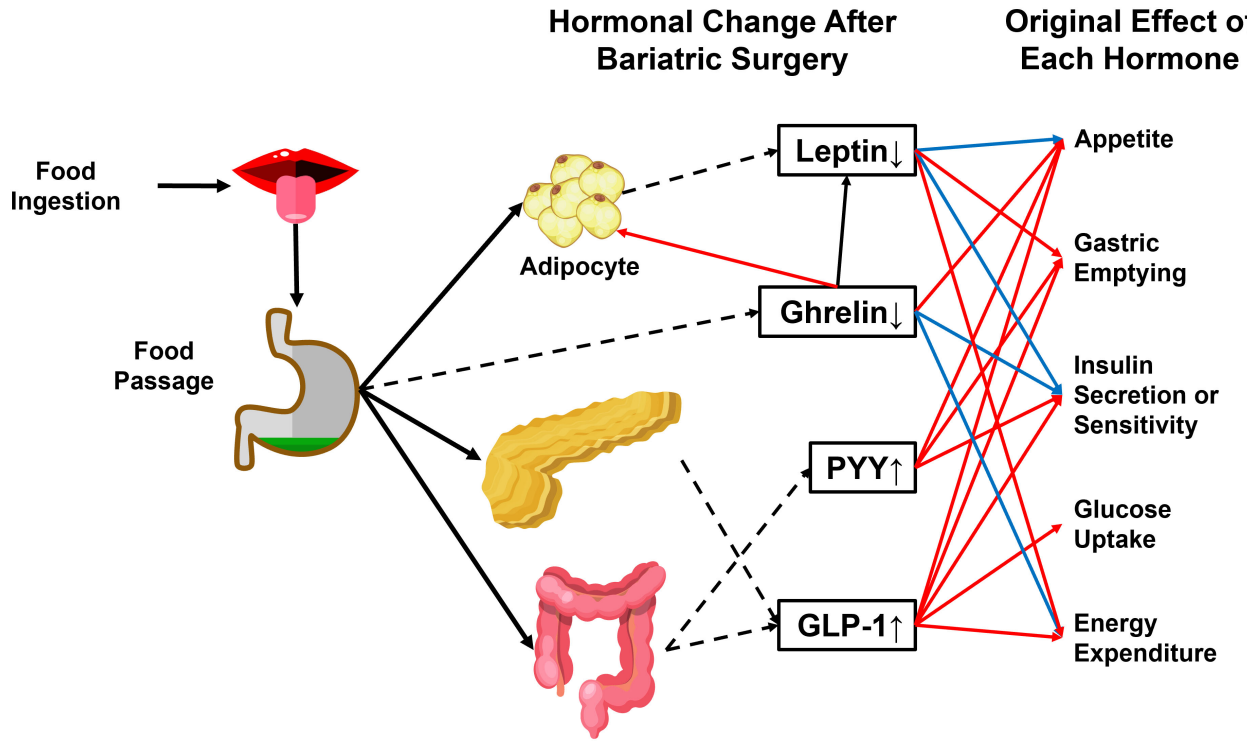

FIGURE 3
Physiological effects of crucial hormones that are altered after bariatric surgery. GLP-1 and PYY are gut-secreted hormones with anti-obesity and antidiabetic actions. The passage of food can stimulate both hormones through the gastrointestinal tract. Ghrelin and leptin are reduced after bariatric surgery. Ghrelin induces energy storage in the form of fat by promoting adipose tissue deposition and fatty acid oxidation, reducing energy expenditure, and blocking insulin secretion. Leptin has an antagonistic effect on ghrelin. PYY, Peptide YY. GLP-1, glucagon-like peptide 1. Dashed arrowhead, hormone secretion. Blue arrowhead, inhibitory effect. Red arrowhead, stimulatory effect.

importance that the rapid post-surgery increase in incretin hormones or bile acids can specifically potentiate β-cell function (85). Altered gut hormone signaling for the reconstructed GI tract was considered a leading cause of insulin secretion and increased blood glucose uptake (86). GLP1 and gastric inhibitory polypeptide (GIP) are two major GI antidiabetic hormones that activate insulin secretion on oral ingestion of food, and each exerts its effect by binding to its receptor (75, 87). The impaired GLP-1 and GIP secretion and function in obese patients were partially restored after gastric bypass surgery or VSG, compared to those who received a low-calorie diet with equivalent weight loss (75, 88, 89). In an obesity cohort (BMI≥35), the post-surgery usage of Ex-9 (a specific GLP-1R antagonist) completely reversed improvements in β-cell glucose sensitivity and glucose tolerance, implicating the critical role of activated GLP-1 response in this process (90). In rare cases, the hyperactivated GLP-1 secretion leads to hyperinsulinemic hypoglycemia, a life-threatening post-RYGB complication that usually arises years after the surgery (91), which highlights the role of the proximal small intestine. In the GK rat model, Ramracheya et al. demonstrated that glucagon secretion was restored after RYGB, while this effect was dependent on a gut hormone, PYY, but not GLP-1 (92).

It is likely that distinct mechanisms account for late-stage post-surgery islet function improvement. Chronic glucose toxicity is one of the leading causes of β-cell degeneration during T2DM development and the fact that β-cell can self-renewal, the removal of glucose toxicity at the early stage caused by other mechanisms at least partially accounts for the prolonged individual glucose-sensing ability and insulin secretion (93). A further hypothesis is that the abatement of insulin resistance decreases the workload of β-cells. Improvement of homeostasis model assessment of β-cell function (HOMA-β) was observed (51).

A later study demonstrated that the Roux limb's morphological and metabolic remodeling adaptation, characterized by intestinal mucosa hyperplasia and hypertrophy, is responsible for improved glucose homeostasis (94). Enhanced GLUT-1–mediated glucose transportation and utilization can be observed under rat abdominal positron emission tomography-computed tomography (PET-CT), which contributes to improved whole-body glucose disposal (94).

The role of β-cell in VSG

As a procedure gaining popularity, VSG has surpassed RYGB to become the most performed BS (95). The procedure involves removing 80% of the stomach by transecting along the greater curvature while preserving the intestinal anatomy's original integrity (96). VSG can help obese patients to achieve weight loss and T2DM remission almost comparable to RYGB, with more straightforward modifications to the GI tract, fewer surgical risks, and reduced postoperative complications (95).

In obese patients, glucose control is quickly restored after VSG, as indicated by apparent reductions in both prandial and fasting glucose levels after the surgery and improvement of insulin resistance (32). VSG promotes β-cell mass increase and cell function restoration as

short-term responses (32, 97–100). Furthermore, histopathological sections of the pancreas displayed a decrease in pancreatic lipid droplet infiltration (32), restoration of islet integrity (99), and β-cell expansion (97) shortly after VSG. Using a positron emission tomography (PET) combing ligand-receptor marking technique, Inabnet et al. were able to demonstrate an increase of Vesicular monoamine transporter type 2 (VMAT2) positive β-cell mass (100). Grong et al. arrived at a similar conclusion and applied a three-dimensional optical projection tomography that can precisely visualize insulin-secreting cells by antibody staining (98). VSG rats had a significantly higher beta-cell density than duodenojejunostomy rats or sham (animals that underwent a false abdominal surgery without changing the GI anatomy) rats (98).

Whether increased insulin secretion or improved insulin sensitivity is the leading cause of glucose homeostasis after VSG remains inconclusive. Abu-Gazala et al. and other groups observed that the operation does not directly affect insulin secretion, while the improved hepatic insulin sensitivity after the surgery played a vital role in the remission of T2DM (32). Other groups hold the view that VSG promoted GSIS (99, 101).

One of the most dramatic post-surgery hormonal changes shared by various bariatric procedures, including VSG, is an over 10-fold increase in the postprandial secretion of GLP-1, a well-established potent stimulator of GSIS (16). There are two distinct sources for GLP-1 elevation after BS. First, the increased influx of insufficiently absorbed nutrients stimulates the secretion of GLP-1 by enteroendocrine L cells in the distal gastrointestinal tract in response to a meal (102). The other source lies within the pancreatic islet. Garibay et al. exploited the β-cell-specific inducible GLP-1R knockout murine model to investigate the role of intra-islet GLP-1R signaling change after VSG. Their result demonstrated that increased GLP-1 in the systemic circulation activated the GLP-1 secretion by α-cell in a β-cell GLP-1R-dependent manner, possibly forming an intra-islet positive feedback loop that promotes insulin secretion (103). However, the exact association between the two GLP-1 secretion pathways remains unclear.

Although the surgery-induced activation of the GLP-1 pathway plays a critical role in GSIS and T2DM remission, it may not be unique. However, patients with diabetes with VSG develop only modest glucose intolerance when treated with the GLP-1R antagonist exendin-[9], similar to a non-operated control group. The lack of disproportionate glucose intolerance during GLP-1R blockade in surgical subjects speaks against increased GLP-1 making a significant contribution to the metabolic improvement after surgery.

In *db/db* mice (a murine model that simulates T2D status related to morbid obesity), VSG reduced glycemia independent of weight loss (32). Single-cell transcriptomic analysis of intra-islet cells acquired from obese mice reveals that in β-cells, the ER-associated protein degradation pathway (ERAD) was activated (97). In the mice that received VSG, the endoplasmic reticulum stress was mitigated due to the augmentation of unfolded protein response. Moreover, the surgery-induced transcription change was exclusive to β-cell rather than other endocrine cells in the islet (97). While in the sham-controlled group, the intra-islet cells retained features of compromised β-cell identity and function and extreme dedifferentiation (97). Using a similar transcriptomic analysis combining pathway enrichment, Douros et al. found an evident activation of calcium signaling for the VSG group mice (101). They hypothesized and verified that increased intra-islet Ca2+ oscillation amplitude in the islet without changing the insulin secretory capacity (101). This alteration fundamentally re-sensitized the islet to glucose concentration, and ex vivo measurement indicated a persistent effect (101).

Since most current studies of the impact of VSG or RYGB on T2DM use mouse models, we should hold a critical understanding of the results by emphasizing a few points. Based on current evidence, although RYGB and VSG lead to comparable weight loss and β-cell function improvement in obese patients, RYGB in mice provides more profound and sustained body weight loss than VSG. The gap between human and animal models has been disputed and recursively highlighted in all biomedical research. Second, it is essential to remember that although the therapeutic effect of bariatric procedures can be compared using unified clinical indicators such as weight loss and insulin concentration, the mechanisms underpinning various procedures can be strikingly different. Even for the same procedure, for example, VSG, the impact of diverse, well-established surgical mouse models and different techniques may have been underestimated (104). As pointed out by Myronovych et al., each of the cohorts of mice used in various studies is of various ages, differing diets, and different lengths of exposure to the diet. The mice's starting weights and body fats also varied considerably from one cohort to another (105). A critical judgment of the effect of BS conferred from animal experiments cannot be overemphasized.

Add-on strategies to promote β-cell regeneration

As mentioned previously, the regenerative ability of pancreatic islets is limited, and they gradually experience cell loss during individual development and growth (106). Although BS has the potential to reverse obesity-induced β-cell dedifferentiation and partially restore cell function, the unavoidable cell degeneration may underlie the postoperative relapse of diabetes and reemergence of other obesity-associated comorbidities (27, 28). Untangling the β-cell pathophysiology during diabetes pathogenesis and BS has shed new light on the development of add-on therapy to mitigate or prevent disease relapse.

The initial success of stem cell therapy (107), hormones therapy, and cytokine therapy (108) in preclinical animal models remind us that the islet regenerative strategy may be a powerful method for adjuvant management of obesity-related T2DM and can be achieved at multiple levels (106). Endogenously, halting β-cell dedifferentiation to maximally preserve β-cell mass and function at an early stage of the disease is fundamental. This goal can be achieved by insulin treatment (57) or diet control (107, 109–111). In db/db mice, simple calory restriction can prevent and possibly reverse β-cell dedifferentiation, as certified by decreased expression of progenitor marker Aldh1a3 and enhanced β-cell markers such as MafA, NeuroD1, and Foxo1 (111). On the one hand, the calory-restricting diet plan overcomes high-fat diet-induced changes and recovers islet calcium oscillation coordination necessary for insulin secretion (112). Conversely, the fasting-mimicking condition upregulated Ngn3 expression, thus

promoting β-cell proliferation and regeneration (113). The application of insulin and other antidiabetic medications permits temporary reduction of systemic hyperglycemia promoted redifferentiation of dedifferentiated β-cells (114–118).

Another approach is to replenish the target cells *via* transplantation of β-cells from donor pancreata or cells derived from human pluripotent stem cells (hPSCs) (106, 119). A shortage of donor organs has largely impeded the clinical feasibility of the former choice; thus, stem cell-based transplantable β-cells therapy has been spotlighted recently (120). The development of β-cells followed a strict pattern regulated by the sequential expression of specific transcription factors (121). In mouse embryos, multipotent pancreatic progenitor cells co-express the critical transcription factors Sox17 and Pdx1 (122). These progenitors then converted epithelial cells with a bipolar destiny: pancreatic duct cells or Ngn3+ precursors that later give rise to all the endocrine in the pancreatic islet, including α cells and β-cells (123). As a further step toward the *in vitro* cell culture of fully functional β cells, Nair et al. first stressed the importance of cell re-clustering after β cell induction from hPSCs to resemble their endogenous counterparts maximally (107). These insights are now exploited to recapitulate aspects of islet formation *in vivo* and formulate novel regenerative tactics by differentiating pluripotent stem cells or reprogramming non-β-cells into transplantable β-cells that may complement BS in the management of T2DM.

Discussion

Numerous high-quality clinical trials have verified the clinical benefits of BS in treating T2DM, making it currently the most effective treatment to control obesity-related T2DM. Nevertheless, heated debate existed on its actual necessity and safety. Although an increasing number of obese patients seek BS, the proportion is lower than 1% of the vast obesity population (124). First, drawbacks exist. The overall mortality rate of BS is 0.5-2%, according to studies based on ample research populations (125–127). The overall complication rate following BS was 10–18% (21), including short-term surgical and long-term nutritional complications.

On the other hand, BS seems not to be a cure for all obese patients. About 40% of patients do not have sustained T2DM remission, and 20-30% of patients with an initial response experience relapse early or late within ten years (27, 28). The SOS project reported a 10-year relapse rate as high as 50% (29).

For one thing, the accurate screening of obese patients that benefit most from the surgery is critical to further recognition and application of BS. Predicting tools based on machine learning methods have been utilized for diabetes remission outcomes after BS. Pedersen et al. developed a heuristic method and concluded that baseline HbA1c and insulin levels, doses of antidiabetic agents such as insulin and insulin-sensitizing medication, and several single nucleotide polymorphisms (SNPs) were informative variables that were related to the response of the surgery (128). Note that all the SNPs had a reported role in insulin secretion, insulin sensitivity, or obesity. Other scoring systems, such as ABCD, IMS, and DiaRem, have also been proposed for short- or long-term diabetes remission (129, 130). However, these scores were developed according to specific bariatric procedures, and none has sufficient predicting power for all patients (131).

While for another, the question needs to be answered why diabetes cannot be controlled after surgery or relapse in certain patients; before that, it is of prime interest to fully understand why BS is effective in the first place. It is indisputable that the mechanism behind surgery-induced T2DM remission is muti-dimensional. Though weight loss has been proven to be a crucial contributor to glycemic control in various bariatric procedures, an increasing body of evidence supports a distinct, weight-independent glucose-lowering mechanism.

As summarized in this review, chronic islet inflammation and glucotoxicity among obese patients progressively impair β-cell function by inducing cell apoptosis and dedifferentiation, while the recovery of β-cell morphology, cell mass, and GSIS after RYGB and VSG seem to be a major cause of rapid improvement of glucose homeostasis. Increased secretion of certain GI hormones accelerates islet function restoration. More research focuses are warranted in the future. First, most current studies with animal models and patients focus on the short-term alteration of islet function, while a longitudinal tracking of the β-cell function after the surgery is lacking. Second, a valid comparison of β-cell function between surgery responders and nonresponders may indicate whether β-cell function improvement is a central indicator of surgery efficacy. Third, the monitoring of β-cell function in initial responders that experiences a late T2DM relapse can help to provide us with insights on novel therapeutics to improve the surgical outcome. Last but not least, Jiménez et al. observed that patients experiencing a later relapse had poorer baseline β-cell reserved function before the surgery, as reflected by dependence on heavy insulin or multiple glucose-lowering agents (98, 99). Correlating the baseline islet function of obese patients and long-term diabetes remission status is critical for choosing the right patient to obtain the most significant benefit from surgery and discriminating the population prone to diabetes relapse that may need additional disease-modifying treatments.

There are no solid and unified recommendations for surgery-refractory obesity or postoperative recurrence due to a lack of high-quality clinical research. Although some pharmacological interventions such as anti-inflammatory and GLP-1 receptor agonists can temporarily improve islet function (132, 133), there is no consistent evidence to support that preoperative or postoperative addition of these drugs and surgery can increase the response rate or lower the diabetes recurrence rate of BS. To elucidate the islet pathophysiology is of critical significance to the understanding of surgical failures. On the other hand, although our current understanding of how the pancreas develops during embryogenesis is scarce, attempts are being made to formulate regenerative strategies that center on induced differentiation of human pluripotent stem cells (hESCs) or reprogramming of non-β-cells. While promising preclinical studies and clinical trials of hESC-induced islet cell regeneration are ongoing, breakthroughs in this direction may hopefully provide us with a radically new strategy to manage obesity-related T2DM and increase the efficacy of BS.

Ethics statement

The authors certify that they have obtained the participant consent forms. In the forms, participants have given their consent for their images and other clinical information to be reported in the journal. The participants understand that their names and initials will not be published, and due efforts will be made to conceal their identity.

Author contributions

TL was responsible for the literature searching and writing. RR and XZ were responsible for the manuscript revision and figure production, and QX was responsible for the supervision and manuscript revision. All authors contributed to the article and approved the submitted version.

Funding

This research was funded by National High Level Hospital Clinical Research Funding (2022-PUMCH-D-001) and National Natural Science Foundation of China (81970763).

Conflict of interest

The authors declare that the research was conducted in the absence of any commercial or financial relationships that could be construed as a potential conflict of interest.

Publisher's note

References

1. Blüher M. Obesity: Global epidemiology and pathogenesis. *Nat Rev Endocrinol* (2019) 15(5):288–98. doi: 10.1038/s41574-019-0176-8

2. Magkos F, Hjorth MF, Astrup A. Diet and exercise in the prevention and treatment of type 2 diabetes mellitus. *Nat Rev Endocrinol* (2020) 16(10):545–55. doi: 10.1038/s41574-020-0381-5

3. Nguyen NT, Varela JE. Bariatric surgery for obesity and metabolic disorders: State of the art. *Nat Rev Gastroenterol Hepatol* (2017) 14(3):160–9. doi: 10.1038/nrgastro.2016.170

4. Chang S-H, Stoll CRT, Song J, Varela JE, Eagon CJ, Colditz GA. The effectiveness and risks of bariatric surgery: An updated systematic review and meta-analysis, 2003-2012. *JAMA Surg* (2014) 149(3):275–87. doi: 10.1001/jamasurg.2013.3654

5. Carlsson LMS, Peltonen M, Ahlin S, Anveden Å, Bouchard C, Carlsson B, et al. Bariatric surgery and prevention of type 2 diabetes in Swedish obese subjects. *N Engl J Med* (2012) 367(8):695–704. doi: 10.1056/NEJMoa1112082

6. Arterburn DE, Telem DA, Kushner RF, Courcoulas AP. Benefits and risks of bariatric surgery in adults: A review. *JAMA* (2020) 324(9):879–87. doi: 10.1001/jama.2020.12567

7. Beamish AJ, Olbers T, Kelly AS, Inge TH. Cardiovascular effects of bariatric surgery. *Nat Rev Cardiol* (2016) 13(12):730–43. doi: 10.1038/nrcardio.2016.162

8. Aung L, Lee W-J, Chen SC, Ser K-H, Wu C-C, Chong K, et al. Bariatric surgery for patients with early-onset vs late-onset type 2 diabetes. *JAMA Surg* (2016) 151(9):798–805. doi: 10.1001/jamasurg.2016.1130

9. Courcoulas AP, Christian NJ, Belle SH, Berk PD, Flum DR, Garcia L, et al. Weight change and health outcomes at 3 years after bariatric surgery among individuals with severe obesity. *JAMA* (2013) 310(22):2416–25. doi: 10.1001/jama.2013.280928

10. Anveden Å, Taube M, Peltonen M, Jacobson P, Andersson-Assarsson JC, Sjöholm K, et al. Long-term incidence of female-specific cancer after bariatric surgery or usual care in the Swedish obese subjects study. *Gynecol Oncol* (2017) 145(2):224–9. doi: 10.1016/j.ygyno.2017.02.036

11. Vest AR, Heneghan HM, Agarwal S, Schauer PR, Young JB. Bariatric surgery and cardiovascular outcomes: A systematic review. *Heart* (2012) 98(24):1763–77. doi: 10.1136/heartjnl-2012-301778

12. Mollan SP, Mitchell JL, Ottridge RS, Aguiar M, Yiangou A, Alimajstorovic Z, et al. Effectiveness of bariatric surgery vs community weight management intervention for the treatment of idiopathic intracranial hypertension: A randomized clinical trial. *JAMA Neurol* (2021) 78(6):678–86. doi: 10.1001/jamaneurol.2021.0659

13. Dixon AE, Pratley RE, Forgione PM, Kaminsky DA, Whittaker-Leclair LA, Griffes LA, et al. Effects of obesity and bariatric surgery on airway hyperresponsiveness, asthma control, and inflammation. *J Allergy Clin Immunol* (2011) 128(3):508–15.e1. doi: 10.1016/j.jaci.2011.06.009

14. Risstad H, Søvik TT, Engström M, Aasheim ET, Fagerland MW, Olsén MF, et al. Five-year outcomes after laparoscopic gastric bypass and laparoscopic duodenal switch in patients with body mass index of 50 to 60: A randomized clinical trial. *JAMA Surg* (2015) 150(4):352–61. doi: 10.1001/jamasurg.2014.3579

15. Angrisani L, Santonicola A, Iovino P, Vitiello A, Zundel N, Buchwald H, et al. Bariatric surgery and endoluminal procedures: IFSO worldwide survey 2014. *Obes Surg* (2017) 27(9):2279–89. doi: 10.1007/s11695-017-2666-x

16. Peterli R, Wölnerhanssen B, Peters T, Devaux N, Kern B, Christoffel-Courtin C, et al. Improvement in glucose metabolism after bariatric surgery: Comparison of laparoscopic roux-en-Y gastric bypass and laparoscopic sleeve gastrectomy: A prospective randomized trial. *Ann Surg* (2009) 250(2):234–41. doi: 10.1097/SLA.0b013e3181ae32e3

17. Schauer PR, Bhatt DL, Kirwan JP, Wolski K, Aminian A, Brethauer SA, et al. Bariatric surgery versus intensive medical therapy for diabetes - 5-year outcomes. *N Engl J Med* (2017) 376(7):641–51. doi: 10.1056/NEJMoa1600869

18. Mehaffey JH, LaPar DJ, Clement KC, Turrentine FE, Miller MS, Hallowell PT, et al. 10-year outcomes after roux-en-Y gastric bypass. *Ann Surg* (2016) 264(1):121–6. doi: 10.1097/SLA.0000000000001544

19. Cavin J-B, Couvelard A, Lebtahi R, Ducroc R, Arapis K, Voitellier E, et al. Differences in alimentary glucose absorption and intestinal disposal of blood glucose after roux-en-Y gastric bypass vs sleeve gastrectomy. *Gastroenterology* (2016) 150(2):454–64.e9. doi: 10.1053/j.gastro.2015.10.009

20. Frühbeck G. Bariatric and metabolic surgery: A shift in eligibility and success criteria. *Nat Rev Endocrinol* (2015) 11(8):465–77. doi: 10.1038/nrendo.2015.84

21. Koch TR, Finelli FC. Postoperative metabolic and nutritional complications of bariatric surgery. *Gastroenterol Clin North Am* (2010) 39(1):109–24. doi: 10.1016/j.gtc.2009.12.003

22. Jaruvongvanich V, Matar R, Storm AC, Beran A, Malandris K, Maselli DB, et al. Endoscopic management of refractory leaks and fistulas after bariatric surgery with long-term follow-up. *Surg Endosc.* (2021) 35(6):2715–23. doi: 10.1007/s00464-020-07702-5

23. Stenberg E, Chen R, Hildén K, Fall K. Pregnancy as a risk factor for small bowel obstruction after laparoscopic gastric bypass surgery. *Ann Surg* (2020) 272(1):125–9. doi: 10.1097/SLA.0000000000003163

24. Kassir R, Debs T, Blanc P, Gugenheim J, Ben Amor I, Boutet C, et al. Complications of bariatric surgery: Presentation and emergency management. *Int J Surg* (2016) 27(27):77–81. doi: 10.1016/j.ijsu.2016.01.067

25. Boerlage TCC, Haal S, Maurits de Brauw L, Acherman YIZ, Bruin S, van de Laar AWJM, et al. Ursodeoxycholic acid for the prevention of symptomatic gallstone disease after bariatric surgery: Study protocol for a randomized controlled trial (UPGRADE trial). *BMC Gastroenterol* (2017) 17(1):164. doi: 10.1186/s12876-017-0674-x

26. Brzozowska MM, Sainsbury A, Eisman JA, Baldock PA, Center JR. Bariatric surgery, bone loss, obesity and possible mechanisms. *Obes Rev* (2013) 14(1):52–67. doi: 10.1111/j.1467-789X.2012.01050.x

27. Conte C, Lapeyre-Mestre M, Hanaire H, Ritz P. Diabetes remission and relapse after bariatric surgery: A nationwide population-based study. *Obes Surg* (2020) 30 (12):4810–20. doi: 10.1007/s11695-020-04924-3

28. Aminian A, Vidal J, Salminen P, Still CD, Nor Hanipah Z, Sharma G, et al. Late relapse of diabetes after bariatric surgery: Not rare, but not a failure. *Diabetes Care* (2020) 43(3):534–40. doi: 10.2337/dc19-1057

29. Sjöström L, Peltonen M, Jacobson P, Ahlin S, Andersson-Assarsson J, Anveden Å, et al. Association of bariatric surgery with long-term remission of type 2 diabetes and with microvascular and macrovascular complications. *JAMA* (2014) 311(22):2297–304. doi: 10.1001/jama.2014.5988

30. Rubino F, Gagner M, Gentileschi P, Kini S, Fukuyama S, Feng J, et al. The early effect of the roux-en-Y gastric bypass on hormones involved in body weight regulation and glucose metabolism. *Ann Surg* (2004) 240(2):236–42. doi: 10.1097/01.sla.0000133117.12646.48

31. Chambers AP, Jessen L, Ryan KK, Sisley S, Wilson-Pérez HE, Stefater MA, et al. Weight-independent changes in blood glucose homeostasis after gastric bypass or vertical sleeve gastrectomy in rats. *Gastroenterology* (2011) 141(3):950–8. doi: 10.1053/j.gastro.2011.05.050

32. Abu-Gazala S, Horwitz E, Ben-Haroush Schyr R, Bardugo A, Israeli H, Hija A, et al. Sleeve gastrectomy improves glycemia independent of weight loss by restoring hepatic insulin sensitivity. *Diabetes* (2018) 67(6):1079–85. doi: 10.2337/db17-1028

33. Jørgensen NB, Jacobsen SH, Dirksen C, Bojsen-Møller KN, Naver L, Hvolris L, et al. Acute and long-term effects of roux-en-Y gastric bypass on glucose metabolism in subjects with type 2 diabetes and normal glucose tolerance. *Am J Physiol Endocrinol Metab* (2012) 303(1):E122–31. doi: 10.1152/ajpendo.00073.2012

34. The National Institutes of Health Consensus Development Conference on GS for SO. Gastrointestinal surgery for severe obesity: National institutes of health consensus development conference statement. *Am J Clin Nutr* (1992) 55(2 Suppl):615S–9S. doi: 10.1093/ajcn/55.2.615s

35. Mechanick JI, Apovian C, Brethauer S, Timothy Garvey W, Joffe AM, Kim J, et al. Clinical practice guidelines for the perioperative nutrition, metabolic, and nonsurgical support of patients undergoing bariatric procedures - 2019 update: Cosponsored by American association of clinical Endocrinologists/American college of endocrinology, the obesity society, American society for metabolic and bariatric surgery, obesity medicine association, and American society of anesthesiologists. *Obes (Silver Spring)* (2020) 28(4): O1–58.

36. Di Lorenzo N, Antoniou SA, Batterham RL, Busetto L, Godoroja D, Iossa A, et al. Clinical practice guidelines of the European association for endoscopic surgery (EAES) on bariatric surgery: uUpdate 2020 endorsed by IFSO-EC, EASO and ESPCOP. *Surg Endosc* (2020) 34(6):2332–58. doi: 10.1007/s00464-020-07555-y

37. Zhou Q, Melton DA. Pancreas regeneration. *Nature* (2018) 557(7705):351–8. doi: 10.1038/s41586-018-0088-0

38. Bernal-Mizrachi E, Wice B, Inoue H, Permutt MA. Activation of serum response factor in the depolarization induction of egr-1 transcription in pancreatic islet beta-cells. *J Biol Chem* (2000) 275(33):25681–9. doi: 10.1074/jbc.M003424200

39. Heit JJ, Apelqvist AA, Gu X, Winslow MM, Neilson JR, Crabtree GR, et al. Calcineurin/NFAT signalling regulates pancreatic beta-cell growth and function. *Nature* (2006) 443(7109):345–9. doi: 10.1038/nature05097

40. Aguayo-Mazzucato C, van Haaren M, Mruk M, Lee TB, Crawford C, Hollister-Lock J, et al. β cell aging markers have heterogeneous distribution and are induced by insulin resistance. *Cell Metab* (2017) 25(4):898–910.e5. doi: 10.1016/j.cmet.2017.03.015

41. Costes S, Bertrand G, Ravier MA. Mechanisms of beta-cell apoptosis in type 2 diabetes-prone situations and potential protection by GLP-1-Based therapies. *Int J Mol Sci* (2021) 22(10). doi: 10.3390/ijms22105303

42. Rojas J, Bermudez V, Palmar J, Martínez MS, Olivar LC, Nava M, et al. Pancreatic beta cell death: Novel potential mechanisms in diabetes therapy. *J Diabetes Res* (2018) 2018:9601801. doi: 10.1155/2018/9601801

43. Kahn SE, Hull RL, Utzschneider KM. Mechanisms linking obesity to insulin resistance and type 2 diabetes. *Nature* (2006) 444(7121):840–6. doi: 10.1038/nature05482

44. Kahn SE, Cooper ME, Del Prato S. Pathophysiology and treatment of type 2 diabetes: Perspectives on the past, present, and future. *Lancet* (2014) 383(9922):1068–83. doi: 10.1016/S0140-6736(13)62154-6

45. Wang Z, York NW, Nichols CG, Remedi MS. Pancreatic β cell dedifferentiation in diabetes and redifferentiation following insulin therapy. *Cell Metab* (2014) 19(5):872–82. doi: 10.1016/j.cmet.2014.03.010

46. Butler AE, Janson J, Bonner-Weir S, Ritzel R, Rizza RA, Butler PC. Beta-cell deficit and increased beta-cell apoptosis in humans with type 2 diabetes. *Diabetes* (2003) 52 (1):102–10. doi: 10.2337/diabetes.52.1.102

47. Thorel F, Népote V, Avril I, Kohno K, Desgraz R, Chera S, et al. Conversion of adult pancreatic alpha-cells to beta-cells after extreme beta-cell loss. *Nature* (2010) 464 (7292):1149–54. doi: 10.1038/nature08894

48. Efrat S. Mechanisms of adult human β-cell *in vitro* dedifferentiation and redifferentiation. *Diabetes Obes Metab* (2016) 18 Suppl 1:97–101. doi: 10.1111/dom.12724

49. Ying W, Fu W, Lee YS, Olefsky JM. The role of macrophages in obesity-associated islet inflammation and β-cell abnormalities. *Nat Rev Endocrinol* (2020) 16(2):81–90. doi: 10.1038/s41574-019-0286-3

50. Eguchi K, Nagai R. Islet inflammation in type 2 diabetes and physiology. *J Clin Invest* (2017). doi: 10.1172/JCI88877

51. Martinussen C, Bojsen-Møller KN, Dirksen C, Jacobsen SH, Jørgensen NB, Kristiansen VB, et al. Immediate enhancement of first-phase insulin secretion and unchanged glucose effectiveness in patients with type 2 diabetes after roux-en-Y gastric bypass. *Am J Physiol Endocrinol Metab* (2015) 308(6):E535–44. doi: 10.1152/ajpendo.00506.2014

52. Ying W, Lee YS, Dong Y, Seidman JS, Yang M, Isaac R, et al. Expansion of islet-resident macrophages leads to inflammation affecting β cell proliferation and function in obesity. *Cell Metab* (2019) 29(2):457–474.e5. doi: 10.1016/j.cmet.2018.12.003

53. Butcher MJ, Hallinger D, Garcia E, Machida Y, Chakrabarti S, Nadler J, et al. Association of proinflammatory cytokines and islet resident leucocytes with islet dysfunction in type 2 diabetes. *Diabetologia* (2014) 57(3):491–501. doi: 10.1007/s00125-013-3116-5

54. Talchai C, Lin HV, Kitamura T, Accili D. Genetic and biochemical pathways of beta-cell failure in type 2 diabetes. *Diabetes Obes Metab* (2009) 11 Suppl 4:38–45. doi: 10.1111/j.1463-1326.2009.01115.x

55. Talchai C, Xuan S, Lin HV, Sussel L, Accili D. Pancreatic β cell dedifferentiation as a mechanism of diabetic β cell failure. *Cell* (2012) 150(6):1223–34. doi: 10.1016/j.cell.2012.07.029

56. Cinti F, Bouchi R, Kim-Muller JY, Ohmura Y, Sandoval PR, Masini M, et al. Evidence of β-cell dedifferentiation in human type 2 diabetes. *J Clin Endocrinol Metab* (2016) 101(3):1044–54. doi: 10.1210/jc.2015-2860

57. Weng J, Li Y, Xu W, Shi L, Zhang Q, Zhu D, et al. Effect of intensive insulin therapy on beta-cell function and glycaemic control in patients with newly diagnosed type 2 diabetes: A multicentre randomised parallel-group trial. *Lancet* (2008) 371 (9626):1753–60. doi: 10.1016/S0140-6736(08)60762-X

58. Lee W-J, Almalki O. Mechanism of diabetes control after metabolic surgery. *Ann Laparosc Endosc Surg* (2017) 2:128–8. doi: 10.21037/ales.2017.07.05

59. Haluzík M. Bariatric surgery and the mechanism of diabetes remission: Are we getting there? *J Clin Endocrinol Metab* (2013) 98(11):4336–8. doi: 10.1210/jc.2013-3698

60. Thaler JP, Cummings DE. Minireview: Hormonal and metabolic mechanisms of diabetes remission after gastrointestinal surgery. *Endocrinology* (2009) 150(6):2518–25. doi: 10.1210/en.2009-0367

61. Jorsal T, Wewer Albrechtsen NJ, Christensen MM, Mortensen B, Wandall E, Langholz E, et al. Investigating intestinal glucagon after roux-en-Y gastric bypass surgery. *J Clin Endocrinol Metab* (2019) 104(12):6403–16. doi: 10.1210/jc.2019-00062

62. Leca BM, Khan U, Abraham J, Halder L, Shuttlewood E, Shah N, et al. Laparoscopic adjustable gastric banding-should a second chance be given? *Obes Surg* (2020) 30(8):2913–9. doi: 10.1007/s11695-020-04613-1

63. Dirksen C, Damgaard M, Bojsen-Møller KN, Jørgensen NB, Kielgast U, Jacobsen SH, et al. Fast pouch emptying, delayed small intestinal transit, and exaggerated gut hormone responses after roux-en-Y gastric bypass. *Neurogastroenterol Motil.* (2013) 25 (4):346–e255. doi: 10.1111/nmo.12087

64. Chambers AP, Smith EP, Begg DP, Grayson BE, Sisley S, Greer T, et al. Regulation of gastric emptying rate and its role in nutrient-induced GLP-1 secretion in rats after vertical sleeve gastrectomy. *Am J Physiol Endocrinol Metab* (2014) 306(4):E424–32. doi: 10.1152/ajpendo.00469.2013

65. Stefater MA, Wilson-Pérez HE, Chambers AP, Sandoval DA, Seeley RJ. All bariatric surgeries are not created equal: Insights from mechanistic comparisons. *Endocr Rev* (2012) 33(4):595–622. doi: 10.1210/er.2011-1044

66. Foo J, Krebs J, Hayes MT, Bell D, Macartney-Coxson D, Croft T, et al. Studies in insulin resistance following very low calorie diet and/or gastric bypass surgery. *Obes Surg* (2011) 21(12):1914–20. doi: 10.1007/s11695-011-0527-6

67. Campos GM, Rabl C, Peeva S, Ciovica R, Rao M, Schwarz J-M, et al. Improvement in peripheral glucose uptake after gastric bypass surgery is observed only after substantial weight loss has occurred and correlates with the magnitude of weight lost. *J Gastrointest Surg* (2010) 14(1):15–23. doi: 10.1007/s11605-009-1060-y

68. Chen X, Zhang J, Zhou Z. Targeting islets: Metabolic surgery is more than a bariatric surgery. *Obes Surg* (2019) 29(9):3001–9. doi: 10.1007/s11695-019-03979-1

69. Maciejewski ML, Arterburn DE, Van Scoyoc L, Smith VA, Yancy WS, Weidenbacher HJ, et al. Bariatric surgery and long-term durability of weight loss. *JAMA Surg* (2016) 151(11):1046–55. doi: 10.1001/jamasurg.2016.2317

70. Wang PYT, Caspi L, Lam CKL, Chari M, Li X, Light PE, et al. Upper intestinal lipids trigger a gut-brain-liver axis to regulate glucose production. *Nature* (2008) 452 (7190):1012–6. doi: 10.1038/nature06852

71. Steinert RE, Feinle-Bisset C, Asarian L, Horowitz M, Beglinger C, Geary N. Ghrelin, CCK, GLP-1, and PYY(3-36): Secretory controls and physiological roles in eating and glycemia in health, obesity, and after RYGB. *Physiol Rev* (2017) 97(1):411–63. doi: 10.1152/physrev.00031.2014

72. Mosinski JD, Aminian A, Axelrod CL, Batayyah E, Romero-Talamas H, Daigle C, et al. Roux-en-Y gastric bypass restores islet function and morphology independent of body weight in ZDF rats. *Am J Physiol Endocrinol Metab* (2021) 320(2):E392–8. doi: 10.1152/ajpendo.00467.2020

73. Zhou X, Qian B, Ji N, Lui C, Liu Z, Li B, et al. Pancreatic hyperplasia after gastric bypass surgery in a GK rat model of non-obese type 2 diabetes. *J Endocrinol* (2016) 228 (1):13–23. doi: 10.1530/JOE-14-0701

74. Li Z, Zhang H-Y, Lv L-X, Li D-F, Dai J-X, Sha O, et al. Roux-en-Y gastric bypass promotes expression of PDX-1 and regeneration of beta-cells in goto-kakizaki rats. *World J Gastroenterol* (2010) 16(18):2244–51. doi: 10.3748/wjg.v16.i18.2244

75. Speck M, Cho YM, Asadi A, Rubino F, Kieffer TJ. Duodenal-jejunal bypass protects GK rats from {beta}-cell loss and aggravation of hyperglycemia and increases enteroendocrine cells co-expressing GIP and GLP-1. *Am J Physiol Endocrinol Metab* (2011) 300(5):E923–32. doi: 10.1152/ajpendo.00422.2010

76. Qian B, Zhou X, Li B, Li B, Liu Z, Wu J, et al. Reduction of pancreatic β-cell dedifferentiation after gastric bypass surgery in diabetic rats. *J Mol Cell Biol* (2014) 6 (6):531–4. doi: 10.1093/jmcb/mju042

77. Chai F, Wang Y, Zhou Y, Liu Y, Geng D, Liu J. Adiponectin downregulates hyperglycemia and reduces pancreatic islet apoptosis after roux-en-y gastric bypass surgery. *Obes Surg* (2011) 21(6):768–73. doi: 10.1007/s11695-011-0357-6

78. Lindqvist A, Spégel P, Ekelund M, Garcia Vaz E, Pierzynowski S, Gomez MF, et al. Gastric bypass improves β-cell function and increases β-cell mass in a porcine model. *Diabetes* (2014) 63(5):1665–71. doi: 10.2337/db13-0969

79. Miskelly MG, Shcherbina L, Thorén Fischer A-H, Abels M, Lindqvist A, Wierup N. GK-rats respond to gastric bypass surgery with improved glycemia despite unaffected insulin secretion and beta cell mass. *Peptides* (2021) 136:170445. doi: 10.1016/j.peptides.2020.170445

80. McGavigan AK, Garibay D, Henseler ZM, Chen J, Bettaieb A, Haj FG, et al. TGR5 contributes to glucoregulatory improvements after vertical sleeve gastrectomy in mice. *Gut* (2017) 66(2):226–34. doi: 10.1136/gutjnl-2015-309871

81. Lin E, Liang Z, Frediani J, Davis SS, Sweeney JF, Ziegler TR, et al. Improvement in ß-cell function in patients with normal and hyperglycemia following roux-en-Y gastric bypass surgery. *Am J Physiol Endocrinol Metab* (2010) 299(5):E706–12. doi: 10.1152/ajpendo.00405.2010

82. Hofsø D, Jenssen T, Bollerslev J, Ueland T, Godang K, Stumvoll M, et al. Beta cell function after weight loss: A clinical trial comparing gastric bypass surgery and intensive lifestyle intervention. *Eur J Endocrinol* (2011) 164(2):231–8. doi: 10.1530/EJE-10-0804

83. Nannipieri M, Mari A, Anselmino M, Baldi S, Barsotti E, Guarino D, et al. The role of beta-cell function and insulin sensitivity in the remission of type 2 diabetes after gastric bypass surgery. *J Clin Endocrinol Metab* (2011) 96(9):E1372–9. doi: 10.1210/jc.2011-0446

84. Camastra S, Gastaldelli A, Mari A, Bonuccelli S, Scartabelli G, Frascerra S, et al. Early and longer term effects of gastric bypass surgery on tissue-specific insulin sensitivity and beta cell function in morbidly obese patients with and without type 2 diabetes. *Diabetologia* (2011) 54(8):2093–102. doi: 10.1007/s00125-011-2193-6

85. Chaudhari SN, Harris DA, Aliakbarian H, Luo JN, Henke MT, Subramaniam R, et al. Bariatric surgery reveals a gut-restricted TGR5 agonist with antidiabetic effects. *Nat Chem Biol* (2021) 17(1):20–9. doi: 10.1038/s41589-020-0604-z

86. Rubino F, Forgione A, Cummings DE, Vix M, Gnuli D, Mingrone G, et al. The mechanism of diabetes control after gastrointestinal bypass surgery reveals a role of the proximal small intestine in the pathophysiology of type 2 diabetes. *Ann Surg* (2006) 244 (5):741–9. doi: 10.1097/01.sla.0000224726.61448.1b

87. Holst JJ. The incretin system in healthy humans: The role of GIP and GLP-1. *Metab Clin Exp* (2019) 96:46–55. doi: 10.1016/j.metabol.2019.04.014

88. Laferrère B, Teixeira J, McGinty J, Tran H, Egger JR, Colarusso A, et al. Effect of weight loss by gastric bypass surgery versus hypocaloric diet on glucose and incretin levels in patients with type 2 diabetes. *J Clin Endocrinol Metab* (2008) 93(7):2479–85. doi: 10.1210/jc.2007-2851

89. le Roux CW, Aylwin SJB, Batterham RL, Borg CM, Coyle F, Prasad V, et al. Gut hormone profiles following bariatric surgery favor an anorectic state, facilitate weight loss, and improve metabolic parameters. *Ann Surg* (2006) 243(1):108–14. doi: 10.1097/01.sla.0000183349.16877.84

90. Jørgensen NB, Dirksen C, Bojsen-Møller KN, Jacobsen SH, Worm D, Hansen DL, et al. Exaggerated glucagon-like peptide 1 response is important for improved β-cell function and glucose tolerance after roux-en-Y gastric bypass in patients with type 2 diabetes. *Diabetes* (2013) 62(9):3044–52. doi: 10.2337/db13-0022

91. Salehi M, Vella A, McLaughlin T, Patti M-E. Hypoglycemia after gastric bypass surgery: Current concepts and controversies. *J Clin Endocrinol Metab* (2018) 103 (8):2815–26. doi: 10.1210/jc.2018-00528

92. Ramracheya RD, McCulloch LJ, Clark A, Wiggins D, Johannessen H, Olsen MK, et al. PYY-dependent restoration of impaired insulin and glucagon secretion in type 2 diabetes following roux-En-Y gastric bypass surgery. *Cell Rep* (2016) 15 (5):944–50. doi: 10.1016/j.celrep.2016.03.091

93. Grams J, Garvey WT. Weight loss and the prevention and treatment of type 2 diabetes using lifestyle therapy, pharmacotherapy, and bariatric surgery: Mechanisms of action. *Curr Obes Rep* (2015) 4(2):287–302. doi: 10.1007/s13679-015-0155-x

94. Saeidi N, Meoli L, Nestoridi E, Gupta NK, Kvas S, Kucharczyk J, et al. Reprogramming of intestinal glucose metabolism and glycemic control in rats after gastric bypass. *Science* (2013) 341(6144):406–10. doi: 10.1126/science.1235103

95. Dang JT, Karmali S. Is RYGB more effective than sleeve gastrectomy? *Nat Rev Endocrinol* (2019) 15(3):134–5. doi: 10.1038/s41574-018-0152-8

96. Welbourn R, Pournaras DJ, Dixon J, Higa K, Kinsman R, Ottosson J, et al. Bariatric surgery worldwide: Baseline demographic description and one-year outcomes from the second IFSO global registry report 2013-2015. *Obes Surg* (2018) 28(2):313–22. doi: 10.1007/s11695-017-2845-9

97. Oppenländer L, Palit S, Stemmer K, Greisle T, Sterr M, Salinno C, et al. Vertical sleeve gastrectomy triggers fast β-cell recovery upon overt diabetes. *Mol Metab* (2021) 54:101330. doi: 10.1016/j.molmet.2021.101330

98. Grong E, Kulseng B, Arbo IB, Nord C, Eriksson M, Ahlgren U, et al. Sleeve gastrectomy, but not duodenojejunostomy, preserves total beta-cell mass in goto-kakizaki rats evaluated by three-dimensional optical projection tomography. *Surg Endosc.* (2016) 30(2):532–42. doi: 10.1007/s00464-015-4236-4

99. Li F, Sheng C, Song K, Zhang M, Bu L, Yang P, et al. Preventative sleeve gastrectomy contributes to maintaining β cell function in db/db diabetic mouse. *Obes Surg* (2016) 26(10):2402–10. doi: 10.1007/s11695-016-2112-5

100. Inabnet WB, Milone L, Harris P, Durak E, Freeby MJ, Ahmed L, et al. The utility of [(11)C] dihydrotetrabenazine positron emission tomography scanning in assessing beta-cell performance after sleeve gastrectomy and duodenal-jejunal bypass. *Surgery* (2010) 147(2):303–9. doi: 10.1016/j.surg.2009.08.005

101. Douros JD, Niu J, Sdao S, Gregg T, Fisher-Wellman K, Bharadwaj M, et al. Sleeve gastrectomy rapidly enhances islet function independently of body weight. *JCI Insight* (2019). doi: 10.1172/jci.insight.126688

102. Hutch CR, Sandoval D. The role of GLP-1 in the metabolic success of bariatric surgery. *Endocrinology* (2017) 158(12):4139–51. doi: 10.1210/en.2017-00564

103. Garibay D, Lou J, Lee SA, Zaborska KE, Weissman MH, Sloma E, et al. β cell GLP-1R signaling alters α cell proglucagon processing after vertical sleeve gastrectomy in mice. *Cell Rep* (2018) 23(4):967–73. doi: 10.1016/j.celrep.2018.03.120

104. Stevenson M, Lee J, Lau RG, Brathwaite CEM, Ragolia L. Surgical mouse models of vertical sleeve gastrectomy and roux-en y gastric bypass: A review. *Obes Surg* (2019) 29 (12):4084–94. doi: 10.1007/s11695-019-04205-8

105. Myronovych A, Lewis A, Seeley RJ. Some caveats when interpreting surgical mouse models of vertical sleeve gastrectomy. *Obes Surg* (2020) 30(4):1582–5. doi: 10.1007/s11695-020-04459-7

106. Aguayo-Mazzucato C, Bonner-Weir S. Pancreatic β cell regeneration as a possible therapy for diabetes. *Cell Metab* (2018) 27(1):57–67. doi: 10.1016/j.cmet.2017.08.007

107. Nair GG, Liu JS, Russ HA, Tran S, Saxton MS, Chen R, et al. Recapitulating endocrine cell clustering in culture promotes maturation of human stem-cell-derived β cells. *Nat Cell Biol* (2019) 21(2):263–74. doi: 10.1038/s41556-018-0271-4

108. Dirice E, Kahraman S, Jiang W, El Ouaamari A, De Jesus DF, Teo AKK, et al. Soluble factors secreted by T cells promote β-cell proliferation. *Diabetes* (2014) 63(1):188–202. doi: 10.2337/db13-0204

109. White MG, Shaw JAM, Taylor R. Type 2 diabetes: The pathologic basis of reversible β-cell dysfunction. *Diabetes Care* (2016) 39(11):2080–8. doi: 10.2337/dc16-0619

110. Ishida E, Kim-Muller JY, Accili D. Pair feeding, but not insulin, phloridzin, or rosiglitazone treatment, curtails markers of β-cell dedifferentiation in db/db mice. *Diabetes* (2017) 66(8):2092–101. doi: 10.2337/db16-1213

111. Sheng C, Li F, Lin Z, Zhang M, Yang P, Bu L, et al. Reversibility of β-Cell-Specific transcript factors expression by long-term caloric restriction in db/db mouse. *J Diabetes Res* (2016) 2016:6035046. doi: 10.1155/2016/6035046

112. Corezola do Amaral ME, Kravets V, Dwulet JM, Farnsworth NL, Piscopio R, Schleicher WE, et al. Caloric restriction recovers impaired β-cell-β-cell gap junction coupling, calcium oscillation coordination, and insulin secretion in prediabetic mice. *Am J Physiol Endocrinol Metab* (2020) 319(4):E709–20. doi: 10.1152/ajpendo.00132.2020

113. Cheng C-W, Villani V, Buono R, Wei M, Kumar S, Yilmaz OH, et al. Fasting-mimicking diet promotes Ngn3-driven β-cell regeneration to reverse diabetes. *Cell* (2017) 168(5):775–788.e12. doi: 10.1016/j.cell.2017.01.040

114. Lee JH, Jaung R, Beban G, Evennett N, Cundy T. Insulin use and new diabetes after acceptance for bariatric surgery: Comparison of outcomes after completion of surgery or withdrawal from the program. *BMJ Open Diabetes Res Care* (2020) 8(2). doi: 10.1136/bmjdrc-2020-001837

115. Lorico S, Colton B. Medication management and pharmacokinetic changes after bariatric surgery. *Can Fam Physician.* (2020) 66(6):409–16.

116. Nicoletti CF, Cortes-Oliveira C, Pinhel MAS, Nonino CB. Bariatric surgery and precision nutrition. *Nutrients* (2017) 9(9). doi: 10.3390/nu9090974

117. RISE Consortium. Restoring insulin secretion (RISE): Design of studies of β-cell preservation in prediabetes and early type 2 diabetes across the life span. *Diabetes Care* (2014) 37(3):780–8. doi: 10.2337/dc13-1879

118. Hallakou-Bozec S, Vial G, Kergoat M, Fouqueray P, Bolze S, Borel A-L, et al. Mechanism of action of imeglimin: A novel therapeutic agent for type 2 diabetes. *Diabetes Obes Metab* (2021) 23(3):664–73. doi: 10.1111/dom.14277

119. Hogrebe NJ, Augsornworawat P, Maxwell KG, Velazco-Cruz L, Millman JR. Targeting the cytoskeleton to direct pancreatic differentiation of human pluripotent stem cells. *Nat Biotechnol* (2020) 38(4):460–70. doi: 10.1038/s41587-020-0430-6

120. Melton D. The promise of stem cell-derived islet replacement therapy. *Diabetologia* (2021) 64(5):1030–6. doi: 10.1007/s00125-020-05367-2

121. Liu H, Yang H, Zhu D, Sui X, Li J, Liang Z, et al. Systematically labeling developmental stage-specific genes for the study of pancreatic β-cell differentiation from human embryonic stem cells. *Cell Res* (2014) 24(10):1181–200. doi: 10.1038/cr.2014.118

122. Qadir MMF, Álvarez-Cubela S, Klein D, van Dijk J, Muñiz-Anquela R, Moreno-Hernández YB, et al. Single-cell resolution analysis of the human pancreatic ductal progenitor cell niche. *Proc Natl Acad Sci USA* (2020) 117(20):10876–87. doi: 10.1073/pnas.1918314117

123. Gribben C, Lambert C, Messal HA, Hubber E-L, Rackham C, Evans I, et al. Ductal Ngn3-expressing progenitors contribute to adult β cell neogenesis in the pancreas. *Cell Stem Cell* (2021) 28(11):2000–2008.e4. doi: 10.1016/j.stem.2021.08.003

124. Gloy VL, Briel M, Bhatt DL, Kashyap SR, Schauer PR, Mingrone G, et al. Bariatric surgery versus non-surgical treatment for obesity: a systematic review and meta-analysis of randomised controlled trials. *BMJ* (2013) 347:f5934. doi: 10.1136/bmj.f5934

125. Gould JC, Kent KC, Wan Y, Rajamanickam V, Leverson G, Campos GM. Perioperative safety and volume: outcomes relationships in bariatric surgery: A study of 32,000 patients. *J Am Coll Surg* (2011) 213(6):771–7. doi: 10.1016/j.jamcollsurg.2011.09.006

126. Quirante FP, Montorfano L, Rammohan R, Dhanabalsamy N, Lee A, Szomstein S, et al. Is bariatric surgery safe in the elderly population? *Surg Endosc* (2017) 31(4):1538–43. doi: 10.1007/s00464-016-5050-3

127. Inge TH, Courcoulas AP, Jenkins TM, Michalsky MP, Helmrath MA, Brandt ML, et al. Weight loss and health status 3 years after bariatric surgery in adolescents. *N Engl J Med* (2016) 374(2):113–23. doi: 10.1056/NEJMoa1506699

128. Pedersen HK, Gudmundsdottir V, Pedersen MK, Brorsson C, Brunak S, Gupta R. Ranking factors involved in diabetes remission after bariatric surgery using machine-learning integrating clinical and genomic biomarkers. *NPJ Genomic Med* (2016) 1:16035. doi: 10.1038/npjgenmed.2016.35

129. Ohta M, Seki Y, Ohyama T, Bai R, Kim SH, Oshiro T, et al. Prediction of long-term diabetes remission after metabolic surgery in obese East Asian patients: A comparison between ABCD and IMS scores. *Obes Surg* (2021) 31(4):1485–95. doi: 10.1007/s11695-020-05151-6

130. Debédat J, Sokolovska N, Coupaye M, Panunzi S, Chakaroun R, Genser L, et al. Long-term relapse of type 2 diabetes after roux-en-Y gastric bypass: Prediction and clinical relevance. *Diabetes Care* (2018) 41(10):2086–95. doi: 10.2337/dc18-0567

131. González Arnáiz E, Ballesteros Pomar MD, Pintor de la Maza B, González Roza L, Ramos Bachiller B, Barajas Galindo D, et al. Diabetes remission after malabsorptive bariatric surgery. *Endocrinol Diabetes Nutr* (2021) 68(4):218–26.

132. de Souza AH, Tang J, Yadev AK, Saghafi ST, Kibbe CR, Linnemann AK, et al. Intra-islet GLP-1, but not CCK, is necessary for β-cell function in mouse and human islets. *Sci Rep* (2020) 10(1):2823. doi: 10.1038/s41598-020-59799-2

133. Carlessi R, Chen Y, Rowlands J, Cruzat VF, Keane KN, Egan L, et al. GLP-1 receptor signalling promotes β-cell glucose metabolism *via* mTOR-dependent HIF-1α activation. *Sci Rep* (2017) 7(1):2661.

Frontiers in Endocrinology

Explores the endocrine system to find new therapies for key health issues

The second most-cited endocrinology and metabolism journal, which advances our understanding of the endocrine system. It uncovers new therapies for prevalent health issues such as obesity, diabetes, reproduction, and aging.

Discover the latest Research Topics

See more →

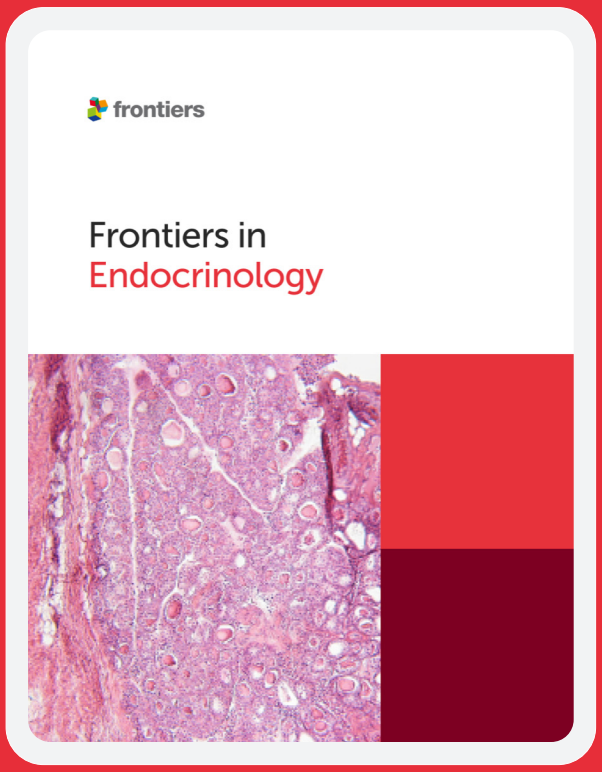

Frontiers

Avenue du Tribunal-Fédéral 34
1005 Lausanne, Switzerland
frontiersin.org

Contact us

+41 (0)21 510 17 00
frontiersin.org/about/contact